CENTRE FOR ECONOMIC POLICY RESEARCH

CEPR PRESS

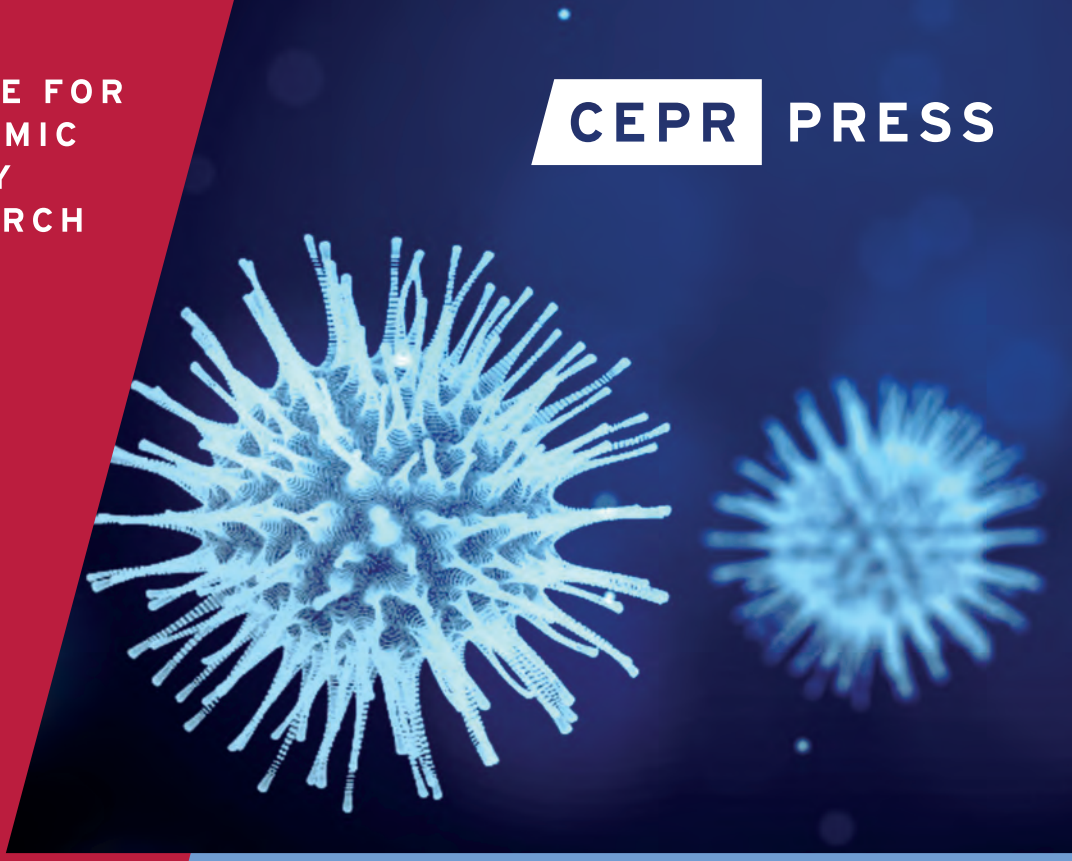

COVID ECONOMICS

VETTED AND REAL-TIME PAPERS

ISSUE 61
11 DECEMBER 2020

Covid Economics
Vetted and Real-Time Papers

Covid Economics, Vetted and Real-Time Papers, from CEPR, brings together formal investigations on the economic issues emanating from the Covid outbreak, based on explicit theory and/or empirical evidence, to improve the knowledge base.

Founder: Beatrice Weder di Mauro, President of CEPR
Editor: Charles Wyplosz, Graduate Institute Geneva and CEPR

Contact: Submissions should be made at https://portal.cepr.org/call-papers-covid-economics. Other queries should be sent to covidecon@cepr.org.

The Centre for Economic Policy Research (CEPR)

The Centre for Economic Policy Research (CEPR) is a network of over 1,500 research economists based mostly in European universities. The Centre's goal is twofold: to promote world-class research, and to get the policy-relevant results into the hands of key decision-makers. CEPR's guiding principle is 'Research excellence with policy relevance'. A registered charity since it was founded in 1983, CEPR is independent of all public and private interest groups. It takes no institutional stand on economic policy matters and its core funding comes from its Institutional Members and sales of publications. Because it draws on such a large network of researchers, its output reflects a broad spectrum of individual viewpoints as well as perspectives drawn from civil society. CEPR research may include views on policy, but the Trustees of the Centre do not give prior review to its publications. The opinions expressed in this report are those of the authors and not those of CEPR.

Editorial Board

Ethics

Covid Economics will feature high quality analyses of economic aspects of the health crisis. However, the pandemic also raises a number of complex ethical issues. Economists tend to think about trade-offs, in this case lives vs. costs, patient selection at a time of scarcity, and more. In the spirit of academic freedom, neither the Editors of *Covid Economics* nor CEPR take a stand on these issues and therefore do not bear any responsibility for views expressed in the articles.

Submission to professional journals

The following journals have indicated that they will accept submissions of papers featured in *Covid Economics* because they are working papers. Most expect revised versions. This list will be updated regularly.

American Economic Review
American Economic Review, Applied Economics
American Economic Review, Insights
American Economic Review, Economic Policy
American Economic Review, Macroeconomics
American Economic Review, Microeconomics
American Journal of Health Economics
Canadian Journal of Economics
*Econometrica**
Economic Journal
Economics of Disasters and Climate Change
International Economic Review
Journal of Development Economics
*Journal of Econometrics**
Journal of Economic Growth
Journal of Economic Theory
*Journal of the European Economic Association**
Journal of Finance
Journal of Financial Economics
Journal of International Economics
*Journal of Labor Economics**
Journal of Monetary Economics
Journal of Public Economics
Journal of Public Finance and Public Choice
Journal of Political Economy
Journal of Population Economics
Quarterly Journal of Economics
*Review of Corporate Finance Studies**
Review of Economics and Statistics
*Review of Economic Studies**
Review of Financial Studies

(*) Must be a significantly revised and extended version of the paper featured in *Covid Economics*.

Covid Economics
Vetted and Real-Time Papers

Issue 61, 11 December 2020

Contents

The value of a cure: An asset pricing perspective[1]

Viral V. Acharya,[2] Timothy Johnson,[3] Suresh Sundaresan[4] and Steven Zheng[5]

Date submitted: 26 November 2020; Date accepted: 26 November 2020

We provide an estimate of the value of a cure using the joint behavior of stock prices and a vaccine progress indicator during the ongoing COVID-19 pandemic. Our indicator is based on the chronology of stage-by-stage progress of individual vaccines and related news. We construct a general equilibrium regime-switching model of repeated pandemics and stages of vaccine progress wherein the representative agent withdraws labor and alters consumption endogenously to mitigate health risk. The value of a cure in the resulting asset-pricing framework is intimately linked to the relative labor supply across states. The observed stock market response to vaccine progress serves to identify this quantity, allowing us to use the model to estimate the economy-wide welfare gain that would be attributable to a cure. In our estimation, and with standard preference parameters, the value of the ability to end the pandemic is worth 5-15% of total wealth. This value rises substantially when there is uncertainty about the frequency and duration of pandemics. Agents place almost as much value on the ability to resolve the uncertainty as they do on the value of the cure itself. This effect is stronger – not weaker – when agents have a preference for later resolution of uncertainty. The policy implication is that understanding the fundamental biological and social determinants of future pandemics may be as important as resolving the immediate crisis.

1 We thank Dick Berner, Rob Engle, Matt Richardson, Venky Venkateswaran, and Olivier Wang for their comments and suggestions. We also received valuable comments from participants at NYU Stern Finance Department seminar, Advisory Board Meeting of NYU Stern Volatility and Risk Institute, and UIUC Gies Finance Department seminar. We are grateful to the Vaccine Centre at the London School of Hygiene & Tropical Medicine for sharing data.

2 New York University, Stern School of Business, NBER, and CEPR.
3 University of Illinois at Urbana-Champaign.
4 Columbia University, Graduate School of Business.
5 New York University, Stern School of Business.

Covid Economics 61, 11 December 2020: 1-72

1 Introduction

Quantifying the scale of the economic damage caused by the coronavirus pandemic is a crucial step in assessing policy responses along social, medical, fiscal, and monetary dimensions. This paper builds on the hypothesis that stock markets may contain valuable information for gauging this magnitude. Stock markets – which corrected by as much as 40-50% at the outbreak of the pandemic – have rebounded robustly within six months. While there are many explanations proposed for the seeming disconnect between the real economy ravaged by the pandemic and the buoyant stock market, one candidate on the table relates to the progress in development of vaccines[1] to end the pandemic. On the one hand, only the arrival of an efficacious vaccine is considered as a definitive event that will end the pandemic and result in robust economic recovery.[2] On the other hand, stock prices – by reflecting forward-looking expectations – should reflect the economic value of credible progress in the development of vaccines; this value arises from the ability of vaccines to end the pandemic and is naturally related to the scale of the economic damage caused by the pandemic.

The relationship between stock prices and vaccine development is well-illustrated by the following examples. On May 18 and July 14, 2020, *Moderna*, one of the vaccine developing companies, announced good news relating to the progress in its Phase I clinical trials and moving to the next stage of trials. Similarly, on November 9, 2020, *Pfizer* and *BioNTech* announced positive news regarding their Phase III clinical trials. In response to these news, the U.S. stocks gained over $1 trillion in cumulative market capitalization over these three days, with several pandemic-exposed sectors such as airlines, cruise ships, and hotels experiencing 10-20% appreciations on each day. These moves were both economically large and indicative of time to deployment of a vaccine being an important factor driving variation in stock market prices.[3]

In this paper, we build upon these observations and offer an asset-pricing perspective to estimate the value of a cure, i.e., the amount of wealth that a representative agent would be willing to pay for obtaining a vaccine that puts an end to the ongoing pandemic. While there are several

[1] We use “cure" and “vaccine" interchangeably to denote something that brings the pandemic to an end, despite being medically very different.

[2] See Lauren Fedor and James Politi, Financial Times, May 18, 2020 in the Appendix.

[3] See (1) Matt Levine, Money Stuff, May 19, 2020, (2) Matt Levine, Money Stuff, July 16, 2020, (3) John Authers, Bloomberg Opinion, November 10, 2020, and (4) Laurence Fletcher and Robin Wigglesworth, Financial Times, November 14, 2020 in the Appendix.

Covid Economics 61, 11 December 2020: 1-72

estimations of how costly the pandemic is to the economy, our approach is different and novel in that it uses stock market data to calculate the value of a cure and indirectly provides an estimate of the pandemic's economic cost.

First, we document empirically the joint behavior of stock returns (for market portfolio and cross-section of industries) and expected time to deployment of a vaccine. To this end, we construct a novel "vaccine progress indicator." Our indicator is based on the chronology of stage-by-stage progress of individual vaccines (obtained from the Vaccine Centre at the London School of Hygiene & Tropical Medicine) and related news (obtained from FactSet). Using data on vaccine development for past epidemics and surveys during the COVID-19 pandemic, we calibrate the probabilities of transition across different stages of vaccine development and use news to "tap" these probabilities up or down. We then simulate over 200 vaccine "trials" corresponding to the vaccines being developed, factoring in a correlation structure between trials based on relevant characteristics such as their approach ("platform"), common company, etc. The result of this exercise is a vaccine progress indicator using all available information at a given point of time expressed in terms of expected time to deployment of a vaccine.[4] The evolution of our indicator is shown in Figure 1.

We then relate stock market returns to changes in the expected time to deployment of a vaccine by regressing the returns on changes in our vaccine progress indicator, controlling for lagged returns as well as large moves attributable to release of other macroeconomic news. Allowing for some lead-lag structure in the relationship, e.g., due to leakage of news or dating noise in our news data, we estimate that a reduction in the expected time to deployment of a vaccine by a year results in an increase in the stock market return as a whole by between 4 to 8% on a daily basis. The joint relationship exhibits the anticipated cross-sectional properties, with the co-movement between returns and changes in the vaccine progress indicator being stronger for sectors most affected by COVID-19 pandemic (see Figure 4).

Second, we build a general equilibrium regime-switching model of pandemics with asset pricing implications to translate this empirical co-movement of stock returns and vaccine progress indicator into the value of a cure. We develop a general equilibrium model of an economy with a

[4] An analogy from credit risk literature is that of a first-to-default basket in which several correlated firms are part of a basket and the quantity of interest is the expected time to a first default.

representative agent that has stochastic differential utility (Epstein-Zin preferences) with endogenous labor and consumption choices. The state of the economy can be "normal," i.e., without a pandemic, or in a pandemic; within the pandemic, there are several regimes mapping into the stages of vaccine development. The economy transitions across these states based on a set of stationary probabilities. Once the economy switches out of a pandemic, another pandemic may occur in future. Labor augments agent's capital stock that can be readily converted into consumption; however, labor exposes the agent to the pandemic in that within the pandemic regime, the agent can be hit by a health shock that destroys forever a part of the agent's capital stock, and this likelihood is proportional to the labor supply.[5] A key feature of the model is that the agent withdraws labor in the pandemic states in order to mitigate the economic exposure to a health shock.

Third, we characterize the solution to the agent's problem of choosing labor and consumption in each state of the economy and the respective objective function values, which are interdependent but are amenable to a straightforward numerical solution of a fixed-point problem. We can then examine the pricing kernel and asset prices in this framework; in particular, we evaluate the value of a claim to future output, and study its relationship with the expected time to switching out of a pandemic state as a theoretical counterpart to our empirical estimate of comovement between stock market return and changes in vaccine progress indicator. A key insight of our asset-pricing perspective is the following: the improvement in the welfare of the agent in switching out of a pandemic is related to the extent of contraction in labor in the pandemic state relative to the non-pandemic one; this same labor contraction is an important statistic (modulated by preference and pandemic parameters) determining how sensitive are stock prices to progress towards deployment of a vaccine. The model delivers the implication that the value of moving from a pandemic state to a non-pandemic state is simply the ratio of marginal propensity to consume in the pandemic state to the marginal propensity to consume in the non-pandemic state, augmented by the intertemporal elasticity of substitution. Thus, the desire to resolve uncertainty sooner is informed by the endogenous consumption choices made by the household in Pandemic states.

[5]The permanent loss of capital stock can be due to a variety of factors such as loss of life, reduced productivity or attrition of human capital in working from home amidst closures of schools and lack of child care support, filing of bankruptcies with deadweight losses in asset value, and firing of labor with difficulty in re-matching to available jobs at a future date.

Covid Economics 61, 11 December 2020: 1-72

Covid Economics 61, 11 December 2020: 1-72

We can therefore readily connect our empirical work to the theoretical asset-pricing perspective. With standard preferences parameters employed in the literature, the value of a cure turns out to be worth 5-15% of wealth (formally, capital stock in the model), corresponding to an approximately 25% contraction of labor during the pandemic relative to the non-pandemic state. The reason why the economy would attach such a large value to the vaccine is because the pandemic causes a permanent loss of capital stock when it effects agents, which in turn is reflected in the significant precautionary contraction of labor during the pandemic. In spite of the simplicity of the model of the pandemic, we can readily examine externalities in the setup. Specifically, the representative agent can impose through its labor choice exposure for all other agents in the economy, but not internalize this spillover; we examine the difference in the value of a cure with a pandemic containment labor choice being made by the representative agent versus that by the central planner. Since the planner contracts the labor more and optimally reduces pandemic exposure for the economy as a whole, the planner attaches a lower value to the cure than the representative agent does.[6]

Our estimate of the value of a cure depends crucially on the frequency and the expected duration of the pandemic. This raises the natural question of parameter uncertainty around these pandemic properties. Such uncertainty is natural given the rare nature of such pandemics and the evolving understanding of connections between various pandemics (SARS, H1N1, COVID-19, etc.).[7]

This is the final exercise we undertake. We specialize our framework to just two states, non-pandemic and pandemic (without individual stages of vaccine development), but allow for uncertainty about frequency and duration of pandemics. The agent learns about these parameters as pandemics arrive and end. We can extend our asset-pricing framework also to this setting with uncertainty and learning. It turns out that the value of the cure rises sharply when there is uncertainty about the frequency and duration of pandemics. Indeed, we find that the representative agent would be willing to pay as much for resolution of this parameter uncertainty as for the cure

[6]Note, however, that the planner may attach a higher value to the cure if the arrival of the pandemic were to result in social costs outside the capital stock dynamics for the agent.

[7]See, for example, "COVID-19 Is Bad. But It May Not Be the 'Big One'", Maryn McKenna, Wired, June 17, 2020, "Coronavirus Response Shows the World Is Not Ready for Climate-Induced Pandemics", Jennifer Zhang, Columbia University Earth Institute, February 24, 2020, and "The next pandemic: where is it coming from and how do we stop it?", Leslie Hook, Financial Times, October 29, 2020.

absent such uncertainty. This effect is stronger – not weaker – when agents have a preference for later resolution of uncertainty (formally, an elasticity of intertemporal substitution, or EIS, which is lower than the inverse coefficient of relative risk aversion) as this induces a more significant contraction of labor during pandemics. Through the learning channel, there can also therefore be "scarring" effects wherein agent's consumption upon exit from a pandemic does not revert to the pre-pandemic levels due to the increase in updated probability of future pandemics. An important policy implication that can be drawn is that understanding the fundamental biological and social determinants of future pandemics, for instance, whether pandemics are related to zoonotic diseases triggered more frequently by climate change, may be as important to mitigating their economic impact as resolving the immediate pandemic-induced crisis.

A few caveats are in order. Our model of pandemics is close to that of rare disasters in asset-pricing literature (Barro, 2006; Gabaix, 2012; Tsai and Wachter, 2015) but with endogenous exposure of the agent to disasters as well as featuring endogenous consumption, labor and asset prices. However, we do not feature SIR-style dynamics of an individual pandemic itself. Finally, our model also does not feature the impact of economic-stabilization policies such as fiscal or monetary support.

The rest of the paper is organized as follows. Section 2 relates to the existing literature. Section 3 describes the construction of vaccine progress indicator and estimates of its covariance with stock market returns. Section 4 presents our general equilibrium regime-switching model of pandemics with endogenous labor and consumption decisions, and asset prices in this framework that in turn help estimate the value of a cure for the pandemic. Section 5 extends (two-state version of) the model to allow for parameter uncertainty and learning to study the impact on the value of a cure from such uncertainty and the value attached to resolving it. Section 6 concludes with some further directions for research. All proofs not in the main text are contained in the Appendix.

2 Related Literature

While the literature studying the economic impact of the pandemic has exploded in a short period of time, there is relatively little focus on the role played by vaccine development and its progress. We first relate to the theoretical literature in asset pricing that is closest to our model; we then

Covid Economics 61, 11 December 2020: 1-72

relate to the empirical literature on observed contraction in employment and consumption during the COVID-19 pandemic.

Hong et al. (2020b) study the effect of pandemics on firm valuation by embedding an asset pricing framework with disease dynamics and a stochastic transmission rate, equipping firms with pandemic mitigation technologies. Similar to our paper, they model vaccine arrival as a Poisson jump process between pandemic and non-pandemic states. Hong et al. (2020a) combine the model of Hong et al. (2020b) with pre- and post-COVID-19 analyst forecasts to infer market expectations regarding the arrival rate of an effective vaccine and to estimate the direct effect of infections on growth rates of earnings. In particular, they develop a regime-switching model of sector-level earnings with shifts in their first and second moments across regimes.

In both these papers, the pricing kernel is exogenously specified for the pandemic and the non-pandemic states. In contrast, our model is general equilibrium in nature with the representative agent choosing labor and consumption (and, in turn, investment in capital) endogenously to mitigate health risk. Deriving asset prices from first principles in a regime-switching framework of pandemics – which allows for several sub-states in a pandemic relating to vaccine progress – is an important theoretical contribution of our paper. We build upon this setup further to introduce learning when there is parameter uncertainty about pandemic parameters.[8]

For empirical work, Hong et al. (2020b) fix expected pandemic duration around one year but show in comparative statics that asset prices show considerable sensitivity to the arrival rate of the vaccine. Hong et al. (2020a) use their model to infer the arrival rate of the vaccine. In contrast, we provide a "vaccine progress indicator" in the form of an estimated time to vaccine deployment using actual data and related news on the clinical trials of vaccines for COVID-19 presently under progress; we relate this vaccine progress indicator to stock market returns to infer labor contraction in the pandemic relative to the non-pandemic state, which we then combine with our asset-pricing framework to provide an estimate of the value that the representative agent would attach to the vaccine.

Elenev et al. (2020) incorporate a "pandemic state" with low but disperse firm productivity that recurs with low probability for studying government intervention in corporate credit mar-

[8]On a technical front, Hong et al. (2020b,a) consider aggregate transmission risk into SIR-style model, whereas our model of health risk arising from a pandemic is closer to the literature on rare disasters cited in the Introduction.

Covid Economics 61, 11 December 2020: 1-72

kets. While we do not model credit markets in our setup, our differentiating novel features are: construction of a vaccine progress indicator and estimation of its joint relationship with stock markets, and mapping it into a general equilibrium regime-switching model of pandemics with asset prices in order to derive an estimate of the value of a cure.

Kozlowski et al. (2020) model learning effects that lead to long-term scarring after the pandemic is over as policy responses relating to debt forgiveness in the current pandemic can lead to lower leverage and consumption in the post-pandemic era.

Collin-Dufresne et al. (2016) show that learning can amplify the pricing of macroeconomic shocks when the representative agent has Epstein-Zin preferences and Bayesian updating. Our results on learning and the impact of parameter uncertainty on the value of a cure are related to the findings of both these papers; our model can generate both long-term scarring in consumption due to updated probability of pandemics and significant contraction of labor and consumption when parameter uncertainty is high, when the Elasticity of Intertemporal Substitution is low. Interestingly, expected time to deployment of a vaccine can be considered as a "macroeconomic shock" in our model that affects asset prices and depends crucially on parameter uncertainty in a manner that interacts with deep preference parameters.

We now turn to the related empirical evidence on labor and consumption. Muellbauer (2020) models a larger drop in consumption than income with a credit-augmented consumption function. Using customized survey data, Coibion et al. (2020a,b) find the pandemic led to a 20 million decline in the number of employed workers by the first week of April, and attributed 60 percent of the decline in the employment-to-population ratio by May to lockdowns. Dingel and Neiman (2020), Mongey et al. (2020) and Beland et al. (2020) classify occupations by their work from home feasibility, documenting more adverse labor market outcomes for occupations with high proximity among coworkers.[9] For those looking for employment, Forsythe et al. (2020) find job vacancies had fallen 40% by April 2020 compared to pre-COVID-19 levels, with the largest declines in leisure, hospitality and non-essential retail. Consequently, Bernstein et al. (2020) find a flight-to-safety effect, with job seekers shifting searches from early-stage ventures to larger firms, while also considering lower salaries, and alternative roles and locations.

[9] Apollo Global Management's Torsten Slok estimates 27 million jobs are in close physical proximity occupations, led by health care, leisure and hospitality, and teachers.

Covid Economics 61, 11 December 2020: 1-72

Covid Economics 61, 11 December 2020: 1-72

Baker et al. (2020a) deploy transaction-level data to study consumption responses to the pandemic, finding an increase in the beginning in an attempt to stockpile home goods, followed by a sharp decrease as the virus spread and stay at home orders were enforced. Using customized survey data, Coibion et al. (2020a) find lockdowns decreased consumer spending by 30 percent, with the largest drops in travel and clothing. Bachas et al. (2020) find a rebound in spending, especially for low-income households, since mid-April. Chetty et al. (2020) further find high-income households significantly reduced spending, especially on services that require in-person interactions, leading to business losses and layoffs in the most affluent neighborhoods. Outside the US, Sheridan et al. (2020) and Andersen et al. (2020) find aggregate spending decreased 27% in the first seven weeks following Denmark's shutdown, with the majority of the decline caused by the virus itself regardless of social distancing laws. Chen et al. (2020) use daily transaction data in China and find severe declines in spending, especially in dining, entertainment and travel sectors.

While this literature estimates the costs of the pandemic for the economy by directly looking at consumption and labor data, our approach is to estimate the value of a cure that takes the economy out of the pandemic. We construct a novel vaccine progress indicator, examine the stock market's sensitivity to this indicator, and then use a structural asset pricing framework to then back out the value of a cure.

A number of papers have modeled climate risk using the approach that long-run risk of climate risk can manifest itself through Poisson shocks to the capital stock, which is the approach we are pursuing here. A detailed survey of this literature is provided by Tsai and Wachter (2015) in the context of better understanding asset pricing puzzles. A number of papers, including Pindyck and Wang (2013), explore the welfare costs associated with climate risk. This paper addresses the issue of how much should society be willing to pay to reduce the probability or impact of a catastrophe.

3 Vaccine Progress Indicator and its Covariance with Stock Returns

As described in the introduction, the paper's hypothesis is that the stock market may convey important information about the social value of resolving the pandemic. This section explains how we attempt to extract that information. There are two distinct steps. First, we construct a method for summarizing the state of vaccine research throughout 2020. Second, we estimate the

stock market response to its changes.

3.1 Measuring Vaccine Progress

Readers are, by now, broadly familiar with the contours of the global effort to develop a vaccine for COVID-19. Through many of the excellent tracker apps, dashboards, and periodic survey articles we were all educated about the dozens of candidates under study, and their progress through pre-clinical work and clinical trials. On any given day, the state of the entire enterprise is a high-dimensional object consisting of multiple pieces of information about all of the projects. Our goal is to reduce that high dimensional object to a single number. Also, crucially, the number should have a tangible physical (or biological or economic) interpretation.

The single most salient aspect of vaccine development, the number that nearly all discussions boiled down to, was the anticipated time until widespread availability of a proven candidate. We therefore construct estimators of that quantity, using information that was available to observers at the time.

To do this, we introduce a stochastic model of candidate progress. We obtain the pre-clinical dates and trial history of vaccine candidates from the London School of Hygiene & Tropical Medicine (LSHTM). The model necessarily involves many parameters for which we have little hope of obtaining precise estimates. Details of our choices of all parameters are explained in Appendix B. We will validate our choices both by examining robustness to reasonable variation and by comparing them to other actual *ex ante* forecasts published during the sample period.[10]

Our stochastic model is a means to simulate, on each day t, the ultimate outcome of each of the candidates given their state of development as of that day. That simulated outcome, for candidate $n \in \{1, \ldots, N\}$, is either success, defined as widespread deployment by some date $T_n > t$, or failure, which can be described as $T_n = \infty$. Using the model, we can then run a large number, M, of joint simulations as of day t encompassing all of the candidates. In each simulation, m, the earliest time to widespread availability is $T_m^\star = \min_n \{T_n\}$. The cross-simulation average value of $T_m^\star < \infty$ is the model's expectation T_t^s for the time to success, conditional on at least one of the active candidates succeeding. Some fraction, μ, of simulations will result in all candidates failing. Our forecast is the full expectation, $\mathbb{E}_t T^\star$ defined as $(1-\mu)T_t^s + \mu T^f$, where T^f is an estimate of the expected time

[10]The appendix also presents evidence that our distributional assumptions are reasonably consistent with the (small) set of observed trial outcomes.

Covid Economics 61, 11 December 2020: 1-72

to first success by a project other than those that are currently active.[11] In addition to the mean, the model also delivers the full distribution, and hence all quantiles, of $T^\star$ as of each date.

The model starts with a standard partition of the clinical trial sequences between pre-clinical, Phases I, II, III, application submission, and approval stages. A candidate in each stage either succeeds and moves to the next stage or fails.[12] We append a final stage: deployment, which an approved vaccine possibly still could not attain, e.g., due to technical infeasibility or emergence of serious safety concerns. Our assumption is that each stage is characterized by an unconditional probability of success, π_s, and an expected duration, τ_s.[13] We model each stage transition as a 2-state Markov chain with exponentially distributed times. Specifically, if we define two exponentially distributed random variables t^u and t^d with intensities

$$\lambda_s^u = \frac{\pi_s}{\tau_s} \quad \text{and} \quad \lambda_s^d = \frac{1-\pi_s}{\tau_s} \tag{1}$$

then it is straightforward to show that $t_s = \min\{t^u, t^d\}$ is exponentially distributed with intensity $1/\tau_s$ and that the probability of success, defined as $t^u < t^d$, is π_s.

Since our objective is to model the joint outcomes of all the vaccine projects, we need to specify the joint distribution of successes and failures. We do this by assuming the exponential times $\{t_n^u\}_{n=1}^N$ are generated by a Gaussian copula with correlation matrix $\mathcal{R}$, and likewise for the times $\{t_n^d\}$. The elements of the correlation matrix are set to positive values to capture the dependence between candidates. This positive dependence arises most obviously because all the vaccines are targeting the same pathogen, and will succeed or fail largely due to its inherent biological strengths and weaknesses. Beyond that, we also capture the dependence of candidates on one of a handful of strategies (or platforms) for stimulating immunological response. If, for example, an RNA-based platform proves to be safe and effective, then all candidates in this family would have a higher likelihood of success.[14] Finally, some research teams (institutes or companies) have sev-

[11] The model does not attempt to forecast the entry of new projects.

[12] This is a simplification. Candidate vaccines will actually undergo multiple overlapping trial sequences with different patient populations, delivery modalities, or medical objectives (endpoints). One sequence could fail while others succeed. Trials can also combine phases I and II or II and III. In our empirical implementation we focus on the most advanced trial of a candidate. This follows Wong et al. (2018).

[13] Our success probabilities are taken from pharmaceutical research firm BioMedTracker and are based upon historical outcomes of infectious disease drug trials. Our duration estimates are based on projections from the pharmaceutical and financial press during 2020. See Appendix A for several examples.

[14] In October, two candidate vaccines had their trials paused due to adverse reactions: both were based on adenovirus platforms.

Covid Economics 61, 11 December 2020: 1-72

eral candidate vaccines. Positive correlation between their outcomes may arise through reliance on common technological components, resources, or abilities.

As described so far, the "state" of a candidate is simply its current clinical-trial phase. This is not realistic in the sense that initiation of a new phase, as captured by the commencement of a new stage trial, is often known in advance. The trial start date (as reported to the U.S. government) may not actually be the date of the arrival of news about the candidate. Likewise, within a stage (as a trial is progressing), the "state" is not static. Information about the trial (preliminary results), or more complete information about earlier trials, may be published or released to the press or leaked. Trial schedule information (delays or acceleration) may be announced. Regulatory actions by non-U.S. authorities may also convey information. For all of these reasons, we modify our framework by adjusting the probability of each candidate's current-stage success on the date of arrival of news specific to it.[15] Because positive news is more likely to be revealed than negative news, we also deterministically depreciate each candidate's success probability in the absence of news. We will verify below that our conclusions about the stock market response to vaccine progress are not driven by our assumptions regarding the arrival of interim trial news.[16]

Our indicator of vaccine progress aims to capture expectations about deployment principally in the U.S. since this is likely to be the primary concern of U.S. markets. Because of political considerations, we believe that observers at the time judged it to be very improbable that vaccines being developed in China and Russia would be the first to achieve widespread deployment in the U.S. Our base case construction for this reason omits candidates coded in the LSHTM data as originating in these countries.[17] This assumption is consistent with the progress of these candidates receiving minimal coverage in the U.S. financial press. We will also verify that including them in our index does not change our primary results.

It is worth acknowledging that, in focusing on the scientific advancement of the individual candidates, our measure does not currently attempt to capture general news about the vaccine development environment and policy. For example, news about the acquisition and deployment of

[15] Our source of news is FactSet StreetAccount. We classify vaccine related stories into seven positive types and six negative types. The types and probability adjustments are given in the appendix.

[16] Technically, altering the marginal success probabilities within a trial induces a non-exponential unconditional marginal distribution of trial duration. We retain the exponential assumption of the Gaussian copula for tractability. Our results are robust to using constant probabilities.

[17] We retain candidates coded as multi-country projects including Russia or China.

Covid Economics 61, 11 December 2020: 1-72

delivery infrastructure by governments (or the failure to do so) could certainly affect estimates of the time to availability. We also do not capture the news content of government financial support programs, or pre-purchase agreements. The Fall of 2020 saw open debate about the standards that would be applied for regulatory approval, the outcome of which could have affected forecasts as well. While we could alter our index based on some subjective assessment of the impact of news of this type, we feel we have less basis for making such adjustments than we do for modeling clinical trial progress.

Figure 1: Expected Time to Vaccine Deployment

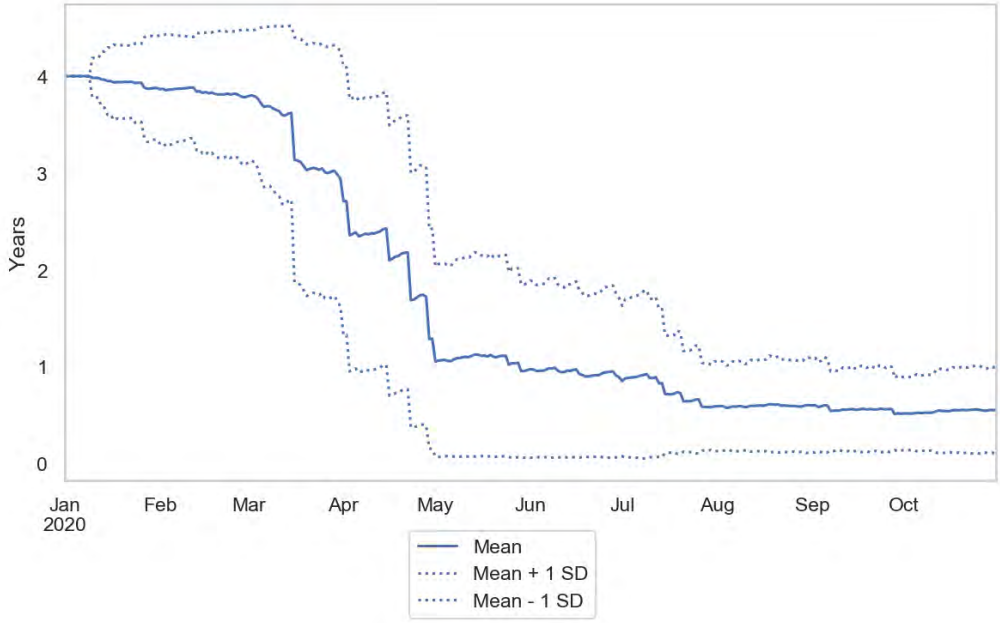

Note: Figure shows our estimate of the expected time to widespread deployment of a COVID-19 vaccine in years. Dashed lines show one standard deviation bands.

Figure 1 shows the model's estimation of the expected time to widespread deployment from January through October of 2020, and Figure 2 shows the number of active vaccine projects. The starting value of the index, in January, is determined by our choice of the parameter T^f because, with very few candidates and none in clinical trials, there was a high probability that the first success would come from a candidate not yet active. However this parameter effectively becomes irrelevant by March when there are dozens of projects. The index is almost monotonically declin-

Covid Economics 61, 11 December 2020: 1-72

ing, since there were no reported trial failures and very few instances of negative news through at least August. The crucial aspects of the index for our purposes are the timing and sizes of the down jumps corresponding to the arrival of good news.

Figure 2: Number of Active COVID-19 Vaccine Projects

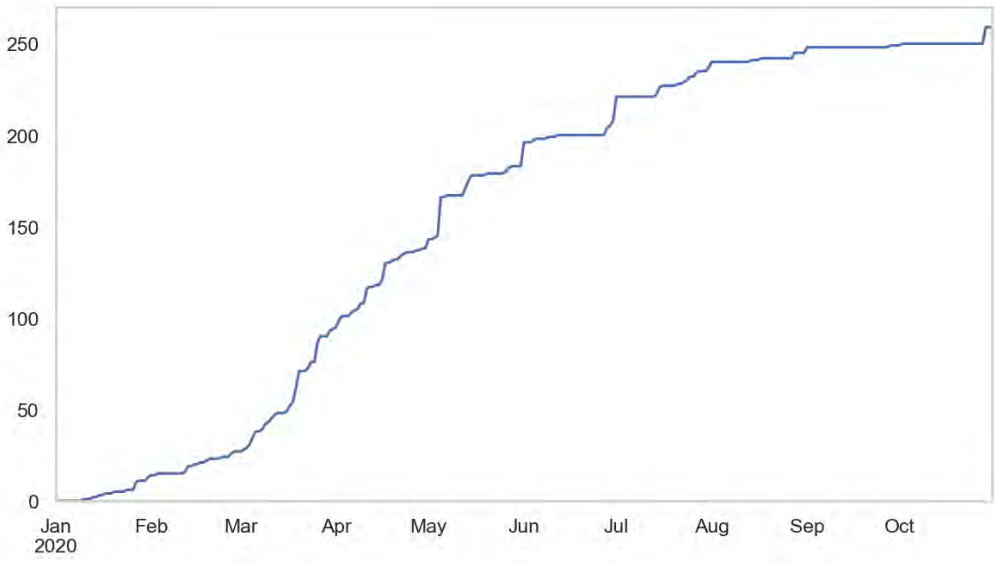

Note: Figure shows the number of active COVID-19 vaccine candidates. Data as of November 2020.

3.1.1 Validation

We are aware of two datasets that contain actual forecasts of vaccine arrival times, as made in real-time. As a validation check, we compare our index to these.

The two data sets are surveys, to which individuals supplied their forecasts of the earliest date of vaccine availability. Comparisons between these pooled forecasts and our index require some intermediate steps and assumptions. In both cases, the outcomes being forecast are given as pre-specified date ranges. Thus, on each survey date, we know the percentage of respondents whose point forecast fell in each bin. For each survey we estimate the median response, assuming a uniform distribution of responses within the bin containing the median.[18] Under the same

[18]While it is tempting to equate the surveys' distribution of forecasts with a forecasted distribution, these are conceptually distinct objects that need not coincide. In addition, in each survey, the farthest out forecast bin is unbounded, meaning that "never" (or "more than 3 years from now") is a possible response. So, for both reasons, it is problematic to compute a weighted average forecast across the response bins. The modal response bin is also not a good summary statistic for the same reason, and also because it depends on the bin widths.

Covid Economics 61, 11 December 2020: 1-72

assumption, we can also tabulate the percentage of forecasters above and below our index.

The first survey is conducted by Deutsche Bank and sent to 800 "global market participants" asking them when they think the first "working" vaccine will be "available". The survey was conducted four times between May and September. The second survey is conducted by Good Judgement Inc., a consulting firm that solicits the opinion of "elite superforecasters." Their question asks specifically "when will enough doses of FDA-approved COVID-19 vaccine(s) to inoculate 25 million people be distributed in the United States?" (Information about the number of responders is not available.) Responses are tabulated daily, starting from April 24th. For brevity, we examine month-end dates. Table 1 summarizes the comparison.

Table 1: Forecast Comparison

	Deutsche Bank		
Date	Survey median	VPI	% respondents below
May	1.158	0.958	35.0
June	1.162	0.893	31.2
July	0.920	0.595	20.8
Sep	0.625	0.561	44.3
	Superforecasters		
Date	Survey median	VPI	% respondents below
April	1.902	1.291	16.1
May	1.603	0.958	14.6
June	1.189	0.893	31.0
July	0.808	0.595	32.7
August	0.519	0.606	58.4
September	0.445	0.518	57.2

Note: Table compares forecasts for the earliest date of vaccine availability in years. The top panel compares the median from a survey conducted by Deutsche Bank, while the bottom panel compares the median from a survey conducted by Good Judgement Inc. The column VPI denotes the forecast from our estimated vaccine progress indicator, and the last column reports the percent of respondents from each survey with forecasts below ours. Survey respondents are reported in calendar intervals. The comparison assumes a uniform distribution of forecasts in time within the median bin. The survey dates are as of the end of the month in the first column, except the Deutsche Bank September survey which is for the week ending September 11, 2020.

Our forecasts align well with those of the Deutsche Bank survey, though ours are more optimistic than the median. The optimism is more pronounced when compared to the superforecasters early in the pandemic. Although we are within the interquartile range of forecasts after May, the

Covid Economics 61, 11 December 2020: 1-72

earlier dates see us in the left-tail of the distribution. A possible reason is the specificity of the particular survey question, which specifies an exact quantity of the vaccine being distributed in the United States. Respondents may have more skeptical of feasible deployment than we have assumed. We will examine robustness of our results below to increasing the probability of an approved vaccine failing in the deployment stage.

3.2 Stock Market Response

Figure 3 plots vaccine progress (inverted) along with the market portfolio's year-to-date performance. In principle, assessing the stock market response to changes in vaccine progress should be straightforward. However, the circumstance of 2020 complicate the task. In a nutshell, there was a lot else going on. The amount of information for markets to digest was enormous and multifaceted. Even the information flow just about coronavirus research *other than vaccine trials* was voluminous. Thus, how to control for non-vaccine related news becomes an important consideration.

Figure 3: Vaccine Progress and Market Performance

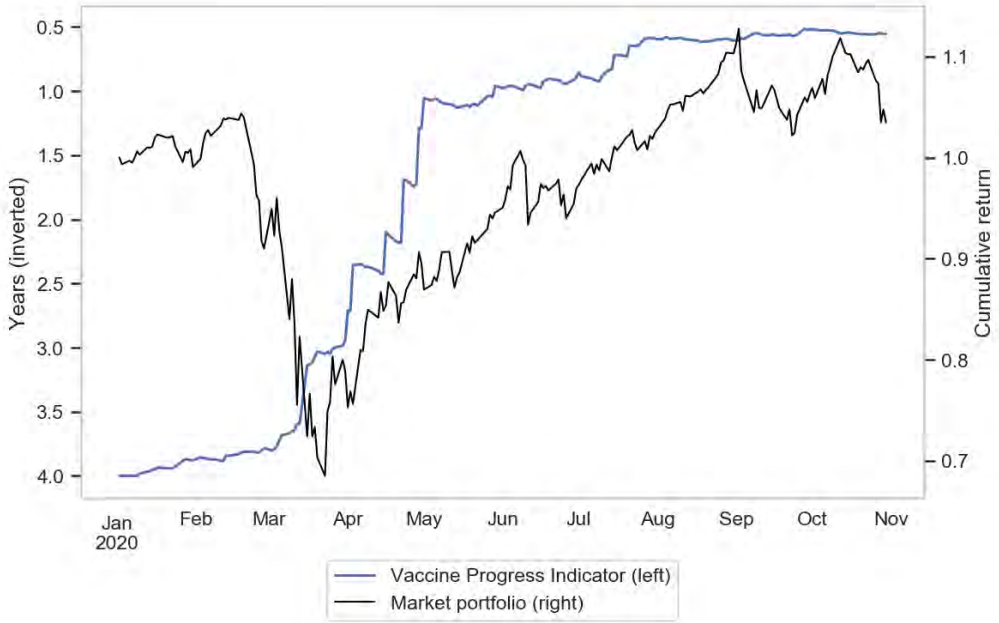

Note: Figure plots vaccine progress (inverted and left axis) along with the cumulated year-to-date excess return on the value-weight CRSP index (right axis). The risk-free rate is the one-month Treasury bill rate.

Covid Economics 61, 11 December 2020: 1-72

Covid Economics 61, 11 December 2020: 1-72

Our approach is to run daily regressions of stock market returns on vaccine progress and exclude days that contained large stock market moves that have been reliably judged to have been due to other sources of news. Specifically, we employ the classification of Baker et al. (2020b) for causes of market moves greater than 2.5% in absolute value. Those authors enlist the opinion of three analysts for each such day and ask them to assign weights to *types* of causes (e.g., corporate news, election results, monetary policy, etc). Under their classification, research on vaccines falls under their "other" category, whereas news about the pandemic itself was usually categorized as "macroeconomic". We view market returns on such days as very unlikely to have been driven by vaccine news if none of the three analysts assigns more than 25% weight to the other category, or if the return was more negative than -2.5%. The latter exclusion is based on the fact that there were no significant vaccine setbacks prior to the end of our data window,[19] and on the prior knowledge that positive vaccine progress cannot be negative news. We include dummies for all of the non-vaccine large-news days. There are 28 such days, 17 of which were in March.

Our approach is imperfect. We have no other controls outside these large move days when there were certainly other factors influencing markets. Including dummy variables effectively reduces our sample size. However, at a minimum we are limiting the ability of our estimation to misattribute the largest market moves to vaccine progress.

Table 2 shows the resulting regression estimates of market impact. These regression specifications include changes in the vaccine progress indicator in a five day window around each day, t, on which stock returns are measured. Including changes on days other than the event day-t guards against our imperfect attribution of the date of news arrival. *A priori* we suspect it is more likely that, if anything, markets have information before it is reflected in our index, meaning the relevant reaction would correspond to the $t+1$ or $t+2$ coefficients. On the other hand, given the sheer volume of news being processed during this period, we do not rule out delayed incorporation of information, which would show up in the $t-1$ or $t-2$ coefficients. The specifications also include two lags of the dependent variable to control for short-term liquidity effects. Specifically,

[19] As of the time of this draft, Baker et al. (2020b)'s website had classified days through June. We append September 3 and September 23 as two dates with negative jumps but arguably were driven by non-vaccine progress related news.

the regression is

$$R^e_{m,t} = \alpha + \sum_{h=-2}^{2} \beta_h \Delta \text{VPI}_{t+h} + \gamma_1 R^e_{m,t-1} + \gamma_2 R^e_{m,t-2} + \sum_{j=1}^{28} \delta_j \mathbb{1}_{\text{jump } j} + \epsilon_t \quad (2)$$

where ΔVPI_t is the change in vaccine progress indicator, and $\mathbb{1}_{\text{jump } j}$ is a dummy equal to one on the jth jump date from Baker et al. (2020b). The dependent variable is the return to the value-weighted CRSP index from January 1 through September 30, 2020. Due to data availability, from October 1 through October 31, 2020 we use the return on the S&P 500 index.

The first column of the table shows results using our baseline vaccine progress indicator. The coefficient pattern shows the largest negative responses on the $t-1$ and $t+2$ index changes. Focusing on the cumulative impact, the sum of the βs is statistically significant at the 1% level. The precisely estimated point estimate implies a stock market increase of 8.6 percent on a decrease in expected time to deployment of one year. This number seems plausible: subsequent to our sample, on November 9th the U.S. stock market opened almost 4% higher in response to positive news from Pfizer on Phase III trial results. This would imply more sensitivity than the OLS estimate if, as seems likely, the news revised estimates of time to deployment by less than six months.[20]

Returning to Table 2, the second and third columns implement the methodology of Kogan et al. (2017) (hereafter KPSS). Those authors use an empirical Bayes procedure to estimate the market value of patents using the stock returns to the patenting firm in an event window surrounding patent publication date. As in our case, economic logic rules out a negative response: vaccine progress cannot be unfavorable news just as the value of a patent must be positive. KPSS employ a truncated normal prior distribution for the unobserved true response. Conditional on knowing the return standard deviation, the posterior mean estimate of the response coefficient is then also distributed as a truncated normal. The estimation methodology generalizes naturally to a multivariate regression setting.[21] (O'hagan (1973).) The table reports posterior mean and stan-

[20] While it is not the focus of the paper, it is also interesting to ask about the total contribution of vaccine progress to the stock market performance during the sample period, and to the post-March rally in particular. From March 23 to October 30 our forecast dropped by 2.5 years, of which 0.6 years was expected. The OLS point estimate then implies that vaccine news in total would have induced a 16.3% positive return. The return on the S&P 500 during this period was 47.7%. Hence, vaccine progress could have been responsible for 34% (16.3/47.7-1) of the rally.

[21] We follow KPSS in assuming a zero mean under the prior for the pre-truncated normal distribution, assuming returns are normally distributed, and in using the regression residual to estimate the return standard deviation. Note that the estimation still includes dummy variable for market jump days making the normality assumption plausible.

dard deviations for the individual response coefficients and for their sum.[22] The methodology is sensitive to the specification of the prior variance of the coefficient distribution. Both column 2 and column 3 assume that the pre-truncated normal distribution for β_t has standard deviation equal to 1, which, after truncation, implies that 84% of the distribution mass is below 1.0. We regard this as a conservative (or skeptical) choice.[23] Results in the second column use the same (independent) prior for all the response coefficients. The third column uses a smaller prior mean for the lead and lag coefficients.[24] Both priors produce posterior means for the sum of the five response coefficients that are lower than the OLS estimate: -6.3% in column 2 and -4.0% in column 3. Note that the estimation is sharp in both cases in the sense that each posterior mean is several standard deviations from zero. The calibrations in the next section will adopt the range of these conservative estimates.

To examine the robustness of the response estimates to the assumptions built into the vaccine progress index, we repeat the OLS specification estimation with five variants. These results are shown in Table 3. The first column repeats the original specification from the prior table. The next two columns vary the assumptions about the effect of news to phase success probabilities. (Column 2 includes no news adjustments. Column 3 applies the news adjustments to only the current trial phase, as opposed to all future phases.) The fourth column increases the base copula correlation from 0.2 to 0.4. The fifth column lowers the assumed probability of successful deployment following approval. Finally the sixth column includes vaccine candidates whose research program is based in Russia or China. In all of these cases the sum of the response coefficients is highly statistically significant and the point estimates are in the same range as those in Table 2.

3.3 Industry Responses

As a validity check for our primary findings, we examine the price impact of vaccine progress in the cross-section of industries. We first gauge each industry's exposure to COVID-19 by its cumulative return from February 1, 2020 to March 22, 2020. This period captures the rapid onset

[22] Moments of the truncated multivariate normal posterior are computed using the algorithm of Kan and Robotti (2017) using software provided by Raymond Kan. http://www-2.rotman.utoronto.ca/~kan/research.htm.

[23] Note that making the prior more diffuse does not, in this case, correspond to making it less informative: the prior mean increases with the standard deviation.

[24] Specifically, the assumption is that pre-truncated standard deviations are 0.7 for the first lead and lag and 0.5 for the second lead and lag.

Covid Economics 61, 11 December 2020: 1-72

Table 2: Stock Market Sensitivity to Vaccine Progress News

	(1) OLS	(2) KPSS (Prior 1)	(3) KPSS (Prior 2)
γ_1	-0.068	-0.088	-0.096
	(0.066)	(0.035)	(0.035)
γ_2	0.126	0.158	0.164
	(0.091)	(0.035)	(0.035)
β_{t-2}	1.226	-0.550	-0.384
	(1.580)	(0.433)	(0.292)
β_{t-1}	-4.365	-2.012	-1.327
	(3.278)	(0.763)	(0.599)
β_t	-0.725	-0.837	-0.881
	(0.895)	(0.561)	(0.577)
β_{t+1}	0.533	-0.561	-0.465
	(1.967)	(0.438)	(0.361)
β_{t+2}	-5.312	-2.344	-0.961
	(1.800)	(0.773)	(0.456)
α	0.199	0.237	0.276
	(0.098)	(0.080)	(0.078)
$\sum_{h=-2}^{2} \beta_{t+h}$	-8.643	-6.305	-4.017
	(0.653)	(1.354)	(1.050)
N	206	206	206

Note: Table shows the results from regression (2). The dependent variable is daily excess returns on the market portfolio in percent. Independent variables include two lags of excess returns on the market portfolio, a five-day window of changes in vaccine progress indicator in years, and dummy variables for each jump date from Baker et al. (2020b) unrelated to news about vaccine progress. The return on the value-weighted CRSP index is used from January 1, 2020 to September 30, 2020, followed by the return on the S&P 500 index until October 31, 2020. All columns are employ the baseline specification with news applying to all states, deterministic depreciation, base copula correlation of 0.2, probability of success in the application state equal to 0.95 and excludes candidates from China and Russia. Column 1 estimates the regression using OLS. Columns 2 and 3 employ the methodology of Kogan et al. (2017) and assume the pre-truncated normal distribution for β_t has standard deviation equal to 1. Column 2 further uses the same prior for all response coefficients, while column 3 uses a pre-truncated standard deviation of 0.7 for the first lead and lag and 0.5 for the second lead and lag. OLS results display Newey-West standard errors with four lags in parentheses and standard deviation of the F-statistic on $\sum_{h=-2}^{2} \beta_{t+h}$. KPSS results show posterior standard deviations in parentheses.

of COVID-19 in the US, with a public health emergency being declared on January 31, 2020[25] and a national emergency declared on March 13, 2020.[26] Importantly, this period precedes the

[25] https://www.hhs.gov/about/news/2020/01/31/secretary-azar-declares-public-health-emergency-us-2019-novel-coronavirus.html

[26] https://www.whitehouse.gov/presidential-actions/proclamation-declaring-national-emergency-concerning-novel-coronavirus-disease-covid-19-outbreak/

Table 3: Stock Market Sensitivity to Vaccine Progress News – Robustness

	(1)	(2)	(3)	(4)	(5)	(6)
News	All states	None	Current state	All states	All states	All states
Depreciation	Y	N	Y	Y	Y	Y
Cor(n, n')	0.2	0.2	0.2	0.4	0.2	0.2
$\pi^{\text{base}}_{\text{approval}}$	0.95	0.95	0.95	0.95	0.85	0.95
Ex-China and Russia	Y	Y	Y	Y	Y	N
γ_1	-0.068	-0.063	-0.065	-0.074	-0.072	-0.083
	(-1.04)	(-0.95)	(-1.00)	(-1.10)	(-1.09)	(-1.54)
γ_2	0.126	0.113	0.121	0.133	0.130	0.111
	(1.39)	(1.31)	(1.40)	(1.43)	(1.43)	(1.38)
β_{t-2}	1.226	2.512	1.596	0.964	0.883	1.708
	(0.78)	(1.16)	(1.00)	(0.52)	(0.56)	(1.00)
β_{t-1}	-4.365	-5.260	-3.359	-3.683	-4.100	-5.396*
	(-1.33)	(-1.37)	(-1.34)	(-1.15)	(-1.31)	(-1.78)
β_t	-0.725	-0.374	-0.259	-0.893	-0.860	1.108
	(-0.81)	(-0.41)	(-0.27)	(-0.99)	(-0.96)	(0.76)
β_{t+1}	0.533	1.878	0.677	0.827	0.452	-0.454
	(0.27)	(0.69)	(0.37)	(0.48)	(0.23)	(-0.28)
β_{t+2}	-5.312***	-7.730***	-4.911***	-4.430**	-4.866**	-4.201
	(-2.95)	(-4.93)	(-3.54)	(-2.36)	(-2.56)	(-1.61)
α	0.199**	0.191*	0.231**	0.216**	0.200**	0.206**
	(2.04)	(1.89)	(2.33)	(2.21)	(2.05)	(2.08)
Jump dummies	Y	Y	Y	Y	Y	Y
$\sum_{h=-2}^{2} \beta_{t+h}$	-8.643	-8.973	-6.256	-7.215	-8.491	-7.234
F-stat	8.13	5.83	5.32	5.48	8.30	3.72
P-value	0.00	0.02	0.02	0.02	0.00	0.06
N	206	206	206	206	206	206

Note: Table shows the results from regression (2). The dependent variable is daily excess returns on the market portfolio in percent. Independent variables include two lags of excess returns on the market portfolio, a five-day window of changes in vaccine progress indicator in years, and dummy variables for each jump date from Baker et al. (2020b) unrelated to news about vaccine progress. The first column is the baseline specification with news applying to all states, deterministic depreciation, base copula correlation of 0.2, probability of success in the application state equal to 0.95 and excludes candidates from China and Russia. Column 2 removes news and depreciation; column 3 restricts news to the current state; column 4 doubles the base copula correlation to 0.4; column 5 decreases the probability of success to 0.85 in the application state; and column 6 includes candidates from China and Russia. The return on the value-weighted CRSP index is used from January 1, 2020 to September 30, 2020, followed by the return on the S&P 500 index until October 31, 2020. The table uses Newey-West standard errors with 4 lags; t-statistics are shown in parentheses. Significance levels: * $p < 0.10$, ** $p < 0.05$, *** $p < 0.01$

Federal Reserve's announcement of the Primary Market Corporate Credit Facility and Secondary

Market Corporate Credit Facility on March 23, 2020[27] and significant advances in vaccine progress, helping us pin down industry covariances with COVID-19 itself, separate from covariances with monetary policy responses and vaccine progress.

We then estimate industry sensitivity to vaccine progress over the non-overlapping sample from March 23, 2020 to September 30, 2020.[28] Specifically, we re-estimate (2) sector-by-sector,

$$R^e_{i,t} = \alpha + \sum_{h=-2}^{2} \beta_{h,i} \Delta \text{VPI}_{t+h} + \gamma_{1,i} R^e_{i,t-1} + \gamma_2 R^e_{i,t-2} + \sum_{j=1}^{28} \delta_{j,i} \mathbb{1}_{\text{jump } j} + \epsilon_{i,t} \tag{3}$$

where $R^e_{i,t}$ denotes value-weighted excess returns on the 49 Fama-French industry portfolios.

Figure 4 presents the results. Each industry's sensitivity to vaccine progress is plotted against its exposure to COVID-19. The relationship is negative and statistically significant – industries that were more exposed to COVID-19 subsequently saw more positive price impact as the vaccine was expected to deploy sooner. The industries also exhibit notable variation. Oil, fabricated products and recreation were among those with higher COVID-19 exposure and vaccine progress sensitivity, while pharmaceutical products, food products and computer software had lower exposure and sensitivity. The association of industry exposure to COVID-19 with its subsequent sensitivity to our index lends confidence to the construction and interpretation of the index as, in fact, measuring vaccine progress. Hence, the results here make it unlikely that our primary findings on the market's sensitivity are due to omitted variables.

[27] https://www.federalreserve.gov/monetarypolicy/pmccf.htm

[28] At the time of writing, industry return data available from Kenneth French's Dartmouth website ends September 30, 2020.

CEPR PRESS

Figure 4: Industry Sensitivity to Vaccine Progress

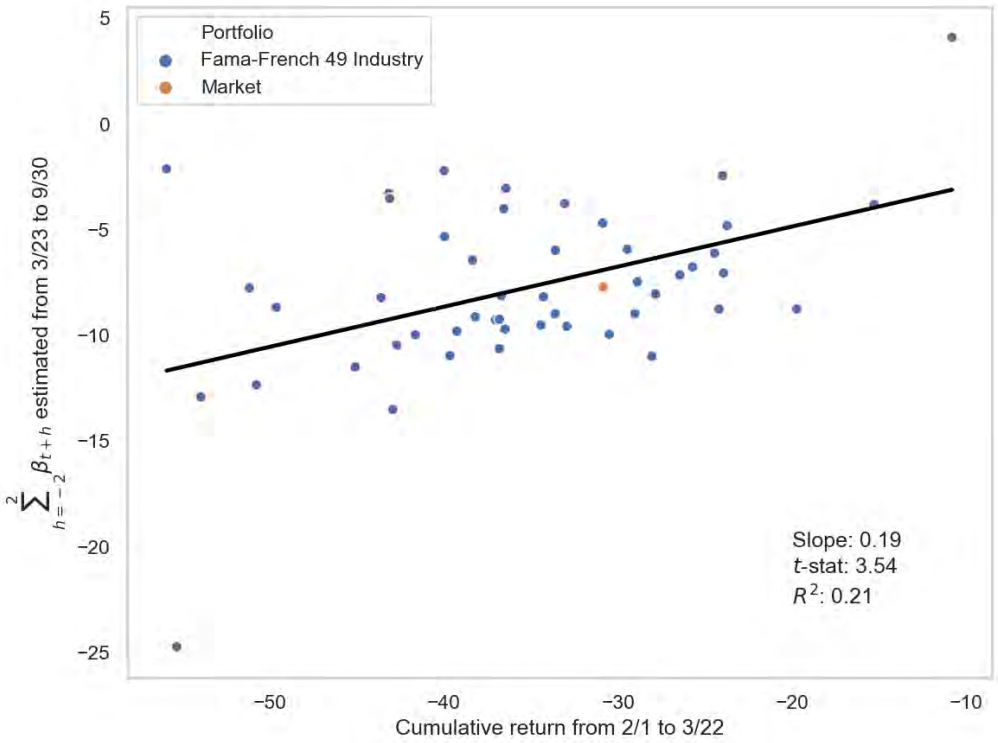

Note: Figure plots industry sensitivity to vaccine progress against exposure to COVID-19 as measured by cumulative returns. Cumulative returns are from February 1, 2020 to March 22, 2020. Sensitivity to vaccine progress is estimated from March 23, 2020 to September 30, 2020 as in (3).

4 Regime-Switching Model of Pandemics

In this section, we introduce a regime-switching model of pandemics in order to derive the value of a cure in terms of the economy's primitive objects, such as the ratio of labor supply or marginal propensity to consume between the pandemic and the non-pandemic states. In order to connect the theory to our empirical exercise, we need a model with four attributes: a description of pandemics; a well-defined notion of the value of ending a pandemic; a depiction of progress towards that objective; and a stock market that is sensitive to that progress.

Covid Economics 61, 11 December 2020: 1-72

4.1 S-State Model

We consider the state of the economy to be either in “non-pandemic" regime or in “pandemic" regime.[29] Within the pandemic regime, there can be several sub-states that correspond in our context to different stages in the development of vaccines. We denote the state as $s \in \{0,1,\ldots,S-1,S\}$, where for ease of notation both state 0 and state S are the same non-pandemic states, and the others are pandemic states. We assume that the economy switches between these states based on a Markov-switching or transition matrix. The transition probabilities are given as follows where η, the probability of switching from the non-pandemic regime to the pandemic regime, and λ_d and λ_u, the respective probabilities in a pandemic state to move “down" or “up" to the adjacent states, are assumed to be exogenous:

$$P(s_{t+dt}=1|s_t=0 \text{ or } S)=\eta dt \tag{4}$$

$$P(s_{t+dt}=s_t|s_t=0 \text{ or } S)=1-\eta dt \tag{5}$$

$$P(s_{t+dt}=s-1|s_t=s\in[1,S-1])=\lambda_d(s)dt \tag{6}$$

$$P(s_{t+dt}=s+1|s_t=s\in[1,S-1])=\lambda_u(s)dt \tag{7}$$

$$P(s_{t+dt}=s_t|s_t=s\in[1,S-1])=1-\lambda_d(s)dt-\lambda_u(s)dt \tag{8}$$

4.1.1 Agents, Labor and Capital Stock

We assume the economy has a unit mass of identical agents, each with the following production function that in the non-pandemic state depends on the labor input l and generates a stochastic output q gross of consumption as:

$$l^{\alpha}q\mu dt+\sigma l^{\alpha/2}qdB_t \tag{9}$$

where $\{B_t,t>0\}$ is a Brownian Motion process. We can view q as capital stock – physical and human – or wealth of the agent that is readily convertible into consumption (a form of “buffer stock" therefore), and $\alpha\in(0,1)$ is the elasticity of instantaneous expected output with respect to labor. The instantaneous expected return is $l^{\alpha}\mu dt$ and the instantaneous variance in output is

[29] In the Appendix, we work out in detail the solution to the 2-state regime-switching model in which the pandemic regime consists of just one state. Besides illustrating the detailed solution to the model (Hamilton-Jacobi-Bellman (HJB) equations, labor and consumption choices, and system to determine the value function), it also serves as the benchmark case for developing the model further with parameter uncertainty.

Covid Economics 61, 11 December 2020: 1-72

$l^{\alpha}\sigma^2 dt$. We will assume $l \in [0, \overline{\ell}]$, where $\overline{\ell}$ is an upper bound representing technological or human constraints on investment into the capital stock.

The production function of agent in the non-pandemic state, net of consumption flow, is therefore:

$$dq = l^{\alpha} q\mu dt - Cdt + \sigma l^{\alpha/2} q dB_t \tag{10}$$

where C is the endogenous consumption rate.

In the pandemic regime, the production function has all of the above features but it becomes exposed to the risk of an economic loss when hit by a "health" disaster:

$$dq = l^{\alpha} q\mu dt - Cdt + \sigma l^{\alpha/2} q dB_t - [l\varepsilon + k + KL] q dP(t). \tag{11}$$

Then let

$$\chi(l, L) \equiv [l\varepsilon + k + KL], \tag{12}$$

where ε is exposure to the pandemic via private labor, k is exposure to the pandemic unrelated to labor, L is aggregate labor supply, and K is exposure to the pandemic via aggregate labor. $P(t)$ is a Poisson process with a parameter ζ and a known jump amplitude $\Delta \in (0,1)$. When the Poisson process is triggered, a part of the agent's capital stock is destroyed and falls to $q(1 - \chi\Delta)$, e.g., due to health-induced disruptions to work, the need to work from home with attendant productivity impact and loss of human capital, filing for bankruptcy with deadweight loss in asset value, and firing of labor with difficulty to re-match at a future date, etc. We will assume parametric restrictions on ε, k and K to be small enough that $(1 - \chi\Delta) \in (0,1)$. The specification allows for both the labor supply choice (l) and the pre-existing conditions of the household unrelated to labor supply (k) to potentially amplify the health shocks. In addition, aggregate labor supply (L) can also amplify exposure to the pandemic as a form of externality. The agent takes the aggregate supply of labor L as given in her optimization problem.

4.1.2 Agent's Preferences

We assume that each agent has stochastic differential utility or Epstein-Zin preferences (Duffie and Epstein, 1992; Duffie and Skiadas, 1994) based on consumption flow rate C, given as

$$\mathbb{J}_t = \mathbb{E}_t \left[\int_t^{\infty} f(C_{t'}, \mathbb{J}_{t'}) dt' \right] \tag{13}$$

and aggregator

$$f(C, \mathbb{J}) = \frac{\rho}{1 - \psi^{-1}} \left[\frac{C^{1-\psi^{-1}} - [(1-\gamma)\mathbb{J}]^{\frac{1}{\theta}}}{[(1-\gamma)\mathbb{J}]^{\frac{1}{\theta}-1}} \right] \tag{14}$$

where $0 < \rho < 1$ is the discount factor, $\gamma \geq 0$ is the coefficient of relative risk aversion (RRA), $\psi \geq 0$ is the elasticity of intertemporal substitution (EIS), and

$$\theta^{-1} \equiv \frac{1 - \psi^{-1}}{1 - \gamma} \tag{15}$$

We also assume that the state of the economy s is known to each agent and so are the transition probabilities. Later on, we will consider parameter uncertainty for a two-state version of the model.

4.1.3 Agent's Optimization Problem and Equilibrium

The representative agent's problem is to choose in each state s optimal consumption $C(s, L^*(s))$ and labor $l(s, L^*(s))$ that maximizes the objective function $\mathbb{J}(s)$; in particular, the agent must have rational expectations about $L^*(s)$, the aggregate labor in equilibrium. In other words, individual agents' decisions in the aggregate should lead to a wealth (consumption) dynamic that is confirmed in equilibrium. This implies the following for wealth dynamics in the pandemic regime:

$$dq(s) = [l(s, L^*(s))]^{\alpha} q\mu dt - C(s, L^*(s))dt + \sigma [l(s, L^*(s))]^{\alpha/2} q dB - \chi(l(s, L^*(s)), L^*(s)) q dP(t) \tag{16}$$

Since $L^*(s)$ is a constant for each s, the above equilibrium dynamics are identical to the dynamics assumed by the agent for $q(s)$ as long as the agent has rational expectations about $L^*(s)$. Substituting for the equilibrium fixed point that $L^*(s) = l(s, L^*(s))$, we can then obtain the rational

Covid Economics 61, 11 December 2020: 1-72

expectations equilibrium outcomes.

4.1.4 Solution

We show in the Appendix how to set up the HJB equation for the optimization problem of the representative agent to determine the optimal consumption $C(s, L^*(s))$ and labor $l(s, L^*(s))$, making the natural conjecture that the value function is given by

$$\mathbb{J}(s) \equiv \frac{H(s)q^{1-\gamma}}{1-\gamma} \tag{17}$$

where $H(s)$ are constants (depending on deeper parameters of the model) to be determined. Given the transitions across states, $H(s)$ are jointly determined as explained below; however, given the structure of the problem, the equilibrium labor choices are more simply derived.

Proposition 1. *Equilibrium labor in the non-pandemic state is given by*

$$L(0) = L(S) = \overline{\ell} \tag{18}$$

Equilibrium labor in pandemic states $L^*(s)$ $\forall s \in \{1, \ldots, S-1\}$ *solves*[30]

$$\chi(L(s), L(s)) = k + (\varepsilon + K)L(s) = \frac{1}{\Delta}\left[1 - (L(s))^{\frac{1-\alpha}{\gamma}}\nu\right] \tag{20}$$

where

$$\nu \equiv \left[\frac{\alpha\left(\mu - \frac{1}{2}\gamma\sigma^2\right)}{\zeta\varepsilon\Delta}\right]^{-\frac{1}{\gamma}} \tag{21}$$

Note: All proofs appear in the appendix.

In the non-pandemic state, the agent faces no cost to supplying labor to augment the capital stock and exerts effort fully. However, in the pandemic states, the agent increases exposure to health risk by supplying labor, which creates a tradeoff between augmenting the capital stock and

[30] It can be shown that given $\alpha \in (0,1)$, the second order condition for a maximum is satisfied whenever

$$\mu - \frac{1}{2}\gamma\sigma^2 > 0 \tag{19}$$

which also implies $\nu > 0$.

Covid Economics 61, 11 December 2020: 1-72

reducing the loss of capital stock that arises when the pandemic hits. A key property of the model is that as the exposure to the pandemic is a function of the labor supply, the agent contracts labor in general relative to the non-pandemic state. We will assume parameter restrictions are such that this is in fact the case.

Next, the constant $H(s)$ that pins down the agent's equilibrium objective function in state s are solved jointly as follows:

Proposition 2. *Denote*

$$g(x,y) \equiv \frac{(1-\gamma)\rho}{(1-\psi^{-1})} - x^{\alpha}(1-\gamma)\left(\mu - \frac{1}{2}\gamma\sigma^2\right) - y\left(\left[1-\chi(x,x)\Delta\right]^{1-\gamma} - 1\right) \tag{22}$$

Then $\{H\}$'s are given by the system of S recursive equations $E(0),\ldots,E(S-1)$ as follows:

$$E(0): g_0 \equiv g(\bar{\ell},0) = \frac{(1-\gamma)}{(\psi-1)}\rho^{\psi}\left(H(0)\right)^{-\psi\theta^{-1}} + \eta\left[\frac{H(1)}{H(0)} - 1\right] \tag{23}$$

$$E(s): g_1 \equiv g(L(s),\zeta) = \frac{(1-\gamma)}{(\psi-1)}\rho^{\psi}\left(H(s)\right)^{-\psi\theta^{-1}} + \lambda_d(s)\left[\frac{H(s-1)}{H(s)} - 1\right] + \lambda_u(s)\left[\frac{H(s+1)}{H(s)} - 1\right] \tag{24}$$

for $s \in \{1,\ldots,S-1\}$, and $H(S) = H(0)$.

This captures another key property of the model. The solution to determining the agent's objective functions depends crucially on the relative values of g_0 and g_1, which serve as an important statistic for the extent of labor contraction in the economy in pandemic states relative to the non-pandemic state. The lower is g_1 relative to g_0, the lower is the objective function in pandemic states relative to the non-pandemic state, and in turn, the greater is the value that the agent attaches to finding a cure that can effect a switch out of the pandemic. This observation will play a crucial role in using our empirical work to infer the value of a cure.

Next,

Proposition 3. *Equilibrium consumption in state s can be determined based on $H(s)$ as*

$$C(s) = \frac{\left(H(s)\right)^{-\psi\theta^{-1}} q}{\rho^{-\psi}} \tag{25}$$

Covid Economics 61, 11 December 2020: 1-72

Marginal propensity to consume, $c(s)$, which is defined as dC/dq, depends on the state (s) and the elasticity of intertemporal substitution (ψ). Figure 5 illustrates for a 10-state regime-switching model that $c(s)$ in the pandemic states, $s \in \{1,\ldots,9\}$, is below (above) that in the non-pandemic state, $s = 0$ or $s = 10$, when ψ is below (above) 1.

Figure 5: Marginal Propensity to Consume in Pandemic and Non-Pandemic States

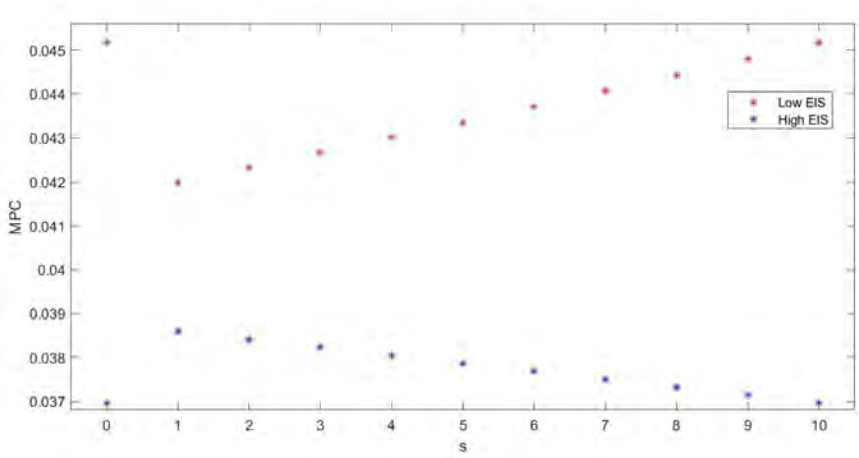

Note: Figure illustrates for a 10-state regime-switching model that $c(s)$ in the pandemic states, $s \in \{1,\ldots,9\}$, is below (above) that in the non-pandemic state, $s = 0$ or $s = 10$, when ψ is below (above) 1. Parameters chosen are in Table 4.

Combining Propositions 2 and 3, the equilibrium can also be characterized in terms of labor and consumption outcomes in different states, s, the solution to the following system of recursive equations,

Corollary 1. *Following Proposition 3, we can write the system of S recursive equations* $\hat{E}(0),\ldots,\hat{E}(S-1)$ *that characterize the* $\{H\}$*'s as:*

$$\hat{E}(0) : g_0 \equiv g(\bar{\ell},0) = \frac{(1-\gamma)}{(\psi-1)}c(0) + \eta\left[\frac{H(1)}{H(0)} - 1\right] \tag{26}$$

$$\hat{E}(s) : g_1 \equiv g(L(s),\zeta) = \frac{(1-\gamma)}{(\psi-1)}c(s) + \lambda_d(s)\left[\frac{H(s-1)}{H(s)} - 1\right] + \lambda_u(s)\left[\frac{H(s+1)}{H(s)} - 1\right] \tag{27}$$

for $s \in \{1,\ldots,S-1\}$, *and* $H(S) = H(0)$.

Covid Economics 61, 11 December 2020: 1-72

4.1.5 Externality and the Central Planner

Before proceeding to the value of a vaccine in this setup, it is worth noting that in our model there is an externality that the impact of labor on the effect of the pandemic via KL term (where L is the aggregate labor) is not internalized by each agent. The planner would factor this in the socially efficient choice of labor for each agent. This is tantamount to replacing ε by $(\varepsilon + K)$ in ν above to obtain ν^{CP}:

$$\nu^{CP} \equiv \left[\frac{\alpha\left(\mu - \frac{1}{2}\gamma\sigma^2\right)}{\zeta(\varepsilon + K)\Delta}\right]^{-\frac{1}{\gamma}} \tag{28}$$

Socially efficient labor choice $L^{CP}(s)$ in the pandemic states is then given by

$$\chi\left(L(s), L(s)\right) = k + (\varepsilon + K)L(s) = \frac{1}{\Delta}\left[1 - \left(L(s)\right)^{\frac{1-\alpha}{\gamma}}\nu^{CP}\right] \tag{29}$$

It is then straightforward to show that $\nu^{CP} > \nu$ for $K > 0$ and $\gamma > 0$, and $L^{CP}(s) < L(s)$, i.e., the socially efficient choice of labor in pandemic states is smaller than the privately optimal one. We will see later that this insight will help understand the wedge between the values attached to a cure by the planner and the private agents.

4.1.6 Value of a Cure

We have now all the ingredients to determine the value of a cure. We define it as the certainty equivalent change in the representative agent's lifetime value function upon a transition from state s to state 0 (or to state S):

$$V(s) = 1 - \left(\frac{H(s)}{H(0)}\right)^{\frac{1}{1-\gamma}} \tag{30}$$

This is the percentage of the agent's stock of wealth q that, if surrendered, would be fully compensated by the utility gain of reverting to the non-pandemic state.[31]

Using the optimal consumption characterized above, we obtain that

[31] We acknowledge that this is essentially a comparative static exercise and the economy does not possess the technology to actually effect this transition. We discuss in the Conclusion ways to enrich our model to introduce the vaccine technology into the model as an important topic for future research, but one that is beyond the immediate scope of this paper.

Covid Economics 61, 11 December 2020: 1-72

Proposition 4. *The value of a cure in the pandemic state s is determined by the ratio of marginal propensity to consume* $(c \equiv dC/dq)$ *in the pandemic state s relative to that in the non-pandemic state, adjusted by the agent's elasticity of intertemporal substitution (EIS):*

$$V(s) = 1 - \left(\frac{c(s)}{c(0)}\right)^{\frac{1}{\psi-1}} = 1 - \left(\frac{C(s)}{C(0)}\right)^{\frac{1}{\psi-1}} \tag{31}$$

Note from Proposition 3 that the ratio of marginal propensities to consume for a given q is simply the ratio of consumptions. Furthermore, when EIS (ψ) is less than one, the value of a cure is higher the greater is the contraction of consumption in the pandemic states relative to the non-pandemic state. Indeed, it can be shown that consumption is lower in the pandemic states relative to the non-pandemic state (for a given q) if and only if $\psi < 1$.

Our next step is to derive this value. To this end, we will derive asset prices in the framework above to show that the value of claim to the economy's output ("stock market") changes in relation to the expected time to switching out of a pandemic ("expected time to deployment of a vaccine") – which we empirically estimated – is crucially determined by the contraction of labor in pandemic state relative to the non-pandemic state, as described by $\frac{g_1}{g_0}$. This then allows us to back out the labor contraction implied by our empirical estimate, and in turn, helps us to estimate the value of a cure under assumptions of standard preference parameters.

4.2 Connection to the Data

We introduced the model in order to first define and study determinants of welfare and the value of a vaccine. The second reason to introduce the model is to allow us to bring financial claims into the picture, and, in particular, to examine the model's counterpart to the sensitivity that we estimated in Section 2.2.

As is standard in the asset pricing literature, we begin by interpreting "the market portfolio" within the model as a claim to the economy's output.[32] Output is the net new resources per unit time, which is implicitly defined by two endogenous quantities: the change in the cumulative physical capital plus consumption, or $dq + Cdt$. (Note that the value of a claim to this flow is not equal to the value of a claim to the capital stock, which is q.) Denote the price of the output claim as $P = P(s,q)$. By the fundamental theorem of asset pricing, the instantaneous expected excess

[32]We defer for now explicitly modeling the dividend share of output or incorporating leverage in the equity claim.

return to holding this claim is equal to minus the covariance of its returns with the pricing kernel. From this, we derive the value of the claim and some key properties in the following proposition.

Proposition 5. *The price of the output claim is $P = p(s)q$ where the the constants $p(s)$ solve a matrix system $Y = Xp$ where X is an $S+1$-by-$S+1$ matrix and Y is an $S+1$ vector both of whose elements are given in the appendix. The system depends on the pandemic parameters through only two quantities, which may be taken to be the risk-neutral expected growth of output and g_1, defined in the preceding section.*

Henceforth we assume the model parameters are such that the matrix X defined in the proposition is of full rank. The behavior of the price-capital ratio, $p(s)$, accords with economic intuition: it declines sharply on a move from state $s = 0$ to $s = 1$, and then gradually (and approximately linearly) recovers as s advances. Thus, the quantity $\Delta \log P = \log p(s+1) - \log p(s)$ is positive for $s > 0$ and, in practice, varies little with s.

Next, define $T^\star$ as the time at which the state S is attained and the pandemic is terminated. Assuming the progression and regression intensities λ_u and λ_d are constant, it is straightforward to show that its time t expectation, $\mathbb{E}_t[T^\star]$ is again given by a linear system, which we omit for brevity. Moreover, for large S, the difference

$$\Delta \mathbb{E}[T^\star] = \mathbb{E}[T^\star|s+1] - \mathbb{E}[T^\star|s] \sim \frac{1}{\lambda_u} \tag{32}$$

is effectively constant as well. (The expression is exact for $s = 1$.)

Combining the above two results, we can readily define the model's analogue of the sensitivity that we empirically estimated as

$$\frac{\Delta \log P}{\Delta \mathbb{E}[T^\star]}. \tag{33}$$

For our purposes the crucial property of this quantity is that it allows us to approximately pin down the pandemic parameters that determine the value of a cure. Specifically, it depends importantly on g_1, modulated by the other pandemic parameters. This is illustrated in Figure 6, which plots the sensitivity for a wide range of model solutions. The horizontal axis is g_1 and each model version corresponds to a single point. Here we allow all of the pandemic parameters to vary, as well as the intensities η and λ_u. From the proposition above, g_1 alone does not suffice to determine

Covid Economics 61, 11 December 2020: 1-72

the pricing function p. However, the second variable that the proposition identifies as mattering – the risk neutral expected growth of output – is codetermined in equilibrium with g_1, and as a practical matter, its residual variation is small. That is, given g_1, the expected growth rate varies only marginally with the remaining parameters.

Figure 6: Stock Market Sensitivity to Vaccine Progress

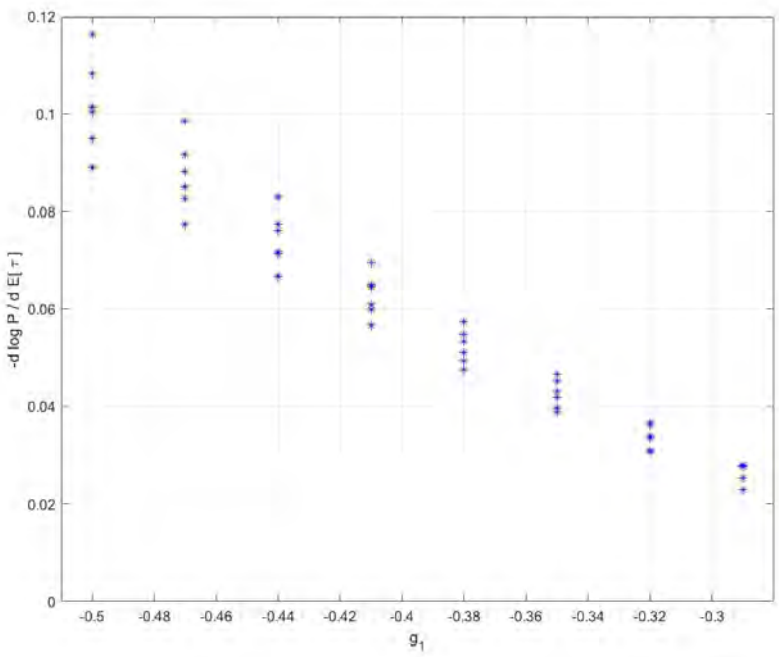

Note: Figure shows the sensitivity $-\Delta \log P / \Delta \mathbb{E}[T^\star]$ as a function of g_1 for model solutions varying the pandemic intensity parameters η and λ and the risk neutral expected growth rate of output as described in the text. Each star corresponds to a single model solution.

Hence, although the identification is not exact, we can infer from the figure that our empirical estimates in the range of 5.0 are consistent with a value of g_1 in range of approximately -0.39 to -0.37, given the non-pandemic parameters used to compute the model solutions shown.

4.3 Calibrating the Value of a Cure

In this section and in Section 5 we present comparative static results exploring the determinants of the value of a cure, V as defined in Section 4.1. In doing this, unless otherwise stated, we will fix the non-pandemic parameters to be the values shown in Table 4. The preference parameters are

Covid Economics 61, 11 December 2020: 1-72

broadly consistent with the asset pricing literature under stochastic differential utility, although we use a relatively low level of risk aversion because higher values of γ can lead to violations of regularity conditions. The growth rate and volatility parameters are chosen as a compromise between two interpretations of the model. On the one hand, we are viewing the output process as representing national income (or GDP), which would suggest smaller mean and volatility. On the other hand, our asset pricing exercise views the same process as depicting dividends, which would suggest higher values for both.[33] In addition, the solutions in this section will set the number of states to be $S = 10$, which is arbitrary but without loss of generality. Our results are not too sensitive to the specific choice of the number of states as it is to the other pandemic parameters. We also set the intensity of regress to be $\lambda_d = 0$, which limits vaccine related volatility. This choice accords with recent experience: the research setbacks through the Fall of 2020 were few and had little impact on our measure of progress.

Table 4: Parameter Values

Parameter	Symbol	Value
Coefficient of relative risk aversion	γ	4.0
Elasticity of intertemporal substitution	ψ	1.5
Rate of time preference	ρ	0.04
Non-pandemic expected output growth	μ	0.055
Non-pandemic output volatility	σ	0.05

Note: Table shows parameter values used in estimating the value of a cure.

Figure 7 plots the value of the cure as a function of the remaining timing parameters, η and λ_u (hereafter we will denote $\lambda_u/(S+1)$ as λ without a subscript). The left panel plots V against $1/\lambda$ the expected duration of the pandemic, while the right panel uses the pandemic frequency η on the horizontal axis. (The left panel sets $\eta = 0.02$ and the right panel sets $\lambda = 0.5$. Both panels take the current state as $s = 1$.) From the left plot, agents in the economy would be willing to give up five percent of their wealth for an immediate transition to state 0 even when the pandemic is only expected to last one year. This value rises to approximately 15% when the expected duration is 4 years. The right panel shows that the value of a cure is actually lower when pandemics are more

[33] An additional consideration is that a relatively high growth rate is needed to obtain a solution when varying the elasticity of intertemporal substitution, which we will do in Section 4.

Covid Economics 61, 11 December 2020: 1-72

frequent. Recall that a "cure" here only applies to the current pandemic. A one-time cure is less valuable when a new one will be needed sooner.

Figure 7: Value of a Cure

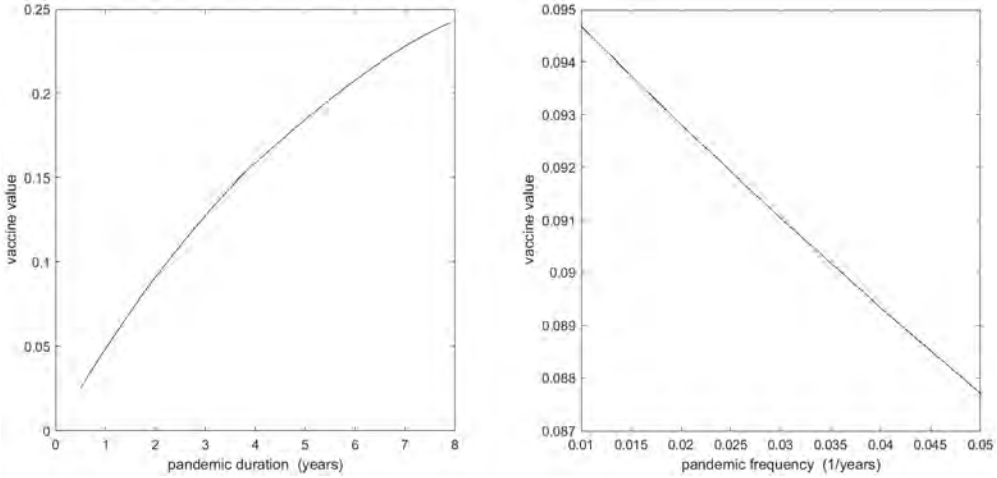

Note: Figure shows the value V as a function of the pandemic intensity parameters η and λ. The left panel plots V against $1/\lambda$. The right panel plots V against η. The left panel sets $\eta = 0.02$ and the right panel sets $\lambda = 0.5$. Both panels take the current state as $s = 1$.

Given the parameters used in the calibration, the (endogenous) expected decline in wealth due to pandemic shocks is approximately 5% per year. Our estimation of the value of a cure is quite close to this expected loss, which is intuitively sensible. Also, while the two quantities are conceptually distinct, the value we are computing here is similar (on a per year basis) to the stock market valuation of a year of pandemic experience as estimated in Section 3.

Table 5 shows the effect on V of the labor market externality, for a range of λ and η. Here the right panel shows the benchmark case while the left panel shows what happens when the labor market response to the pandemic is determined by a welfare maximizing central planner. The result shows a small but not insignificant increase in the value of the vaccine in the presence of the externality. In effect, the extra degree of lock-down that the planner would impose and the vaccine are substitutes as countermeasures. We acknowledge though that if the arrival of the pandemic were to result in social costs that are outside the capital stock dynamics for the agent, then this result could reverse and the planner might value the vaccine more than the representative agent.

Covid Economics 61, 11 December 2020: 1-72

Table 5: Value of a Cure: The Effect of Externality

		Central Planner				Benchmark		
		λ				λ		
		0.2	0.5	1.0		0.2	0.5	1.0
η	0.01	0.197	0.094	0.048	η 0.01	0.242	0.116	0.058
	0.05	0.154	0.084	0.045	0.05	0.185	0.102	0.055

Note: Table shows the fraction of wealth that the representative would be willing to surrender for a one-time transition out of the pandemic state. The right panel shows the results when the labor supply decision is made by individual agents acting atomistically. The left panel shows the case where the labor policy is determined by a central planner. All cases use $\gamma = 4, \psi = 1.5, \rho = 0.04, \alpha = 0.5, \sigma = 0.05, \mu = 0.055, \Delta = 0.06, \epsilon = 0.4, k = 0.1, K = 0.4$ and $\zeta = 1$.

Covid Economics 61, 11 December 2020: 1-72

5 Learning and Uncertainty

We have used the S-state version of our model to study the reaction of markets to vaccine news within a pandemic. Relating its predictions to the empirical evidence in Section 3 has provided evidence on plausible parameters affecting the value of a vaccine. Now we return to the two-state version of our model in order to examine the role of vaccine news from a different angle. Specifically, we are interested in the accumulation of information over longer horizons about the frequency and duration of pandemics. We study the effect upon the value of a vaccine of uncertainty about these quantities and of differing attitudes towards uncertainty.

5.1 Information Structure

Recall that in the two-state model η is the intensity of switching from state 0 ("off") to state 1 ("on") and λ is the intensity of switching from 1 to 0. In this section, we assume that agents have imperfect information about these intensities.

Let us stipulate that at time zero the agent has beliefs about the two parameters that are described by gamma distributions, which are independent of each other. Each gamma distribution has a pair of non-negative hyperparameters, a^η, b^η and a^λ, b^λ, that are related to the first and second moments via

$$\mathbb{E}[\eta] = \frac{a^\eta}{b^\eta}, \qquad \text{Std}[\eta] = \frac{\sqrt{a^\eta}}{b^\eta}, \tag{34}$$

and likewise for λ.

Covid Economics 61, 11 December 2020: 1-72

By Bayes' rule, under this specification, as the agent observes the switches from one regime to the next, her beliefs remain in the gamma class with the hyperparameters updating as follows

$$\begin{aligned} a_t^\eta &= a_0^\eta + N_t^\eta \\ b_t^\eta &= b_0^\eta + t^\eta \end{aligned}$$

where t^η represents the cumulative time spent in state 0 and N_t^η represents the total number of observed switches from 0 to 1. Analogous expressions apply for λ. Thus, during the "off" regime, the only information that arrives (on a given day, say) is whether or not we have switched to "on" on that day. If that has occurred, the counter N^η increments by one and the clock t^η turns off (and t^λ turns on). In this version of the model, that is the entirety of the information revelation. In contrast to the previous section, no good or bad news arrives about progress during a regime. Although this setting lessens the model's ability to speak to high-frequency dynamics, it allows us to study the role of uncertainty in the econmy's longer term evolution.

Under the above information structure, the economy is characterized by a six-dimensional state vector consisting of the stock of wealth, q, $a^\eta, b^\eta, a^\lambda, b^\lambda$ and the regime indicator S. However this six-dimensional space can actually be reduced to three.

Since the switches between states alternate, let us define an integer index M_t to be the total number of switches $N_t^\eta + N_t^\lambda$ and then (assuming we are in state 0 at time 0) $N_t^\eta = M_t/2$ when M is even, and $N_t^\lambda = (M_t + 1)/2$ when M is odd. Knowing M (along with the priors a_0^η and a_0^λ) is equivalent to knowing a_t^η and a_t^λ. Given these values, specifying the current estimates

$$\hat{\eta}_t \equiv \mathbb{E}_t[\eta] \quad \text{and} \quad \hat{\lambda}_t \equiv \mathbb{E}_t[\lambda] \tag{35}$$

is equivalent to specifying the remaining hyperparameters b_t^η and b_t^λ. Thus, solutions to the model can be described as a sequence of functions $H_M(\hat{\eta}, \hat{\lambda})$ for the agent's value function at step M.

Compared to the full-information model in Section 4, within each regime the only new changes to the state come through variation in the estimates $\hat{\eta}_t$ and $\hat{\lambda}_t$ which change deterministically with

the respective clocks t^η and t^λ. Holding M fixed, the dynamics of $\hat{\eta}_t$ are given by

$$d\hat{\eta}_t = d\frac{a_t^\eta}{b_t^\eta} = a_l^\eta d\frac{1}{b_t^\eta} \tag{36}$$

$$= -\frac{a_t^\eta}{(b_t^\eta)^2}\, dt \tag{37}$$

$$= -\frac{(\hat{\eta}_t)^2}{a_t^\eta}\, dt. \tag{38}$$

Under partial information, we proceed as in Section 4 to write-out the HJB equation with the state variables following the dynamics determined by the representative agent's information set. As before, we can conjecture a form of the value function

$$V = \frac{q^{1-\gamma}}{1-\gamma}\, H(\hat{\eta}, \hat{\lambda}, M; C, \ell). \tag{39}$$

And, as before the first order condition for consumption yields $C = q\ (\rho^\psi)\ H_1^e$ (where e_1 is defined in Section 4.1). This follows because consumption does not enter into any of the new terms involving the information variables. Also fortunately, none of the information variables appears in terms affected by labor supply, ℓ, and the function H drops out of the first-order condition for ℓ. (Intuitively, nothing about the likelihood of changing regimes affects the optimal choice of labor within a regime.) This means that the solutions for $\ell^\star$ can be computed independent of the rest of the system.

Using these the results, the HJB system can be written as the infinite-dimensional linked PDEs:

$$g_0 = \rho^\psi \left(\frac{\theta}{\psi}\right) H_M^{-\psi/\theta} + \hat{\eta}\left(\frac{H_{M+1}}{H_M} - 1\right) - \frac{(\hat{\eta})^2}{a^\eta H_M}\frac{\partial H_M}{\partial \hat{\eta}} \tag{40}$$

$$g_1 = \rho^\psi \left(\frac{\theta}{\psi}\right) H_{M+1}^{-\psi/\theta} + \hat{\lambda}\left(\frac{H_{M+2}}{H_{M+1}} - 1\right) - \frac{(\hat{\lambda})^2}{a^\lambda H_{M+1}}\frac{\partial H_{M+1}}{\partial \hat{\lambda}} \tag{41}$$

where M runs over the even integers.[34]

For large M, the estimation errors for both η and λ, expressed as a fraction of the posterior

[34]The constants g_0 and g_1 are as defined in Section 4.

estimates, go to zero:

$$\frac{\text{Std}[\eta]}{\mathbb{E}[\eta]} = \frac{1}{\sqrt{a^{\eta}}} = \frac{1}{\sqrt{a_0^{\eta} + M_t}}. \tag{42}$$

Hence the system always converges to the full-information solution. This provides a boundary condition, which, together with the single-regime solutions on the edges of the $(\hat{\eta}, \hat{\lambda})$ plane, enables computation of all the individual H functions.[35] It can be shown that, as in the full-information case, a necessary and sufficient condition for existence of a solution is $g_0 > g_1$.

As in the previous section, once the value function is obtained, we can characterize the certainty equivalent value of a vaccine that produces an immediate transition from the pandemic state to the non-pandemic state. The next section performs this calculation and analyzes the drivers of variation in that value.

5.2 Results

Table 6 shows numerical solutions for the value of a vaccine using the benchmark parameters from Section 4 but varying the elasticity of intertemporal substitution (EIS). The upper two panels show the full-information solution, with the upper right case corresponding to the benchmark $\psi = 1.5$, whereas the left panel lower the EIS to $\psi = 0.15$. There is almost no difference between the two solutions (which verifies the robustness of the conclusions in Section 4 on this dimension). The bottom two panels show the results under partial information. Specifically, results are computed under the assumption that agents' standard deviation of beliefs about the two parameters are equal to their mean beliefs. Comparing the right-hand panels, we see that this degree of parameters uncertainty has the effect of raising the level of wealth agents in the economy would be willing to surrender for a cure in the baseline case of a high EIS by between 7 and 15 percentage points, or up to a factor of three times the full information value. The left hand panels show the same effect, but amplified to an extreme level. With a low intertemporal elasticity, the representative agent would be willing to sacrifice on the order of 50 to 60 percent of accumulated wealth.

An additional computation that our framework can address is the value of a permanent cure.

[35] Knowing the solution for higher M enables direct evaluation of the jump-terms in (40)-(41). Knowing the solution on the inner edges enables explicit approximation of the first partial derivatives.

Covid Economics 61, 11 December 2020: 1-72

Table 6: Value of a Cure under Parameter Uncertainty

	Low Uncertainty / Low EIS			Low Uncertainty / High EIS		
	$\hat{\lambda}$			$\hat{\lambda}$		
$\hat{\eta}$	0.2	0.5	1.0	0.2	0.5	1.0
0.01	0.242	0.114	0.058	0.242	0.116	0.058
0.05	0.192	0.102	0.055	0.185	0.102	0.055

	High Uncertainty / Low EIS			High Uncertainty / High EIS		
	$\hat{\lambda}$			$\hat{\lambda}$		
$\hat{\eta}$	0.2	0.5	1.0	0.2	0.5	1.0
0.01	0.633	0.613	0.558	0.379	0.302	0.222
0.05	0.456	0.479	0.477	0.256	0.222	0.186

Note: Table shows the fraction of wealth that the representative agent would be willing to surrender for a one-time transition out of the pandemic state. The cases labeled High EIS set $\psi = 1.5$. Cases labeled Low EIS set $\psi = 0.15$. Cases labeled Low Uncertainty correspond to agents knowing the parameters λ and η. Cases labeled High Uncertainty correspond to agents having a posterior standard deviation for those parameters that is equal to their point estimates of them. All cases use $\gamma = 4, \rho = 0.04, \alpha = 0.5, \sigma = 0.05, \mu = 0.05, \Delta = 0.06, \epsilon = 0.4, k = 0.1, K = 0.4$ and $\zeta = 1$.

Table 7 shows the fraction of wealth agents in the economy would exchange to live in a world with no pandemics. (Formally, this is equivalent to letting λ go to infinity.) As expected, the values now show the same pattern as in Table 6, but exaggerated still further. In this case, eliminating the threat *and* resolving the parameter uncertainty can lead to valuation of 25 to 50 percent for high EIS agents and 60 to 80 percent for low EIS agents.

The latter finding may be counterintuitive based on the common understanding of Epstein-Zin preferences under which agents with $\psi < 1/\gamma$ can be viewed as having a preference for "later resolution of uncertainty." In the current model, agents facing a pandemic are much worse off with parameter uncertainty. This is verified in Table 8 where we compute the value that agents would pay to resolve parameter uncertainty *without* ending the on-going pandemic.

For both values of the EIS the numbers are again extremely high, and for the low EIS case they are even higher than in the previous table. Apparently, in this economy, low-EIS agents would pay dearly for early resolution of uncertainty. The source of the extreme welfare loss in this case is the endogenous consumption response. Recall that low-EIS agents cut their consumption

Covid Economics 61, 11 December 2020: 1-72

Table 7: Value of a Permanent Cure

	Low Uncertainty / Low EIS				Low Uncertainty / High EIS			
			$\hat{\lambda}$				$\hat{\lambda}$	
		0.2	0.5	1.0		0.2	0.5	1.0
$\hat{\eta}$	0.01	0.308	0.136	0.068	0.01	0.327	0.148	0.074
	0.05	0.430	0.214	0.111	0.05	0.429	0.239	0.130
	High Uncertainty / Low EIS				High Uncertainty / High EIS			
			$\hat{\lambda}$				$\hat{\lambda}$	
		0.2	0.5	1.0		0.2	0.5	1.0
$\hat{\eta}$	0.01	0.813	0.720	0.613	0.01	0.503	0.378	0.265
	0.05	0.831	0.751	0.658	0.05	0.538	0.435	0.335

Note: Table shows the fraction of wealth that the representative agent would exchange to live in a world with no pandemics. High uncertainty denotes agents having a posterior standard deviation for the regime parameters λ and η that is equal to their point estimates of them. Low uncertainty denotes full information. The cases labeled High EIS set $\psi = 1.5$. Cases labeled Low EIS set $\psi = 0.15$. All cases use $\gamma = 4, \rho = 0.04, \alpha = 0.5, \sigma = 0.05, \mu = 0.05, \Delta = 0.06, \epsilon = 0.4, k = 0.1, K = 0.4$ and $\zeta = 1$.

during a pandemic. With parameter uncertainty this response becomes extreme because agents cannot rule out the worst case scenario that $\lambda \sim 0$, i.e., that there will never be a cure and the pandemic effectively lasts forever. This possibility leads to extreme savings and, consequently, very little utility flow from consumption.

Even with high EIS however, the effect of parameter uncertainty is economically large, and is again due to agents being unable to rule out worst-case scenarios. From a policy perspective, the implication of this finding is that, while working to end the current pandemic is enormously valuable, equally and perhaps even more valuable is anything that resolves uncertainty about the frequency and, especially, the duration of current and future pandemics. In addition to developing cures and vaccines, understanding the fundamental science behind the fight against viral pathogens and investing in the infrastructure for future responses can provide crucial gains to welfare.

Table 8: Value of Information

		Low EIS				High EIS		
		$\hat{\lambda}$				$\hat{\lambda}$		
		0.2	0.5	1.0		0.2	0.5	1.0
$\hat{\eta}$	0.01	0.733	0.675	0.587	0.01	0.270	0.273	0.209
	0.05	0.708	0.682	0.617	0.05	0.200	0.255	0.236

Note: Table shows the fraction of wealth that the representative would be willing to surrender for a one-time transition from high parameter uncertainty to low parameter uncertainty. High uncertainty denotes agents having a posterior standard deviation for the regime parameters λ and η that is equal to their point estimates of them. Low uncertainty denotes full information. The cases labeled High EIS set $\psi = 1.5$. Cases labeled Low EIS set $\psi = 0.15$. All cases use $\gamma = 4, \rho = 0.04, \alpha = 0.5, \sigma = 0.05, \mu = 0.05, \Delta = 0.06, \epsilon = 0.4, k = 0.1, K = 0.4$ and $\zeta = 1$.

6 Conclusion

In this paper, we estimated the value of a "cure" – vaccine for a pandemic – using the joint behavior of stock prices and a novel vaccine progress indicator based on the chronology of stage-by-stage progress of individual vaccine candidates and related news. We developed a general equilibrium regime-switching model of repeated pandemics and stages of vaccine progress, wherein the representative agent withdraws labor and alters consumption endogenously to mitigate the economic consequences of health risk arising from pandemics. We showed that the value of cure is pinned down by the ratio of marginal propensity to consume in the pandemic state to the marginal propensity to consume in the non-pandemic state augmented by the elasticity of intertemporal substitution. In the resulting asset-pricing framework, we showed that the covariance of stock prices with the vaccine progress indicator gives an indirect estimate of labor contraction during the pandemic relative to the non-pandemic states; in turn, the empirical estimate of the covariance helps pin down the labor contraction which is an important statistic for the value attached by the representative agent to finding a cure.

With standard preferences parameters, the value of a cure turns out to be worth 5-15% of wealth (formally, capital stock in the model). The value of the cure rises sharply when there is uncertainty about the frequency and duration of pandemics. Indeed, we find that the representative agent would be willing to pay as much for resolution of this parameter uncertainty as for the cure

absent such uncertainty. This effect is stronger – not weaker – when agents have a preference for later resolution of uncertainty. An important policy implication is that understanding the fundamental biological and social determinants of future pandemics, for instance, whether pandemics are related to zoonotic diseases triggered more frequently by climate change, may be as important to mitigating their economic impact as resolving the immediate pandemic-induced crisis.

An interesting extension of our regime-switching framework could be one where as the pandemic evolves through various stages of vaccine progression, it may be simultaneously evolving in its own characteristics. For instance, the arrival intensity (ζ) of the health shock might decline due to "herd immunity" building up or its impact on capital stock (Δ) be mitigated due to learning-by-doing in working from home. Such variations across pandemic states would also generate the realistic implication that labor contraction across pandemic states reduces as the pandemic gets "weaker." Theoretically, this would add richness to the existing framework we have proposed, though empirically, it would require substantially greater statistical power to estimate state-by-state covariance of stock returns with changes in the vaccine progress indicator or progression across the pandemic states.

Our empirical work could be extended in several directions. First, long-short or "factor mimicking" portfolios can be constructed to map into changes in the vaccine progress indicator for use in future asset-pricing tests. Secondly, changes in the vaccine progress indicator may also be relevant for fixed income markets and expectations of future interest rates; more generally, progress in finding a cure could affect expectations of monetary and fiscal policies, which we did not consider in this paper. Thirdly, we can numerically consider regression in progress of the vaccine by allowing λ_d in our state-transition matrix to be greater than zero, a feature that can have significant implications for asset price volatility, and in turn, for options markets. Finally, vaccines may be more readily available for early deployment in some countries (developed, for example) versus others; this would imply patterns in sensitivity of cross-country returns to the vaccine progress indicator, which can be teased out in data.

One caveat to our estimate of the value of a cure is that it is essentially a comparative static exercise. In particular, the economy in our model does not possess the technology to actually effect the transition out of a pandemic. In reality, there is a "real option" to invest in vaccine technology that affects the probability of switching out of a pandemic. Indeed, there are many such candidates

Covid Economics 61, 11 December 2020: 1-72

as we empirically exploit in the construction of our vaccine progress indicator. It is an interesting open question for future research to embed the vaccine production technologies into the model, allowing policy analysis that can help answer questions such as: How much should the central planner invest or co-fund the investment in vaccines given their value to the society far exceeds the value to individual vaccine production companies? Should the central planner cap user fees for deployment of the vaccine once developed? How do these choices affect competition in the speed of development of the vaccine and the endogenous probability of switching out of pandemics? Our asset-pricing perspective on the value of a cure is hopefully a useful first step for further inquiry along these lines.

Covid Economics 61, 11 December 2020: 1-72

References

Asger Lau Andersen, Emilt Toft Hansen, Niels Johannsesen, and Adam Sheridan. Consumer responses to the covid-19 crisis: Evidence from bank account transaction data. Technical report, CEPR, April 2020. URL https://cepr.org/sites/default/files/news/CovidEconomics7.pdf.

Natalie Bachas, Peter Ganong, Pascal J Noel, Joseph S Vavra, Arlene Wong, Diana Farrell, and Fiona E Greig. Initial impacts of the pandemic on consumer behavior: Evidence from linked income, spending, and savings data. Working Paper 27617, National Bureau of Economic Research, July 2020. URL http://www.nber.org/papers/w27617.

Scott Baker, R.A. Farrokhnia, Steffen Meyer, Michaela Pagel, and Constantine Yannelis. How does household spending respond to an epidemic? consumption during the 2020 covid-19 pandemic. *Covid Economics*, May 2020a. URL https://cepr.org/sites/default/files/CovidEconomics18.pdf#Paper3.

Scott R Baker, Nicholas Bloom, Steven J Davis, Kyle Kost, Marco Sammon, and Tasaneeya Viratyosin. The Unprecedented Stock Market Reaction to COVID-19. *The Review of Asset Pricing Studies*, 07 2020b. ISSN 2045-9920. doi: 10.1093/rapstu/raaa008. URL https://doi.org/10.1093/rapstu/raaa008. raaa008.

Robert J. Barro. Rare Disasters and Asset Markets in the Twentieth Century*. *The Quarterly Journal of Economics*, 121(3):823–866, 08 2006. ISSN 0033-5533. doi: 10.1162/qjec.121.3.823. URL https://doi.org/10.1162/qjec.121.3.823.

Louis-Philippe Beland, Abel Brodeur, and Taylor Wright. Covid-19, stay-at-home orders and employment: Evidence from cps data. Working Paper 13282, IZA Institute of Labor Economics, May 2020. URL http://ftp.iza.org/dp13282.pdf.

Shai Bernstein, Richard R Townsend, and Ting Xu. Flight to safety: How economic downturns affect talent flows to startups. Working Paper 27907, National Bureau of Economic Research, October 2020. URL http://www.nber.org/papers/w27907.

Covid Economics 61, 11 December 2020: 1-72

Haiqiang Chen, Welan Qian, and Qiang Wen. The impact of the covid-19 pandemic on consumption: Learning from high frequency transaction data. Technical report, Working Paper, 2020. URL https://ssrn.com/abstract=3568574.

Raj Chetty, John N Friedman, Nathaniel Hendren, Michael Stepner, and The Opportunity Insights Team. How did covid-19 and stabilization policies affect spending and employment? a new real-time economic tracker based on private sector data. Working Paper 27431, National Bureau of Economic Research, June 2020. URL http://www.nber.org/papers/w27431.

Olivier Coibion, Yuriy Gorodnichenko, and Michael Weber. The cost of the covid-19 crisis: Lockdowns, macroeconomic expectations, and consumer spending. *Covid Economics*, May 2020a. URL https://cepr.org/sites/default/files/CovidEconomics20.pdf#Paper1.

Olivier Coibion, Yuriy Gorodnichenko, and Michael Weber. Labor markets during the covid-19 crisis: A preliminary view. *Covid Economics*, May 2020b. doi: 10.3386/w27017. URL https://cepr.org/sites/default/files/CovidEconomics21.pdf#Paper2.

Pierre Collin-Dufresne, Michael Johannes, and Lars A. Lochstoer. Parameter learning in general equilibrium: The asset pricing implications. *American Economic Review*, 106(3):664–98, March 2016. doi: 10.1257/aer.20130392. URL https://www.aeaweb.org/articles?id=10.1257/aer.20130392.

Jonathan I Dingel and Brent Neiman. How many jobs can be done at home? *Covid Economics*, April 2020. URL https://cepr.org/sites/default/files/CovidEconomics1.pdf.

Darrell Duffie and Larry G. Epstein. Asset pricing with stochastic differential utility. 5:411–436, 1992.

Darrell Duffie and Costis Skiadas. Continuous-time security pricing: A utility gradient approach. *Journal of Mathematical Economics*, 23:107–132, 1994.

Vadim Elenev, Tim Landvoigt, and Stijn Van Nieuwerburgh. Can the covid bailouts save the economy. *Covid Economics*, May 2020. URL https://cepr.org/sites/default/files/CovidEconomics17.pdf#Paper4.

Covid Economics 61, 11 December 2020: 1-72

Eliza Forsythe, Lisa B Kahn, Fabian Lange, and David G Wiczer. Labor demand in the time of covid-19: Evidence from vacancy postings and ui claims. Working Paper 27061, National Bureau of Economic Research, April 2020. URL http://www.nber.org/papers/w27061.

X. Gabaix. Variable rare disasters: An exactly solved framework for ten puzzles in macro-finance. *Quarterly Journal of Economics*, 127(2):645–700, 2012.

Harrison Hong, Jeffrey Kubik, Neng Wang, Xiao Xu, and Jinqiang Yang. Pandemics, vaccines and corporate earnings. Technical report, Working Paper, 2020a.

Harrison Hong, Neng Wang, and Jinqiang Yang. Implications of stochastic transmission rates for managing pandemic risks. Working Paper 27218, National Bureau of Economic Research, May 2020b. URL http://www.nber.org/papers/w27218.

Raymond Kan and Cesare Robotti. On moments of folded and truncated multivariate normal distributions. *Journal of Computational and Graphical Statistics*, 26(4):930–934, 2017.

Leonid Kogan, Dimitris Papanikolaou, Amit Seru, and Noah Stoffman. Technological innovation, resource allocation, and growth. *The Quarterly Journal of Economics*, 132(2):665–712, 2017.

Julian Kozlowski, Laura Veldkamp, and Venky Venkateswaran. Scarring body and mind: The long-term belief-scarring effects of covid-19. *Covid Economics*, April 2020. URL https://cepr.org/sites/default/files/CovidEconomics8.pdf.

Simon Mongey, Laura Pilossoph, and Alex Weinberg. Which workers bear the burden of social distancing policies? *Covid Economics*, May 2020. URL https://cepr.org/sites/default/files/CovidEconomics12.pdf.

John Muellbauer. The coronavirus pandemic and us consumption. *Vox EU*, 2020. URL https://voxeu.org/article/coronavirus-pandemic-and-us-consumption.

A. O'hagan. Bayes estimation of a convex quadratic. *Biometrika*, 60(3):565–571, 1973.

Robert S. Pindyck and Neng Wang. The economic and policy consequences of catastrophes. *American Economic Journal: Economic Policy*, 5(4):306–39, November 2013. doi: 10.1257/pol.5.4.306. URL https://www.aeaweb.org/articles?id=10.1257/pol.5.4.306.

Covid Economics 61, 11 December 2020: 1-72

Adam Sheridan, Asger Lau Andersen, Emil Toft Hansen, and Niels Johannesen. Social distancing laws cause only small losses of economic activity during the covid-19 pandemic in scandinavia. *Proceedings of the National Academy of Sciences*, 117(34):20468–20473, 2020. ISSN 0027-8424. doi: 10.1073/pnas.2010068117. URL https://www.pnas.org/content/117/34/20468.

Jerry Tsai and Jessica A. Wachter. Disaster risk and its implications for asset pricing. *Annual Review of Financial Economics*, 7(1):219–252, 2015. doi: 10.1146/annurev-financial-111914-041906. URL https://doi.org/10.1146/annurev-financial-111914-041906.

Chi Heem Wong, Kien Wei Siah, and Andrew W Lo. Estimation of clinical trial success rates and related parameters. *Biostatistics*, 20(2):273–286, 01 2018. ISSN 1465-4644. doi: 10.1093/biostatistics/kxx069. URL https://doi.org/10.1093/biostatistics/kxx069.

Covid Economics 61, 11 December 2020: 1-72

Appendix

A News Articles

This section quotes news articles from the Introduction and includes news articles as cited in Section 3.

A.1 News Articles from the Introduction

On May 18, 2020 *Moderna* released positive interim clinical data from their Phase I trials and announced a Phase III trial.

> Federal Reserve chair Jay Powell has warned that a full US economic recovery may take until the end of next year and require the development of a COVID-19 vaccine: "For the economy to fully recover, people will have to be fully confident. And that may have to await the arrival of a vaccine", Mr. Powell told CBS News on Sunday"
>
> Lauren Fedor and James Politi, Financial Times, May 18, 2020

> U.S. stocks gained about $1 trillion of market capitalization yesterday, and while there are lots of reasons why any particular stock may have gone up or down, good news about a vaccine that might allow reopening of the economy seems like a common factor for a lot of stocks.
>
> "U.S. Stocks Surge as Hopes for Coronavirus Vaccine Build," was the Wall Street Journal's headline, citing the Moderna results... It is almost fair to say that Moderna added $1 trillion of value to all the other stocks yesterday.
>
> Matt Levine, Money Stuff, May 19, 2020

On July 14, 2020 *Moderna* publishes positive Phase I data in the New England Journal of Medicine, highlighted by its vaccine candidate producing antibodies in all patients.

> The most interesting correlation in the stock market right now is the one between (1) the prices of airline stocks and (2) the amount of antibodies produced by coronavirus vaccine candidates in clinical trials. So far the vaccines are experimental and uncertain.

Covid Economics 61, 11 December 2020: 1-72

> If you knew that they'd work really well—protect everyone perfectly, no side effects, easy to produce, etc.—then you'd know with a pretty high degree of certainty that airline stocks (and cruise ships, hotels, casinos, retailers, etc.) would go up. If you knew that they'd be a disaster then you'd probably be short airlines.
>
> So on Tuesday Moderna announced good news, and yesterday:... Royal Caribbean Cruises Ltd. was up 21.2%. Norwegian Cruise Line Holdings Ltd. was up 20.7%. Carnival Corp. was up 16.2%. American Airlines Group Inc. was also up 16.2%. United Airlines Holdings was up 14.6%. The biggest gainers were the vaccine sensitive industries, not Moderna itself.
>
> Matt Levine, Money Stuff, July 16, 2020

On November 9, 2020 *Pfizer* and *BioNTech* announced positive news regarding interim analysis from their Phase III Study.

> Markets received a shot in the arm Monday from Pfizer Inc. and its encouraging Stage III tests on a COVID-19 vaccine. As a result, the S&P 500, the MSCI World and the MSCI All-World indexes all rose to records. But that misses the point of the impact. The news triggered the biggest single-day market rotation I've witnessed in the 30 years since I started covering markets...
>
> In technical terms, the clearest expression of the violence of the turnaround comes from tracking the performance of stocks that have had the greatest positive momentum, relative to the market. Bloomberg's measure of the pure momentum factor in the U.S. stock market shows that momentum dropped 4% Monday. Since Bloomberg started tracking daily moves in 2008, it had never before fallen as much as 2%.
>
> John Authers, Bloomberg Opinion, November 10, 2020
>
> Monday's news that a COVID-19 vaccine being developed by Pfizer and Germany's BioNTech was more than 90 per cent effective sent markets soaring. But it also prompted

Covid Economics 61, 11 December 2020: 1-72

an abrupt switch out of sectors that have prospered during the pandemic, such as technology, and into beaten-down stocks such as real estate and airlines — and triggered an earthquake in some popular investment "factors" such as value and momentum...

The value factor, which is centred on lowly-priced, unfashionable stocks, enjoyed a 6.4 per cent uplift, its strongest one-day gain since the 1980s, while the momentum factor — essentially stocks on a hot streak — tumbled 13.7 per cent, its worst ever loss, according to JPMorgan.

Laurence Fletcher and Robin Wigglesworth, Financial Times, November 14, 2020

A.2 News Articles from Section 3

Our duration estimates are based on projections from the pharmaceutical and financial press during 2020. For example, see (1) Damian Garde, STAT News, January 24, 2020, (2) Chelsea Weidman Burke, BioSpace, February 17, 2020, (3) Hannah Kuchler, Clive Cookson and Sarah Neville, Financial Times, March 5, 2020, (4) Bill Bostock, Business Insider, April 1, 2020, (5) Derek Lowe, Science Translational Medicine, April 15, 2020, (6) The Economist, April 16, 2020, (7) Nicoletta Lanese, Live Science, April 16, 2020, and (8) James Paton, Bloomberg, April 27, 2020.

B Vaccine Progress Indicator

This section describes the simulation procedure, data and parameters for the vaccine progress indicator.

B.1 Simulation Procedure

Start with N positively correlated vaccine candidates, with correlation matrix $\mathcal{R}$. Each candidate n is in a state $s \in S$, where

$$S = \{\text{failure, preclinical, phase 1, phase 2, phase 3,}$$
$$\text{application, approval, deployment}\}$$

and each state has known expected duration τ_s and baseline probability of success π_s^{base}.

Covid Economics 61, 11 December 2020: 1-72

Next we augment the state-level, baseline probability of successes with candidate-specific news. Let $\omega_{n,t} \in \Omega$ denote news published at time t about candidate n. For example, Ω could span positive data releases, negative data releases, next state announcements, etc. Then let $\Delta\pi :\rightarrow [-1,1]$ be a mapping from news to changes in probabilities. For each candidate, we cumulate the changes in probabilities from all news from the beginning of our sample t_0 up to time t,

$$\Delta\pi_{n,t}^{\text{news}} = \sum_{t'=t_0}^{t} \Delta\pi\left(\omega_{n,t'}\right). \tag{A.1}$$

Finally, we combine it with the baseline probability of success, resulting in a candidate-specific probability of success that potentially varies overtime, even within the same state,

$$\pi_{n,s,t}^{\text{total}} = \frac{\exp Y_{n,s,t}}{1+\exp Y_{n,s,t}} \tag{A.2}$$

where $Y_{n,s,t} = \log \frac{\pi_s^{\text{base}}}{1-\pi_s^{\text{base}}} + 2\Delta\pi_{n,t}^{\text{news}}$.

Figure A.1 outlines the simulation procedure. We simulate stage-by-stage progress of each candidate and generate the expected time to first vaccine deployment, similar to a first to "default" model. Specifically, on each day, one run of the simulation repeats steps one to three until candidates have all failed or deployed:

1. Draw two N-dimensional multivariate Normal random variables

$$z_t^u,\ z_t^d \sim \mathcal{N}(0,\mathcal{R}) \tag{A.3}$$

2. For each candidate, transform to exponentially driven time to success and failure,

$$t_{n,s,t}^u = -\frac{\log\Phi(z_{n,t}^u)}{\lambda_{n,s,t}^u} \quad \text{and} \quad t_{n,s,t}^d = -\frac{\log\Phi(z_{n,t}^d)}{\lambda_{n,s,t}^d} \tag{A.4}$$

where

$$\lambda_{n,s,t}^u = \frac{\pi_{n,s,t}^{\text{total}}}{\tau_s} \quad \text{and} \quad \lambda_{n,s,t}^d = \frac{1-\pi_{n,s,t}^{\text{total}}}{\tau_s} \tag{A.5}$$

3. If $t_{n,s,t}^u > t_{n,s,t}^d \implies$ candidate's run is over

Covid Economics 61, 11 December 2020: 1-72

If $t^u_{n,s,t} < t^d_{n,s,t} \implies$ candidate advances states, continue run

4. Calculate each candidate's time to vaccine deployment as

$$T_n = \begin{cases} \sum_s t^u_{n,s,t} & \text{candidate deploys} \\ \infty & \text{candidate fails} \end{cases}$$

5. Then calculate minimum time to vaccine deployment across candidates

$$T^*_m = \min_n T_n \tag{A.6}$$

That finishes one run of the simulation. Repeat for $M = 50{,}000$ runs and then advance to $t + 1$.

On each day across runs, we calculate the average

$$\mathbb{E}[T^*] = (1 - \mu)T^s_t + \mu T^f, \tag{A.7}$$

where some fraction, μ, of simulations will result in all candidates failing, so we incorporate T^f, an estimate of the expected time to first success by a project other than those currently active.

B.2 Data and Parameters

The simulation takes as input a timeline of COVID-19 vaccine candidates' stage-by-stage progress from the London School of Hygiene & Tropical Medicine.[1] For each of the 259 candidates, we observe the start dates of each pre-clinical and clinical trial, along with their vaccine strategy. Table A.1 breaks down the number of candidates at each state at the end of our sample. Vaccines typically take years of research and testing, and in an effort to accelerate the timeline, institutes have combined phases. Following Wong et al. (2018), we adopt each candidate's most advanced state. We also observe each candidate's vaccine strategy. Table A.2 summaries the main strategies along with the number of candidates following each.

Since candidates share a common virus target, and potentially common institutes or strategies,

[1]This version of the paper uses the timeline available on November 2, 2020.

we define pairwise correlations in an additive manner:

$$\rho(n,n') = \begin{cases} 0.2 & \text{baseline} \\ \text{add } 0.2 & \text{if shared institute} \\ \text{add } 0.1 & \text{if shared strategy} \end{cases}$$

for two candidates $n \neq n'$.

Table A.3 lists our parameter choices of state-level durations and baseline probabilities of success. Table A.4 summarizes the distribution of days spent in each state in our simulation. Following Wong et al. (2018), we adopt each candidate's most advanced state. We track days spent in each state until the next state starts, only among candidates that have successfully transitioned to the next state. The realized outcomes for state durations are reasonably consistent with our choices of parameters, in particular for Phase I and Phase II. And the standard deviations of durations are less than the mean is consistent with the Gaussian copula assumption of positively correlated outcomes.

We then augment π_s^{base} with 233 news articles from FactSet StreetAccount, split into positive and negative news types. Table A.5 lists the news types along with their changes in probabilities. Table A.6 shows the number of articles by news type, while Table A.7 shows the top ten candidates by news count. And finally, we set T^f equal to four years.

Covid Economics 61, 11 December 2020: 1-72

Figure A.1: Simulation Flow Chart

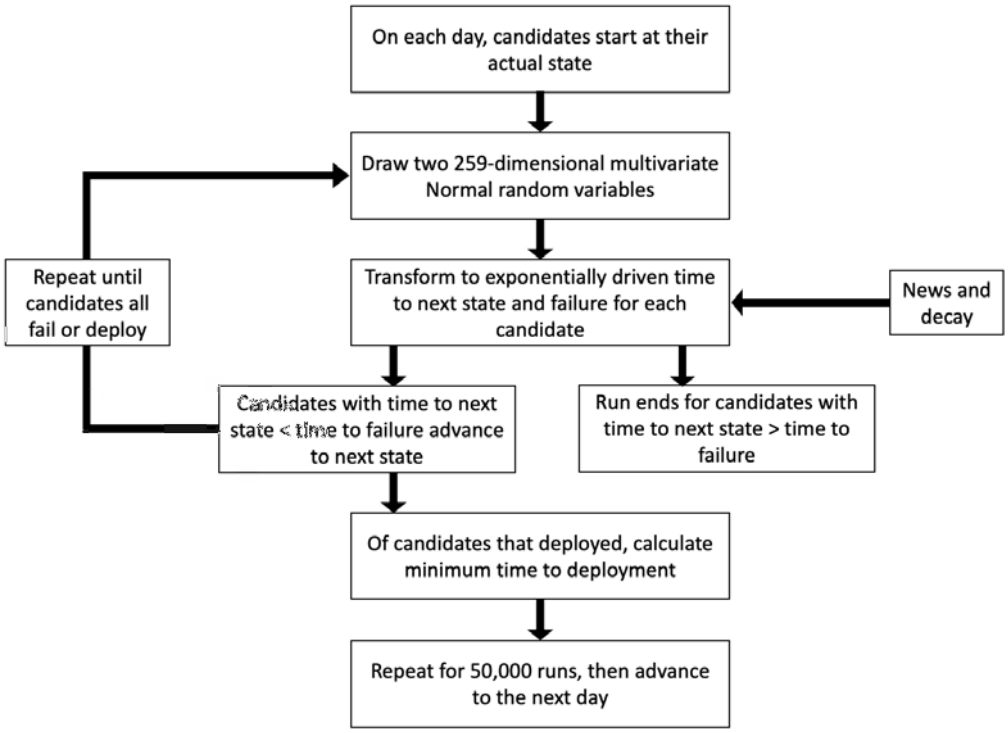

Note: Figure sketches the simulation procedure for estimating the expected time until vaccine deployment.

Covid Economics 61, 11 December 2020: 1-72

Table A.1: Vaccine States

State	# Candidates	Example Candidates
Preclinical	210	Amyris Inc Baylor College of Medicine Mount Sinai
Phase I Safety Trials	20	Clover/GSK/Dynavax CSL/University of Queensland Imperial College London
Phase II Expanded Trials	18	Arcturus/Duke Osaka/AnGes/Takara Bio Sanofi Pasteur/GSK
Phase III Efficacy Trials	11	AstraZeneca/Oxford BioNTech/Fosun/Pfizer Moderna

Note: Table describes the number of vaccine candidates in each state, along with example institutes. Data are from the London School of Hygiene & Tropical Medicine's COVID-19 Tracker. Data are as of November 2, 2020.

Covid Economics 61, 11 December 2020: 1-72

Table A.2: Vaccine Strategies

Type	Description	# Candidates
RNA (genetic)	Consist of messenger RNA molecules which code for parts of the target pathogen that are recognised by our immune system ('antigens'). Inside our body's cells, the RNA molecules are converted into antigens, which are then detected by our immune cells.	33
DNA (genetic)	Consist of DNA molecules which are converted into antigens by our body's cells (via RNA as an intermediate step). As with RNA vaccines, the antigens are subsequently detected by our immune cells.	21
Viral Vector	Consist of harmless viruses that have been modified to contain antigens from the target pathogen. The modified viruses act as delivery systems that display antigens to our immune cells. Replicating make extra copies of themselves in our body's cells. Non-replicating do not.	56
Protein	Consist of key antigens from the target pathogen that are recognised by our immune system.	78
Inactivated	Consist of inactivated versions of the target pathogen. These are detected by our immune cells but cannot cause illness.	16
Attenuated	Consist of living but non-virulent versions of the target pathogen. These are still capable of infecting our body's cells and inducing an immune response, but have been modified to reduce the risk of severe illness.	4

Note: Table describes the number of vaccine candidates in each strategy. 51 candidates have other, virus-like particle or unknown strategies. Data from the London School of Hygiene & Tropical Medicine's COVID-19 Tracker. Data as of November 2, 2020.

Covid Economics 61, 11 December 2020: 1-72

Table A.3: State Durations and Probabilities of Success

State	τ_s (years)	π_s^{base} (%)
Preclinical	0.6	5
Phase I	0.2	70
Phase II	0.2	44
Phase III	0.4	69
Application	0.1	88
Approval	0.5	95

Note: Table shows the duration and probability of success at each state.

Covid Economics 61, 11 December 2020: 1-72

Table A.4: Vaccine States

	Days in State				
	Min	Max	Mean	Median	SD
Preclinical	1.0	242.0	105.2	105.5	67.5
Phase I Safety Trials	17.0	103.0	51.9	27.0	39.8
Phase II Expanded Trials	6.0	152.0	86.8	89.0	54.5
Phase III Efficacy Trials	-	-	-	-	-

Note: Table shows statistics on the number of days spent in each state before transitioning to the next. Following Wong et al. (2018), we adopt each candidate's most advanced state. We track days spent in each state until the next state starts, among candidates that have successfully transitioned to the next state. Data are from the London School of Hygiene & Tropical Medicine's COVID-19 Tracker. Data are as of November 2, 2020.

Covid Economics 61, 11 December 2020: 1-72

Table A.5: News and Changes in Probabilities

Positive		Negative	
News type	$\Delta\pi$ (%)	News type	$\Delta\pi$ (%)
Announce next state	+5	Pause in state	-25
State ahead of schedule	+2	State behind schedule	-15
Release positive data	+5	Release negative data	-60
Positive regulatory action	+3	Negative regulatory action	-50
Positive preclinical progress	+1	Negative preclinical progress	-2
Positive enrollment	+1	Negative enrollment	-5
Dose starts	+1		
State resumes after pause	+5		

Note: Table shows the positive and negative news types, along with their changes in probabilities.

Covid Economics 61, 11 December 2020: 1-72

Table A.6: Number of Articles by News Type

News Type	Number of Articles
Release positive data	76
Announce next state	59
Positive regulatory action	22
Positive preclinical progress	20
Announce dosage start	21
Positive enrollment	15
State ahead of schedule	7
State resumed	5
State paused	4
State behind schedule	2
Negative regulatory action	1
Negative enrollment	1
Total	233

Note: Table shows the count of news articles by news type.

Covid Economics 61, 11 December 2020: 1-72

Table A.7: Number of Articles by Top 10 Candidates

Candidate	Number of Articles
Moderna	33
Oxford / AstraZeneca	21
Johnson & Johnson / Beth Israel Deaconess Medical Center	20
BioNTech / Fosun Pharma / Pfizer	19
Inovio Pharmaceuticals	17
Novavax	12
Arcturus / Duke	9
Vaxart	8
Medicago / GSK / Dynavax	7
Takis / Applied DNA / Evvivax	7

Note: Table the number of news articles for the top ten candidates by article count.

Covid Economics 61, 11 December 2020: 1-72

C Proofs to Section 4

C.1 Proof of Proposition 1

Proof. From the evolution of capital stock for the representative agent (16), we obtain the Hamilton-Jacobi-Bellman (HJB) equation as follows for each state $s \in \{1,\dots,S-1\}$

$$0 = \max_{C,l} \Big[f(C,\mathbb{J}(s)) - \rho\mathbb{J}(s) + \mathbb{J}_q(s)(l^\alpha q\mu - C) + \frac{1}{2}\mathbb{J}_{qq}(s) l^\alpha q^2\sigma^2 + \xi\left[\mathbb{J}(s)\left(q(1-\chi\Delta)\right) - \mathbb{J}(s)(q)\right] + \lambda_u(s)\left[\mathbb{J}(s+1)(q) - \mathbb{J}(s)(q)\right] + \lambda_d(s)\left[\mathbb{J}(s-1)(q) - \mathbb{J}(s)(q)\right]\Big] \tag{A.8}$$

Using the conjecture for the objective function (17) for $\mathbb{J}(s)$, calculating the derivatives with respect to q, $\mathbb{J}_q(s) = H(s)q^{-\gamma}$ and $\mathbb{J}_{qq}(s) = -\gamma H(s)q^{-\gamma-1}$, and differentiating with respect to labor l, we obtain the first-order condition as

$$\mathbb{J}_q(q)\alpha l^{\alpha-1}\mu q + \frac{1}{2}\mathbb{J}_{qq}(q)\alpha l^{\alpha-1}\sigma^2 q^2 - \mathbb{J}_q\left(q(1-\chi\Delta)\right)\xi\varepsilon\Delta q = 0 \tag{A.9}$$

where we have suppressed state s in the notation. This in turn simplifies to

$$\left[\frac{\alpha\left(\mu - \frac{1}{2}\gamma\sigma^2\right)}{\xi\varepsilon\Delta}\right] l^{\alpha-1} - [1-\chi\Delta]^{-\gamma} = 0 \tag{A.10}$$

where $\chi(l,L) = \kappa + \varepsilon l + KL$. In rational expectations equilibrium $L(s) = l(s)$, which gives us that optimal labor in pandemic state $L^\star(s)\ \forall s \in \{1,\dots,S-1\}$ satisfies (20):

$$\chi\left(L(s),L(s)\right) = \kappa + (\varepsilon+K)L(s) = \frac{1}{\Delta}\left[1 - (L(s))^{\frac{1-\alpha}{\alpha}}\nu\right] \tag{A.11}$$

where

$$\nu \equiv \left[\frac{\alpha\left(\mu - \frac{1}{2}\gamma\sigma^2\right)}{\xi\varepsilon\Delta}\right]^{-1/\gamma}. \tag{A.12}$$

The second-order condition with respect to l is satisfied (footnote 7, equation 19) whenever $\left(\mu - \frac{1}{2}\gamma\sigma^2\right) > 0$. For the non-pandemic state $s = 0$ or $s = S$, the third term in first-order condition (A.9) is absent; therefore, we obtain that labor is at the highest possible level $L(0) = L(S) = \bar{\ell}$, whenever

Covid Economics 61, 11 December 2020: 1-72

$\alpha\left(\mu - \frac{1}{2}\gamma\sigma^2\right) > 0.$ □

C.2 Proof of Propositions 2 and 3

Proof. Taking the first-order condition with respect to $C(s)$ in HJB equation (A.8), we obtain

$$f_c(C,\mathbb{J}(s)) - \mathbb{J}_q(s) = 0. \tag{A.13}$$

Using $f(C,\mathbb{J})$ from (14) and taking the derivative with respect to C, we obtain

$$f_c = \frac{\rho C^{-\psi^{-1}}}{[(1-\gamma)\mathbb{J}(s)]^{\frac{1}{\theta}-1}}, \tag{A.14}$$

which substituting for conjecture $\mathbb{J}(s)$ in equation (16) yields

$$f_c = \frac{\rho C^{-\psi^{-1}}}{H(s)^{\frac{\gamma-\psi^{-1}}{1-\gamma}} q^{\gamma-\psi^{-1}}}. \tag{A.15}$$

Then, for state $s \in \{0,\ldots,S\}$, we obtain by substituting $\mathbb{J}_q(s)$ in (A.13), and simplifying:

$$C(s) = \frac{H(s)^{-\theta\psi^{-1}} q}{\rho^{-\psi}}, \tag{A.16}$$

which proves Proposition 3.

To obtain the solution to state-by-state constants $H(s)$, we

1. substitute the optimal controls $\{C(s), L(s)\}$ into the HJB equation (A.8) for each s;
2. cancel the terms in q which have the same exponent; and
3. group terms not involving $H(s)$ constants into $g(\overline{\ell},0)$ for state $s = 0$ and $g(L(s),\xi)$ for state $s \in \{1,\ldots,S-1\}$

to reach equations (22) - (24). This system of recursive equations can then be solved numerically with the final condition in Proposition 2: $H(s) = H(0)$, that states 0 and S are both non-pandemic states. □

The detailed derivation of these equations for the two-state case ($S = 2$) is provided for illustration in the online appendix where we refer to the non-pandemic state 0 and 2 as "Off" state and

the pandemic state 1 as "On" state. □

C.3 Proof of Proposition 4

Proof. The value of a cure (vaccine) $V(s)$ satisfies:

$$\mathbb{J}(0)(q) = \mathbb{J}(0)\left[(1 - V(s))\, q\right] \tag{A.17}$$

where $\mathbb{J}(0)$ is evaluated at $(1 - V(s))\, q$. Substituting for $\mathbb{J}(s)$ from (17), we obtain

$$\frac{H(0)q^{1-\gamma}}{(1-\gamma)} = \frac{H(0)\left[(1 - V(s))\, q\right]^{1-\gamma}}{(1-\gamma)} \tag{A.18}$$

which yields

$$V(s) = 1 - \left(\frac{H(s)}{H(0)}\right)^{\frac{1}{1-\gamma}}. \tag{A.19}$$

Then, substituting for $C(s)$ from (25) and recognizing marginal propensity to consume, $c(s)$, equals $\frac{dC}{dq} = \frac{C(s)}{q}$, yields Proposition 4. □

D Asset Pricing

Proposition 5. *The price of the output claim is $P = p(s)q$ where the constants $p(s)$ solve a matrix system whose elements are given below. The system depends on the pandemic parameters through only two quantities, which may be taken to be the risk-neutral expected growth of output and g_1, defined in Section 4.*

Proof. To begin, we derive the pricing kernel and the risk-free rate. Under stochastic differential utility, the kernel can be represented as

$$\Lambda_t = e^{\int_0^t f_{\mathbb{J}} du} f_C \tag{A.20}$$

where

$$f(C, J) = \rho \frac{C^{\varrho}}{\varrho}\left((1-\gamma)\mathbb{J}\right)^{1-\frac{1}{\theta}} - \rho\theta\mathbb{J} \tag{A.21}$$

where $\varrho = 1 - \frac{1}{\psi}, \theta = \frac{1-\gamma}{\varrho}$. As shown in Section 4, the value function and the consumption flow

rates are:

$$\mathbb{J} = q^{1-\gamma} H(s)/(1-\gamma) \quad \text{and} \quad C = \rho^{\psi} H(s)^{e}\, q(s) q \tag{A.22}$$

where $e = \frac{1-\psi}{1-\gamma}$. Together these imply

$$f_C = \rho C^{\varrho-1} \left((1-\gamma)\mathbb{J}\right)^{1-\frac{1}{\theta}} \tag{A.23}$$

or

$$f_C = \rho \left(\rho^{\psi} H(s)^{e} q\right)^{\varrho-1} \left((1-\gamma)\left(q^{1-\gamma} H(s)/(1-\gamma)\right)\right)^{1-\frac{1}{\theta}}. \tag{A.24}$$

Simplifying, we get:

$$f_C = \rho^{1+\psi(\varrho-1)} H(s)^{e(\varrho-1)+\frac{\theta-1}{\theta}} q^{(\varrho-1)+\frac{(1-\gamma)(\theta-1)}{\theta}}. \tag{A.25}$$

The exponent of ρ is: $1+\psi(\varrho-1) = 1+\psi(-\frac{1}{\psi}) = 0$. The exponent of q is: $(\varrho-1)+\frac{(1-\gamma)(\theta-1)}{\theta}$. Substitute $\theta = \frac{1-\gamma}{\varrho}$ to get: $(\varrho-1)+\varrho(\frac{1-\gamma}{\varrho}-1) = -\gamma$. The exponent of $H(s)$ is

$$e(\varrho-1)+\frac{\theta-1}{\theta} \Rightarrow \frac{1-\psi}{1-\gamma}\left(-\frac{1}{\psi}\right)+\frac{1-\gamma\psi}{\psi(1-\gamma)} = 1 \tag{A.26}$$

Hence, $f_C = H(s) q^{-\gamma}$. Next, to evaluate $f_{\mathbb{J}}$, note that

$$f_{\mathbb{J}} = \rho \frac{C^{\varrho}}{\varrho}\left(1-\frac{1}{\theta}\right)\left[(1-\gamma)\mathbb{J}\right]^{-\frac{1}{\theta}}(1-\gamma) - \rho\theta \tag{A.27}$$

Plugging in for C and $\mathbb{J}$ we get:

$$f_{\mathbb{J}} = \rho \frac{\left(\rho^{\psi} H(s)^{e} q\right)^{\varrho}}{\varrho}\left(1-\frac{1}{\theta}\right)\left[(1-\gamma)\left(q^{1-\gamma} H(s)/(1-\gamma)\right)\right]^{-\frac{1}{\theta}}(1-\gamma) - \rho\theta \tag{A.28}$$

or

$$f_{\mathbb{J}} = \rho \frac{\left(\rho^{\psi} H(s)^{e} q\right)^{\varrho}}{\varrho}\left(\frac{\theta-1}{\theta}\right)\left[\left(q^{1-\gamma} H(s)\right)\right]^{-\frac{1}{\theta}}(1-\gamma) - \rho\theta. \tag{A.29}$$

Covid Economics 61, 11 December 2020: 1-72

This can be expressed as:

$$f_{\mathbb{J}} = \frac{1}{\varrho}\rho^{1+\psi\varrho}H(s)^{e\varrho}q^{\varrho}\left(\frac{\theta-1}{\theta}\right)(1-\gamma)q^{\frac{\gamma-1}{\theta}}H(s)^{-\frac{1}{\theta}} - \rho\theta. \tag{A.30}$$

Collecting terms:

$$f_{\mathbb{J}} = \frac{1}{\varrho}\rho^{1+\psi\varrho}H(s)^{e\varrho-\frac{1}{\theta}}q^{\varrho+\frac{\gamma-1}{\theta}}\left(\frac{\theta-1}{\theta}\right)(1-\gamma) - \rho\theta. \tag{A.31}$$

Here the exponent of ρ is : $1+\psi\varrho = \psi$, and the exponent of $H(s)$ is: $e\varrho - \frac{1}{\theta} = e\varrho - \frac{\varrho}{1-\gamma} = e$, and the exponent of q is: $\varrho + \frac{\gamma-1}{\theta} = 0$. Hence,

$$f_{\mathbb{J}} = \frac{1}{\varrho}\rho^{\psi}H(s)^{e}\left(\frac{\theta-1}{\theta}\right)(1-\gamma) - \rho\theta = \rho^{\psi}H(s)^{e}(\theta-1) - \rho\theta = c(s)(\theta-1) - \rho\theta. \tag{A.32}$$

So, we conclude that

$$\Lambda_t = e^{\int_0^t f_{\mathbb{J}}du}f_C = q^{-\gamma}H(s)e^{\int_0^t[c(s)(\theta-1)-\rho\theta]du}. \tag{A.33}$$

The riskless interest rate, $r(s)$ is minus the expected change of $d\Lambda/\Lambda$ per unit time. Applying Itô's lemma to the above expression yields drift (or dt terms)

$$c\,(\theta-1) - \rho\theta - \gamma(\ell^{\alpha}\mu - c) + \gamma(\gamma+1)\ell^{\alpha}\sigma^2 \tag{A.34}$$

where $\ell(0) = \bar{\ell} = 1$ and $\ell(s) = \ell^{\star}$ for $s > 0$. Note that the term $(\ell^{\alpha}\mu - c)$ is the drift of dq/q. To these terms we add the expected change from the jumps in the state s for $s = 0$:

$$\eta\left(\frac{H(1)}{H(0)} - 1\right) \equiv \tilde{\eta} - \eta \tag{A.35}$$

which serves to define the risk-neutral jump intenstity $\tilde{\eta}$. For $s > 0$ the expected jumps include both up and down changes in s as well as jumps in $q^{-\gamma}$:

$$\lambda_u\left(\frac{H(s+1)}{H(s)} - 1\right) + \lambda_d\left(\frac{H(s-1)}{H(s)} - 1\right) + \zeta((1-\chi\Delta)^{-\gamma} - 1) \equiv (\tilde{\lambda_u} - \lambda_u) + (\tilde{\lambda_d} - \lambda_d) + (\tilde{\zeta} - \zeta) \tag{A.36}$$

where the risk neutral intensities are defined as for η. The full expression for $r(0)$ is then

$$-\left\{c(0)\ (\theta-1)-\rho\theta-\gamma(\mu-c(0))+\gamma(\gamma+1)\sigma^2+(\tilde{\eta}-\eta)\right\}. \tag{A.37}$$

For $s>0$ we have $r(s)$ as

$$-\left\{c(s)(\theta-1)-\rho\theta-\gamma((\ell^\star)^\alpha\mu-c(s))+\frac{1}{2}\gamma(\gamma+1)(\ell^\star)^\alpha\sigma^2+(\tilde{\lambda_u}-\lambda_u)+(\tilde{\lambda_d}-\lambda_d)+(\tilde{\zeta}-\zeta))\right\}. \tag{A.38}$$

We return to these expressions after deriving the pricing equation for the output claim.

By the fundamental theorem of asset pricing, the instantaneous expected excess return to the claim $P(q,s)$ must equal minus covariance of the returns to P with the pricing kernel. Deriving these two quantities and setting them equal yields the pricing system, to which the proof will construct the solution.

The expected excess return to the claim $P(q,s)$ is the sum of its expected capital gain and its expected payout, minus rP. In the nonpandemic state, this is

$$\frac{1}{2}\sigma^2q^2P_{qq}(q,0)+(\mu-c(0))qP_q(q,0)+\eta(P(q,1)-P(q,0))+\mu q-r(0)P(q,0) \tag{A.39}$$

whereas in the pandemic states it is

$$\begin{aligned}&\frac{1}{2}(\ell^\star)^\alpha\sigma^2q^2P_{qq}(q,s)+((\ell^\star)^\alpha\mu-c(s))qP_q(q,s)\\&+\lambda_u(P(q,s+1)-P(q,s))+\lambda_d(P(q,s-1)-P(q,s))+\zeta(P((1-\chi\Delta)q,s)-P(q,s))\\&+\mu(\ell^\star)^\alpha q-\zeta\chi\Delta q-r(s)P(q,s).\end{aligned} \tag{A.40}$$

Next, we need to derive the covariance of the returns to P with $d\Lambda/\Lambda$. As mentioned in the text, in addition to the usual contribution of covariance from the capital gains dP/P, the covariance also includes the contribution from the dividends themselves, which are risky in this model. There

are also contributions from both Brownian comovement and co-jumps in q and s. The Brownian terms are

$$-\gamma(\ell^\star)^\alpha\sigma^2[qP(q,s)-q] \tag{A.41}$$

for $s>0$, or just $-\gamma\sigma^2[qP-q]$ for $s=0$. The co-jump terms for $s>0$ are

$$\begin{aligned}&\zeta[P((1-\chi\Delta)q,s)-P(q,s)-\chi\Delta q]\,[(1-\chi\Delta)^{-\gamma}-1]\\&+\lambda_u[P(q,s+1)-P(q,s)]\left[\frac{H(s+1)}{H(s)}-1\right]+\lambda_d[P(q,s-1)-P(q,s)]\left[\frac{H(s-1)}{H(s)}-1\right]\end{aligned} \tag{A.42}$$

or

$$\begin{aligned}&[P((1-\chi\Delta)q,s)-P(q,s)-\chi\Delta q]\,[\tilde{\zeta}-\zeta]\\&+[P(q,s+1)-P(q,s)][\tilde{\lambda_u}-\lambda_u]+[P(q,s-1)-P(q,s)][\tilde{\lambda_d}-\lambda_d].\end{aligned} \tag{A.43}$$

For $s=0$ the corresponding expression is just

$$[P(q,1)-P(q,0)][\tilde{\eta}-\eta]. \tag{A.44}$$

We now equate the expected excess return to minus the above covariance to obtain the difference/differential equation system that P must solve. Rather than repeating the general expressions, we instead conjecture that the the solutions are linear in q and deduce the resulting system. Under linearity $P_{qq}=0$ and $P_q=p$, a constant that depends on s.

Plugging in the conjectured form, and cancelling a q, in states $s>0$ the pricing equation says

$$\begin{aligned}&((\ell^\star)^\alpha\mu-c(s))p(s)+\lambda_u(p(s+1)-p(s))+\lambda_d(p(s-1)-p(s))-\chi\Delta\zeta p(s)+\mu(\ell^\star)^\alpha-\zeta\chi\Delta-r(s)p(s)\\&-\gamma(\ell^\star)^\alpha\sigma^2[p(s)+1]-\chi\Delta[p(s)+1]\,[\tilde{\zeta}-\zeta]+[p(s+1)-p(s)][\tilde{\lambda_u}-\lambda_u]+[p(s-1)-p(s)][\tilde{\lambda_d}-\lambda_d]\\&=0.\end{aligned} \tag{A.45}$$

Covid Economics 61, 11 December 2020: 1-72

Leaving the constant terms on the left, the right side consists of

$$p(s+1) \quad \text{terms:} \quad -\lambda_u - [\tilde{\lambda_u} - \lambda_u] = -\tilde{\lambda_u}, \tag{A.46}$$

$$p(s-1) \quad \text{terms:} \quad -\lambda_d - [\tilde{\lambda_d} - \lambda_d] = -\tilde{\lambda_d}, \tag{A.47}$$

and $p(s)$ terms:

$$-((\ell^\star)^\alpha \mu - c(s)) + \lambda_u + \lambda_d + \chi\Delta\zeta + r(s) + \gamma(\ell^\star)^\alpha\sigma^2 + \chi\Delta[\tilde{\zeta} - \zeta] + [\tilde{\lambda_u} - \lambda_u] + [\tilde{\lambda_d} - \lambda_d] \tag{A.48}$$

or

$$r(s) + c(s) - (\ell^\star)^\alpha(\mu - \gamma\sigma^2) + \tilde{\lambda_u} + \tilde{\lambda_d} + \chi\Delta\tilde{\zeta}. \tag{A.49}$$

The remaining constants on the left are

$$\mu(\ell^\star)^\alpha - \zeta\chi\Delta - \gamma(\ell^\star)^\alpha\sigma^2 - \chi\Delta[\tilde{\zeta} - \zeta]. \tag{A.50}$$

or

$$(\ell^\star)^\alpha(\mu - \gamma\sigma^2) - \chi\Delta\tilde{\zeta}. \tag{A.51}$$

The above equations define a linear system for $p(1)$ to $p(S-1)$. The pricing equation for $s = 0$ says

$$(\mu - c(s))p(0) + \eta(p(1) - p(0)) + \mu - r(0)p(0) - \gamma\sigma^2[p(0) + 1] + [p(1) - p(0)][\tilde{\eta} - \eta] = 0, \tag{A.52}$$

or

$$\mu - \gamma\sigma^2 = p(0)[r(0) + c(0) - (\mu - \gamma\sigma^2) + \tilde{\eta}] - p(1)\,\tilde{\eta}. \tag{A.53}$$

This equation closes the system on the low end. At the high end, the system is closed via $p(S) = p(0)$.

Covid Economics 61, 11 December 2020: 1-72

Altogether the system may be written in matrix form,

$$\begin{bmatrix} r(0)+c(0)-(\mu-\gamma\sigma^2)+\tilde{\eta} & -\tilde{\eta} & 0 & \cdots \\ -\tilde{\lambda_d} & r(s)+c(s)-(\ell^\star)^\alpha(\mu-\gamma\sigma^2)+\chi\Delta\tilde{\zeta}+\tilde{\lambda_d}+\tilde{\lambda_u} & -\tilde{\lambda_u} & 0 \\ 0 & \ddots & \ddots & \ddots \\ \vdots & \ddots & \ddots & \ddots \\ -\tilde{\lambda_u} & 0 & \cdots & \end{bmatrix} p = \begin{bmatrix} (\mu-\gamma\sigma^2) \\ (\ell^\star)^\alpha(\mu-\gamma\sigma^2)-\chi\Delta\tilde{\zeta} \\ \vdots \\ \vdots \\ \vdots \end{bmatrix}.$$

Assuming the parameters are such that the right-hand matrix is of full rank, the system has a unique, finite solution. Since the output flow being priced is not guaranteed to be positive, it need not be the case that the price of the claim is positive either.

Finally, the proposition also identifies a minimal set of parameters that characterize the system. It has been shown that the value function solution functions $H(s)$ and consumption propensities $c(s)$ depend only on the pandemic parameters $\alpha, k, K, \epsilon, \zeta, \Delta, \chi$, and $\ell^\star$ (the latter two of which are endogenous) via the important variable we have called g_1. The pricing system explicitly references $\alpha, \zeta, \Delta, \chi$, and $\ell^\star$. We now show that the equations can be written in terms of g_1 and one additional combination of these variables.

In fact, the second combination of parameters is the constant term on the right hand side, $(\ell^\star)^\alpha(\mu-\gamma\sigma^2)-\chi\Delta\tilde{\zeta}$, which may be seen to be the risk-neutral expected outpu per unit time in the pandemic. So it suffices to show that the diagonal term can be written solely in terms of g_1.

To do this, it is necessary to unpack the dependence of the riskless rate on the parameters. From above, the diagonal coefficient for $s > 0$ is

$$r(s)+c(s)-(\ell^\star)^\alpha(\mu-\gamma\sigma^2)+\chi\Delta\tilde{\zeta}+(\tilde{\lambda_u}-\lambda_u)+(\tilde{\lambda_d}-\lambda_d)+(\lambda_u+\lambda_d) \tag{A.54}$$

And $r(s)$ is

$$-[c(s)\ (\theta-1)-\rho\theta-\gamma((\ell^\star)^\alpha\mu-c(s))+\frac{1}{2}\gamma(1+\gamma)(\ell^\star)^\alpha\sigma^2+(\tilde{\lambda_u}-\lambda_u)+(\tilde{\lambda_d}-\lambda_d)+(\tilde{\zeta}-\zeta)]. \tag{A.55}$$

Covid Economics 61, 11 December 2020: 1-72

Collecting terms, we have

$$\rho\theta + [(1-\theta)+(1-\gamma)]c(s) + [\lambda_u + \lambda_d] - (\tilde{\zeta} - \zeta) + \chi\Delta\tilde{\zeta} - (\ell^\star)^\alpha(1-\gamma)\mu + (\ell^\star)^\alpha(\gamma - \frac{1}{2}\gamma(1+\gamma)). \tag{A.56}$$

Recall that we defined

$$g_1 = \rho\theta - (\ell^\star)^\alpha(1-\gamma)(\mu - \frac{1}{2}\gamma\sigma^2) - \zeta((1-\chi\Delta)^{1-\gamma} - 1). \tag{A.57}$$

Then note that $\gamma - \frac{1}{2}\gamma(1+\gamma) = -\frac{1}{2}\gamma(1-\gamma)$, and that

$$\zeta((1-\chi\Delta)^{1-\gamma} - 1) = \zeta((1-\chi\Delta)(1-\chi\Delta)^{-\gamma} - 1) \tag{A.58}$$

$$= \zeta((1-\chi\Delta)^{-\gamma} - 1) + \zeta\chi\Delta(1-\chi\Delta)^{-\gamma} \tag{A.59}$$

$$= \tilde{\zeta} - \zeta - \chi\Delta\tilde{\zeta}. \tag{A.60}$$

Using these, the expression for the coefficient becomes

$$g_1 + [(1-\theta)+(1-\gamma)]c(s) + [\lambda_u + \lambda_d]. \tag{A.61}$$

This establishes the claim.

□

Are banks catching corona? Effects of COVID on lending in the US

Thorsten Beck[1] and Jan Keil[2]

Date submitted: 2 December 2020; Date accepted: 2 December 2020

We exploit geographic variation in the exposure of US banks to COVID-19 and lockdown policies to document the impact of the pandemic and consequent economic crisis on banks. Combining county-level data on COVID-19 and lockdown policies with bank-level data on loan performance and lending growth, and syndicated loan data, we document that banks geographically more exposed to the pandemic and lockdown policies show (i) an increase in loan loss provisions and non-performing loans, (ii) an increase in lending to small businesses, but not in other lending categories, and (iii) an increase in interest spreads and decrease in loan maturities. These findings show that banks have already seen the negative impact of the pandemic and have reacted to higher lending risk with an adjustment in loan conditionality, but have also responded to higher loan demand and government support programmes.

Covid Economics 61, 11 December 2020: 73-120

1 Professor of Banking and Finance; The Business School (formerly Cass), City, University London and CEPR.
2 Research Associate; Humboldt Universität zu Berlin, School of Business and Economics.

Covid Economics 61, 11 December 2020: 73-120

I. Introduction

The COVID-19 pandemic has hit the U.S. economy fast and hard. Unemployment claims spiked up in the first half of 2020 at an unprecedented speed. While such a shock is unlikely to leave banks unaffected, equity buffers have improved significantly since the 2007 financial crisis and fiscal, monetary and regulatory policy responses were swift and radical. In this paper we examine if and how banks' health is affected and if there have been changes in lending growth and loan conditionality. Our results can shed light on how deep and long the trough and how speedy the economic recovery will be after the shockwave, both of which depend crucially on liquidity provision by financial intermediaries.

While negative economic shocks have often quick effects on loan performance and should thus be reflected in non-performing loans (NPL) and loan loss provisions, regulatory easing might counter these negative effects, at least to a certain extent. And while economic recessions and crises often result in a drop in demand for and supply of loans, the COVID-19 crisis shows unique characteristics in its effect on both real economy and financial system. Drops in aggregate demand have been swift but temporary, related to both the fear of contagion and to lockdown restrictions, resulting in an increase rather than decrease in corporate loan demand, as companies in affected sectors require liquidity for survival. Similar, while higher uncertainty and lower risk appetite tends to reduce loan supply during such a crisis, aggressive monetary and regulatory policy measures, combined with loan guarantees by government counter some of these effects. It is thus an empirical question how bank lending has reacted to the pandemic.

This paper combines county-, bank-, and loan-level data from several sources to provide a first assessment of the effect of COVID-19 and lockdown policies on the banking system, exploiting variation in pandemic outbreaks and lockdown policies

across U.S. counties. Our results suggest that both COVID outbreaks and lockdowns are associated with increases in unemployment and worse loan performance. COVID outbreaks and lockdown policies are also associated with higher small business lending growth but not growth in other lending types. Finally, we find that COVID outbreaks are associated with higher interest spreads and shorter maturities in syndicated lending, suggesting a higher risk premium and tighter conditionality.

The U.S. offers a unique laboratory to test the impact of the pandemic and policy reactions. COVID-19 outbreaks were initially concentrated in urban centers on both coasts before the pandemic moved Mid-West and ultimately into the South and Southwest. Given the variation in regional exposure of banks, different banks were affected to a different degree by the pandemic as well as at different points in time. Similarly, state and county governments across the U.S. have shown quite some variation in lockdown policies. Over the course of 2020 there has been thus a wide variation across different parts of the country in terms of pandemic impact, which we can use to look beyond general trends to link COVID-19 to bank- and loan-level outcomes. As in many other advanced countries, fiscal, monetary and regulatory authorities have reacted swiftly and resolutely to the crisis, including one-time tax rebates, extended unemployment benefits, loan (guarantees), some of them specifically targeted at small businesses, lowering the federal funds rate to 0-0.25%, a variety of funding facilities targeted at commercial paper and corporate credit issuers and dealers and issuers of small business loans, among others, lowering of regulatory capital and liquidity buffers and easing of loan classification requirements.[1]

Theory and evidence from previous crises provide contradictory evidence on whether macroeconomic shocks result in lending retrenchment or not. On the one hand, theory and evidence suggests lending retrenchment, due to dropping collateral values and thus increasing agency conflicts (Gertler & Bernanke, 1989) or due to losses re-

[1] For more detail, see this cross-country compilation by the IMF on Policy Responses to COVID-19.

Covid Economics 61, 11 December 2020: 73-120

ducing bank capital and banks' limited ability to raise additional capital (see Ivashina & Scharfstein, 2010; Cornett, McNutt, Strahan & Tehranian, 2011). However, Kahle & Stulz (2013) find no evidence for a credit supply shock during the Global Financial Crisis, but rather evidence for a demand reduction. And while Ivashina & Scharfstein (2010) show a sharp downturn in syndicated lending from mid-2007 onwards, they also show an increase in C&I loans on the aggregate balance sheet of the U.S. banking sector between September and October 2008, due to drawdown of credit lines. Similarly, initial evidence from the current shock suggests that loan demand has increased substantially, with many firms drawing down credit lines or tapping capital markets (Acharya & Steffen, 2020). At the same time and as described above, there have been aggressive measures by central banks to encourage banks to keep lending to the real economy, while they also mitigated to an extent an immediate deterioration of loan performance. It is thus a-priori not clear whether the reaction of banks will be the same during the current as during previous crises. While the evidence on lending growth is thus ambiguous, it points more clearly to an increase in interest spreads, related to reduced net worth of borrowers (and thus collateral value), higher funding costs for banks, and increased uncertainty (see Santos (2010) for evidence from the Global Financial Crisis). A similar effect can be expected in the context of the current crisis, related to lower asset prices and lower revenue streams reducing net worth of borrowers, while increasing demand for liquidity by firms.

Our first set of results shows that unemployment rates (the most accurate and most rapidly available indicator of economic activity) co-varies significantly across counties in the US in the first three quarters of 2020 with COVID outbreaks and lockdown policies. While not a focus of our work, our results thus also speak to the discussion on whether it is COVID outbreaks and/or lockdown policies that are responsible for the drop in economic activity we have observed. Taking unemployment as the most accurate regularly and quickly published economic activity gauge, we find that both

Covid Economics 61, 11 December 2020: 73-120

COVID outbreaks and lockdown policies have dampened economic activity.

Our second set of results show that the increase in loan loss provisions over 2020 can be related to banks' exposure to COVID-19 outbreaks and lockdown policies, while the results are somewhat less robust for non-performing loans (NPLs). This increase in loan loss provisions and NPLs is primarily driven by household loans. At the same time, banks have been expanding lending in response to COVID-19, though primarily to small businesses.

Our third set of results shows that banks more affected by the COVID increased interest spreads on syndicated loans; interestingly, this is driven by exposure to COVID outbreaks rather than to lockdown policies. Similarly, we find that such banks grant shorter maturity loans, although this finding is somewhat less robust.

Our paper is related to a small literature on the effect of COVID-19 on the banking system. Specifically, using bank regulatory filings Li, Strahan & Zhang (2020) document the largest ever liquidity demand by firms drawing down preexisting credit lines; banks were able to accommodate the liquidity demand due to cash inflows from the Fed and from depositors. Using loan-level data, Greenwald, Krainer & Paul (2020) show that bank lending increased following the March 2020 U.S. COVID-19 outbreak, concentrated on C&I lending, and in the form of credit line draw-downs. Halling, Yu & Zechner (2020) gauge U.S. firms' access to public capital markets and show that particularly highly rated firms issued public debt after the onset of the pandemic, but substantially less equity. Focusing on the firm-side, Acharya & Steffen (2020) show that while AAA-A-rated firms raised cash through bond and equity issuances (in addition to credit line drawdowns), BBB-rated firms mainly increased cash holdings through credit line drawdowns and term loan issuances; non-investment grade and unrated firms had to rely fully on credit-line drawdowns and term loans from banks. Chodorow-Reich, Darmouni, Luck & Plosser (2020) show that the increase in bank credit in the first two quarters of 2020 are almost completely due to drawdowns

Covid Economics 61, 11 December 2020: 73-120

Covid Economics 61, 11 December 2020: 73-120

by large firms of lines of credit.[2] Our paper adds to this literature by considering a larger time horizon, through 30 September 2020, exploiting cross-bank exposure to the pandemic and lockdown measures and gauging the impact on loan performance, lending growth and loan conditionality.[3]

Our paper is also related to a more established literature on the transmission of macroeconomic shocks through credit markets. Gertler & Gilchrist (1993) show a rise in credit following contractionary monetary shocks, and also argue that this increase is biased toward larger firms. Using loan-level data and a structural model Greenwald et al. (2020) do not only look at the COVID-19 shock but also identified monetary policy shock based on the approach of Romer & Romer (2004) and show an increase in overall lending after shocks, due to a credit line draw-downs, while term lending to smaller firms drops. We add to this literature by focusing specifically on the COVID shock but looking both at bank-level lending and loan-level conditionality and exploiting cross-bank exposure to the pandemic.

While our results are for the U.S., they offer important lessons for other advanced countries in terms of the impact of the pandemic and lockdown policies on banking systems. Before proceeding, we would like to stress the tentative nature of our exercise. Rather than testing different contrasting hypotheses, our analysis is mostly descriptive in documenting the impact of the pandemic on the banking system. And while we can differentiate across banks according to their exposure to the pandemic and – separately – to lockdown policies, we cannot separate out the effect of federal support policies.

The remainder of the paper is organised as follows. The next section introduces

[2] Duchin & Hackney (2020) show that firms with prior lending relationships or personal connections to bank executives are more likely to obtain Paycheck Protection Program loans. Darmouni & Siani (2020) show that corporate bond issuance is used to increase holdings of liquid assets rather than for real investment and that most issuers, including many riskier "high-yield" firms, prefer issuing bonds to borrowing from their bank.

[3] Hasan, Politsidis & Sharma (2020) also focus on the pricing of syndicated loans, but in a cross-country setting and using a text-based approach based on transcripts of quarterly conference calls held by companies. Similar to us, they find an increase in interest spreads for higher firm and lender exposure to the pandemic.

the different data sources and variables we use in our analysis. Section III provides evidence on the relationship between COVID-19 and unemployment across U.S. counties. Section IV presents bank-level regressions on the effect of COVID-19 on loan performance and lending, while Section V uses loan-level data to assess the impact of COVID-19 on interest spreads and maturities of syndicated loans. Section VI concludes.

II. Data and Variables

We combine data from a number of data sources to assess the impact of COVID-19 and lockdown policies on real economy and banking system in the US. Descriptive statistics for all the variables used in county, bank, and loan level analyses are in tables A1, A2, and table A3 in the appendix, respectively, while we present the most important variables in Table 1.

A. COVID-19 and lockdown policies

In our first set of tests we gauge the impact of the pandemic and policy responses on unemployment across 3,142 counties in the US. We capture exposure to the pandemic by COVID-19 related deaths per 100,000, based on data from the New York Times, except for the 5 counties that are part of New York City, which the New York Times sums up into one metropolitan aggregate. For consistency we use CDC data for these counties. Population data come from the U.S. Census. Observations are per county and either 2020 cumulative deaths or the number of new deaths in a quarter. In county regressions we use the logarithm of 1 + the number of deaths per 100,000 inhabitants. The descriptive statistics in Table 1 shows an increase in the average COVID-19 deaths from 0.5 per 100,000 in the first quarter to 17 in the second quarter to 26.8 in the third quarter, but with significant variation across counties.

Covid Economics 61, 11 December 2020: 73-120

To capture lockdown policies, we use the non-pharmaceutical intervention (NPI) index from Olivier Lejeune. The NPI index is defined on the state level (there is little to no variation within states), ranging from 0 (no or few containment measures in place) to 6 (harsh lockdown where citizens are not allowed to come out of their home). The descriptive statistics in Table 1 shows an increase in the average NPI from 0.7 in the first quarter to 3.2 in the second quarter and a decline to 1.7 in the third quarter, but again with significant variation across states and thus counties.

Not surprisingly, there is a high correlation between COVID-deaths and NPI of 0.624 (see Appendix Table A4) and we therefore run regressions where we introduce the two variables separately and regressions where we include them together.

We rely on unemployment data comes from BLS Local Area Unemployment Statistics. While the average over the three quarters is 5.5%, it ranges from a 10th percentile of 2.7% to a 90th percentile of 10%.

Other county level controls are from Jie Ying Wu's COVID-19 database and from 2019. We include the number of ICU beds, persons older than 65, the share of African-American and hispanics (all weighted by total county population), median income, population density, 2-digit NAICS and government employment shares.

B. Bank-level data

In our second set of regressions, we focus on a sample 1,293 banks and their loan losses and lending growth. We construct a measure of bank exposure to deaths and NPIs from bank branch deposit distributions, and thus only use banks with a "significant branch network". This excludes, for example, de-facto investment banks like Goldman Sachs, or any bank with $10 billion or more in assets but less than 10 branches, banks with $5 billion or more and less than 5 branches, $3 billion or more and less than 3 branches, or $1 billion or more and only 1 branch. Observations are excluded if zero or missing values are reported for total bank assets, equity capital, deposits, income,

Covid Economics 61, 11 December 2020: 73-120

total loans and leases, loan loss provisions, or unused commitments outstanding.

For bank level exposure to COVID-19 deaths, we compute the "average exposure" to areas in which the bank is physically present, using 2019 bank branch deposit shares in total bank deposits as weights for each county, using data from the Federal Deposit Insurance Corporation's Summary of Deposits. We illustrate this idea visually with the examples of Citibank and Zions Bancorp in Q2 2020 in Figure 5. Citi branches (red dots) are concentrated in city centers, with a particularly heavy exposure to the New York City metropolitan area – the early epicenter of the U.S. pandemic. Zions (blue circles) is a counter example, operating a relatively dispersed network of locations across the western U.S. with presence in rural areas and cities less affected by COVID in the first half of 2020.[4] Computed on the bases of new Q2 deaths, this exposure amounts to 67 for Citibank and 13 for Zions. Table A5 in the appendix lists the 35 largest U.S. banks in the sample with their respective COVID exposures. Appendix Figure A1 shows the branch and deposit intensity across the US.

Other bank level variables are from the Federal Financial Institutions Examination Council's Call Reports. To increase observation counts in the loan level analysis, total assets and deposits come from Summary of Deposits and not Call Reports.

We use a number of variables as dependent variables. First, we use growth in loan loss provisions and NPLs, both relative to total loans and leases and measured for each quarter to gauge the effect of the crisis and policy responses on banks' loan losses. Growth in loan loss provisions relative to the corresponding pre-year quarter varies between -100% (10th percentile) and 137% (90th percentile), with a mean of 13.6%, while growth in NPLs varies between -88% and 103%, with a mean of 3.6%. Second, we use the growth in loans and leases to test the effect of the pandemic and policy responses on banks' lending activities. Over our sample period, loan growth varied between -1.2% (10th percentile) and 19.5% (90th percentile), with a mean of 8.3%.

[4]Notable overlaps are only in California and Las Vegas.

Covid Economics 61, 11 December 2020: 73-120

We also consider growth in three categories of lending: commercial and industrial loans including loans secured by commercial real estate (all C&I loans are included irrespectively of their size); household loans including loans secured by real estate and not assigned to C&I or agricultural loans; finally, small business loans, defined as in Call Reports filings and including small C&I and small agricultural loans (with an original amount of 1 million or less).

Bank controls in tables 3-4 are the logarithm of total assets, income, equity, deposits, liquidity, unused commitments, and loans and leases in percent of total assets. All bank controls are from the respective pre-year quarter.

C. *Loan-level data*

In our final set, we focus on syndicated loan data to gauge the effect of the pandemic and policy reactions on loan conditionality. Loan level data come from the Thompson Reuters LPC's DealScan database and company level data are from DealScan and Standard & Poor's Compustat. We use the DealScan-Compustat linking table used in Chava & Roberts (2008) and made available on Michael Robert's homepage to match borrowers in both databases. We also use an updated version of the link extension for their table from Keil (2018) to match DealScan borrowers to Compustat firms for years after 2016. To match banks from DealScan to their financial information from Call Reports and Summary of Deposits we created a linking table where we fuzzy-matched via name similarity scores, location, year, and other information contained in both files (table, algorithm, and additional technical details are available upon request). Following Bharath, Dahiya, Saunders & Srinivasan (2011); Schwert (2018, 2020) a "loan" refers to a "facility" in DealScan. Our broadest estimation sample contains 13,150 loans over the period 2017 Q1 to 2020 Q2.[5]

We focus on maturity in months and interest rate spread over LIBOR, defined as

[5]Unlike for county and bank-regressions, third quarter 2020 data were not available yet.

Covid Economics 61, 11 December 2020: 73-120

the all-in-spread, which is the amount paid by borrowers in basis points for each dollar that is actually drawn-down. The interest rate spread varies from 113 (10th percentile) to 400 (90th percentile), with a mean of 233 basis points. The maturity varies from 19 (10th percentile) to 69 months (90th percentile), with a mean of 51 months.

Basic bank controls come from Summary of Deposits as they are available for a considerably larger number of banks than the Call Reports and are matched to DealScan in loan level estimations. They include the logarithm of total assets and deposits over total assets. Loan type fixed effects are for term loans, revolving credit lines, and other (or loans classified as both). Detailed loan controls comprise of the respectively left out loan term, the logarithm of loan volume, fixed effects for loan purpose, collateral, and refinanced loans.

III. Economic Impact of COVID-19 across U.S. Counties

The pandemic has had adverse affects on the U.S. economy. In our first empirical analysis, we assess the impact of COVID-19 on local economies across the US. We also differentiate between the impact of national trends, geographic variation in COVID outbreaks and non-pharmaceutical interventions (NPI) on local economies. As a graphic illustration of the regional variation, Figures 1, 2, and 3 chart quarterly county level exposures to new COVID-19 related deaths (per 100,000 inhabitants), state level NPIs, and county level unemployment rates in the first three quarters of 2020 across contiguous U.S. counties (Panels A, B, and C, respectively). Figure 1 illustrates the spread of COVID-19 and shows that COVID deaths were initially concentrated around population centers, especially along coastal areas and the Great Lakes in Q2, before moving increasingly South and Southwest in Q3.[6] Figure 2 shows that NPIs have been tougher in the North and Northeast and were dramatically higher in Q2 than before or after.

[6] Appendix Figure A4 shows a similar pattern of COVID-19 infections.

Covid Economics 61, 11 December 2020: 73-120

Similarly, Figure 3 shows that unemployment rates were the highest in Q2 and elevated especially along costal areas and the Northeast.

Figure 4 Panel A confirms the positive correlation between unemployment and COVID-19 death suggested by the geospatial plots, charting the median monthly unemployment rates over the period March 2019 to September 2020 for U.S. counties with zero deaths and in counties with cumulative Q3 2020 COVID-19 related deaths per 100,000 inhabitants above the median of counties with more than zero deaths. While there is no clear difference in unemployment rates between these two groups until March 2020, counties hit hard by COVID death rates experience much steeper and more persistent increases in unemployment rates than counties without COVID-19 deaths. Panel B shows similar adverse effects of NPIs on economic activities, splitting counties into those below and above the median NPIs in the first three quarters of 2020.

As these results may be driven by other factors, such as population density, infrastructure (travel hubs vs. remote and isolated areas), or clustering of economic sectors (sectors with different cyclicality or import dependence) that correlate with COVID-19 deaths and economic losses, we next turn to regression analysis. Specifically, we run the following regression to assess the impact of COVID-19 deaths and NPIs on unemployment across counties and over the period Q1 2019 to Q3 2020:

$$\begin{aligned} Unempl.\ Rate_{c,t} =& \beta_1 Q1\ 2020_t + \beta_2 Q2\ 2020_t + \beta_3 Q3\ 2020_t + \beta_4 COVID\ Deaths_{c,t} \\ &+ \beta_5 NPI\ Index_{c,t} + \gamma \boldsymbol{X_c} + \eta_t + \delta_c + \epsilon_{c,t}. \end{aligned} \tag{1}$$

where subscripts c and t indicate counties and quarters. In some specifications, we control for pre-crisis population density, employment shares in different sectors, demographic characteristics, income, ICU bed density (in $\boldsymbol{X_c}$), while in others we absorb local factors in county fixed effects, δ_c. We include quarter-fixed effects η_t, but fo-

cus our attention on the estimates for the Q1, Q2 and Q3 2020 fixed effects (included separately for emphasis in regression 1), with Q4 2019 being the omitted period. We include COVID related death rates and an NPI index jointly or separately, as the two variables are highly correlated (Appendix Table A4). Standard errors $\epsilon_{c,t}$ are clustered on the county level.

Table 2 suggests that it is both COVID-19 outbreaks *and* NPIs that can explain time and regional variation in unemployment rates. Here we present eight different models, four with county-level controls and four with county-fixed effects, including (i) quarter dummies only, (ii) adding COVID deaths per 100,000, (iii) adding NPIs, and (iv) including both. The results in columns (1) and (2) show a significant increase in unemployment in 2020 compared to the last quarter of 2019, with unemployment rates increasing by almost one percentage point in Q1, around 7 percentage points in Q2, and over 3 percentage points in Q3, compared to a 5.5% sample mean. Beyond this general trend, however, there is geographic co-variation in unemployment with COVID outbreaks and lockdown measures. The results in columns (3) and (4) confirm the positive relationship between COVID death rates and unemployment rates, while the three 2020 quarter dummies continue to enter positively and significantly, although of smaller size. When we include NPIs in columns (5) and (6), on the other hand, the dummies for Q2 and Q3 of 2020 lose significance and the Q1 dummy turns negative and significant; the NPI index, on the other hand enters positively and significantly, a finding confirmed in columns (7) and (8) where we include both COVID-19 deaths and NPIs. This suggests that unemployment across the US over the course of 2020 was less driven by national trends, but by exposure to the pandemic and especially by lockdown policies. Even though COVID-19 deaths and NPIs are highly correlated, they enter with similar coefficient sizes and significance across the different specifications, suggesting that they drive increases in unemployment independently.

The findings are not only statistically but also economically significant. The coeffi-

Covid Economics 61, 11 December 2020: 73-120

cient estimates for COVID deaths in column (8) implies that doubling COVID deaths within a county is associated with increase in the unemployment rate of 0.3 percentage points, compared to a mean of 5.5 percent. Coefficient estimates imply that an increase in the NPI index by one step (out of six) is associated with an increase in the unemployment rate of 2.1 percentage points within a state.

IV. Bank Level Evidence

Having shown that both COVID outbreaks and lockdowns can explain geographic variation in unemployment (and thus economic activity) across the US, we now turn to the implications of the crisis for the banking sector, gauging first the impact on loan losses and NPLs and then on loan volumes.

A. Effects on Loss Provisions and NPLs

The tremendous economic shock illustrated in the analysis in the previous section suggests that banks may generally start to experience problems in their loan portfolio. On the other hand, fiscal, monetary and regulatory support measures might either reduce the impact of these problems on banks' balance sheet or might delay their recognition by banks. We first gauge the impact of COVID-19, NPIs and the associated economic downturn on banks' loan losses and NPLs. We exploit regional variation in COVID-19 to construct a measure of the exposure of each bank to COVID outbreaks based on branch locations, as described in section 2.

As in the previous section, we first provide a graphic illustration of the impact of COVID-19 on loan losses. Specifically, we plot loss provisions and non-performing loans (NPLs) indexed to 100 in Q4 2019 in panels A and B in Figure 6. The sample is split into banks below and above the median bank exposure to cumulative September 30th COVID deaths per 100,000. There is a steep increase in loss provisions for all

Covid Economics 61, 11 December 2020: 73-120

banks, but more so for banks with above median COVID exposure – growing by 80% in Q2 2020 relative to Q4 2019 for highly exposed banks and 50% for less exposed. Similarly, Panel B shows that NPLs increase considerably more for highly exposed banks (9%), while elevating only modestly for banks with below average exposure (less than 5%). Notably, low exposure banks see NPLs decline in Q3 2020, while high exposure banks maintain elevated NPLs. In the appendix (panels A and B in Figure A1) we show that time trends for non-performing C&I loans diverge similarly to (presumably more local) loans to households. When comparing the development of NPLs during 2020 to the development after Q4 2006 during the Global Financial Crisis, we note that the current increase is relatively muted, while we observe an almost four-time increase in 2007/8 (a considerably longer time period than ours). From a difference-in-differences perspective, both graphs suggest parallel trends before the start of the COVID shock.[7]

To test the effect of COVID-19 exposure on banks' growth in loan loss provisions and NPLs more formally, we run the following bank-quarter panel regression:

$$\begin{aligned} Y_{b,t} =& \beta_1 Q1\ 2020_t + \beta_2 Q2\ 2020_t + \beta_3 Q3\ 2020_t + \beta_4 COVID\ Deaths_{b,t} \\ &+ \beta_5 NPI\ Index_{b,t} + \gamma \boldsymbol{X_{b,t}} + \eta_t + \delta_b + \epsilon_{b,t}. \end{aligned} \tag{2}$$

where subscripts b and t indicate banks and quarters, respectively. We allow for clustering of error terms $\epsilon_{b,t}$ on the bank level. All regressions absorb time-invariant bank and general quarter-specific effects, η_t and δ_b, respectively. Fixed effects for the first, second and third quarters of 2020 measure the general effect on all banks (the omitted fixed effect is again for Q4 2019). Time-variant bank controls $\boldsymbol{X_{b,t}}$ include current percentage changes in deposits and unused credit line commitments and lagged values of the logarithm of total assets, loan portfolio shares, and income, equity, de-

[7] Appendix Figure A3 shows parallel trends also for some of the bank-level variables, notably liquidity, equity, unused commitments and deposits. While equity is higher for above-COVID-19 median exposure banks throughout 2019 and 2020, this gaps closes in 2020. There is a somewhat higher increase in unused commitments for low-exposure banks in 2020.

Covid Economics 61, 11 December 2020: 73-120

posits, liquidity, unused commitments, and loans and leases in percent of total assets.

The results in Panel A of Table 3 show, in line with the visual findings from Figure 6 that exposure to COVID-19 and to NPIs can explain bank variation in loan loss provisions and NPLs over time. Fixed effects for the first three quarters of 2020 are both highly significant with growth in loan loss provisions as the dependent variable in panel A columns (1) and (2), while the Q3 dummy turns negative and significant once we control for banks' exposure to COVID-19 deaths and/or NPIs in columns (3) to (8). Bank exposure to both COVID outbreaks and NPIs enter positively and significantly, though the coefficient size of NPIs drops by a third once we also include exposure to COVID-19 deaths.

The results are not only statistically but also economically significant. The Q2 2020 fixed effect in column (2) suggests a 57% increase in loan loss provisions. Bank exposure to COVID deaths has a considerable additional differential effect on loss provisions (columns 3-4 and 7-8 in panel A). The coefficient in column (8) suggests the growth rate of loan loss provisions increases by 9 percentage points when bank exposure to the logarithm of COVID deaths doubles. This is sizable given the 13.6% sample average and the 69% sample average in Q2 2020. Increasing the NPI index by one notch implies a 27.7 percentage point increase in the growth rate of loan loss provisions.

The results in Panel B of Table 3 show that there is no significant general increase in NPLs during the first three quarters of 2020. Across the first two columns, the 2020 quarterly dummies enter mostly insignificantly. Both exposure to COVID-19 deaths and exposure to NPIs enter positively and significantly in columns (3) to (8), (while the 2020 quarter fixed effects turn negative). Using the coefficient in column (8) as a reference, the percentage change in NPLs is 4.2 percentage points higher when the logarithm of the exposure to the COVID deaths doubles. An increase in the NPI by one notch implies an increase of 7.5 percentage points in growth in NPLs. In table A6 in

Covid Economics 61, 11 December 2020: 73-120

the appendix we show that positive effects on NPLs are driven more significantly and robustly by household loans and less by C&I loans.[8]

B. *Effects on Lending Growth*

In the previous subsection IV.A we showed that there are general and differential adverse effects of the pandemic on banks' balance sheets, showing up in loss provisions and NPLs. In this subsection we explore if exposure to the pandemic and lockdown measures are associated with any early effects on lending volumes on the bank level. In addition to total loans and leases, we also gauge the impact of the pandemic on three sub-categories: small business loans, C&I loans and household loans. As in previous analyses, we first undertake graphic illustration before proceeding to regression analysis, differentiating between banks above and below the average exposure to COVID-19 outbreaks (Figure 6, volumes are indexed to 100 in Q4, 2019). While there are steep increases for total loans and leases in Q2, 2020, there is no difference between the two groups of banks (Panel C). The increase in small business loans is on average considerably larger than the increase in total loans and leases and somewhat larger for banks more exposed to COVID related deaths (Panel D). As shown in Appendix Figure A1 the increase for C&I loans is similar to those for total loans and leases, with no difference across the two bank groups, while loans to households remain relatively flat. Using the same regression set-up as for loan loss provisions and NPLs, we next explore the relationship between the pandemic and lending volumes more formally.

The regressions in Table 4 show that bank exposure to COVID outbreak and lockdown policies has had no significant effect on growth in C&I loans and household loans, but a positive and significant impact on growth in small business loan volume. Here we run similar regressions as in Table 3, but using percentage changes in total loan volumes, small business loan volume, C&I loan volume and household loan vol-

[8] We do not observe a breakdown for small business NPLs separately.

Covid Economics 61, 11 December 2020: 73-120

Covid Economics 61, 11 December 2020: 73-120

ume as dependent variables.

The results in Panel A of Table 4 show no consistently significant average change in growth of total loans and leases in the first three quarters of 2020. Q2 and Q3 dummies enter positively and significantly, as long as we do not control for time-variant bank characteristics. While bank-level exposures to COVID-19 deaths per 100,000 enters positively and significantly, there is no significant effect from bank-exposure to lockdown measures. In terms of economic significance, we find that a doubling in exposure to COVID-19 deaths is associated with a 0.3 percentage point higher loan growth (compared to an average growth in total loans and leases of 8.3%). These findings are consistent with an increase in loan demand during the COVID-19 pandemic, which outweighed any possibly negative effect of the crisis on loan supply. Our findings are consistent with Acharya & Steffen (2020), Chodorow-Reich et al. (2020) and Li et al. (2020).

The results in Panel B, on the other hand, show a positive and significant effect of bank exposure to both COVID outbreaks and lockdown policies on small business lending. While we find a negative and significant Q1 dummy, suggesting that lending to small business dropped significantly in the first three months of 2020, the Q2 and Q3 dummies enter positively and significantly in columns (1) to (4) and as long as we do not include exposure to NPIs. Bank-level exposures to both COVID-19 deaths per 100,000 and to NPIs enter positively and significantly at the 1% level. While the size of both coefficients decreases when we include both exposure measure together (columns 7 and 8), bank exposures to both COVID outbreaks and lockdown policies continue to enter statistically and economically significantly. The coefficient in column (8), Panel B suggests that a doubled exposure to COVID deaths is associated with a 2.2 percentage point increase in the growth rate of small business loan volumes (which has a mean of 8% in the full estimation sample and 24.5% in Q2 2020), a rather large increase. An increase of the NPI index by one notch implies an increase of 6 percentage points in

the growth of small business lending. As the findings in Panel A, these results suggests a significant increase in loan demand both due to the pandemic and the lockdown policies, but the substantially larger effects for small business than overall loans is an indication that loan supply to this specific group was supported by policy measures (in line with findings by Chodorow-Reich et al. (2020)), while smaller firms also rely more on banks than larger firms that have access to public capital markets.

The results in Panel C show that there was a positive and significant increase in C&I loan growth in the second and third quarter of 2020 (compared to the last quarter of 2019), while the bank-level exposure to COVID outbreaks and lockdown policies do not enter significantly. While there was thus an increase in C&I loan growth during the second and third quarter (relative to 2019 Q4), this loan growth did not vary across banks with exposure to the pandemic or lockdown policies. This can be interpreted in two different ways. First, larger corporates are more diversified across different states within the US and are thus exposed economically and thus in their loan demand more to national than to local trends. Second, corporate loans are more likely to be given by bank headquarters and geographic distribution of corporate loans might mirror banks' geographic branch distribution less than small business loans.

The results in Panel D, finally, show some evidence for slower loan growth to households in the second and third quarter of 2020, though the coefficient do not always enter significantly. We find no significant variation of household loan growth with bank exposure to COVID outbreaks and lockdown policies.

V. Loan-Level Effects on Terms

We have shown in section IV that banks are adversely affected through their geographical exposure to the pandemic, while providing increasing loan volumes, especially to small businesses with loan volumes up to 1 million. In this section we explore if there

Covid Economics 61, 11 December 2020: 73-120

Covid Economics 61, 11 December 2020: 73-120

are effects on interest spreads and maturities in the market for medium and large syndicated loans in the U.S. Average loan volumes in our sample are 498 million and average borrowers have total assets of 66 billion.

Figure 7 provides the graphical illustration. Floating interest quoted as spreads over LIBOR plotted in panel A increase for all loans, but considerably more so for loans issued by banks that are more exposed to areas severely hit by the pandemic. Similarly, maturities on newly granted loans in Panel B drop across the board, but seem to experience a slightly steeper decline for loans issued by banks more present where COVID outbreaks are more severe.

To explore the effect of the pandemic on loan conditionality (interest spreads in percentage points and of maturities in months), we adjust the regression model used in the previous section as follows:

$$\begin{aligned} Y_{l,i,b,t} =& \beta_1 Q1\ 2020_t + \beta_2 Q2\ 2020_t + \beta_3 COVID\ Deaths_{b,t} \\ &+ \beta_4 NPI\ Index_{b,t} + \gamma \boldsymbol{X_{b,t}} + \tau \boldsymbol{Z_l} + \eta_t + \delta_b + \epsilon_l, \end{aligned} \tag{3}$$

where the subscripts l, i b, and t refer to loan facilities, industries, banks and quarters, respectively. Compared to the previous bank level analysis, this estimation includes not only bank controls, but also loan controls $\boldsymbol{Z_l}$ and higher dimensionality fixed effects, including bank-fixed effects, loan type fixed effects, industry × state and industry × quarter fixed effects (similar to Berg, Saunders, Schäfer & Steffen, 2019).[9] Standard errors are clustered at the bank level to control for any unobservable bank-specific pricing differences.

The results in columns (1) and (2) of Table 5 show that, in line with the graphical evidence, interest spreads experienced a significant uptick in the second quarter of 2020. Using the coefficient in column 2 as reference they increased by about 55 basis

[9]Note that the latter set of fixed effects absorbs simple quarter fixed effects.

Covid Economics 61, 11 December 2020: 73-120

points in Q2 2020 relative to Q4 2019, corresponding to 23.7% of the sample mean (233 basis points). Columns (3), (4), (7) and (8), however, show that this increase is entirely driven by bank exposure to COVID-19 deaths, which enters positively and significantly while the Q2 dummy turns insignificant. The magnitude of the coefficient in column (8) implies that the interest spread on a new loan increases by 30 basis points for a doubled exposure to COVID-19 deaths. While this result is similar to findings by Hasan et al. (2020), the economic effect seems significantly larger, though we work with very different samples (US vs. cross-country). The results in columns (5) to (8), on the other hand, show that bank-level exposure to NPIs has no significant measurable effect on interest spreads. The coefficient varies sign is mostly positive. The inclusion of NPI in the regression does not affect the coefficient estimates of the COVID exposure variables.

The results in Table 6 show similar though weaker results for maturities. The coefficient of the Q2 2020 fixed effect enters negatively and highly significant in columns (1) and (2), with the coefficient sizes suggesting 15 months shorter loans, a 29% drop compared to the mean of 51 months. However, the Q2 dummy turns insignificant once we control for bank exposure to COVID-19 deaths and/or NPIs. Bank exposure to COVID outbreaks enters negatively throughout, but significantly at the 5%-level only in columns (3) and (7). In terms of economic effects, the result suggest a four month drop in maturity for a doubled exposure to COVID-19 deaths. As in the interest spread regressions, the coefficient on the NPI exposure does not enter significantly.

In summary, the loan-level results suggest that there was a tightening of loan conditionality due to COVID-exposures of banks, both in terms of interest spreads and loan maturity. Variation across banks in this tightening is related to their exposure to the pandemic, but not to exposure to lockdown measures. Comparing these findings to the earlier results on C&I lending growth, there was thus a national trend in lending, but not related to banks' exposure to COVID-19, while the tightening of loan

conditionality varies with banks' exposure to COVID-19. Lockdown measures do not explain either lending growth or loan conditionality.

VI. Conclusion

This paper has documented the impact of the COVID-19 pandemic and lockdown measures on the performance and behavior of the US banking system. We find that counties and states more exposed to COVID-19 deaths and (independently) lockdown measures experience higher increases in unemployment. Both the pandemic and the public-health response also explain variation in loan performance across banks. While overall lending growth increases with bank exposure in COVID-19 deaths, C&I lending growth sees a general increase in the second and third quarter of 2020, but no variation across banks with exposure to the pandemic or lockdown measures, while we find strong growth in small business lending, which varies with banks' exposure to the pandemic and lockdown policies. Finally, we find that banks more exposed to the pandemic increase interest spreads and reduce the maturity more for syndicated loans.

Our findings are consistent with previous papers showing an increase in corporate and small business lending and with work that shows an increase in interest spreads. More generally, our findings are consistent with Gertler & Gilchrist (1993) and Greenwald et al. (2020) of a positive effect of macroeconomic shocks on lending, but also consistent with evidence of an increased risk premium following such a shock.

References

Acharya, V. V. & Steffen, S. (2020). The Risk of Being a Fallen Angel and the Corporate Dash for Cash in the Midst of COVID. *The Review of Corporate Finance Studies*.

Covid Economics 61, 11 December 2020: 73-120

Berg, T., Saunders, A., Schäfer, L., & Steffen, S. (2019). 'brexit'and the contraction of syndicated lending. *Available at SSRN*.

Bharath, S. T., Dahiya, S., Saunders, A., & Srinivasan, A. (2011). Lending relationships and loan contract terms. *Review of Financial Studies*, *24*(4), 1141–1203.

Chava, S. & Roberts, M. R. (2008). How does financing impact investment? The role of debt covenants. *The Journal of Finance*, *63*(5), 2085–2121.

Chodorow-Reich, G., Darmouni, O., Luck, S., & Plosser, M. C. (2020). Bank liquidity provision across the firm size distribution. *National Bureau of Economic Research Working Paper 27945*.

Cornett, M. M., McNutt, J. J., Strahan, P. E., & Tehranian, H. (2011). Liquidity risk management and credit supply in the financial crisis. *Journal of Financial Economics*, *101*(2), 297–312.

Darmouni, O. & Siani, K. (2020). Crowding out bank loans: Liquidity-driven bond issuance. *CEPR Covid Economics*, *51*(7), 74–133.

Duchin, R. & Hackney, J. (2020). Electoral politics and the allocation of government capital. *Available at SSRN 3708462*.

Gertler, M. & Bernanke, B. (1989). Agency costs, net worth and business fluctuations. In *Business Cycle Theory*. Edward Elgar Publishing Ltd.

Gertler, M. & Gilchrist, S. (1993). The cyclical behavior of short-term business lending: Implications for financial propagation mechanisms. *European Economic Review*, *37*(2), 623 – 631.

Greenwald, D. L., Krainer, J., & Paul, P. (2020). The credit line channel. Federal Reserve Bank of San Francisco.

Covid Economics 61, 11 December 2020: 73-120

Halling, M., Yu, J., & Zechner, J. (2020). How Did COVID-19 Affect Firms' Access to Public Capital Markets?*. *The Review of Corporate Finance Studies*, *9*(3), 501–533.

Hasan, I., Politsidis, P., & Sharma, Z. (2020). Bank lending during the covid-19 pandemic. *MPRA Paper No. 103565*.

Ivashina, V. & Scharfstein, D. (2010). Bank lending during the financial crisis of 2008. *Journal of Financial economics*, *97*(3), 319–338.

Kahle, K. M. & Stulz, R. M. (2013). Access to capital, investment, and the financial crisis. *Journal of Financial economics*, *110*(2), 280–299.

Keil, J. (2018). The value of lending relationships when creditors are in control? *Working Paper, available online*.

Li, L., Strahan, P. E., & Zhang, S. (2020). Banks as lenders of first resort: Evidence from the covid-19 crisis. *The Review of Corporate Finance Studies*, *9*(3), 472–500.

Romer, C. D. & Romer, D. H. (2004). A new measure of monetary shocks: Derivation and implications. *American Economic Review*, *94*(4), 1055–1084.

Santos, J. A. C. (2010). Bank Corporate Loan Pricing Following the Subprime Crisis. *The Review of Financial Studies*, *24*(6), 1916–1943.

Schwert, M. (2018). Bank capital and lending relationships. *The Journal of Finance*, *73*(2), 787–830.

Schwert, M. (2020). Does borrowing from banks cost more than borrowing from the market? *The Journal of Finance*, *75*(2), 905–947.

Covid Economics 61, 11 December 2020: 73-120

Covid Economics 61, 11 December 2020: 73-120

Figure 1: COVID-19 Related Deaths

Panel A: Q1 2020

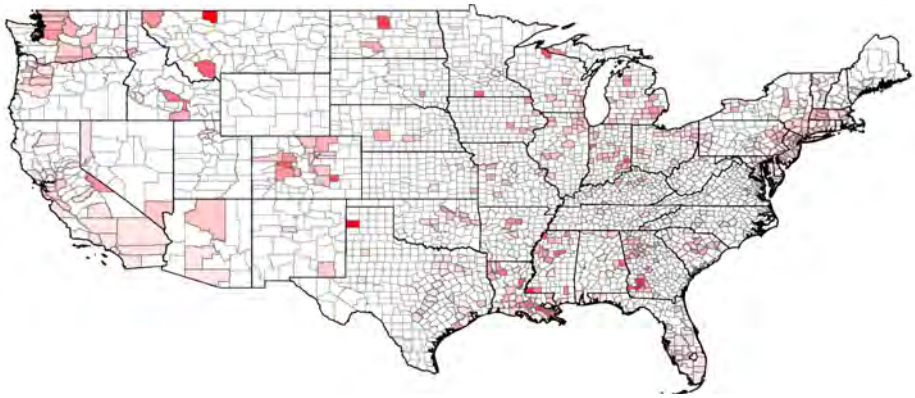

Panel B: Q2 2020

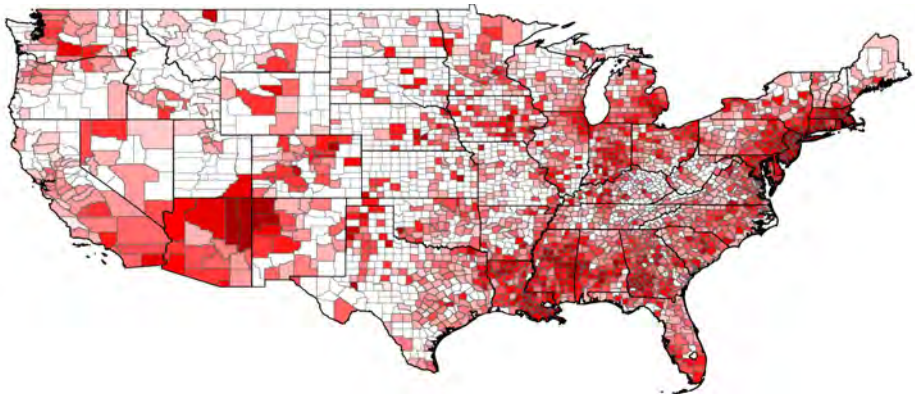

Panel C: Q3 2020

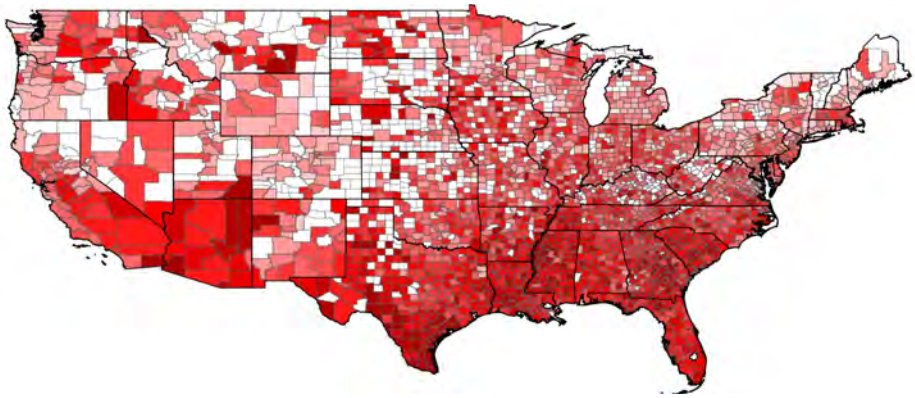

Coloring of contiguous U.S. counties follows a heat map scheme with identical thresholds across all panels. The darker the red, the higher the number of new quarterly COVID-19 related deaths per 100,000 inhabitants.

Covid Economics 61, 11 December 2020: 73-120

Figure 2: Non-pharmaceutical Interventions

Panel A: Q1 2020

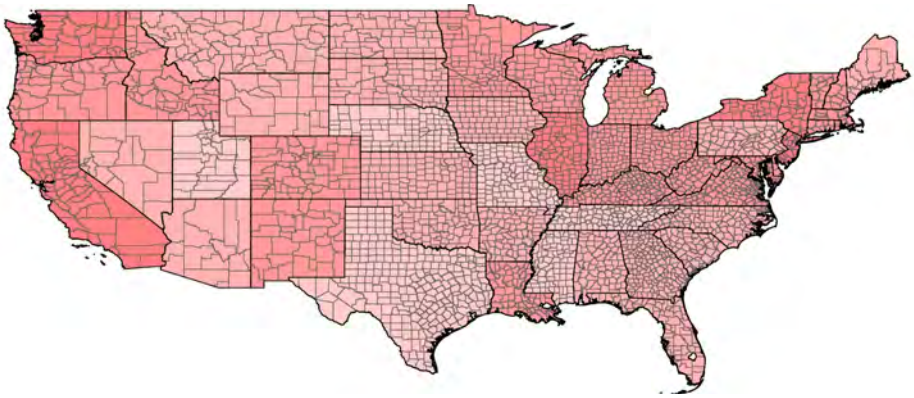

Panel B: Q2 2020

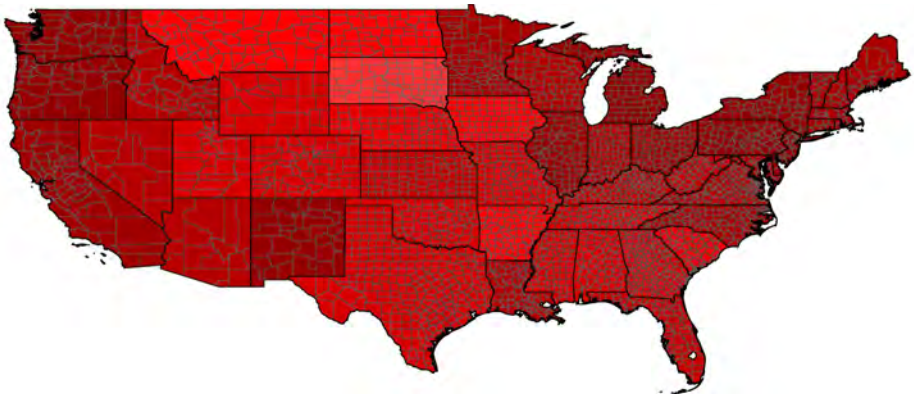

Panel C: Q3 2020

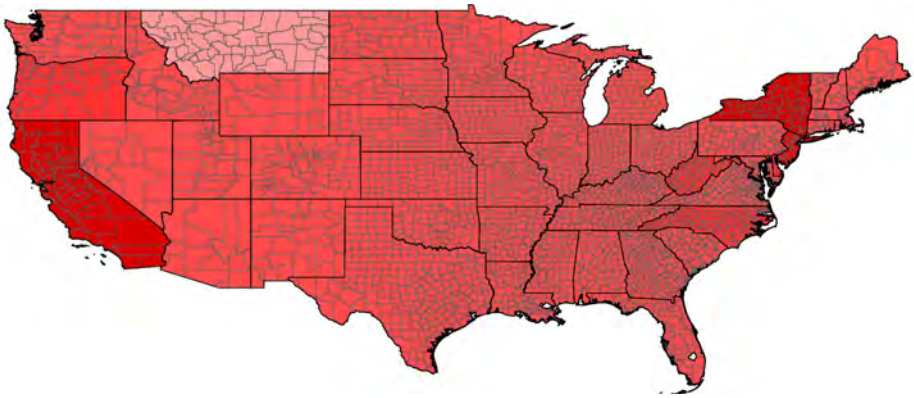

Coloring of contiguous U.S. counties follows a heat map scheme with identical thresholds across all panels. The darker the red, more restrictive the NPIs as measured by a state level index from Olivier Lejeune.

Covid Economics 61, 11 December 2020: 73-120

Figure 3: Unemployment Rates

Panel A: Q1 2020

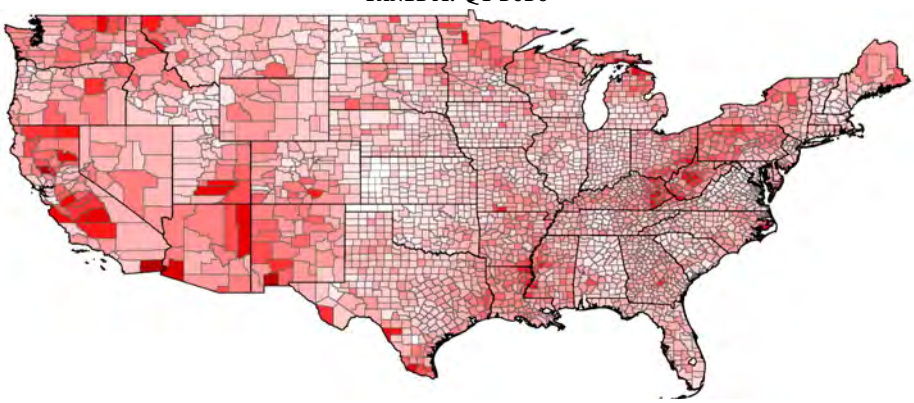

Panel B: Q2 2020

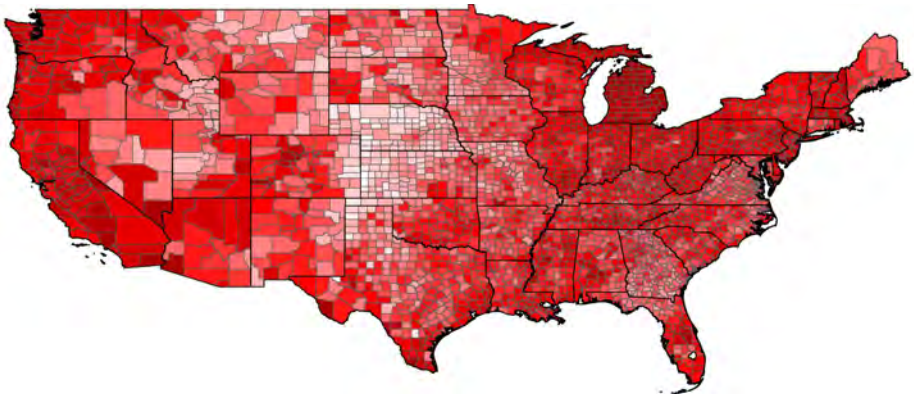

Panel C: Q3 2020

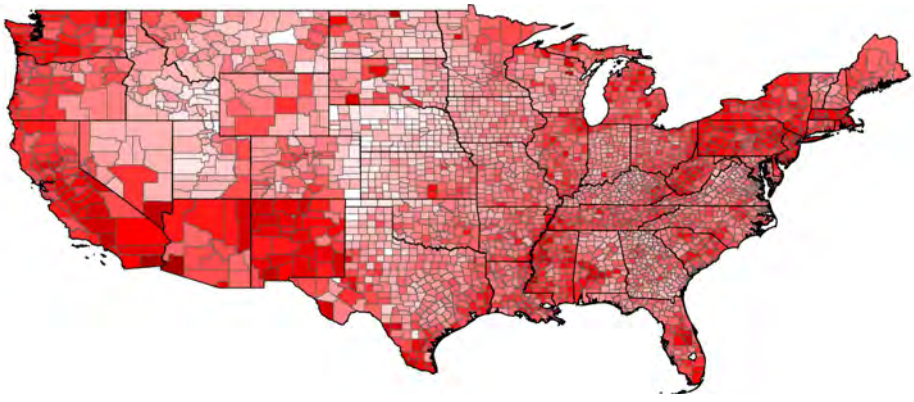

Coloring of contiguous U.S. counties follows a heat map scheme with identical thresholds across all panels. The darker the red, the higher the unemployment rate

Covid Economics 61, 11 December 2020: 73-120

Figure 4: Unemployment in Counties with Different Exposures

Panel A: Exposure to COVID Deaths

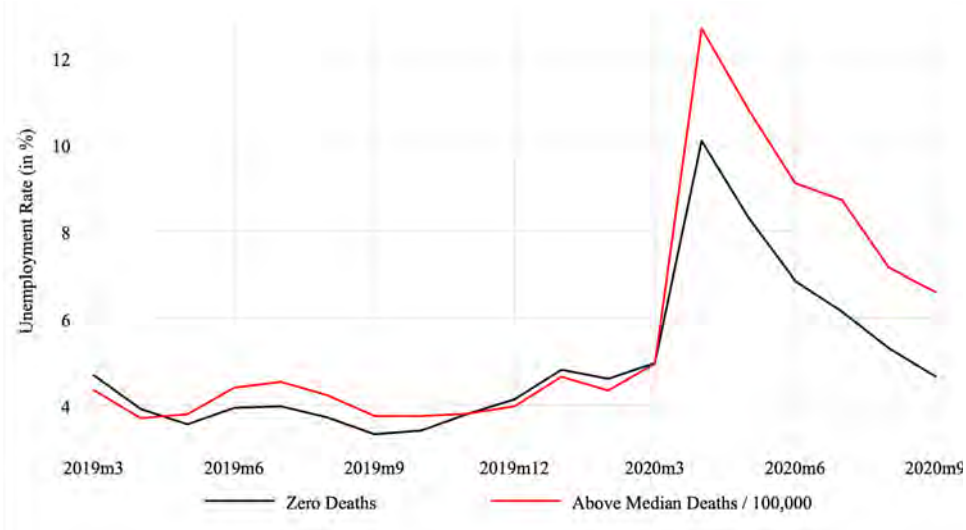

Panel B: Exposure to NPIs

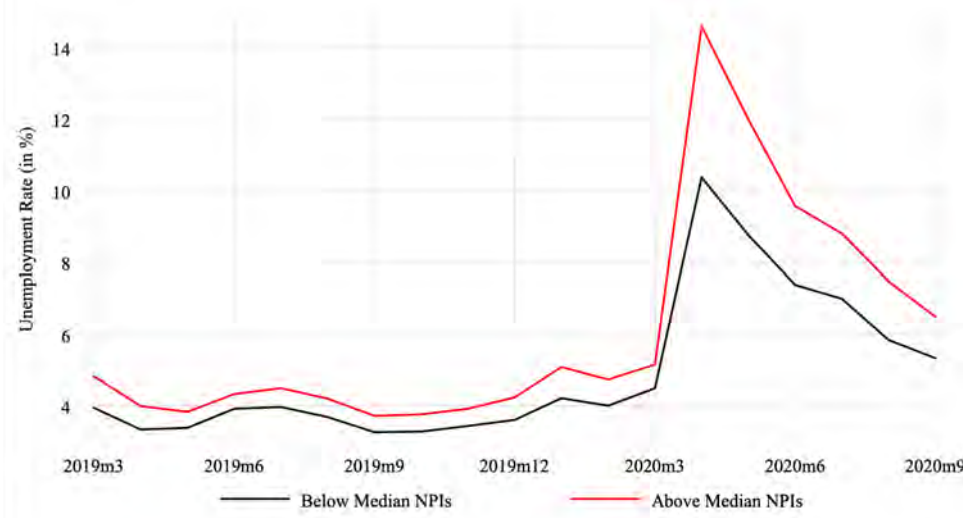

This figure displays median monthly unemployment rates for U.S. counties. Panel A divides them into groups with zero deaths and cumulative Q3 2020 COVID-19 related deaths / 100,000 inhabitants above the median of counties with more than 0 deaths. Panel B separates counties into those with below and above median NPIs in the first three quarters of 2020.

Figure 5: Examples for Differential Exposures – Citibank and Zions Bankcorp

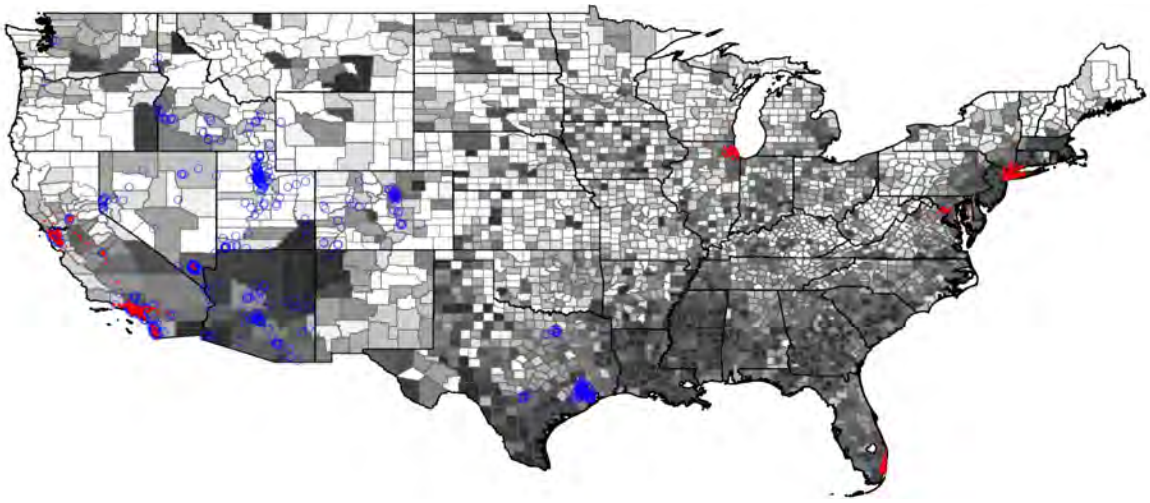

Red dots (blue circles) represent June 2019 Citibank (Zions Bancorp) branches. Citibank (Zions) is an example for a commercial bank with a relatively high (low) geographical exposure to COVID deaths. Coloring of contiguous U.S. counties follows a heat map scheme, corresponding to the number of cumulative Q3 2020 COVID-19 related deaths per 100,000 inhabitants. The darker the gray, the higher the death rate.

Covid Economics 61, 11 December 2020: 73-120

Covid Economics 61, 11 December 2020: 73-120

Figure 6: Health and Lending by Banks with Differential Geographical Exposures to COVID

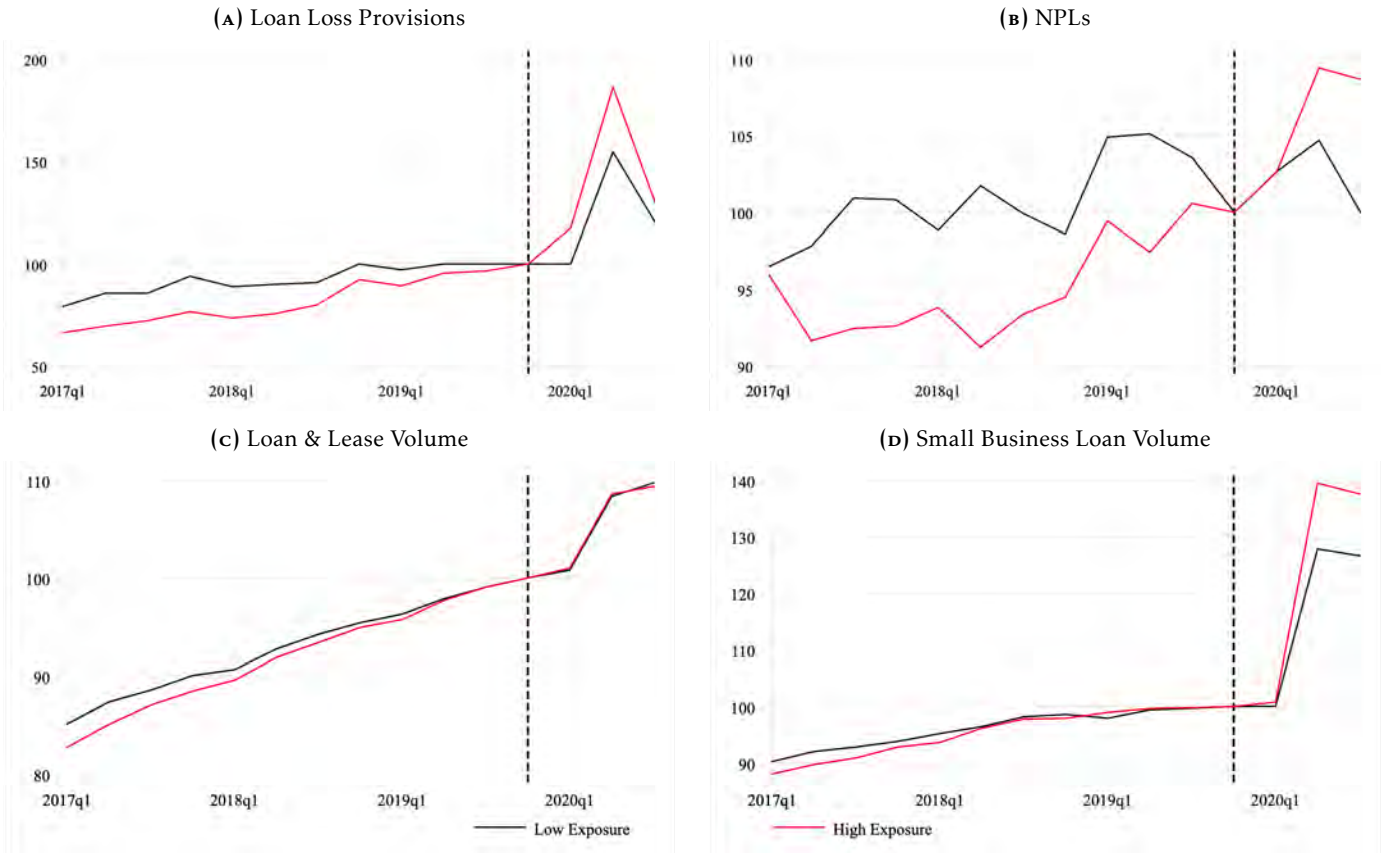

This figure shows U.S. banks' median quarterly loan loss provisions in panel A, non-performing loans in panel B, total and small business lending volumes in panels C-D (all indexed to 100 in Q4 2019). The figure differentiates according to banks' geographical exposure to COVID. The latter is the deposit weighted number of cumulative COVID-19 related deaths / 100,000 inhabitants during the three quarters of 2020. The black (red) line represents the group of banks below (above) the median exposure. The vertical black dashed line indicates the pre-COVID quarter Q4 2019.

Covid Economics 61, 11 December 2020: 73-120

Figure 7: Syndicated Loans and Exposure to COVID

Panel A: Loan Spreads

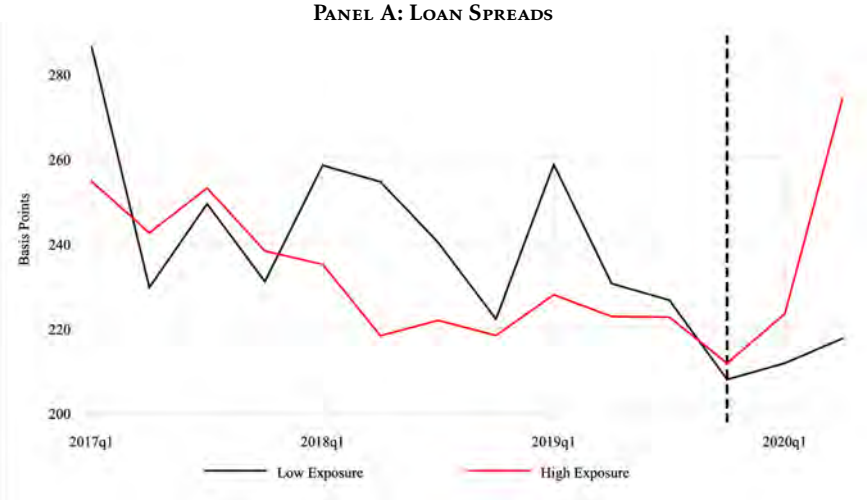

Panel B: Maturities

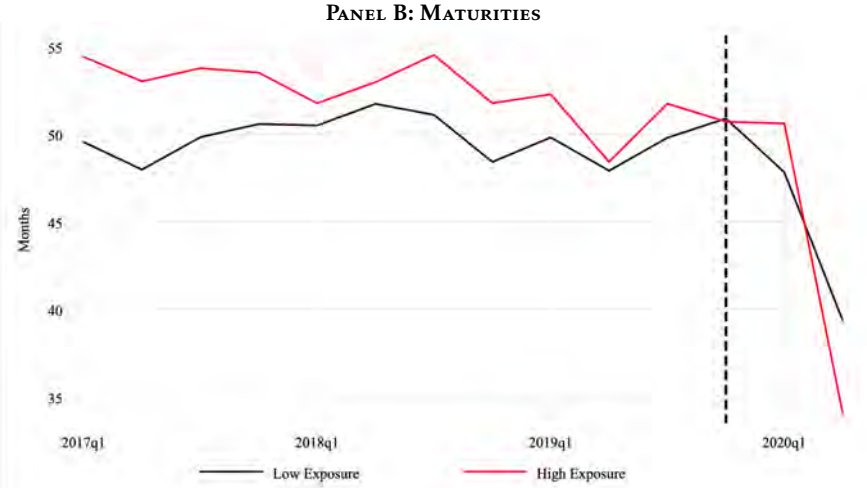

This figure shows quarterly basis point spreads over LIBOR for syndicated loans (panel A) and maturities in months (B). It differentiates according to banks' geographical exposure to COVID. The latter is the deposit weighted number of cumulative COVID-19 related deaths / 100,000 inhabitants during the first half of 2020. The black (red) line represents the group of banks below (above) the mean exposure. The vertical black dashed line indicates the pre-COVID quarter Q4 2019.

Table 1: Descriptive Statistics

Variable	N	10th Perc.	Median	90th Perc.	Mean	SD
Panel A: County-Level						
Covid Deaths/100,000	21,987	0	0	17	6.3	21.5
Q1 2020 Covid Deaths/100,000	21,987	0	0	.869	.464	2.259
Q2 2020 Covid Deaths/100,000	21,987	0	4.4	47.3	17	34.2
Q3 2020 Covid Deaths/100,000	21,987	0	13.8	66.6	26.3	37
NPI Index	21,987	0	0	2.923	.802	1.16
Q1 2020 NPI Index	21,987	.464	.71	1	.713	.221
Q2 2020 NPI Index	21,987	2.44	3.055	4.011	3.197	.564
Q3 2020 NPI Index	21,987	1.674	1.674	2	1.738	.285
Unemployment Rate	21,987	2.7	4.3	9.8	5.4	3.2
Panel B: Bank-Level						
Covid Deaths/100,000	19,388	0	0	5.8	3.44	15.47
Q1 2020 Covid Deaths/100,000	1,293	0	.04	1.39	.65	1.87
Q2 2020 Covid Deaths/100,000	1,293	0	10.49	78.66	27.34	41.27
Q3 2020 Covid Deaths/100,000	1,293	2.99	15.25	53	23.57	27.57
NPI Index	19,388	0	0	1.67	.39	.92
Q1 2020 NPI Index	1,293	.46	.73	1.04	.73	.24
Q2 2020 NPI Index	1,293	2.6	3.09	3.95	3.27	.53
Q3 2020 NPI Index	1,293	1.67	1.67	2	1.78	.32
Growth in Loss Provisions	19,388	-100	1.72	137.5	13.64	132.63
Growth in NPLs	18,949	-88.29	0	102.86	3.61	77.85
Growth in Loans and Leases	19,388	-1.2	6.48	19.46	8.29	9.9
Growth in Small Bus Loans	13,329	-7.5	4.24	30.89	7.98	17.96
Growth in C&I Loans	19,388	-4.82	8.29	28.23	10.36	14.48
Growth in Household Loans	19,388	-5.89	4.88	20.66	6.56	12.33
Panel C: Loan-Level						
Covid Deaths/100,000	10,789	0	0	.62	2.81	12.76
Q1 2020 Covid Deaths/100,000	707	.62	1.36	4.16	1.86	1.38
Q2 2020 Covid Deaths/100,000	521	28.1	49.2	83.1	55.6	20.9
NPI Index	10,789	2.067	2.34	2.551	2.317	.203
Q1 2020 NPI Index	707	.77	.869	.923	.858	.087
Q2 2020 NPI Index	521	3.126	3.639	3.915	3.613	.343
Spread over LIBOR (BPS)	10,789	113	200	400	233	132
Maturity (Months)	10,765	19	60	69	52	19

This table contains summary statistics for main variables of interest used in the county-, bank-, and loan-level analyses (panels A, B, and C, respectively). Observations are those used in regressions 2, table 2, regression 1, table 3, and regression 1, table 5. "COVID Deaths/100,000" variables and "NPI Index" in panels B and C refer to the bank level exposures to COVID, computed as the deposit weighted number of new COVID-19 related deaths/100,000 inhabitants (or the NPI index value) during a quarter in a U.S. county.

Covid Economics 61, 11 December 2020: 73-120

CEPR PRESS

Table 2: County Unemployment Rates and Exposure to COVID

	(1)	(2)	(3)	(4)	(5)	(6)	(7)	(8)
Q1 2019 – Q3 2019 FE	Yes	Yes	Yes	Yes	Yes	Yes	Yes	Yes
County FE		Yes		Yes		Yes		Yes
County Controls	Yes	–	Yes	–	Yes	–	Yes	–
Q1 2020 FE	0.909***	0.907***	0.835***	0.846***	-1.214***	-0.661*	-1.200***	-0.608*
	(0.000)	(0.000)	(0.000)	(0.000)	(0.003)	(0.074)	(0.003)	(0.098)
Q2 2020 FE	7.391***	6.724***	6.650***	6.090***	-1.918	-0.230	-2.182	-0.292
	(0.000)	(0.000)	(0.000)	(0.000)	(0.182)	(0.871)	(0.123)	(0.834)
Q3 2020 FE	3.419***	3.111***	2.416***	2.192***	-1.661*	-0.710	-2.271**	-1.210
	(0.000)	(0.000)	(0.000)	(0.000)	(0.057)	(0.416)	(0.011)	(0.164)
Covid Deaths/100,000			0.395***	0.377***			0.307***	0.308***
			(0.000)	(0.000)			(0.000)	(0.000)
NPI Index					2.883***	2.199***	2.786***	2.054***
					(0.000)	(0.000)	(0.000)	(0.000)
Adj. R^2	0.64	0.77	0.65	0.77	0.68	0.79	0.69	0.79
Observations	15,589	21,987	15,589	21,987	15,589	21,987	15,589	21,987

This table contains county panel regressions from Q1 2019 to Q3 2020. The dependent variable is the average quarterly unemployment rate. Independent variables of interest are the logarithm of 1 + the number of COVID-19 related deaths / 100,000 inhabitants and a state level NPIs index. Controls are from 2019 and include the number of ICU beds, persons older than 65, blacks and hispanics weighted by total county population, median income, population density, 2-digit NAICS and government employment shares. Standard errors are clustered by state. ***, **, and * indicate statistical significance at 1%, 5%, and 10%. P-values are in parenthesis.

Covid Economics 61, 11 December 2020: 73-120

Table 3: Bank Health and the COVID Shock

	(1)	(2)	(3)	(4)	(5)	(6)	(7)	(8)
Q1 2017 – Q3 2019 FE	Yes	Yes	Yes	Yes	Yes	Yes	Yes	Yes
Bank FE	Yes	Yes	Yes	Yes	Yes	Yes	Yes	Yes
Bank Controls		Yes		Yes		Yes		Yes
Panel A: Loss Provisions								
Q1 2020 FE	47.092***	74.549***	43.587***	70.177***	20.329***	48.757***	21.251***	50.414***
	(0.000)	(0.000)	(0.000)	(0.000)	(0.001)	(0.000)	(0.001)	(0.000)
Q2 2020 FE	69.598***	56.512***	41.282***	27.139***	-50.096***	-56.092***	-56.112***	-56.527***
	(0.000)	(0.000)	(0.000)	(0.000)	(0.009)	(0.005)	(0.003)	(0.005)
Q3 2020 FE	46.584***	36.346***	15.426**	4.937	-18.399*	-26.177**	-34.328***	-37.673***
	(0.000)	(0.000)	(0.040)	(0.622)	(0.100)	(0.044)	(0.003)	(0.004)
Covid Deaths/100,000			11.456***	11.984***			9.191***	8.932***
			(0.000)	(0.000)			(0.000)	(0.000)
NPI Index					36.585***	34.344***	31.480***	27.799***
					(0.000)	(0.000)	(0.000)	(0.000)
Adj. R^2	0.01	0.02	0.02	0.02	0.02	0.03	0.02	0.03
Observations	19,388	14,932	19,388	14,932	19,388	14,932	19,388	14,932
Banks								
Panel B: Non-Performing Loans								
Q1 2020 FE	3.285	3.266	1.941	1.406	-4.839	-4.665	-4.499	-3.939
	(0.113)	(0.261)	(0.370)	(0.636)	(0.184)	(0.261)	(0.216)	(0.343)
Q2 2020 FE	6.753**	-2.063	-4.050	-14.413***	-29.513**	-36.614***	-32.089**	-37.013***
	(0.012)	(0.507)	(0.382)	(0.007)	(0.025)	(0.009)	(0.015)	(0.008)
Q3 2020 FE	0.908	-3.427	-10.950**	-16.631***	-18.754**	-22.599***	-25.271***	-28.145***
	(0.767)	(0.412)	(0.029)	(0.005)	(0.013)	(0.007)	(0.002)	(0.001)
Covid Deaths/100,000			4.361***	5.033***			3.720***	4.220**
			(0.002)	(0.002)			(0.009)	(0.012)
NPI Index					11.072***	10.525***	9.045**	7.492*
					(0.004)	(0.010)	(0.021)	(0.074)
Adj. R^2	0.05	0.06	0.05	0.06	0.05	0.06	0.05	0.06
Observations	18,954	14,635	18,954	14,635	18,954	14,635	18,954	14,635
Banks	1,285	1,263	1,285	1,263	1,285	1,263	1,285	1,263

This table contains bank panel regressions from Q1 2017 to Q3 2020. Dependent variables are %-changes in loan loss provisions (panel A) and total non-performing loans and leases relative to the pre-year quarter (B). Independent variables of interest are fixed effects for 2020 quarters, the logarithm of 1 + the bank level exposure to COVID related deaths, and an NPI index. Exposure to COVID deaths is the deposit weighted number of new COVID-19 related deaths / 100,000 inhabitants during a quarter in a U.S. county. The state level NPI index is linked to banks equivalently. Controls include current %-changes in deposits and unused credit line commitments and lagged values of the logarithm of total assets, loan portfolio shares, and income, equity, deposits, liquidity, unused commitments, and loans and leases in percent of total assets. Standard errors are clustered by bank. ***, **, and * indicate statistical significance at 1%, 5%, and 10%. P-values are in parenthesis.

Covid Economics 61, 11 December 2020: 73-120

Table 4: Outstanding Loan Volumes and the COVID Shock

	(1)	(2)	(3)	(4)	(5)	(6)	(7)	(8)
Q1 2017 – Q3 2019 FE	Yes	Yes	Yes	Yes	Yes	Yes	Yes	Yes
Bank FE	Yes	Yes	Yes	Yes	Yes	Yes	Yes	Yes
Bank Controls		Yes		Yes		Yes		Yes
Panel A: Loans & Leases								
Q1 2020 FE	0.222	-0.119	0.094	-0.234	0.082	-0.422	0.125	-0.368
	(0.126)	(0.524)	(0.532)	(0.221)	(0.839)	(0.211)	(0.759)	(0.274)
Q2 2020 FE	5.682***	0.176	4.648***	-0.598	5.056***	-1.150	4.780***	-1.164
	(0.000)	(0.541)	(0.000)	(0.169)	(0.003)	(0.373)	(0.005)	(0.366)
Q3 2020 FE	5.252***	-1.173***	4.114***	-1.999***	4.912***	-1.908**	4.182***	-2.288***
	(0.000)	(0.002)	(0.000)	(0.000)	(0.000)	(0.015)	(0.000)	(0.005)
Covid Deaths/100,000			0.418**	0.315**			0.421**	0.295**
			(0.010)	(0.022)			(0.010)	(0.034)
NPI Index					0.191	0.404	-0.043	0.188
					(0.706)	(0.291)	(0.934)	(0.627)
Adj. R^2	0.40	0.77	0.40	0.77	0.40	0.77	0.40	0.77
Observations	19,395	14,937	19,395	14,937	19,395	14,937	19,395	14,937
Banks	1,293	1,272	1,293	1,272	1,293	1,272	1,293	1,272
Panel B: Small Business Loans								
Q1 2020 FE	-0.591	-1.113**	-1.796***	-2.216***	-5.561***	-6.927***	-5.183***	-6.547***
	(0.271)	(0.017)	(0.001)	(0.000)	(0.000)	(0.000)	(0.000)	(0.000)
Q2 2020 FE	20.647***	14.271***	13.160***	7.171***	-1.082	-11.156***	-1.249	-11.231***
	(0.000)	(0.000)	(0.000)	(0.000)	(0.790)	(0.003)	(0.758)	(0.003)
Q3 2020 FE	24.168***	17.575***	16.090***	9.967***	12.062***	3.415	8.763***	0.583
	(0.000)	(0.000)	(0.000)	(0.000)	(0.000)	(0.117)	(0.000)	(0.792)
Covid Deaths/100,000			3.005***	2.896***			2.466***	2.211***
			(0.000)	(0.000)			(0.000)	(0.000)
NPI Index					6.633***	7.755***	4.809***	6.125***
					(0.000)	(0.000)	(0.000)	(0.000)
Adj. R^2	0.31	0.53	0.31	0.54	0.31	0.54	0.31	0.54
Observations	13,330	13,330	13,330	13,330	13,330	13,330	13,330	13,330
Banks	1,293	1,272	1,293	1,272	1,293	1,272	1,293	1,272

	(1)	(2)	(3)	(4)	(5)	(6)	(7)	(8)
Q1 2017 – Q3 2019 FE	Yes	Yes	Yes	Yes	Yes	Yes	Yes	Yes
Bank FE	Yes	Yes	Yes	Yes	Yes	Yes	Yes	Yes
Bank Controls		Yes		Yes		Yes		Yes
Panel A: Commercial & Industrial Loans								
Q1 2020 FE	0.450**	0.702**	0.372	0.681*	0.513	0.639	0.541	0.649
	(0.049)	(0.038)	(0.131)	(0.056)	(0.428)	(0.312)	(0.404)	(0.304)
Q2 2020 FE	14.916***	9.739***	14.286***	9.596***	15.197***	9.462***	15.019***	9.459***
	(0.000)	(0.000)	(0.000)	(0.000)	(0.000)	(0.000)	(0.000)	(0.000)
Q3 2020 FE	14.883***	7.979***	14.189***	7.827***	15.036***	7.825***	14.564***	7.757***
	(0.000)	(0.000)	(0.000)	(0.000)	(0.000)	(0.000)	(0.000)	(0.000)
Covid Deaths/100,000			0.255	0.058			0.272	0.053
			(0.367)	(0.834)			(0.345)	(0.853)
NPI Index					-0.086	0.084	-0.237	0.046
					(0.914)	(0.901)	(0.769)	(0.948)
Adj. R^2	0.38	0.61	0.38	0.61	0.38	0.61	0.38	0.61
Observations	19,395	14,937	19,395	14,937	19,395	14,937	19,395	14,937
Banks	1,293	1,272	1,293	1,272	1,293	1,272	1,293	1,272
Panel B: Loans to Households								
Q1 2020 FE	0.086	-0.693**	0.150	-0.607*	0.292	-0.637	0.272	-0.683
	(0.692)	(0.024)	(0.503)	(0.052)	(0.583)	(0.259)	(0.609)	(0.226)
Q2 2020 FE	-1.143***	-6.559***	-0.624	-5.978***	-0.220	-6.312***	-0.090	-6.300***
	(0.000)	(0.000)	(0.254)	(0.000)	(0.920)	(0.004)	(0.967)	(0.004)
Q3 2020 FE	-1.742***	-8.567***	-1.171*	-7.946***	-1.241	-8.430***	-0.899	-8.110***
	(0.000)	(0.000)	(0.063)	(0.000)	(0.317)	(0.000)	(0.488)	(0.000)
Covid Deaths/100,000			-0.210	-0.237			-0.198	-0.249
			(0.262)	(0.257)			(0.286)	(0.230)
NPI Index					-0.282	-0.075	-0.172	0.107
					(0.667)	(0.907)	(0.793)	(0.869)
Adj. R^2	0.32	0.58	0.32	0.58	0.32	0.58	0.32	0.58
Observations	19,395	14,937	19,395	14,937	19,395	14,937	19,395	14,937
Banks	1,268	1,268	1,268	1,268	1,268	1,268	1,268	1,268

This table contains bank panel regressions from Q1 2017 to Q3 2020. Dependent variables are %-changes in loan volumes outstanding (relative to the pre-year quarter) – total loans and leases (panel A), small businesses loans (B), commercial & industrial loans (C), and private household loans (D). Independent variables of interest are fixed effects for 2020 quarters, the logarithm of 1 + the bank level exposure to COVID related deaths, and an NPI index. Exposure to COVID deaths is the deposit weighted number of new COVID-19 related deaths / 100,000 inhabitants during a quarter in a U.S. county. The state level NPI index is linked to banks equivalently. Controls include current %-changes in deposits and unused credit line commitments and lagged values of the logarithm of total assets, loan portfolio shares, and income, equity, deposits, liquidity, unused commitments, and loans and leases in percent of total assets. Standard errors are clustered by bank. ***, **, and * indicate statistical significance at 1%, 5%, and 10%. P-values are in parenthesis.

CEPR PRESS

Covid Economics 61, 11 December 2020: 73-120

Table 5: Interest Spreads of Syndicated Loans and the COVID Shock

	(1)	(2)	(3)	(4)	(5)	(6)	(7)	(8)
Q1-Q3 2019 FE	Yes	Yes	Yes	–	Yes	–	Yes	–
Bank FE	Yes	Yes	Yes	Yes	Yes	Yes	Yes	Yes
Loan Type FE	Yes	Yes	Yes	Yes	Yes	Yes	Yes	Yes
Industry * State FE	Yes	Yes	Yes	Yes	Yes	Yes	Yes	Yes
Industry * Quarter FE				Yes		Yes		Yes
Loan Controls		Yes		Yes		Yes		Yes
Bank Controls		Yes		Yes		Yes		Yes
Q1 2020 FE	1.629	-0.827	-15.083		-6.056		-11.432	
	(0.806)	(0.921)	(0.189)		(0.668)		(0.318)	
Q2 2020 FE	41.192***	55.228***	-28.837		8.895		-13.478	
	(0.000)	(0.000)	(0.407)		(0.863)		(0.734)	
Covid Deaths/100,000			17.394**	30.180**			18.667**	30.137**
			(0.032)	(0.017)			(0.039)	(0.025)
NPI Index					8.952	22.775	-5.678	0.132
					(0.530)	(0.181)	(0.639)	(0.994)
Adj. R^2	0.36	0.45	0.36	0.47	0.36	0.47	0.36	0.47
Observations	10,904	10,879	10,904	10,757	10,904	10,757	10,904	10,757
Borrowers	4,696	4,679	4,696	4,631	4,696	4,631	4,696	4,631
Banks	32	30	32	30	32	30	32	30

This table contains syndicated loan-level regressions from Q1 2017 to Q2 2020. The dependent variable is the interest spread over LIBOR (BPS). Independent variables of interest are fixed effects for the first two quarters of 2020, the logarithm of 1 + the bank level exposure to COVID related deaths, and an NPI index. Exposure to COVID deaths is the deposit weighted number of new COVID-19 related deaths / 100,000 inhabitants during a quarter in a U.S. county. The state level NPI index is linked to banks equivalently. Loan type fixed effects are for term loans, revolving credit lines, and other or both. Loan controls comprise of maturity, loan volume, fixed effects for loan purpose, collateral, and refinanced loans. Bank controls include current %-changes in deposits and unused credit line commitments and lagged values of the logarithm of total assets, loan portfolio shares, and income, equity, deposits, liquidity, unused commitments, and loans and leases in percent of total assets. Standard errors are clustered by the bank's headquarter state. ***, **, and * indicate statistical significance at 1%, 5%, and 10%. P-values are in parenthesis.

CEPR PRESS

Covid Economics 61, 11 December 2020: 73-120

Table 6: Maturities of Syndicated Loans and the COVID Shock

	(1)	(2)	(3)	(4)	(5)	(6)	(7)	(8)
Q1-Q3 2019 FE	Yes	Yes	Yes	–	Yes	–	Yes	–
Bank FE	Yes	Yes	Yes	Yes	Yes	Yes	Yes	Yes
Loan Type FE	Yes	Yes	Yes	Yes	Yes	Yes	Yes	Yes
Industry * State FE	Yes	Yes	Yes	Yes	Yes	Yes	Yes	Yes
Industry * Quarter FE				Yes		Yes		Yes
Loan Controls		Yes		Yes		Yes		Yes
Bank Controls		Yes		Yes		Yes		Yes
Q1 2020 FE	-2.228**	-3.061*	1.984		1.456		2.454	
	(0.032)	(0.055)	(0.503)		(0.792)		(0.658)	
Q2 2020 FE	-15.465***	-15.035***	2.587		-0.038		4.541	
	(0.000)	(0.000)	(0.792)		(0.998)		(0.816)	
Covid Deaths/100,000			-4.548**	-4.316*			-4.390**	-5.428
			(0.044)	(0.067)			(0.045)	(0.107)
NPI Index					-4.269	-0.700	-0.714	3.579
					(0.448)	(0.859)	(0.893)	(0.523)
Adj. R^2	0.25	0.29	0.25	0.30	0.25	0.30	0.25	0.30
Observations	13,162	12,912	13,162	12,805	13,162	12,805	13,162	12,805
Borrowers	5,800	5,624	5,800	5,585	5,800	5,585	5,800	5,585
Banks	34	31	34	31	34	31	34	31

This table contains syndicated loan-level regressions from Q1 2017 to Q2 2020. The dependent variable is maturity in months. Independent variables of interest are fixed effects for the first two quarters of 2020, the logarithm of 1 + the bank level exposure to COVID related deaths, and an NPI index. Exposure to COVID deaths is the deposit weighted number of new COVID-19 related deaths / 100,000 inhabitants during a quarter in a U.S. county. The state level NPI index is linked to banks equivalently. Loan type fixed effects are for term loans, revolving credit lines, and other or both. Loan controls comprise of interest spread, loan volume, fixed effects for loan purpose, collateral, and refinanced loans. Bank controls include current %-changes in deposits and unused credit line commitments and lagged values of the logarithm of total assets, loan portfolio shares, and income, equity, deposits, liquidity, unused commitments, and loans and leases in percent of total assets. Standard errors are clustered by the bank's headquarter state. ***, **, and * indicate statistical significance at 1%, 5%, and 10%. P-values are in parenthesis.

Appendix

Table A1: County-Level Descriptive Statistics

Variable	N	10th Perc.	Median	90th Perc.	Mean	SD
Covid Deaths/100,000	21,987	0	0	17	6.3	21.5
Q1 2020 Covid Deaths/100,000	21,987	0	0	.869	.464	2.259
Q2 2020 Covid Deaths/100,000	21,987	0	4.4	47.3	17	34.2
Q3 2020 Covid Deaths/100,000	21,987	0	13.8	66.6	26.3	37
NPI Index	21,987	0	0	2.923	.802	1.16
Q1 2020 NPI Index	21,987	.464	.71	1	.713	.221
Q2 2020 NPI Index	21,987	2.44	3.055	4.011	3.197	.564
Q3 2020 NPI Index	21,987	1.674	1.674	2	1.738	.285
Unemployment Rate	21,987	2.7	4.3	9.8	5.4	3.2
ICU Beds	21,987	0	0	32.9	13.4	53.5
Share of Elderly (above 65)	21,987	.137	.189	.253	.192	.045
Median Income	21,987	10.5	10.8	11.1	10.8	.2
Population Density	21,973	4.2	45.2	379.4	259.4	1,725
Share of Black and Hispanic	21,980	.013	.044	.318	.107	.141
Emp Share Primary Sector	20,041	.003	.029	.176	.063	.085
Emp Share Construction	19,782	.028	.056	.11	.064	.037
Emp Share Manufacturing	19,341	.035	.138	.335	.164	.119
Emp Share Trade, Transp, Util	21,861	.169	.236	.327	.245	.066
Emp Share Information	16,723	.004	.01	.023	.012	.009
Emp Share FIRE	20,874	.025	.042	.075	.047	.022
Emp Share Professional Services	20,811	.031	.072	.157	.085	.052
Emp Share Education + Health	21,203	.078	.165	.268	.17	.075
Emp Share Leisure Hospitality	21,399	.064	.118	.2	.13	.067
Emp Share Other Services	19,390	.017	.031	.05	.033	.014
Emp Share Government	21,903	.119	.206	.368	.228	.101

This table contains summary statistics for variables used in county-level regressions, in figures, or for bank exposure calculations. Observations are those used in regression 2, table 2.

Covid Economics 61, 11 December 2020: 73-120

Table A2: Bank-Level Descriptive Statistics

Variable	N	10th Perc.	Median	90th Perc.	Mean	SD
Covid Deaths/100,000	19,388	0	0	5.8	3.44	15.47
Q1 2020 Covid Deaths/100,000	1,293	0	.04	1.39	.65	1.87
Q2 2020 Covid Deaths/100,000	1,293	0	10.49	78.66	27.34	41.27
Q3 2020 Covid Deaths/100,000	1,293	2.99	15.25	53	23.57	27.57
NPI Index	19,388	0	0	1.67	.39	.92
Q1 2020 NPI Index	1,293	.46	.73	1.04	.73	.24
Q2 2020 NPI Index	1,293	2.6	3.09	3.95	3.27	.53
Q3 2020 NPI Index	1,293	1.67	1.67	2	1.78	.32
Growth in Loss Provisions	19,388	-100	1.72	137.5	13.64	132.63
Growth in NPLs	18,949	-88.29	0	102.86	3.61	77.85
Growth in NPLs (C&I)	17,298	-159.3	-4.1	168.1	1.1	107.3
Growth in NPLs (Households)	18,489	-102.19	-2.65	107.33	-.36	84.42
Growth in Loans and Leases	19,388	-1.2	6.48	19.46	8.29	9.9
Growth in Small Bus Loans	13,329	-7.5	4.24	30.89	7.98	17.96
Growth in C&I Loans	19,388	-4.82	8.29	28.23	10.36	14.48
Growth in Household Loans	19,388	-5.89	4.88	20.66	6.56	12.33
Income/Assets	14,212	.12	.28	.46	.28	.14
Equity/Assets	14,212	8.68	10.73	14.25	11.22	2.46
Liquidity/Assets	14,212	10.18	20.97	42.39	23.68	12.78
Deposits/Assets	14,212	75.53	84.37	89.45	83.29	5.57
Loans and Leases/Assets	14,212	51.45	72.59	84.56	70.14	12.93
Undrawn Commitments/Assets	14,212	4.47	11.93	23	13.3	8.42
Assets (Bn)	14,212	.1	.4	4.4	9.9	102.8
Growth in Deposits	19,388	-1.64	5.81	20.07	8.11	11.16
Growth in Undrawn Commitm	19,388	-15.51	7.75	34.85	8.87	23.95
C&I/Tot Loans & Leases	14,212	4.41	12.04	27.54	14.31	9.85
Agricul/Tot Loans & Leases	14,212	0	.9	21.46	6.19	10.46
Househ/Tot Loans & Leases	14,212	.46	3.41	15.04	6.29	8.4
Real Est/Tot Loans & Leases	14,212	47.01	75.74	92.09	72.58	17.42
Small Bus/Tot Loans & Leases	9,892	5.98	21.96	43.84	23.73	14.46

This table contains summary statistics for variables used in bank-level regressions or figures. Observations are those used in regression 1, table 3. "COVID Deaths/100,000" variables and "NPI Index" refer to the bank level exposures to COVID, computed as the deposit weighted number of new COVID-19 related deaths / 100,000 inhabitants (or the NPI index value) during a quarter in a U.S. county.

Covid Economics 61, 11 December 2020: 73-120

Covid Economics 61, 11 December 2020: 73-120

Table A3: Loan-Level Descriptive Statistics

Variable	N	10th Perc.	Median	90th Perc.	Mean	SD
Covid Deaths/100,000	10,789	0	0	.62	2.81	12.76
Q1 2020 Covid Deaths/100,000	707	.62	1.36	4.16	1.86	1.38
Q2 2020 Covid Deaths/100,000	521	28.1	49.2	83.1	55.6	20.9
NPI Index	10,789	2.067	2.34	2.551	2.317	.203
Q1 2020 NPI Index	707	.77	.869	.923	.858	.087
Q2 2020 NPI Index	521	3.126	3.639	3.915	3.613	.343
Spread over LIBOR (BPS)	10,789	113	200	400	233	132
Maturity (Months)	10,765	19	60	69	52	19
Facility Amount (M)	10,789	25	200	1,200	498	973
Term Loan (1/0)	10,789	0	0	1	.4	.5
Revolving Loan (1/0)	10,789	0	1	1	.56	.496
Purpose CAPX (1/0)	10,789	0	0	0	.048	.213
Purpose Working Cap (1/0)	10,789	0	0	0	.009	.096
Purpose Corporate (1/0)	10,789	0	0	1	.156	.362
Purpose M&A (1/0)	10,789	0	1	1	.7	.5
Purpose Debt Repaym (1/0)	10,789	0	0	0	.025	.158
Purpose Other (1/0)	10,789	0	0	0	.051	.22
Secured Loan (1/0)	10,789	0	0	1	.351	.477
Refinancing Loan (1/0)	10,789	0	1	1	.654	.476
Assets (Bn)	10,780	143	1,758	2,338	1,463	835
Deposit Growth	10,777	.24	3.25	14.94	5.53	8.9
Unused Commitm Growth	10,777	-1.62	3.58	9.28	4.34	13.06
Deposits/Assets	10,777	56	72	77	68	11
Liquity/Assets	10,777	18	27	31	26	5
Equity/Assets	10,777	9.5	10.8	12.7	11.1	2.1
Income/Assets	10,777	.217	.295	.411	.297	.087
Loans & Leases/Assets	10,777	36	48	66	50	12
Unused Commitm/Assets	10,777	39	51	57	50	12
C&I/Tot Loans & Leases	10,769	19	29	38	27	8
Agricult/Tot Loans & Leases	10,769	.048	.078	.544	.192	.239
Househ/Tot Loans & Leases	10,769	9.1	20.2	23.9	18.6	8
Real Est/Tot Loans & Leases	10,769	35.9	42.8	52.8	43.5	7.2
Sm Bus/Tot Loans & Leases	10,766	2.97	4.06	4.65	3.91	1.21

This table contains summary statistics for variables used in loan-level regressions or figures. Observations are those used in regression 1, table 5. "COVID Deaths/100,000" refers to the bank level exposure to COVID, computed as the deposit weighted number of new COVID-19 related deaths / 100,000 inhabitants during a quarter in a U.S. county.

Table A4: Pairwise Correlations of COVID Related Variables

Variables	Q1 2020	Q2 2020	Q3 2020	Covid Deaths	NPI Index
Q1 2020	1.000				
Q2 2020	-0.167	1.000			
	(0.000)				
Q3 2020	-0.167	-0.167	1.000		
	(0.000)	(0.000)			
Covid Deaths	-0.145	0.346	0.590	1.000	
	(0.000)	(0.000)	(0.000)		
NPI Index	-0.031	0.831	0.329	0.624	1.000
	(0.000)	(0.000)	(0.000)	(0.000)	

This table contains pairwise correlations of all independent variables of interest defined on the county level. COVID deaths refer to the logarithm of 1 plus the number COVID Deaths/100,000. Significance levels are in brackets.

Covid Economics 61, 11 December 2020: 73-120

Table A5: Exposure of the Largest U.S. Banks to COVID in the First Half of 2020

				Covid Deaths/100,000		
Bank	**Headquarters**	**Assets**	**Branches**	**New Q1**	**New Q2**	**New Q3**
Signature Bank	New York, NY	51	31	8	190	13
New York Community Bank	Westbury, NY	54	241	6	175	19
HSBC Bank USA	Tysons, VA	173	225	7	160	16
Santander Bank	Wilmington, DE	85	613	3	139	16
People's United Bank	Bridgeport, CT	58	414	3	116	9
JPMorgan Chase Bank	Columbus, OH	2,338	5,024	4	102	22
TD Bank	Wilmington, DE	320	1,244	2	92	16
Citizens Bank	Providence, RI	166	1,105	1	84	15
The Northern Trust Company	Chicago, IL	136	56	1	68	24
Capital One	McLean, VA	329	488	3	74	16
City National Bank	Los Angeles, CA	61	71	2	62	26
Comerica Bank	Dallas, TX	73	436	3	67	21
Citibank	Sioux Falls, SD	1,454	709	2	67	16
Manufacturers & Traders Trust Company	Buffalo, NY	119	788	1	71	10
BMO Harris Bank	Chicago, IL	138	590	1	61	15
TCF National Bank	Sioux Falls, SD	47	330	1	60	13
Bank of America	Charlotte, NC	1,853	4,335	1	50	23
PNC Bank	Wilmington, DE	398	2,398	1	52	17
Synovus Bank	Columbus, GA	48	296	1	21	47
First Republic Bank	San Francisco, CA	116	81	2	55	13
East West Bank	Pasadena, CA	44	111	1	35	28
CIT Bank	Pasadena, CA	45	66	1	31	32
Regions Bank	Birmingham, AL	126	1,460	1	23	37
BBVA USA	Birmingham, AL	93	642	0	13	42
Fifth Third Bank	Cincinnati, OH	168	1,224	1	36	17
Wells Fargo Bank	Sioux Falls, SD	1,713	5,570	1	33	21
The Huntington National Bank	Columbus, OH	109	909	1	38	15
KeyBank	Cleveland, OH	143	1,125	1	38	12
MUFG Union Bank	San Francisco, CA	133	350	1	21	28
Branch Banking & Trust Company	Charlotte, NC	461	1,791	0	22	25
TIAA, FSB	Jacksonville, FL	42	13	0	8	37
U.S. Bank	Cincinnati, OH	486	2,979	1	28	17
First Tennessee Bank	Memphis, TN	43	291	0	13	27
Zions Bancorporation	Salt Lake City, UT	69	435	0	13	26
Bank of the West	San Francisco, CA	93	554	1	15	18

This table contains information on the 35 largest U.S. banks. Total assets (in billion USD) and numbers of branches are from 2019. The exposure to COVID is based on the county-level death rates in new quarterly deaths (COVID-19 related deaths / 100,000 inhabitants). The bank level exposure variables in this table bank's weighted averages using the county-level branch deposit share in the bank's total deposits as weights. The list (and all tables and plits) exclude institutes that are formally commercial banks but do not operate a significant branch network (excluding those banks with $ 10 Bn or more in assets but less than 10 branches, those with at least 5 Bn and less than 5 branches, 3 Bn and less than 3 branches, or 1 Bn and only 1 branch).

Table A6: Bank Health and the COVID Shock

	(1)	(2)	(3)	(4)	(5)	(6)	(7)	(8)
Q1 2017 – Q3 2019 FE	Yes	Yes	Yes	Yes	Yes	Yes	Yes	Yes
Bank FE	Yes	Yes	Yes	Yes	Yes	Yes	Yes	Yes
Bank Controls		Yes		Yes		Yes		Yes
Panel C: Non-Performing C&I Loans								
Q1 2020 FE	5.951*	7.428*	4.536	5.692	-0.254	1.583	-0.056	2.109
	(0.061)	(0.099)	(0.164)	(0.213)	(0.963)	(0.808)	(0.992)	(0.747)
Q2 2020 FE	8.399**	0.014	-3.094	-11.695	-19.186	-25.311	-23.027	-26.763
	(0.025)	(0.997)	(0.653)	(0.136)	(0.352)	(0.234)	(0.265)	(0.209)
Q3 2020 FE	4.578	0.406	-7.889	-11.959	-10.402	-13.673	-18.141	-19.697
	(0.297)	(0.946)	(0.289)	(0.172)	(0.381)	(0.294)	(0.146)	(0.146)
Covid Deaths/100,000			4.553**	4.677*			4.135*	4.166*
			(0.034)	(0.055)			(0.060)	(0.096)
NPI Index					8.408	7.699	6.397	4.970
					(0.169)	(0.217)	(0.304)	(0.438)
Adj. R^2	0.05	0.05	0.05	0.05	0.05	0.05	0.05	0.05
Observations	17,296	13,484	17,296	13,484	17,296	13,484	17,296	13,484
Banks	1,255	1,227	1,255	1,227	1,255	1,227	1,255	1,227
Panel D: Non-Performing Loans to Households								
Q1 2020 FE	0.193	1.999	-1.168	0.291	-14.117***	-11.770**	-13.835***	-11.264**
	(0.934)	(0.522)	(0.630)	(0.928)	(0.000)	(0.010)	(0.001)	(0.014)
Q2 2020 FE	1.354	-7.790**	-9.574*	-19.214***	-62.522***	-67.816***	-64.724***	-68.067***
	(0.648)	(0.025)	(0.073)	(0.001)	(0.000)	(0.000)	(0.000)	(0.000)
Q3 2020 FE	-5.213	-8.528*	-17.169***	-20.653***	-39.801***	-41.830***	-45.299***	-45.542***
	(0.110)	(0.064)	(0.003)	(0.002)	(0.000)	(0.000)	(0.000)	(0.000)
Covid Deaths/100,000			4.385***	4.626**			3.126*	2.856
			(0.006)	(0.011)			(0.051)	(0.121)
NPI Index					19.483***	18.267***	17.778***	16.197***
					(0.000)	(0.000)	(0.000)	(0.000)
Adj. R^2	0.05	0.06	0.05	0.06	0.05	0.06	0.05	0.06
Observations	18,493	14,308	18,493	14,308	18,493	14,308	18,493	14,308
Banks	1,273	1,246	1,273	1,246	1,273	1,246	1,273	1,246

This table contains bank panel regressions from Q1 2017 to Q3 2020. Dependent variables are %-changes in non-performing C&I loans (panel A) and loans to private households (B) relative to the respective pre-year quarter. Independent variables of interest are fixed effects for 2020 quarters, the logarithm of 1 + the bank level exposure to COVID related deaths, and an NPI index. Exposure to COVID deaths is the deposit weighted number of new COVID-19 related deaths / 100,000 inhabitants during a quarter in a U.S. county. The state level NPI index is linked to banks equivalently. Controls include current %-changes in deposits and unused credit line commitments and lagged values of the logarithm of total assets, loan portfolio shares, and income, equity, deposits, liquidity, unused commitments, and loans and leases in percent of total assets. Standard errors are clustered by bank. ***, **, and * indicate statistical significance at 1%, 5%, and 10%. P-values are in parenthesis.

Covid Economics 61, 11 December 2020: 73-120

Figure A1: Health and Lending by Banks with Differential Geographical Exposures to COVID

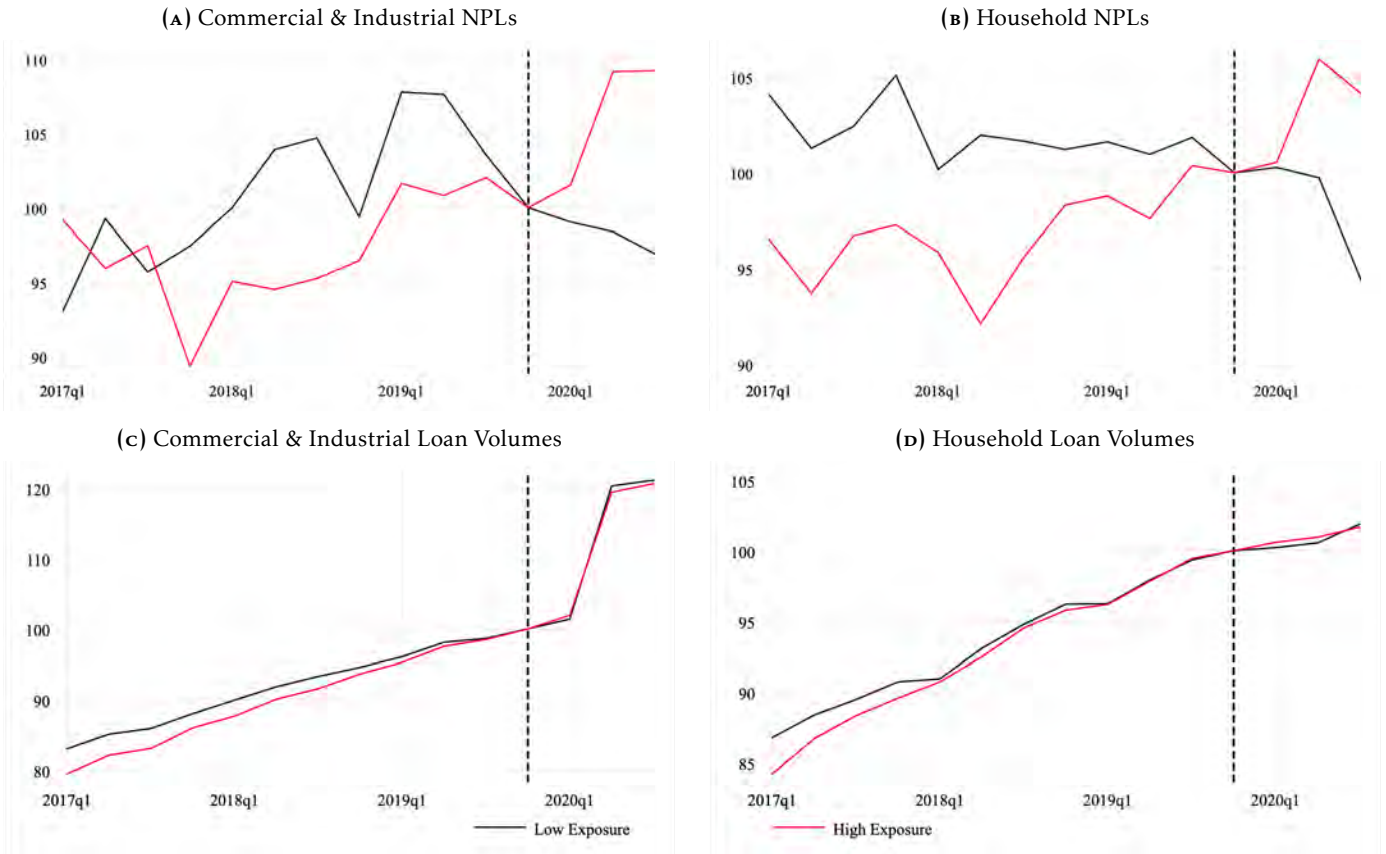

This figure shows U.S. banks' median quarterly loan loss provisions (in % of total loans & leases) in panel A and non-performing loans (indexed to 100 in Q4 2019) in panels B-D. The figure differentiates according to banks' geographical exposure to COVID. The latter is the deposit weighted number of cumulative COVID-19 related deaths / 100,000 inhabitants during the first half of 2020. The black (red) line represents the group of banks below (above) the median exposure. The vertical black dashed line indicates the pre-COVID quarter Q4 2019.

Covid Economics 61, 11 December 2020: 73-120

Figure A2: Geographical Footprint of Banks

Panel A: Bank Branches

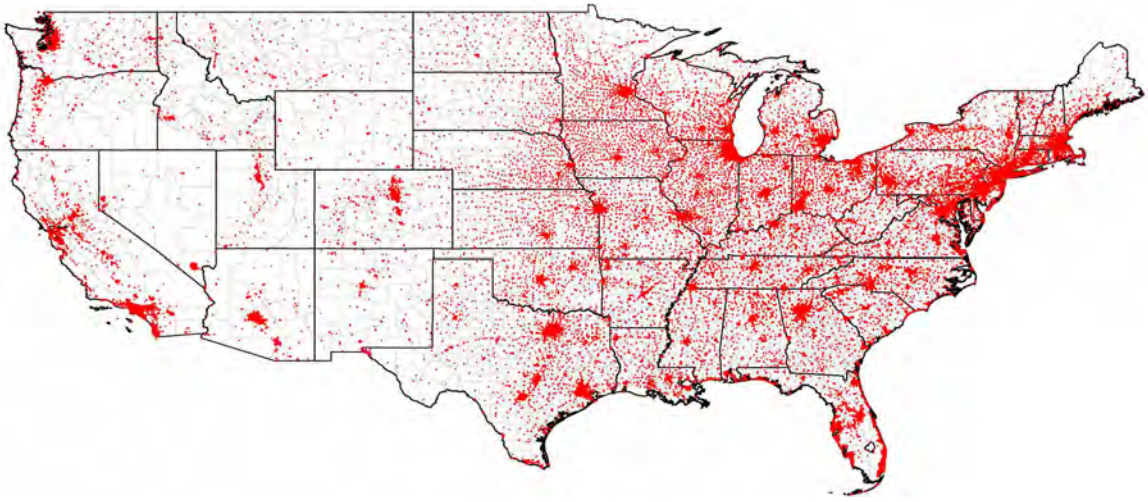

Panel B: Deposit Distribution

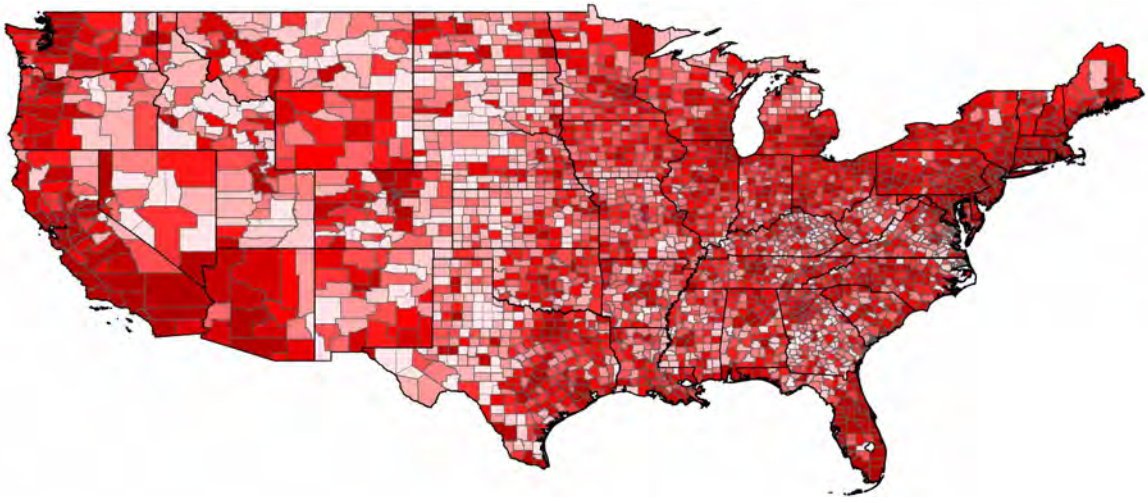

Every dot in panel A represents a bank branch in June 2019 in the contiguous states of the U.S. Coloring of counties in panel B follows a heat map scheme, corresponding to 2019 deposits at bank branches in a county. A darker red means more deposits.

Covid Economics 61, 11 December 2020: 73-120

Figure A3: Other Variables of Banks with Differential Exposures to COVID

(A) Liquidity

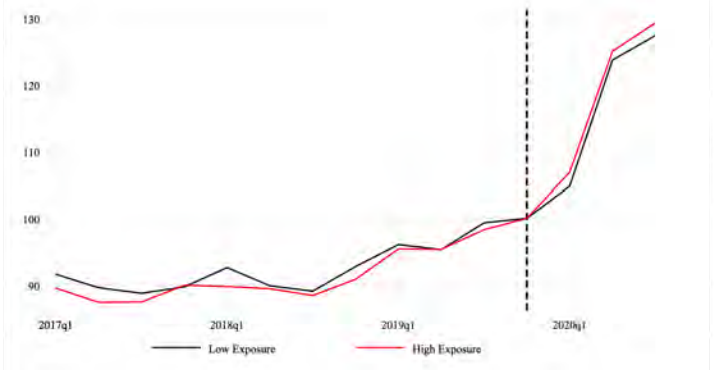

(B) Equity

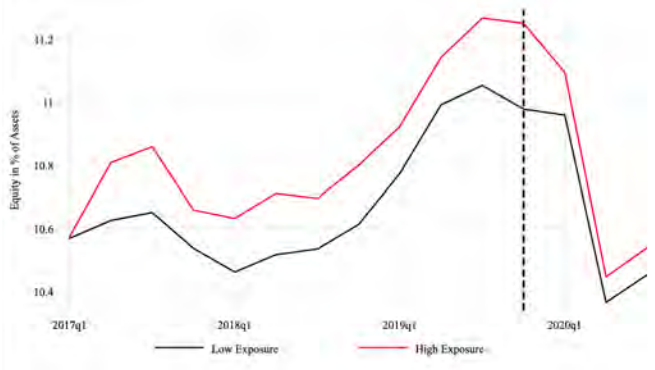

(C) Unused Commitments Outstanding

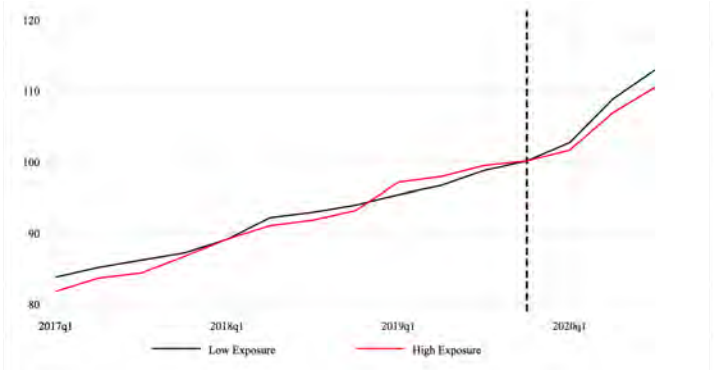

(D) Deposits

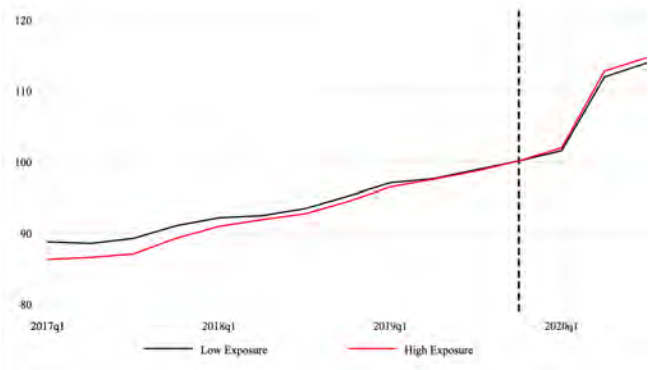

Panels A, C, and D shows U.S. banks' mean quarterly liquidity, unused commitments outstanding, and deposits indexed to 100 in Q4 2019 respectively. Panel B shows U.S. banks' mean equity / total assets. The figure differentiates according to banks' geographical exposure to COVID. The latter is the deposit weighted number of cumulative COVID-19 related deaths / 100,000 inhabitants during the first half of 2020. The black (red) line represents the group of banks below (above) the median exposure. The vertical black dashed line indicates the pre-COVID quarter Q4 2019.

Covid Economics 61, 11 December 2020: 73-120

Figure A4: COVID-19 Infections

Panel A: Q1 2020

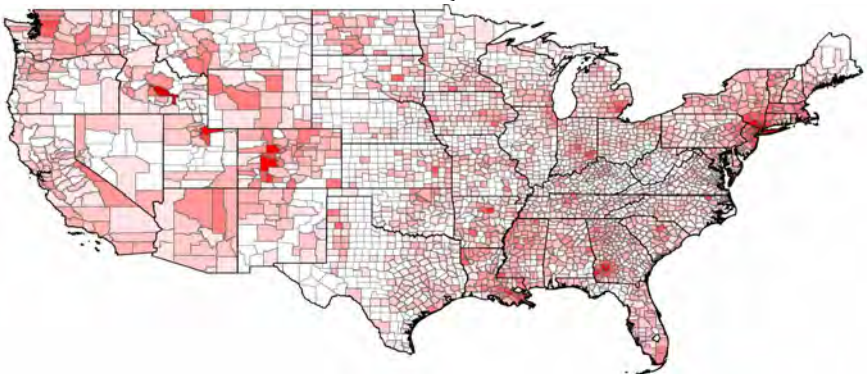

Panel B: Q2 2020

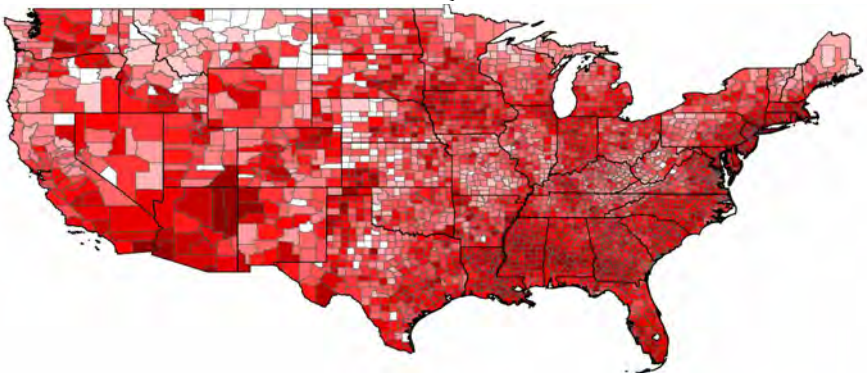

Panel C: Q3 2020

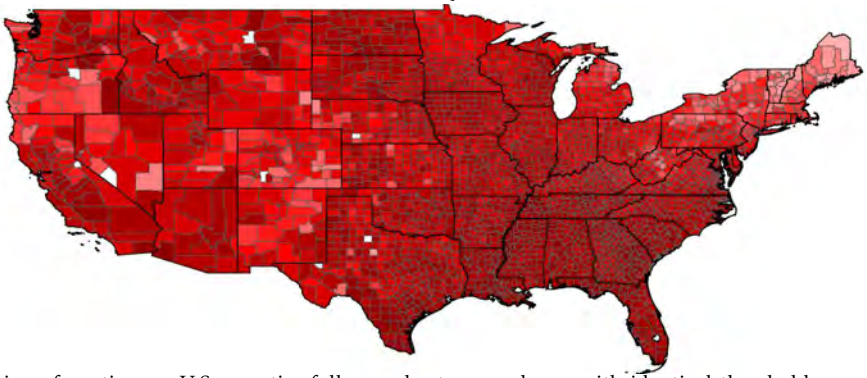

Coloring of contiguous U.S. counties follows a heat map scheme with identical thresholds across all panels. The darker the red, the higher the number of new quarterly COVID-19 infections per 100,000 inhabitants.

US churches' response to Covid-19: Results from Facebook[1]

Eva Raiber[2] and Paul Seabright[3]

Date submitted: 6 December 2020; Date accepted: 8 December 2020

This study investigates U.S. churches' response to the SARS-CoV-2 pandemic by looking at their public Facebook posts. For religious organizations, in-person gatherings are at the heart of their activities. Yet religious in-person gatherings have been identified as some of the early hot spots of the pandemic, but there has also been controversy over the legitimacy of public restrictions on such gatherings. Our sample contains information on church characteristics and Facebook posts for nearly 4000 churches that posted at least once in 2020. The share of churches that offer an online church activity on a given Sunday more than doubled within two weeks at the beginning of the pandemic (the first half of March 2020) and stayed well above baseline levels. Online church activities are positively correlated with the local pandemic situation at the beginning, but uncorrelated with most state interventions. After the peak of the first wave (mid April), we observe a slight decrease in online activities. We investigate heterogeneity in the church responses and find that church size and worship style explain differences consistent with churches facing different demand and cost structures. Local political voting behavior, on the other hand, explains little of the variation. Descriptive analysis suggests that overall online activities, and the patterns of heterogeneity, remain unchanged through end-November 2020.

1 We are grateful to Amandine Belard and Paulina Rebolledo Guzmán for excellent research assistance. We thank participants of the Institute for Advanced Study in Toulouse religious reading group and the lunch seminar, the ASREC 24h conference, and members of the Network of Female Researchers in Behavioral Economics and Development for their suggestions. Eva Raiber acknowledges support from the French National Research Agency Grants ANR-17-EURE-0020. Paul Seabright acknowledges IAST funding from the French National Research Agency (ANR) under the Investments for the Future (Investissements d'Avenir) program, grant ANR-17-EURE-0010.

2 Aix-Marseille University, CNRS, AMSE, Marseille, France.

3 Toulouse School of Economics (IAST), University of Toulouse, France.

Covid Economics 61, 11 December 2020: 121-171

1 Introduction

For religious organisations, in-person gatherings are at the heart of their activities. They are where members of the organisation interact, a platform for prayer and religious rituals, and exchange with the religious leaders. Unfortunately, religious in-person gatherings have been identified as some of the early hot spots of the novel coronavirus (SARS-CoV-2).[1] Religious gatherings usually take place indoors, with large groups, and often involve singing and close contact between the members. These points have been identified as key features that facilitate the spread of SARS-CoV-2.[2] At the same time, in-persons gatherings are the way in which members' commitment to fellow members and to the organisation is strengthened, in a way that often translates directly into revenues for the organisation. This obviously creates important conflicts of interest for such organisations - how have they responded?

We investigate the response of US Christian churches to the coronavirus pandemic and to the interventions imposed by the governments to limit the virus propagation. Specifically, we ask to what extent churches have responded to the pandemic by moving their gatherings online, and which types of churches have done so most. We use a data set of nearly 4000 Christian churches in the United States that have a public Facebook profile, and that are registered at usachurches.org. With the support of CrowdTangle, a Facebook-owned tool that tracks interactions on public content from Facebook pages and groups, we obtained all public Facebook posts of those churches from January 2020 to October 2020 (CrowdTangle Team [2020]).

To identify church online activities, we hand coded 1600 church posts and then use a random forest algorithm to predict the advertisement of an online church activity in a Sunday post for the rest of the sample. The prediction algorithm evaluates the type of the post (video, link, live stream, etc), as well as the post text. We then observe the extent to which the churches' online activities are correlated with state and county regulations and numbers of Covid-19 cases in the period between

[1] For example an annual prayer meeting at an evangelical megachurch in France https://www.washingtonpost.com/world/europe/how-a-prayer-meeting-at-a-french-megachurch-may-have-led-to-scores-of-coronavirus-deaths/2020/04/01/fe478ca0-7396-11ea-ad9b-254ec99993bc_story.html and a Muslim gathering in India https://www.washingtonpost.com/world/asia_pacific/india-coronavirus-tablighi-jamaat-delhi/2020/04/02/abdc5af0-7386-11ea-ad9b-254ec99993bc_story.html. See also James et al. [2020].

[2] World Health Organization [2020], July 2020 version.

Covid Economics 61, 11 December 2020: 121-171

January and June 2020. We verify the results using the share of churches that post at least one video on a given Sunday as another proxy for online activity. We investigate heterogeneity in the reaction according to the size and the worship style of the church, as well as voting behavior at the county level in the 2016 presidential election.

Stories of religious organisations that held in-person gatherings despite the coronavirus pandemic and despite governmental orders are easy to find in the media.[3] Indeed, many religious organisations and denominations were presented as responding irresponsibly to the crisis.[4] Yet stories of churches defying public health guidance are undeniably more newsworthy and perhaps more relevant for enforcement of public health measures, which suggests they may not be representative of the behavior of churches overall. The issue of in-person religious gatherings has again become central to the political debate on the legitimacy of public health measures, in the wake of the US Supreme Court decision on 25th November 2020 striking down restrictions on religious services imposed in New York by Governor Andrew M. Cuomo.[5] We try to provide a more objective measure of the response of US churches in moving their gatherings online, to the extent that is possible from the limited available data. This may help formulate public health policies that may be necessary due to the continuation of the pandemic, as well as to future crises arising from other types of infectious disease.

In a pandemic, it seems likely that individuals turn to figures of authority for guidance on how to behave. Those figures of authority may be in government or in other components of civil society, and may include church leaders. The role of other sources is likely to be particularly important where the message from government is either not clear or not trusted by the people. The United States is especially suitable for this study because it is a country with a federal structure as well as high level of religious participation. There are multiple sources of advice and authority for individuals to listen to even within the government, and they are likely to have given particular weight

[3] For example, https://www.bbc.com/news/world-us-canada-52232384, accessed 2020-09-18.

[4] Forexample, https://www.nytimes.com/2020/03/30/us/coronavirus-pastor-arrested-tampa-florida.html?auth=login-facebook, accessed 2020-06-18, and https://www.independent.co.uk/news/world/americas/kenneth-copeland-blow-coronavirus-pray-sermon-trump-televangelist-a9448561.html, accessed 2020-06-18.

[5] See "Splitting 5 to 4, Supreme Court Backs Religious Challenge to Cuomo's Virus Shutdown Order", *New York Times*, 26th November 2020, https://www.nytimes.com/2020/11/26/us/supreme-court-coronavirus-religion-new-york.html?action=click&module=Top%20Stories&pgtype=Homepage.

to decisions by churches on how to respond to the pandemic.

We find that the proportion of churches offering an online activity more than doubled between February and April 2020. While around 28 percent of churches in our sample already posted an online alternative in February, around another 16 percent of churches responded very quickly and already posted an online alternative in the weekend after the international travel ban (March 11) and another 16 percent the weekend after. We also find a positive association between positive Covid cases or Covid deaths on the county level and churches online activity, even when controlling for governmental regulations, in the introduction period, defined as between January 1 and April 15, 2020.

Looking at the period between April 15 and June 30, the relaxation period, we find that the proportion of churches offering an online alternative slowly goes down over time. Yet the decrease is not correlated with the number of Covid cases or deaths. There is a correlation with lifting governmental regulations, yet it becomes insignificant once a trend is included. We thus cannot distinguish a relationship between lifting restrictions and online activities from a general fatigue effect. In the end, though, the proportion does not go down to the baseline levels but stays at a much higher level than before. Furthermore, we confirm that this high level of online activity continues through to the end of October.

We do not expect that churches would all react in the same way. For example, large churches that already have a significant online presence might find the cost of moving their activities entirely online is smaller than for smaller churches. If true, this might apply not only to their direct costs of moving online , but also to their opportunity costs: small churches may rely on appeals to funds delivered in person to their physical congregations, whereas larger churches may have more sophisticated online fundraising skills. The demand that churches face according to their size and worship style might also be different. Larger churches may be more attractive to a different type of population. Also, a contemporary church event might be easier to broadcast online and might have a higher take-up than a traditional church service.

Covid Economics 61, 11 December 2020: 121-171

Investigating heterogeneity in the church responses, we find that mega and large churches were indeed very fast in their response. The share of mega churches offering an online alternative on Sunday was already high before the pandemic (around 50%) but still increased significantly after the first weekend (after the international travel ban came into place). Relatedly, 36% of churches who have a contemporary worship style already offered an online alternative before the pandemic and the proportion increased strongly in the first two weekends of the pandemic. Large and mega churches also do not seem to decrease their online offer in the relaxation period as much, suggesting a more permanent shift to a hybrid model.

Medium and small churches, which started from a lower baseline level, were slower to respond. Yet the proportion of medium and small churches offering an online activity on a Sunday in the week after the federal guidelines on the coronavirus were issued (March 16) increased by 20 - 26 percentage points. This implies that the number offering an online alternative also doubled within the first weeks of the pandemic. However, there is a stronger decreasing trend for small churches in the relaxation period, suggesting that some might go back to solely in-person gatherings. Similarly, churches with a traditional worship style started with a lower baseline proportion but more than doubled the share offering an online activity on Sundays. Yet their decrease is the strongest in the relaxation period.

The ruling of the Supreme Court in favor of religious gatherings seems likely to entrench a view of the behavior of churches in the pandemic as reflecting primarily ideological or political beliefs, and as motivated by the political convictions of their leaders rather than the well-being or safety of their members. Yet when we interact churches' responses with the share of Republican votes in the county at the 2016 Presidential election we find almost no effect. A slight dampening of the move online can be observed in states with religious exemptions to stay-home orders, which tend to lean Republican. However, controlling for the nature of the stay-home orders, churches in Republican counties show a slightly greater tendency to move online, and the two effects more or less offset each other. In short, if their is a political effect of Republican support on online activity it appears to operate through a political channel (the type of state-level health measures imposed) rather than a religious channel (the decisions of church leaders).

Covid Economics 61, 11 December 2020: 121-171

Covid Economics 61, 11 December 2020: 121-171

It is hardly surprising that churches should become a focus of attention in a pandemic. A now substantial literature has shown that religious activities can help individuals to deal with stress, uncertainty, and negative shocks. Recent studies show that people become more religious if they recently experienced an earthquake close by (Bentzen [2019]) and that church members in Ghana made less charitable donations when they were enrolled in a formal insurance policy (Auriol et al. [2020]).[6] This phenomenon is likely to be particularly important in societies lacking comprehensive mechanisms of insurance against various risks including health risks.

The coronavirus pandemic is therefore likely to change the demand for religion. Indeed, Bentzen [2020] describes how the pandemic lead to a global increase in the demand for prayers measured by an increase in relative Googles searches. A survey conducted by Pew Research Center survey at the end of March 2020 finds that 55% of U.S. adults state that they have prayed for an end of the pandemic (Pew Research Center [2020]). Yet among those who usually attend religious services at least once or twice a month, 59% scaled back on attendance of religious gatherings. The coronavirus pandemic thus combines a change in the cost of holding in-person gatherings (due to regulations but also due to the health risk for members) with a shift in the demand for religious activities.

This economic view of the activities of religious organizations - that they primarily act to supply services for which they perceive a demand on the part of their actual and potential members - contrasts with a more ideological or political view, according to which church leaders have a significant ability to persuade church members to adopt the leaders' narrowly political or more broadly ideological beliefs. In our heterogeneity analysis, we find no evidence that supply-driven ideological factors have played a substantial part in shaping the churches' responses. Size and worship style are important sources of heterogeneity, while political orientation is not. Of course, we cannot rule out that churches are using their persuasive power to advance political messages in ways that escape our analysis. But if the majority of churches were opposing public health measures on a large scale we would expect to see evidence of this in our data, and we do not.

[6] See also Chen [2010] and Ager and Ciccone [2016].

2 Covid-19 in the US: Cases and regulations

The first case of Covid-19 in the US was confirmed on 20 January 2020 and from the beginning of March cases began to increase exponentially (see figure 10 in the Appendix). On March 11, the federal government banned foreign travel, trying to avoid infected travellers from abroad spreading the virus in the US. Just a few days later, on Monday March 16, the federal government published guidelines that should be implemented to mitigate the spread of the virus. It urged citizens to stay at home if they were sick, lived with someone who was tested positive, or were in an at-risk group. It also encouraged working from home and avoiding gatherings of more than 10 people.[7]

At around the same time, state governments reacted to the increase of cases in their states. We use regulation data from Killeen et al. [2020] which summarizes and groups state and district orders. Public schools in all states were closed with state orders being released between March 15 and April 2. Restaurants and entertainment establishments were told to close at around the same time in all states (except South Dakota). Most states also banned gatherings of more than 500 people or of more than 50 people. The different state regulations were often released within the same week, yet there are some states that had a one or two-week time lag between the regulations, and some regulations were implemented at the county level. Between March 21 and April 6, most states issued a stay-at-home order. Some states defined religious organisations as essential businesses and/or allowed small religious gatherings, while others did not.

The number of daily deaths due to Covid-19 reached its peak in the middle of April 2020. Confirmed Covid-19 cases decreased slightly after April. They stayed at a high level also due to more extensive testing with the number of tests doubling between mid-May and the end of June. The number of positive Covid-19 cases increased again from the middle of June onward with an increase of death from July onward which was less pronounced than the surge observed in April. As a reaction to the decreasing number of deaths and hospitalization, states rolled back their stay-home orders between April 24 and June 15. Similarly, restaurants and entertainment establishments were allowed to reopen between April 24 and June 22. At the end of June, several states still had

[7] https://www.whitehouse.gov/wp-content/uploads/2020/03/03.16.20_coronavirus-guidance_8.5x11_315PM.pdf, accessed 2020-09-16.

Covid Economics 61, 11 December 2020: 121-171

restrictions on the number of people being allowed to gather in one place.

3 Church Data

3.1 Church characteristics and Facebook pages from usachurches.org

On May 29, 2020, we collected information on churches from the usachurches.org website. usachurches.org is an online platform offering information for people searching for a church in the United States. It contains relevant information regarding the main characteristics of churches, such as denominations, location, size and the programs and services they offer. The platform was first established in 2000 in Columbus, Ohio and expanded to other states in 2005. Any website user can register their church and indicate their information. This implies that any member of the church, not only the church leaders, can register their church. The information is then reviewed and approved by the platform.

The website contains rich information on 10,190 churches in nearly all states. Estimating the total number of churches in the US at 350,000[8], the registry includes around 3% of all US churches. However, the website does not report when the information was registered nor when it was last updated. Also, because the information can be registered by any church member, it might omit certain programs and services or miscalculate the size of their church. Self-registration also implies that more technology-friendly churches, as well as those that are publicly advertising their congregation as a place to join, are more likely to be in our data set. Potential selection bias should therefore be borne in mind in interpreting our results.

Importantly, the registry includes information about the social media presence of the church, as well as some characteristics of interest. First, the church size is defined according to the church's average weekly attendance. Small churches are defined as receiving up to 50 people, medium churches between 51 and 300 people; large churches correspond to between 301 and 2000 people, and mega-churches receive on average over 2000 people a week. According to these definitions,

[8]Estimate by the Hartfort institute: http://hirr.hartsem.edu/research/fastfacts/fast_facts.html#numcong.

Covid Economics 61, 11 December 2020: 121-171

32.7% of the churches are small, 49% are medium, 12.5% are large, and the remaining 5.8% are mega-churches. Additionally, 3.6% of churches declare that they have more than one worship site. Comparing these numbers to the results of the National Congregation Study (Chaves [2019]) there are proportionately fewer small churches in our data set than in the National Congregation Study where they make up 42.7%. We also have proportionately more megachurches present in our data set than on average in the US.[9]

Secondly, churches declare their denomination. The raw data contains 159 different denominations; we categorize them into 18 broader Christian denominations according to the definitions presented in the USA Churches Directory. 27% of the churches are either non-denominational or independent churches. The most important denominations in the sample are Baptist (22.7%), Pentecostal (15.8%), and Methodist (5.3%). Thirdly, the directory contains information on the worship style which is either contemporary, traditional, or a blend of the two.

Finally, churches can provide links to their social media profiles. 43.4% provide a link to their public Facebook profile, 20.6% indicate a Twitter profile, and 5.9% provide a YouTube link. As Facebook is the most widespread social media platform, we decide to focus on their online Facebook presence.

Table 3 in the Appendix shows the difference between churches that provide a public Facebook link and those that do not. Not surprisingly, in the sample that provides a Facebook link there are more large and mega churches and fewer small churches. More churches with a Facebook link describe themselves as having a contemporary worship style. The two samples are similar in their denominational structure, with more Methodist and slightly fewer Baptist churches providing a Facebook link. Finally, churches that provide a Facebook link also more often provide a YouTube or Twitter link.

[9]The definitions for medium and large churches are unfortunately not the same in the two data sets.

Covid Economics 61, 11 December 2020: 121-171

3.2 Public posts on Facebook

To study the churches' social media response to the coronavirus pandemic, we use Facebook as a proxy for online activity. Facebook is the social media platform that has the highest prevalence of the three in the church data set. Furthermore, Facebook still has one of the highest numbers of users in the US among all social media. According to the Pew Research Center (Perrin and Anderson [2019]), 69% say they have ever used the platform. Only usage of YouTube is higher, and this can be easily connected with Facebook. Among users, 74% visit Facebook at least once per day, which is much higher than usage of YouTube or Twitter. Furthermore, Facebook usage is more evenly distributed across most age and socio-economic categories, compared to most other social platforms. Finally, compared to social media such as WhatApp, information posted on public websites can be accessed and readily collected.

Nearly half (43%) of the 10,190 churches from the usachurches.org provide a link to a public Facebook page. Of those 91% were active on September 1st, 2020. To access the posts on Facebook, we partnered with CrowdTangle, a Facebook-owned tool that tracks interactions on public content from Facebook pages and groups.[10] We retrieved all posts that were posted by one of the churches in our data base, that were still online on July 1st, and that were posted between January 1st, 2020 and June 30th, 2020. The data set contains 644,752 posts of 3,897 churches that had made at least one publication in this period. The posts can be connected to the church characteristics via their Facebook Id. The information about the posts includes the date and time, the message (the text of the post, link text or picture text), the type of posts (different types of video, photo, link or just text "status"), the number of reactions, the number of comments and the number of shares.

[10] https://www.CrowdTangle.com/

Covid Economics 61, 11 December 2020: 121-171

Fig. 1. Total number of Facebook posts per day between January 1 and June 30, 2020

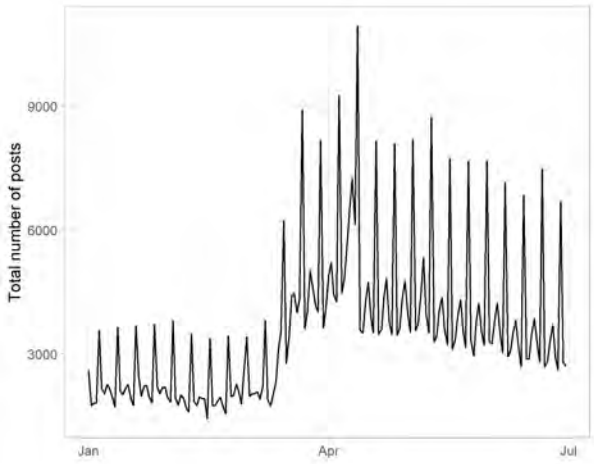

Note: Total number of posts made by public U.S. church profiles between January 2020 and June 30 2020 on Facebook. Facebook IDs were obtained from usachurch.org and Facebook posts by CrowdTangle.

4 Empirical Strategy

4.1 Church posting behavior

Figure 1 illustrates the number of posts made by the churches in our data set from January to June 2020. We can see regular spikes in the number of posts. Zooming in on January in Figure 11 in the Appendix, we see that churches post most on Sunday, the day of worship. As we focus on the question whether churches moved their in-person gatherings online, we restrict our study to their posting behavior on Sundays. In particular, the same weekday pattern can be observed in Figure 2 for posts that contain a video (live videos, videos directly posted to Facebook or YouTube videos). Even before the pandemic, churches primarily posted videos on Sundays. On weekdays, they are more likely to post a photo. Links and statuses are not as common.

Even before the coronavirus pandemic (defined as before March 2020), 47% of churches in our sample posted on a given Sunday, as illustrated in Figure 3. Also, 30% posted at least one video on a given Sunday before the pandemic and 4% a link. Overall in April, at the height of the pandemic, 82% of churches posted on a given Sunday, 81% if Easter Sunday is excluded. 70% of churches

Covid Economics 61, 11 December 2020: 121-171

Covid Economics 61, 11 December 2020: 121-171

Fig. 2. Total number of Facebook posts per day between January 1 and June 30, 2020 by type of post

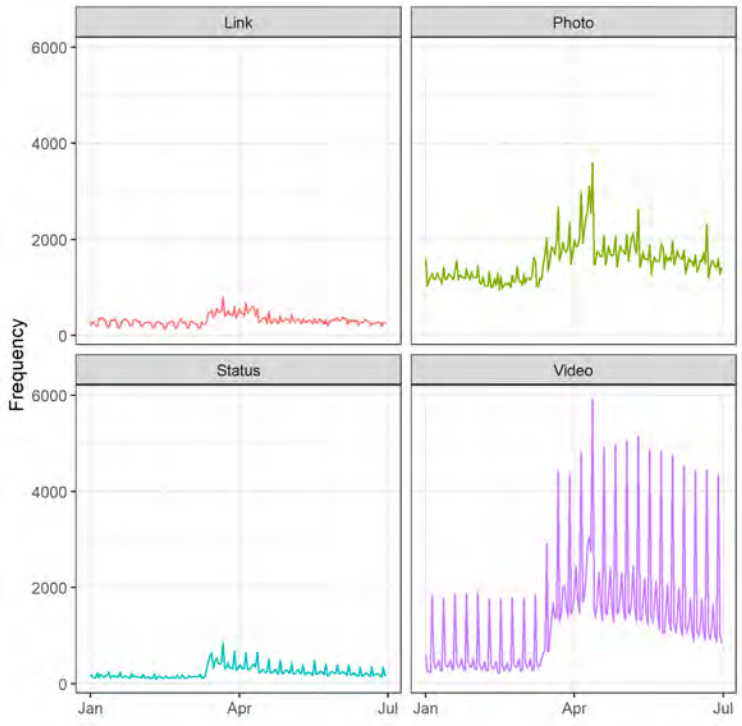

Note: Number of posts made by public U.S. church profiles between January 2020 and June 30 2020 on Facebook by type of post. Video includes live videos (including scheduled and completed live videos), native videos (video files posted directly to Facebook) and YouTube videos. Status describes posts that only contain text. Facebook IDs were obtained from usachurch.org and Facebook posts by CrowdTangle.

CEPR PRESS

Fig. 3. Proportion of churches that post at least once on Sunday between January 1 and June 30, 2020 overall and by type of post

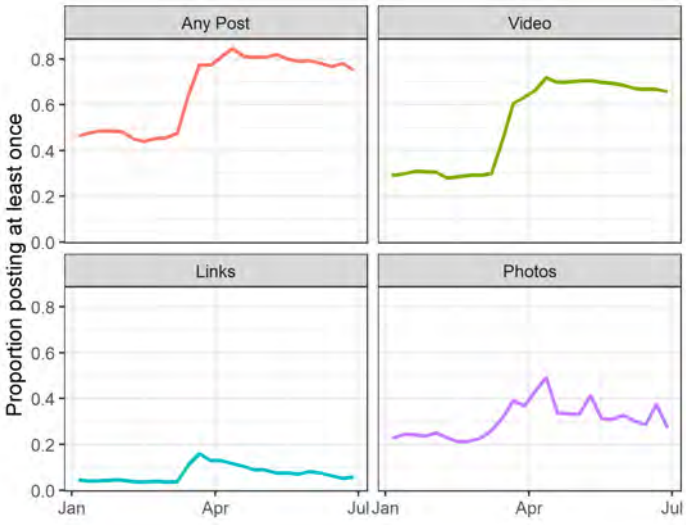

Note: Proportion of U.S. churches posting at least once on Sunday between January 2020 and June 30 2020 on Facebook overall and by type of post. Video includes live videos (including scheduled and completed live videos), native videos (video files posted directly to Facebook) and YouTube videos. Status describes posts that only contain text. Facebook IDs were obtained from usachurch.org and Facebook posts by CrowdTangle.

posted at least one video (69% excluding Easter Sunday) and 11% a link (10.7% excluding Easter Sunday). Therefore, nearly twice as many churches posted on a given Sunday in April than did before March 2020. The proportion of churches posting a video more than doubled, as did the number of links.

4.2 Proxying online gatherings

The first proxy for making online worship attendance possible is whether churches post a video. Videos include videos posted directly to Facebook, embedded YouTube videos, and live videos (including completed or scheduled). Table 4 shows 9 randomly selected Sunday posts with a message that are marked as video and 9 that are not. Most video posts seem to be connected to Sunday worship, yet there are some which are not directly related to Sunday worship (in this case a pastor

Covid Economics 61, 11 December 2020: 121-171

offering health advice). Some posts that are not marked as videos are connected to Sunday online service. For example, one post clearly announces a live Facebook video. In this case, we still record this church as posting at least one video on this Sunday because the follow-up post would be captured. Yet we do not capture whether churches announce an online service on Facebook but then stream the video via a different platform without linking it through Facebook. This would be the case, for example, if churches stream the video directly to their website or via WhatsApp.

In order to improve the online activity proxy we hand-coded 1600 posts[11] and identified those describing a "church activity that was clearly online" using the message text and the post type. Church activities include Sunday services, but also smaller group activities. 49% of all posts are related to a church activity in our training sample, and 74% of Sunday posts. 7% of all posts refer to a social event, 6% give information about the church, and 25% are defined are purely "motivational" (an inspiring quote or psalm). The rest is either unclear (5%), are congratulatory posts (celebrating for example the anniversary of the church - around 2%), talk about a charitable activity (3%) or include some political message (less than 1%). 4% of posts after March 01 2020 have a clear reference to Covid.

We use the hand-coded posts as the training sample for a random forest algorithm predicting online church activities.[12] As predictors, we use the type of the post and the 200 most commonly used words in the post texts. Figure 12 summarizes the most frequently used words churches use, both overall and on Sundays. The text analysis excludes stop words such as 'and' or 'or', as well as words that only consist of a number.[13] Figure 13 summarizes the most frequent words before March 2020 and after March 2020. We can see that "https" (also captured in the post type), "live", "online" and "watch" either improve in the ranking or enter the top 20 most frequent words.

The random forest prediction algorithm reaches an average 15% error rate.[14] Figure 14 in the

[11] We randomly selected 100 posts for each month from January to September 2020, as well as for March and April 2019. To this we added a random selection of 500 posts drawn from January to September 2020.
[12] We use the randomForest R package with 500 trees. The number of predictors used at each node minimizes the out-of-bag error rate.
[13] Covid-19 is therefore not excluded but if the message includes for example 'John 1:33', then only 'John' is counted as a word.
[14] 8% for wrong zeros and 27% for wrong 1.

Appendix illustrates the most important predictors for the random forest prediction. Not surprisingly, the type of the post is the most informative characteristic. However, we can also see expected keywords such as "online", "live", but also "facebook", "join" and "youtube". We use the prediction algorithm to predict online church activity for the whole sample. In 93% of the posts, the random forest based online indicator and the indicator for posting at least one video give the same result. In 3% of the cases, the algorithm predicts an online activity but there is no video posted, and in 4% of the cases a video is posted, but the algorithm does not predict the post as an online activity. Figure 4 illustrates the time trends in the two online activity proxies. Though the trend before the pandemics are quite similar, there seem to be some differences during the pandemic and afterwards.

In what follows we use the predicted online measure as our variable of interest, as we suggest that it is an improvement over the "naive" proxy that only uses the fact of posting a video. We report in the Appendix some robustness tests using the share of churches posting a video on a given Sunday.[15]

4.3 Intervention data, Introduction and Relaxation Period

To estimate the churches' responses to governmental regulations, we use the county-level information about government intervention collected by Killeen et al. [2020]. We supplement the intervention database with information about religious exemptions to the stay home order. First, we define states that either define religious organisations as essential businesses and allow individuals to go there, or who allow small gatherings for religious purpose while they implemented their stay home order as having an religious exemption. States that do neither of those in their executive orders are defined as not having a religious exemption. Second, we use the definition used by the Pew Research Center that differentiates between 4 categories: religious gatherings forbidden, limited to 10 people or less, limited in other ways, or exempt from the stay home order.

We also use county level information on the number of confirmed positive cases, deaths and

[15] In the multivariate analysis we find that coefficients on regressors of interest under the first proxy are generally smaller and somewhat less statistically significant than their counterpart coefficients under the second. This suggests the presence of attenuation bias due to measurement error, and that the first proxy might suffer more from measurement error than the second.

Covid Economics 61, 11 December 2020: 121-171

Covid Economics 61, 11 December 2020: 121-171

Fig. 4. Churches' online behavior over time

(a) At least one video post on a Sunday

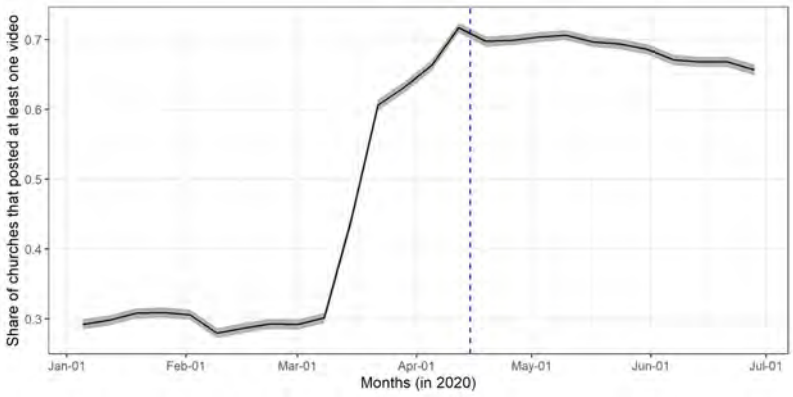

(b) At least one post predicted as online activity on a Sunday

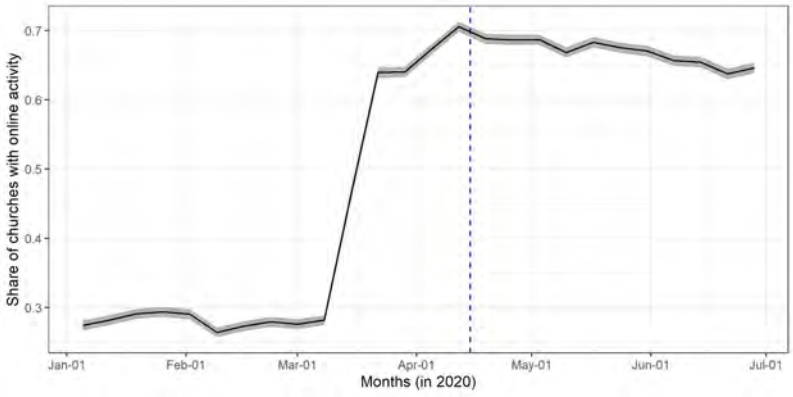

Note: Share of churches with a predicted online church activity on a Sunday from January to June 2020. Public Facebook posts obtained via CrowdTangle, Facebook IDs from usachurches.org. The dashed line separates the introduction and relaxation periods. Shaded area indicates the standard deviation.

hospitalizations from Killeen et al. [2020], based on numbers released by the Johns Hopkins University. We merge this information with the panel set of Facebook posts and the church characteristics using the FIPS code of the church address. For the heterogeneity analysis, we use information of county-level voting in the 2016 presidential election from Kirkegaard [2016], based on data from the New York Times[16].

We distinguish two different time periods: the introduction period and the relaxation period. The introduction period is defined from January 1 to April 15 and covers the time when federal guidelines were issued and states issued regulations. The relaxation period is defined as the time after April 15 until the end of June. It covers the time span where stay home orders were lifted, restaurant and entertainment establishments were allowed to reopen and some states allowed gatherings of more than 50 or 500 people. We choose to look at the two periods separately as we expect that introducing or lifting a governmental restriction would have different effects. The boundary between the two time periods is illustrated by the dashed line in figure 4.

As the state interventions are highly correlated among each other (given that we use weekly and not daily information), we merge the following measures: First, gatherings forbidden indicates if gatherings are limited to at least less than 500 people. Second, a restaurant and entertainment establishments closed indicator that equals one if both restaurant and entertainment establishments are order to closed, and 0.5 if only one category of both is ordered to close.

4.4 Empirical Specification

We regress our predicted online indicator on publicly available information about the severity of the coronavirus pandemic. For this we use the number of confirmed Covid-19 cases and deaths. Though both of the measures underestimate the true spread of the virus, particularly in the first quarter of the year, they are pieces of information available to the churches. We also use federal, state and district interventions as regressors. These include dummy variables for the periods after the travel ban, after the federal guidelines were issued, after public schools closed, and during state or district interventions and stay-at-home orders.

[16] https://www.nytimes.com/elections/2016/results/president

Covid Economics 61, 11 December 2020: 121-171

$$church\_activity_{itc} = \alpha.interventions_{tc} + \beta.Covid_{tc} + X_t + \gamma_i + \epsilon_{itc} \quad (1)$$

This regression is described in Equation 1: Church activity of church i at Sunday t in county c is regressed on the interventions in place in county c on Sunday t, and the Covid-cases in district c in the week before Sunday t. We also add controls X which include a dummy for Easter Sunday and a linear week in one specification for the relaxation period. Finally, we always use church fixed Effects (γ_i). Standard errors are clustered at the state level.

None of the coefficients should be interpreted in a causal way. Covid-19 cases are potentially correlated with religious demand factors in many ways: population density and economic activity, education and trust in science. Religious demand then shapes the religious supply that churches are offering and is correlated with political opinion. Simultaneously, religious activity can have an effect on Covid-19 cases. Finally, religious organisations that want to stay open and continue to gather in person might lobby against strict regulations at the state or county level and so influence the intervention variable.

Covid Economics 61, 11 December 2020: 121-171

5 Results

5.1 Average Effects

Table 1 displays the churches' online activities on Sundays in the introduction period, defined as lasting from January 01 to April 15, 2020, in relation to Covid-19 cases, deaths and regulations. In odd numbered columns we use reported infections as a measure of the spread of the pandemic by county, while in even numbered columns we use reported deaths. Results are qualitatively similar with some differences in points of detail. The same regression using the fact of posting a video on Sunday as proxy for online activity is shown in table 5 in the Appendix.

Online activity is positively correlated with the numbers of confirmed Covid cases and Covid deaths in previous weeks. To get an idea of the magnitude of the correlation, a 20% rise in infec-

tions or deaths is associated with a one percentage point increase in online presence (compared to an average of around 30% in February). The coefficients are smaller but still significantly positive when we control for governmental interventions (column 3 to 8).

Online activity increased dramatically on the Sunday after international travel was banned (by between 16 and 18 percentage points) and again after the Federal guidelines were issued (by between 16 and 18 percentage points according to specification). Apart from this, there is little sign of an impact from statewide public health orders, except for a negative effect of stay-home orders (which were typically implemented some time after the Federal orders) in column 3.

Covid Economics 61, 11 December 2020: 121-171

Table 1: Effect of Covid-19 and interventions on churches posting behavior on Sundays: Introduction Period (before April 15)

	Dependent variable: Predicted Online Church Activity on Sunday							
	(1)	(2)	(3)	(4)	(5)	(6)	(7)	(8)
Log Infections previous week (county)	0.047***		0.021***		0.022***		0.022***	
	(0.002)		(0.008)		(0.008)		(0.007)	
Log deaths previous week (county)		0.052***		0.019*		0.019*		0.020*
		(0.002)		(0.011)		(0.011)		(0.011)
After International Travel Ban (March 11)			0.156***	0.178***	0.157***	0.179***	0.156***	0.178***
			(0.013)	(0.009)	(0.013)	(0.009)	(0.013)	(0.010)
After Federal guidelines issued (March 16)			0.160***	0.181***	0.161***	0.182***	0.158***	0.179***
			(0.027)	(0.026)	(0.027)	(0.026)	(0.027)	(0.025)
After Public Schools Closed			−0.009	−0.015	−0.008	−0.014	−0.006	−0.012
			(0.014)	(0.012)	(0.014)	(0.012)	(0.015)	(0.012)
Gatherings forbidden			−0.011	0.003	−0.012	0.002	−0.011	0.003
			(0.014)	(0.013)	(0.015)	(0.014)	(0.014)	(0.013)
Restaurants/Entertainment closed			−0.015	0.007	−0.017	0.006	−0.016	0.006
			(0.029)	(0.026)	(0.029)	(0.026)	(0.028)	(0.025)
During Stay Home Order			−0.044**	−0.039				
			(0.019)	(0.024)				
Stay Home: with religious exemption					−0.054**	−0.045		
					(0.022)	(0.027)		
Stay Home: without religious exemption					−0.024	−0.028		
					(0.018)	(0.022)		
Stay home: Rel. gatherings prohibited							−0.047*	−0.050
							(0.025)	(0.030)
Stay home: Exempt from limits							−0.065***	−0.058*
							(0.023)	(0.029)
Stay home: Limited to 10							−0.016	−0.010
							(0.021)	(0.022)
Stay home: Limited otherwise							0.007	−0.003
							(0.048)	(0.041)
Average in February (Sunday)	0.277	0.277	0.277	0.277	0.277	0.277	0.277	0.277
Number of churches	3893	3893	3893	3893	3893	3893	3893	3893
Observations	58,395	58,395	58,395	58,395	58,395	58,395	58,395	58,395
Adjusted R^2	0.570	0.530	0.594	0.590	0.594	0.590	0.594	0.590

Note: *p<0.1; **p<0.05; ***p<0.01. Includes church fixed effects and an Easter Sunday dummy. Standards error clustered on state level. Includes Sundays between 2020-01-01 and 2020-04-15. Columns 4 and 5: Religious exemptions according to own categorization. Columns 7 and 8: Categorization from Pew Research Center. Number of states (clusters): 51

Covid Economics 61, 11 December 2020: 121-171

Though the negative coefficient of the stay-home order may be a statistical fluke, we explore the matter further in columns 5 to 8 by differentiating between different types of stay-home orders according to whether or not there were exemptions for religious organisations. In columns 5 and 6, we use our own categorization, which differentiates between orders that did and did not have an exemption for a religious gatherings. In column 7 and 8, we use a categorization from the Pew research institute, which differentiates between prohibiting religious gatherings, exempting them from any limit, or limiting them to 10 persons, or limiting otherwise[17]. When we control for the number of infections in the previous week (columns 5 and 7), there is a substantially and significantly negative coefficient on states with complete exemption of religious gatherings from limits. Controlling for the number of deaths, the coefficient becomes insignificant when using our own categorization (column 6) and is only significant at 10% for the Pew categorization (column 8). We cautiously interpret this as being likely due to a relaxation of their previously increased online presence in states where the stay-home orders allowed this.

Table 2 displays the results for the relaxation period, defined as lasting from April 15 to June 30, 2020.[18] There is not much evidence of any responsiveness to reports of deaths or infections in the county, suggesting that such reports may have played a part in the initial phase in bringing home to churches the seriousness of the pandemic, but once the pandemic was established such reports made little difference. Although public health orders are positively correlated with online church activity in columns 3, 5 and 7, once we control for a time trend that effect disappears. This suggests that a general effect of fatigue with the restrictions may have been at work, rather the restrictions *per se*.

Overall, it is possible to be impressed by the speed with which many churches moved activities online once the pandemic began, while also noting that there remained a substantial share of churches that did not have any perceptible online activity even at the height of the first wave of the pandemic. It should be kept in mind however, that other church behavior such as offering online activities on other platforms or offering drive though prayers, is not captured in these results.

[17] More than 10 persons, but still limited.
[18] And table 6 shows the results using posting a video as dependent variable.

CEPR PRESS

Covid Economics 61, 11 December 2020: 121-171

Table 2: Effect of Covid-19 and interventions on churches posting behavior on Sundays: Relaxation Period (after April 15)

	Dependent variable: Predicted Online Church Activity on Sunday							
	(1)	(2)	(3)	(4)	(5)	(6)	(7)	(8)
Log Infections previous week (county)	−0.004		−0.002	0.0002	−0.002	0.0003	−0.002	−0.0004
	(0.003)		(0.002)	(0.002)	(0.002)	(0.002)	(0.002)	(0.002)
Log deaths previous week (county)		0.001						
		(0.002)						
Gatherings forbidden			0.026**	0.016	0.026**	0.017	0.025**	0.015
			(0.010)	(0.010)	(0.010)	(0.010)	(0.011)	(0.010)
Restaurants/Entertainment closed			0.012	−0.001	0.013*	−0.0002	0.012	−0.001
			(0.008)	(0.007)	(0.007)	(0.007)	(0.007)	(0.007)
During Stay Home Order			0.017**	−0.002				
			(0.007)	(0.007)				
Stay Home: with religious exemption					0.019**	−0.0001		
					(0.008)	(0.008)		
Stay Home: without religious exemption					0.010	−0.006		
					(0.009)	(0.010)		
Stay home: Rel. gatherings prohibited							0.028***	0.011
							(0.010)	(0.011)
Stay home: Exempt from limits							0.018*	−0.001
							(0.009)	(0.009)
Stay home: Limited to 10							0.005	−0.013
							(0.010)	(0.010)
Stay home: Limited otherwise							0.033*	0.012
							(0.017)	(0.017)
Linear week trend				−0.005***		−0.005***		−0.005***
				(0.001)		(0.001)		(0.001)
Average in April (Sunday)	0.688	0.688	0.688	0.688	0.688	0.688	0.688	0.688
Number of churches	3893	3893	3893	3893	3893	3893	3893	3893
Number of States (clusters)	51	51	51	51	51	51	51	51
Observations	42,823	42,823	42,823	42,823	42,823	42,823	42,823	42,823
Adjusted R^2	0.671	0.671	0.671	0.672	0.671	0.672	0.671	0.672

Note: *p<0.1; **p<0.05; ***p<0.01. Dependent variable: At least one post predicted to offer an online church activity on a given Sunday. Includes church fixed effects. Standards error clustered on state level. Includes Sundays between 2020-04-15 and 2020-06-30. Columns 4 and 5: Religious exemptions according to own categorization. Columns 7 and 8: Categorization from Pew Research Center.

Covid Economics 61, 11 December 2020: 121-171

5.2 Heterogeneity

We now look at heterogeneity among churches in their response to the pandemic, concentrating in particular on the dimensions of church size, worship style and political environment. Figure 5 shows the evolution over time of online activity according to the size of the church. Unsurprisingly, size matters a lot. Already before the pandemic, half of megachurches were posting online activity on any given Sunday, and that proportion rose very rapidly to over 80%. More surprisingly, even medium and small churches, though beginning from lower levels, saw almost equally substantial rises in their online activity. In the relaxation period all sizes of church saw some decline in their online activity, though this was more marked among smaller churches.

A similar pattern can be seen comparing churches by worship style, illustrated in Figure 6. Those that report a contemporary worship style posted more prior to the pandemic and the more mainline churches that report a traditional worship style posting less. All types see a rapid and substantial increase, with a subsequent slight decline that is more marked among the traditional churches.

The comparison by political environment is interesting for what it does not show. Figure 7 compares churches in counties in the highest 40 percentile and the lowest percentile of Republican vote share in the 2016 presidential election. Given the strong political polarisation surrounding pandemic management, it might have been expected that churches in strongly Republican areas would respond less to the pandemic than those in strongly Democrat areas. The evolution of activity in these two types of county is almost identical. Indeed, even if the curves are slightly different at the beginning of the pandemic, they converge and are nearly identical from May onward. Of course this is a pure description of average activity, and it may be that more detailed analysis may reveal more traces of polarisation. But if polarisation had been as deep as many media commentators appeared to suggest we would have expected to see a difference in the development of these averages, and we do not.

The multivariate regression analysis in the Appendix tends to corroborate these findings and

Covid Economics 61, 11 December 2020: 121-171

Fig. 5. Churches' online activity over time by church size.

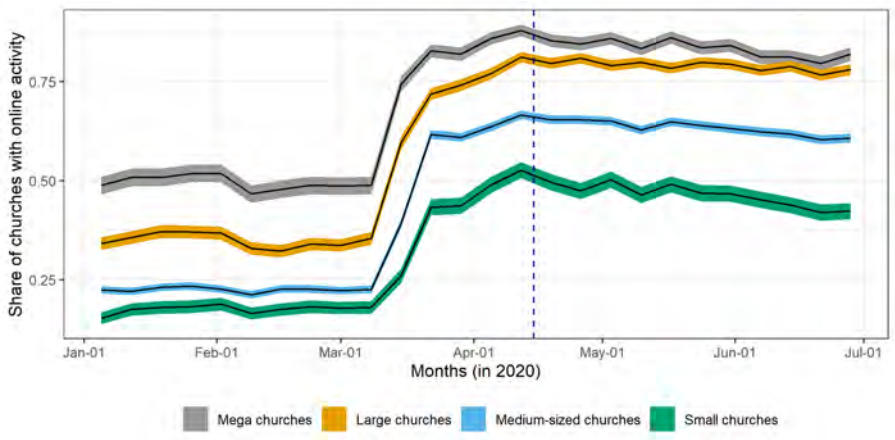

Note: Share of churches with a predicted online church activity on a Sunday from January to June 2020 according to church size. Public Facebook posts obtained via CrowdTangle, Facebook IDs from usachurches.org. The dashed line separates the introduction and relaxation periods. Shaded areas indicate the standard deviation. Small churches are defined as receiving up to 50 people on a regular Sunday, medium churches between 51 and 300, large churches between 301 and 500 and mega churches over 2000. Size characterization from usachurches.org.

CEPR PRESS

Fig. 6. Churches' online activity over time by church worship style.

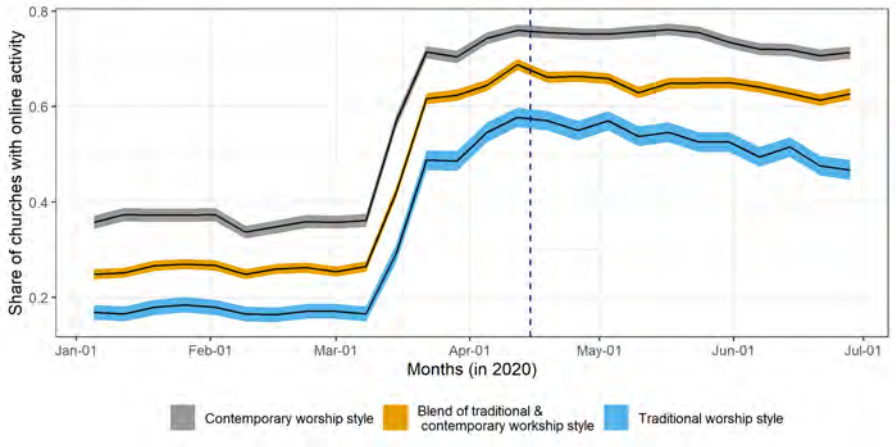

Note: Share of churches with a predicted online church activity on a Sunday from January to June 2020 according to church worship style. Public Facebook posts obtained via CrowdTangle, Facebook IDs from usachurches.org. The dashed line separates the introduction and relaxation periods. Shaded areas indicate the standard deviation. Worship style characterization from usachurches.org.

adds some points of detail. However, it should be noted that in our regressions we always use church fixed effects and control for public health measures, so that the coefficients cannot be interpreted in exactly the same way as the lines in the Figures, which show raw averages by category. Table 7 confirms that Mega and large churches both had higher average postings prior to the pandemic and reacted faster (after March 11th) than medium and small churches. Nevertheless, the latter responded almost as fast, with a strong response to the Federal guidelines on the 16th of March. There is an interesting difference between these two groups in association with the closure of public schools, which has a positive impact on online activity in the larger churches and a negative impact on activity in smaller churches. This makes sense since smaller churches probably rely on volunteers to manage online activity, and these volunteers may have been constrained by childcare responsibilities. Finally, the correlation between the report of infections in the county in the previous week and small churches' online behavior is insignificant.

Table 8, for the relaxation period, shows little impact of public health measures, but a negative

Covid Economics 61, 11 December 2020: 121-171

week trend reflecting probably a fatigue effect, that seems faster for smaller churches. Table 9 confirms the impression of Figure 6 with respect to differences of worship style during the introduction period, and Table 10 shows, as for size, no major effect of public health measures, only a generalized negative weekly trend.

Finally, Tables 11 and 12 confirm that there is no tendency for churches in strongly Republican counties to respond less to public health measures. If anything there are slightly positive coefficients on the interaction of Republican vote share with certain of the announced measures. However, as Table 12 shows, there is a strong negative coefficient on the presence of a religious exemption in a stay home order. There may well be a tendency for churches in strongly Republican counties to be located in states that have religious exemptions, and those religious exemptions seem to be very clearly associated with lower online activity. But given the nature of the stay-home order, churches in strongly Republican counties do seem to have posted more online. This might indicate that such orders were perceived as more legitimate in Republican counties - though at this stage that remains a conjecture.

Overall, though, the absence of any visible negative association of a county's Republican vote share on the level of online activity remains striking in the light of the expectations generated by widespread press reports of political polarisation in churches' response to the pandemic.

Covid Economics 61, 11 December 2020: 121-171

Covid Economics 61, 11 December 2020: 121-171

Fig. 7. Churches' online activity over time by previous political voting behavior on the county level.

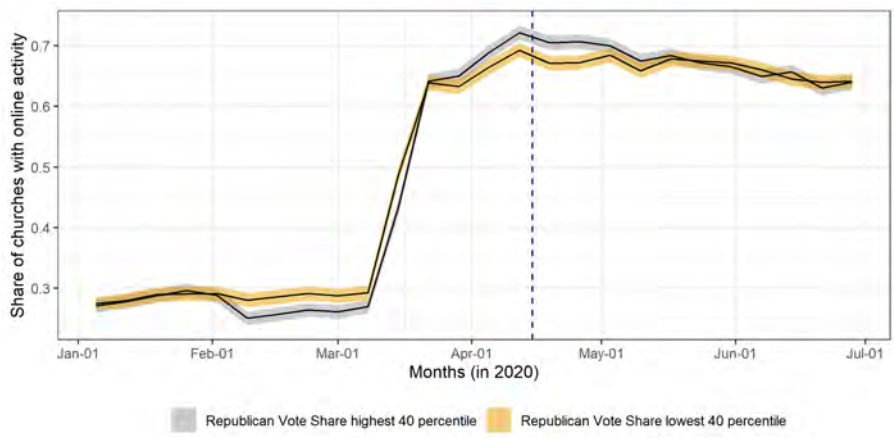

Note: Share of churches with a predicted online church activity on a Sunday from January to June 2020, according to if the county the church is located in is within the top of bottom 40 percentile of the vote share for the Republican party in the 2016 presidential elections. Public Facebook posts obtained via CrowdTangle, Facebook IDs from usachurches.org. The dashed line separates the introduction and relaxation periods. Shaded areas indicate the standard deviation.

5.3 Developments through end-November 2020

In this section we show the equivalents of Figures 4 through 7 on Facebook data until the end of November 2020. Though we do not perform multivariate analysis for the larger sample (since updated information about public health measures is not yet available), it is nevertheless possible to note a number of salient features. First, as we can see from Figure 8, after an initial dip in the relaxation period from the middle of April until the end of June, average online activity levels off and shows no tendency to decline further. This may reflect the fact (shown in Figure 10 in the Appendix), that confirmed cases and deaths from Covid-19 rose in July and August 2020 in the United States. This contrasts with the European Union where they fell to low levels until they caught up with and overtook US levels by November 2020. Even if churches relaxed their vigilance after the April peak, they may quickly have realized the pandemic was not under control.

However, it is also notable that online activity shows no further increase. All the response of church online activity to the pandemic seems to have happened within the first month of the pandemic. One might have expected a significant proportion of churches to develop an online presence gradually over the following months, but there is no sign of this in our data. Yet it should be noted that the constant levels of online activities could hide some churches stopping while new churches offer online activities as the pandemic becomes more important in different parts of the country.

Next, Figure 9 shows that heterogeneity by both church size and worship style remained more or less constant until the end of November (panels (a) and (b)). Most interestingly of all, panel (c) shows that activity of churches in strongly Republican and strongly Democrat areas show no tendency to diverge through to mid-October, even though the period covered the run-up to a very partisan election with an unprecedentedly high voter turnout. There is a slight divergence during November though the gap is small. This corroborates our impression, reported above in our discussion of the content of Facebook posts, that churches overwhelmingly use their posts to advertise their services and to provide inspirational content for members rather than to communicate politically partisan messages.

Covid Economics 61, 11 December 2020: 121-171

Covid Economics 61, 11 December 2020: 121-171

Fig. 8. Churches' online activities until November 2020

(a) At least one video post on a Sunday

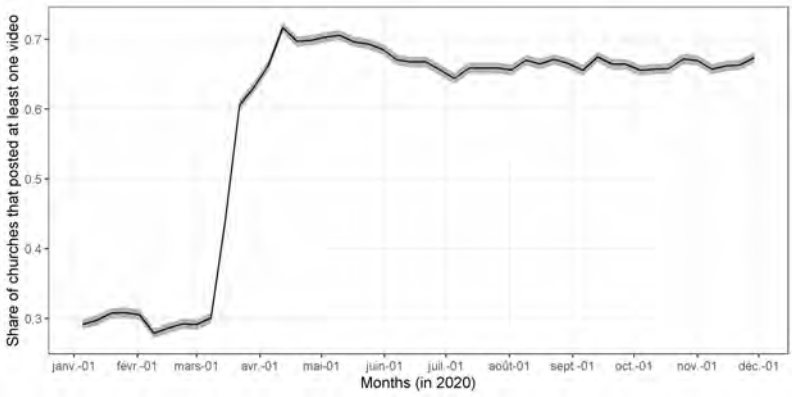

(b) At least one post predicted as online church activity on a Sunday

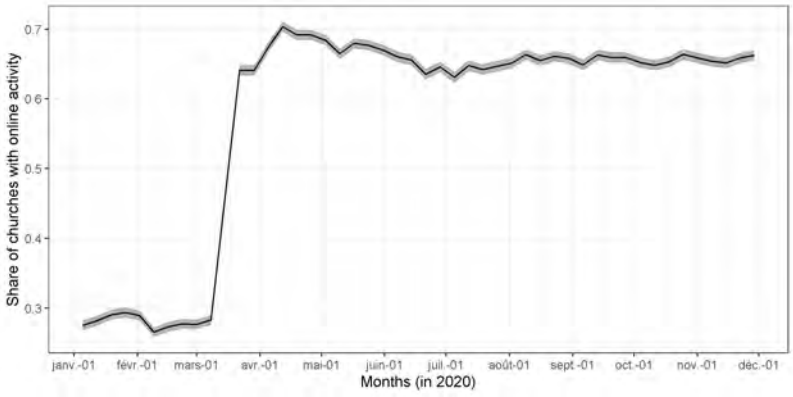

Note: Share of churches with a predicted online church activity on a Sunday from January to end-November 2020. Public Facebook posts obtained via CrowdTangle, Facebook IDs from usachurches.org. The dashed line separates the introduction and relaxation periods. Shaded area indicates the standard deviation.

Covid Economics 61, 11 December 2020: 121-171

Fig. 9. Churches' online activities until November 2020

(a) Heterogeneity in Church Size

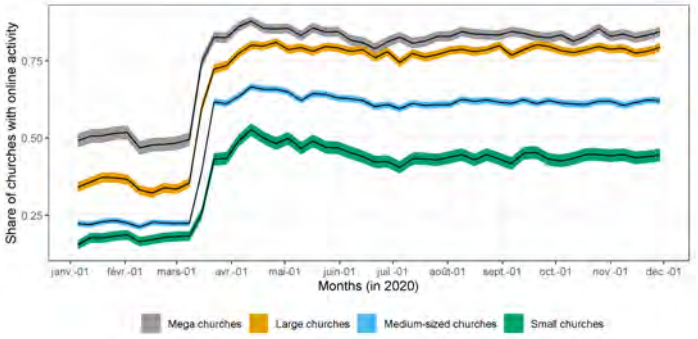

(b) Heterogeneity in Worship Style

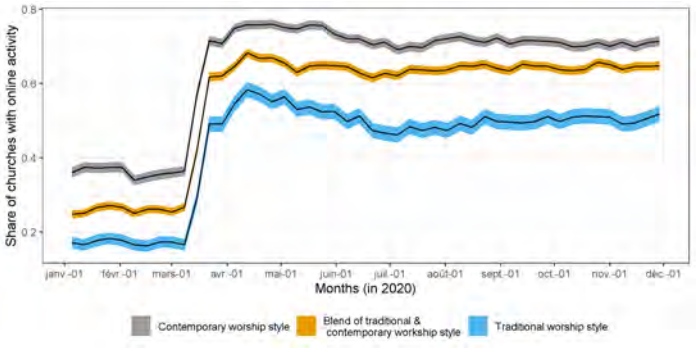

(c) Heterogeneity in Voting Behavior

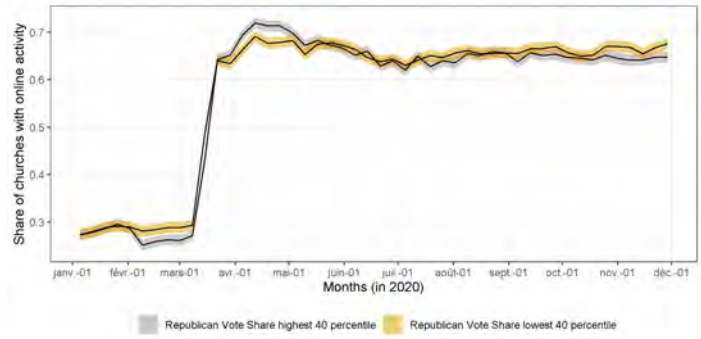

Note: Share of churches with a predicted online church activity on a Sunday from January to end-November 2020 according to (a) church size, (b) worship style, and (c) whether the county in which the church is located lies within the top or bottom 40 percentile of the vote share for the Republican party in the 2016 presidential elections. Public Facebook posts obtained via CrowdTangle, Facebook IDs, size, worship style and location from usachurches.org, from usachurches.org. Shaded areas indicate the standard deviation.

6 Conclusion

In this paper we have examine the way in which US churches responded in their online behavior to the unexpected challenge of the Covid-19 pandemic. We draw a contrast between two broad models of churches' operations. Under the economic model, churches respond to the demand of their members for ritual and communitarian activities, as well as for some other services that may be bundled with these. For such churches, the pandemic represents both a shock to demand and a shock to supply. The shock to demand comes in the form of an unexpected increase in demand for online services. Larger churches can typically meet this demand at a lower marginal cost, and the increase might be different according to the service style. The supply shock takes the form of an increase in the cost of in-person religious gatherings which again might be different according to the average number of people attending. We find that US churches with Facebook pages responded rapidly to these two shocks, with two-third of churches showing evidence of online activity each Sunday from the middle of April compared to less than one-third prior to the beginning of March. Consistent with the economic model, churches of all sizes and worship styles responded, but larger churches and those with more contemporary worship styles had higher levels of online activity throughout the period than smaller and more traditional churches.

An alternative model of churches' operations, in which they use their ideological influence over the beliefs of church members to reinforce partisan political divides and resist public health measures that would diminish their revenues, is one that we cannot rule out but for which we find no evidence in our data. Churches in strongly Republican and churches in strongly Democrat counties display very similar behavior. Religious exemptions from stay-home orders are indeed associated with lower levels of online activity, but such exemptions are the result of political decisions at the state level. Conditional on exemptions there is no evidence that political factors influence church responses.

Our sample is drawn from Christian churches that already have a significant online presence through at least a Facebook page. We decided to focus on Christian churches to compare religious organisations that are part of the Christian majority. There might be very different dynamics for

Covid Economics 61, 11 December 2020: 121-171

religious organisations that are of a minority religion. Furthermore, this more technology-friendly sample may overestimate the increase in online activities in the general church population. It would be of interest to analyse the creation of new public church Facebook pages during the pandemic, which so far escapes our analysis. This omission also leaves open the possibility that selection bias, as well as the choice to analyse Facebook posts, may have hidden from us evidence of a more ideological role for churches' behavior. This remains an important avenue for future research. Yet in view of the politically charged nature of controversies during the pandemic it is useful to draw attention to the apparently bipartisan nature of churches' general responses to the pandemic.

Covid Economics 61, 11 December 2020: 121-171

References

Philipp Ager and Antonio Ciccone. Agricultural Risk and the Spread of Religious Communities. *Journal of the European Economic Association*, 16(4):1021–1068, 2016.

Emmanuelle Auriol, Julie Lassebie, Amma Panin, Eva Raiber, and Paul Seabright. God insures those who pay? Formal insurance and religious offerings in Ghana. *Quarterly Journal of Economics*, 2020.

Jeanet Bentzen. Acts of God? Religiosity and natural disasters across subnational world districts. *The Economic Journal*, 129(622):2295–2321, 2019.

Jeanet Bentzen. In crisis, we pray: Religiosity and the COVID-19 pandemic. *Covid Economics*, 20, 2020.

Mark A Chaves. National Congregations Study, Cumulative Dataset (1998, 2006-2007, and 2012), Version 2. *ICPSR version. Mark A. Chaves, National Opinion Research Center [producer]*, 2019.

Daniel Chen. Club Goods and Group Identity: Evidence from Islamic Resurgence during the Indonesian Financial Crisis. *Journal of Political Economy*, 118(2):300–354, 2010.

CrowdTangle Team. CrowdTangle. *Facebook, Menlo Park, California, United States. List ID: 1403116*, 2020.

Allison James, Lesli Eagle, Cassandra Phillips, D Stephen Hedges, Cathie Bodenhamer, Robin Brown, J Gary Wheeler, and Hannah Kirking. High COVID-19 attack rate among attendees at events at a church—Arkansas, March 2020. 2020.

Benjamin D. Killeen, Jie Ying Wu, Kinjal Shah, Anna Zapaishchykova, Philipp Nikutta, Aniruddha Tamhane, Shreya Chakraborty, Jinchi Wei, Tiger Gao, Mareike Thies, and Mathias Unberath. A County-level Dataset for Informing the United States' Response to COVID-19. April 2020.

Emil OW Kirkegaard. Inequality across US counties: an S factor analysis. *Open Quantitative Sociology & Political Science*, 2016.

Andrew Perrin and Monica Anderson. Share of USadults using social media, including Facebook, is mostly unchanged since 2018. *Pew Research Center*, 10, 2019.

Pew Research Center. Most Americans Say Coronavirus Outbreak Has Impacted Their Lives. 2020, 2020.

World Health Organization. Transmission of SARS-CoV-2: implications for infection prevention precautions: scientific brief, 09 July 2020. Technical report, World Health Organization, 2020.

Covid Economics 61, 11 December 2020: 121-171

Covid Economics 61, 11 December 2020: 121-171

7 Appendix

7.1 Additional Figures

Fig. 10. The evolution of confirmed cases and deaths from Covid-19 in the United States and the European Union from February to December 2020.

(a)

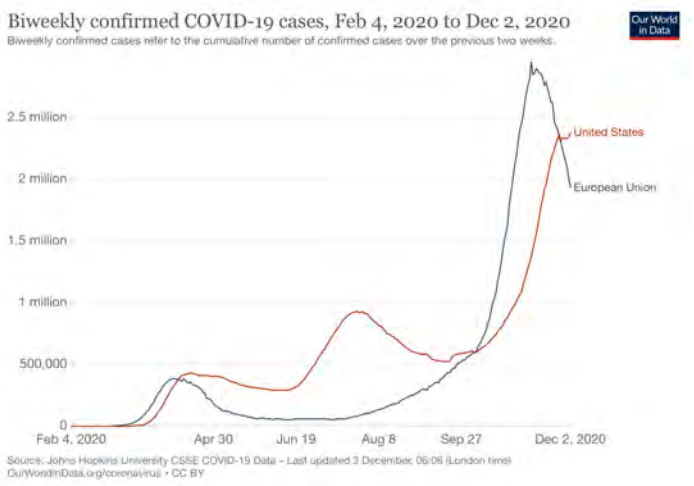

(b)

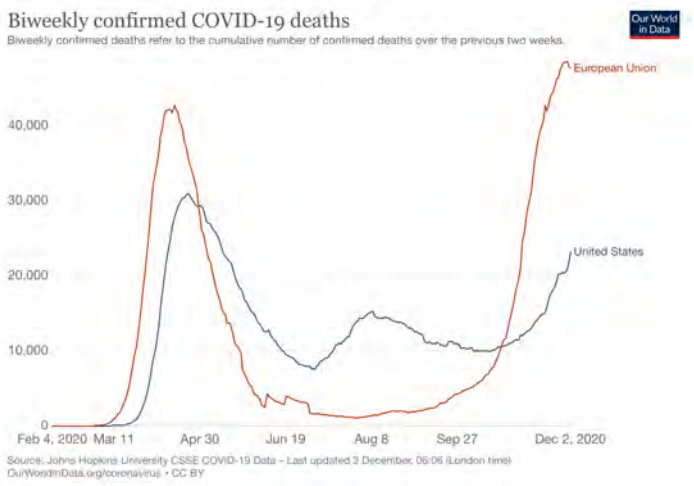

Source: Our World in Data

Covid Economics 61, 11 December 2020: 121-171

Fig. 11. Total number of Facebook posts per day in January 2020 with information about the weekday

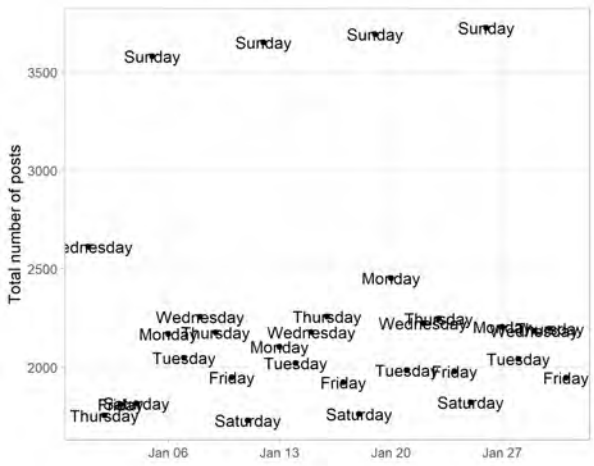

Note: Number of posts made by public U.S. church profiles in January 2020. The weekday is added to each day. Facebook IDs were obtained from usachurch.org and Facebook posts by CrowdTangle.

Covid Economics 61, 11 December 2020: 121-171

Fig. 12. 20 most common words in church posts overall and on Sunday

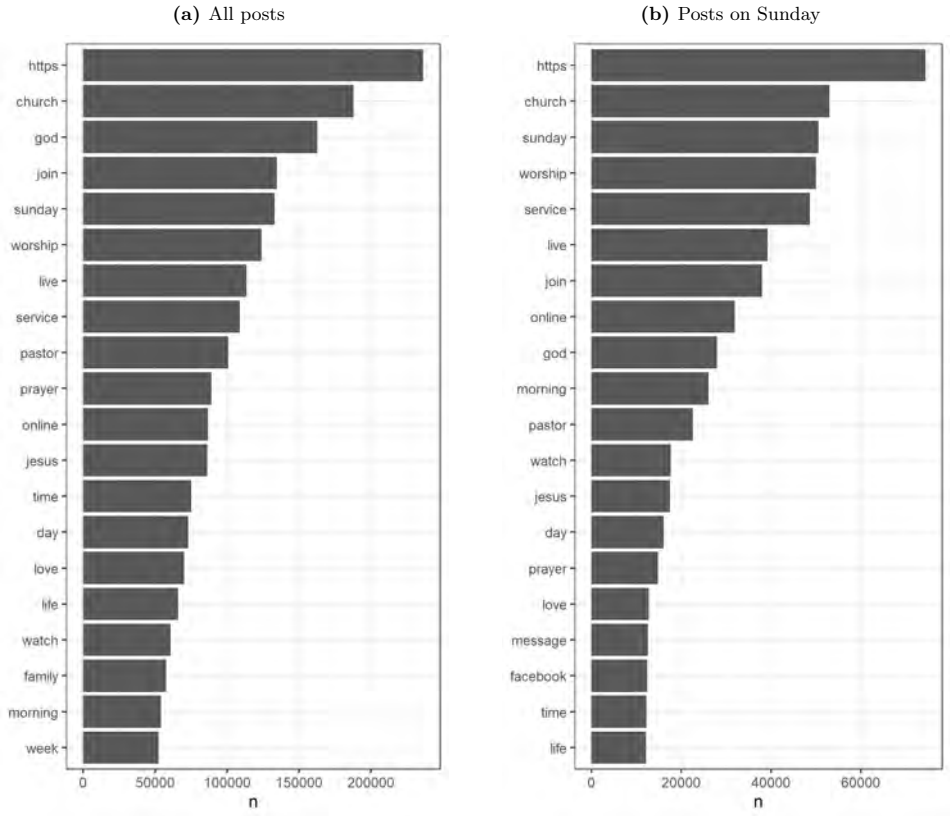

Note: Displays the 20 most common words in the messages of posts including all days (panel a) and on Sundays (panel b) made by churches from January to June 2020. Stop words and numbers are excluded. Posts are obtained from Facebook public profiles via CrowdTangle. Facebook IDs obtained via usachurches.org

Covid Economics 61, 11 December 2020: 121-171

Fig. 13. 20 most common words in church posts before and after March 2020

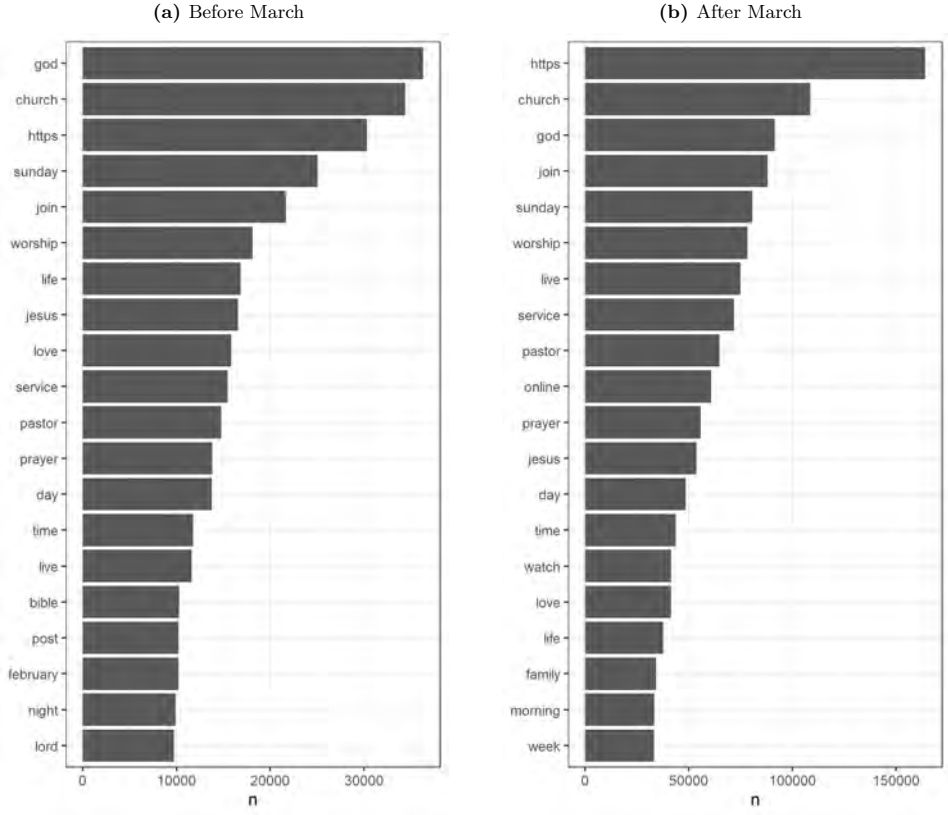

Note: Displays the 20 most common words in the messages of posts including all days made by churches before March 2020 (panel a) and after March 2020 (panel b). Stop words and numbers are excluded. Posts are obtained from Facebook public profiles via CrowdTangle. Facebook IDs obtained via usachurches.org

Covid Economics 61, 11 December 2020: 121-171

Fig. 14. Most important predictors for online activity

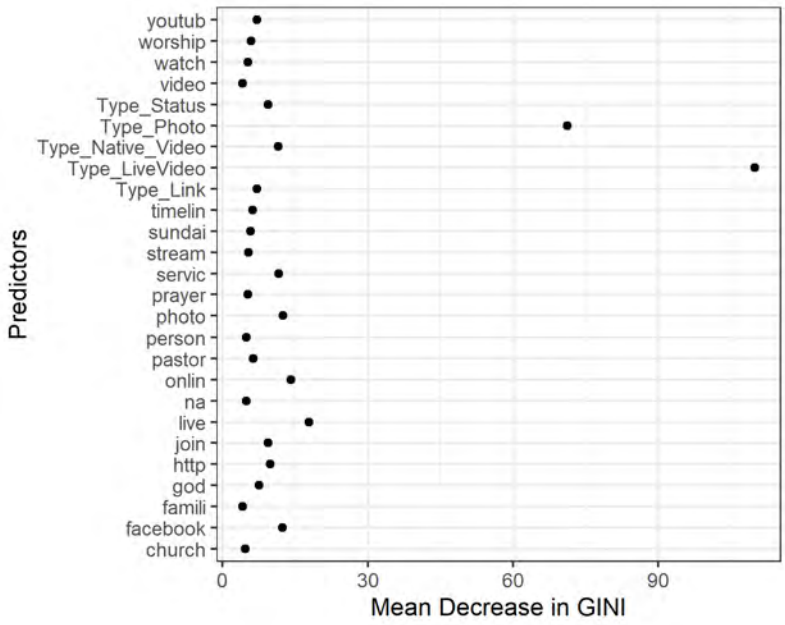

Note: Illustrates the "importance" of each predictor in the online forest prediction algorithm that identifies online church activities, measured as the mean decrease in the GINI. Based on a training set of 1600 hand coded public Facebook posts. Predictors included the word stem of the 200 most used words and the post type.

Covid Economics 61, 11 December 2020: 121-171

Fig. 15. Church online Sunday activity according to the Republican vote share in 2016 on the county level separately for states that eventually had a stay home order with and without a religious exemption

(a) States that issued a stay home order with an exemption for religious gatherings

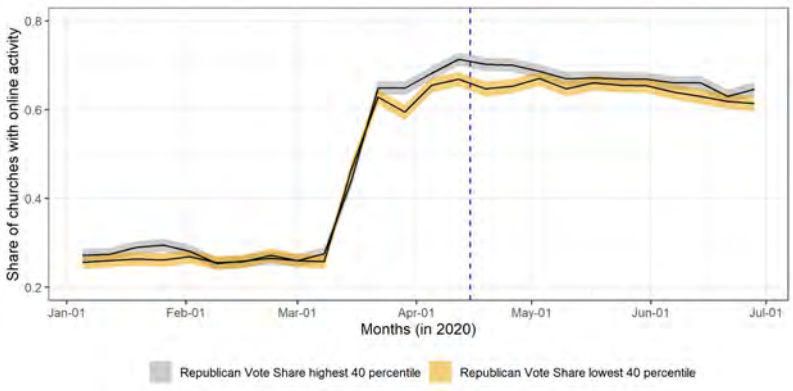

(b) States that issued a stay home order without an exemption for religious gatherings

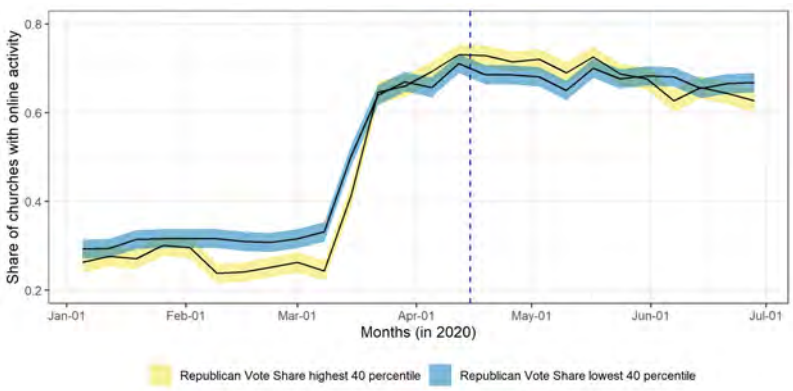

Note: Share of churches with a predicted online church activity on a Sunday according to if the county the church is located within the top or bottom 40 percentile of Republican vote shares in the 2016 presidential elections. Panel (a) includes only states that issued a stay home order with an exemption for religious gatherings, panel (b) includes only states that issued a stay home order without an exemption.

7.2 Additional Tables

Table 3: Comparing churches with and without Facebook Link Provided on usachurches.org

Variable	Without Facebook Link	With Facebook Link	Difference	P-Value
Church Size: Small	0.440	0.180	0.260	0.000
Church Size: Medium	0.490	0.490	-0.005	0.609
Church Size: Large	0.060	0.210	-0.150	0.000
Church Size: Mega	0.010	0.120	-0.104	0.000
Denomination: Baptist	0.230	0.220	0.019	0.024
Denomination: Catholic	0.010	0.010	0.002	0.377
Denomination: Lutheran	0.030	0.030	-0.006	0.068
Denomination: Methodist	0.040	0.070	-0.024	0.000
Denomination: Pentecostal	0.170	0.140	0.030	0.000
Denomination: Non-denominational or Independent	0.270	0.280	-0.005	0.542
Traditional worship style	0.260	0.150	0.108	0.000
Blend of traditional and and contemporary worship style	0.500	0.430	0.067	0.000
Contemporary worship style	0.200	0.310	-0.113	0.000
Twitter Provided	0.030	0.430	-0.399	0.000
YouTube provided	0.010	0.120	-0.113	0.000
N	5763	4427		

Note: Information from usachurches.org, accessed in May 2020, according to if the church information included a Facebook link or not. P-values from a two-sided t-test comparing the means. Small churches are defined as receiving up to 50 people on a regular Sunday, medium churches between 51 and 300, large churches between 301 and 500 and mega churches over 2000. Broad denomination according to the entry's own definition and church name. Worship style could be selected between traditional, contemporary, blend of contemporary and traditional, and other.

Covid Economics 61, 11 December 2020: 121-171

Table 4: Examples of posts with text defined as with and without at video

Posts with Video	**Posts without Video**
Sunday is here! Watch live at 9:30 and 11:00 AM.	Psalm 139 1-6 God knows you 7-12 God is close to you 13-18 God made you 19-24 God protects you
Welcome to our Sunday Service Live Streaming - April 19, 2020 Ptr. Jose Butao Message: " SEASONS OF PRAYER." #worshipjesusfellowship	What an awesome way to start a new year. 8 baptisms.
On Father's Day, Worship with your family. Watch Valley Baptist.	*YouTubeLink*
Pastor Danny launches us into Day 1 of 21 Days of Prayer and Fasting with a devotional message on Romans 5! Let us know how God is speaking to you through Romans 5 today!	Join us tomorrow online or in person!!! Service begins at 10:45 AM. There will be NO Children's Church or Nursery, children will remain with their parents. Hope to see you there!!
Attend Church right from your living room! Join us live right now as Pastor Josh Surratt shares how we can become Unshakable, even in scary and uncertain times. teachers.	Today, our #pandemicprayer is to pray for the parents
During the welcome today, Pastor Matt shared with us some steps that we are taking to stay healthy, as well as a change in how we are going to take communion starting next week. Check it out below!	Its a beautiful day to worship! Join us this morning as we gather together, virtually! WAYS TO WATCH: FACEBOOK LIVE (9:30am) *church website* (9:30am & 11am) FBCA Mobile APP (9:30am & 11am)
Live Event	$Emoji$ There is no fear in love. But perfect love drives out fear, because fear has to do with punishment. The one who fears is not made perfect in love. 1 John 4:18 $Emoji$
Sunday Livestream	JOIN US for our Sunday afternoon online services, 2PM, 4PM & 6PM, where Pastor Corey will be chatting LIVE at 2PM, Pastor Yolie at 4PM and Pastor Tammy at 6PM. Each will be offering prayer and encouragement right here on Facebook LIVE! Don't forget to tag a friend or SHARE this post! See you soon!
Sunday Service: 31 May 20: Sunday Morning Worship	If you are making disciples, who are not making disciples, then you are not making disciples

Note: Randomly selected public posts with a message defined as with and without a video. Posts obtained via CrowdTangle. Facbooks ID from usachurches.org

Covid Economics 61, 11 December 2020: 121-171

7.2.1 Posting at least one video on a given Sunday as dependent variable

Covid Economics 61, 11 December 2020: 121-171

Table 5: Effect of Covid-19 and interventions on churches posting behavior on Sundays: Introduction Period (before April 15)

	Dependent variable: Posted at least one video on Sunday							
	(1)	(2)	(3)	(4)	(5)	(6)	(7)	(8)
Log Infections previous week (county)	0.041***		0.016**		0.016**		0.016**	
	(0.002)		(0.006)		(0.006)		(0.006)	
Log deaths previous week (county)		0.047***		0.014*		0.014*		0.015*
		(0.003)		(0.008)		(0.008)		(0.008)
After International Travel Ban (March 11)			0.122***	0.139***	0.123***	0.139***	0.122***	0.138***
			(0.011)	(0.008)	(0.011)	(0.009)	(0.011)	(0.009)
After Federal guidelines issued (March 16)			0.165***	0.181***	0.166***	0.181***	0.163***	0.178***
			(0.026)	(0.025)	(0.026)	(0.025)	(0.026)	(0.024)
After Public Schools Closed			−0.019	−0.023	−0.017	−0.022	−0.016	−0.020
			(0.019)	(0.016)	(0.019)	(0.016)	(0.020)	(0.017)
Gatherings forbidden			0.005	0.015	0.003	0.014	0.004	0.015
			(0.014)	(0.012)	(0.014)	(0.013)	(0.014)	(0.012)
Restaurants/Entertainment closed			−0.009	0.007	−0.010	0.006	−0.009	0.007
			(0.026)	(0.024)	(0.026)	(0.024)	(0.025)	(0.023)
During Stay Home Order			−0.014	−0.010				
			(0.017)	(0.020)				
Stay Home: with religious exemption					−0.023	−0.017		
					(0.019)	(0.022)		
Stay Home: without religious exemption					0.006	0.003		
					(0.019)	(0.020)		
Stay home: Rel. gatherings prohibited							−0.012	−0.015
							(0.027)	(0.028)
Stay home: Exempt from limits							−0.033	−0.027
							(0.021)	(0.024)
Stay home: Limited to 10							0.009	0.013
							(0.020)	(0.020)
Stay home: Limited otherwise							0.017	0.010
							(0.049)	(0.042)
Average in February (Sunday)	0.291	0.291	0.291	0.291	0.291	0.291	0.291	0.291
Number of churches	3893	3893	3893	3893	3893	3893	3893	3893
Observations	58,395	58,395	58,395	58,395	58,395	58,395	58,395	58,395
Adjusted R^2	0.564	0.533	0.586	0.583	0.586	0.583	0.586	0.584

Note: *p<0.1; **p<0.05; ***p<0.01. Dependent variable: At least one post includes a video (YouTube video, live video, scheduled and completed, native video) on a given Sunday. Includes church fixed effects and an Easter Sunday dummy. Standards error clustered on state level. Includes Sundays between 2020-01-01 and 2020-04-15. Columns 4 and 5: Religious exemptions according to own categorization. Columns 7 and 8: Categorization from Pew Research Center. Number of states (clusters): 51.

CEPR PRESS

Covid Economics 61, 11 December 2020: 121-171

Table 6: Effect of Covid-19 and interventions on churches posting behavior on Sundays: Relaxation Period (after April 15)

	Dependent variable: Posted at least one video on Sunday							
	(1)	(2)	(3)	(4)	(5)	(6)	(7)	(8)
Log Infections previous week (county)	−0.004		−0.002	−0.0004	−0.002	−0.0002	−0.003	−0.001
	(0.003)		(0.003)	(0.002)	(0.003)	(0.002)	(0.003)	(0.002)
Log deaths previous week (county)		0.003**						
		(0.002)						
Gatherings forbidden			0.022**	0.012	0.022**	0.013	0.020**	0.010
			(0.010)	(0.010)	(0.010)	(0.009)	(0.009)	(0.009)
Restaurants/Entertainment closed			0.011	−0.002	0.012*	−0.001	0.012	−0.002
			(0.007)	(0.006)	(0.007)	(0.006)	(0.007)	(0.006)
During Stay Home Order			0.014*	−0.005				
			(0.007)	(0.007)				
Stay Home: with religious exemption					0.017**	−0.003		
					(0.008)	(0.006)		
Stay Home: without religious exemption					0.008	−0.008		
					(0.010)	(0.011)		
Stay home: Rel. gatherings prohibited							0.030**	0.012
							(0.014)	(0.015)
Stay home: Exempt from limits							0.014	−0.005
							(0.011)	(0.008)
Stay home: Limited to 10							0.008	−0.011*
							(0.007)	(0.006)
Stay home: Limited otherwise							0.010	−0.011
							(0.012)	(0.012)
Linear week trend				−0.005***		−0.005***		−0.005***
				(0.001)		(0.001)		(0.001)
Average in April (Sunday)	0.694	0.694	0.694	0.694	0.694	0.694	0.694	0.694
Number of churches	3888	3888	3888	3888	3888	3888	3888	3888
Number of States (clusters)	50	50	50	50	50	50	50	50
Observations	42,823	42,823	42,823	42,823	42,823	42,823	42,823	42,823
Adjusted R^2	0.706	0.706	0.707	0.707	0.707	0.707	0.707	0.707

Note: *p<0.1; **p<0.05; ***p<0.01. Dependent variable: At least one post includes a video (YouTube video, live video, scheduled and completed, native video) on a given Sunday. Includes church fixed effects. Standards error clustered on state level. Includes Sundays between 2020-04-15 and 2020-06-30. Columns 4 and 5: Religious exemptions according to own categorization. Columns 7 and 8: Categorization from Pew Research Center.

7.2.2 Heterogeneity Analysis

Table 7: Effect of Covid-19 and interventions on churches posting behavior on Sundays according to size of the church: Introduction Period (before April 15)

	Dependent variable: Predicted Online Church Activity on Sunday			
	Mega churches	Large churches	Medium churches	Small churches
	(1)	(2)	(3)	(4)
Log Infections previous week (county)	0.027***	0.023***	0.022**	0.009
	(0.005)	(0.007)	(0.009)	(0.007)
After International Travel Ban (March 11)	0.194***	0.223***	0.147***	0.058***
	(0.022)	(0.021)	(0.016)	(0.019)
After Federal guidelines issued (March 16)	0.022	0.035	0.262***	0.177***
	(0.058)	(0.047)	(0.038)	(0.063)
After Public Schools Closed	0.069**	0.086***	−0.072***	−0.058
	(0.032)	(0.021)	(0.027)	(0.064)
Gatherings forbidden	0.027	−0.002	−0.024	−0.002
	(0.034)	(0.028)	(0.017)	(0.027)
Restaurants/Entertainment closed	−0.094	−0.039	−0.008	0.054
	(0.060)	(0.052)	(0.034)	(0.035)
During Stay Home Order	−0.054**	−0.051**	−0.052**	−0.003
	(0.025)	(0.023)	(0.026)	(0.026)
Average in February (Sunday)	0.488	0.34	0.223	0.177
Number of churches	504	888	1912	589
Number of States (clusters)	43	50	51	48
Observations	7,560	13,320	28,680	8,835
Adjusted R^2	0.574	0.589	0.569	0.582

Note: *p<0.1; **p<0.05; ***p<0.01. Dependent variable: At least one post predicted to offer an online church activity on a given Sunday. Includes church fixed effects and an Easter Sunday dummy. Standards error clustered on state level. Includes Sundays between 2020-01-01 and 2020-04-15. Small churches are defined as receiving up to 50 people on a regular Sunday (column 4), medium churches between 51 and 300 (column 3), large churches between 301 and 500 (column 2) and mega churches over 2000 (column 1).

CEPR PRESS

Table 8: Effect of Covid-19 and interventions on churches posting behavior on Sundays according to size of the church: Relaxation Period (after April 15)

	Dependent variable: Predicted Online Church Activity on Sunday							
	Mega churches	Mega churches	Large churches	Large churches	Medium churches	Medium churches	Small churches	Small churches
	(1)	(2)	(3)	(4)	(5)	(6)	(7)	(8)
Log Infections previous week (county)	0.007	0.011	−0.008	−0.006	−0.004	−0.002	0.005	0.007
	(0.007)	(0.008)	(0.005)	(0.005)	(0.004)	(0.004)	(0.006)	(0.006)
Gatherings forbidden	0.022	0.011	0.034**	0.027*	0.030**	0.021*	0.0003	−0.016
	(0.021)	(0.022)	(0.015)	(0.015)	(0.012)	(0.012)	(0.023)	(0.023)
Restaurants/Entertainment closed	−0.004	−0.016	−0.012	−0.021	0.019*	0.007	0.034**	0.012
	(0.014)	(0.014)	(0.012)	(0.013)	(0.010)	(0.010)	(0.017)	(0.016)
During Stay Home Order	0.046***	0.031*	0.009	−0.004	0.012	−0.007	0.023*	−0.006
	(0.016)	(0.017)	(0.008)	(0.011)	(0.008)	(0.009)	(0.013)	(0.018)
Linear week trend		−0.004**		−0.003*		−0.005***		−0.008**
		(0.002)		(0.002)		(0.001)		(0.003)
Average in April (Sunday)	0.859	0.859	0.797	0.797	0.652	0.652	0.496	0.496
Number of churches	504	504	888	888	1912	1912	589	589
Number of States (clusters)	43	43	50	50	51	51	48	48
Observations	5,544	5,544	9,768	9,768	21,032	21,032	6,479	6,479
Adjusted R^2	0.594	0.595	0.594	0.594	0.657	0.658	0.709	0.710

Note: *p<0.1; **p<0.05; ***p<0.01. Dependent variable: At least one post predicted to offer an online church activity on a given Sunday. Includes church fixed effects and an Easter Sunday dummy. Standards error clustered on state level. Includes Sundays between 2020-04-15 and 2020-06-30. Small churches are defined as receiving up to 50 people on a regular Sunday, medium churches between 51 and 300, large churches between 301 and 500 and mega churches over 2000.

Covid Economics 61, 11 December 2020: 121-171

Table 9: Effect of Covid-19 and interventions on churches posting behavior on Sundays according to worship style of the church: Introduction Period (before April 15)

	Dependent variable: Predicted Online Church Activity on Sunday		
	Contemporary worship style	Traditional worship style	Blend of the 2 worship styles
	(1)	(2)	(3)
Log Infections previous week (county)	0.025***	0.011	0.019**
	(0.006)	(0.009)	(0.009)
After International Travel Ban (March 11)	0.179***	0.109***	0.128***
	(0.016)	(0.023)	(0.019)
After Federal guidelines issued (March 16)	0.155***	0.309***	0.132***
	(0.044)	(0.041)	(0.035)
After Public Schools Closed	−0.061**	−0.080***	0.030
	(0.029)	(0.025)	(0.019)
Gatherings forbidden	−0.013	−0.001	−0.001
	(0.019)	(0.029)	(0.020)
Restaurants/Entertainment closed	−0.017	−0.048	0.003
	(0.043)	(0.042)	(0.037)
During Stay Home Order	−0.020	−0.028	−0.056**
	(0.019)	(0.029)	(0.026)
Average in February (Sunday)	0.355	0.17	0.26
Number of churches	1222	580	1655
Number of States (clusters)	50	47	51
Observations	18,330	8,700	24,825
R^2	0.621	0.593	0.620
Adjusted R^2	0.594	0.563	0.593

Note: *p<0.1; **p<0.05; ***p<0.01. Dependent variable: At least one post predicted to offer an online church activity on a given Sunday. Includes church fixed effects and an Easter Sunday dummy. Standards error clustered on state level. Includes Sundays between 2020-01-01 and 2020-04-15. Worship style could be selected between traditional, contemporary, blend of contemporary and traditional, and other.

Covid Economics 61, 11 December 2020: 121-171

CEPR PRESS

Table 10: Effect of Covid-19 and interventions on churches posting behavior on Sundays according to worship style of the church: Relaxation Period (after April 15)

	Dependent variable: Predicted Online Church Activity on Sunday					
	Contemporary worship style	Contemporary worship style	Traditional worship style	Traditional worship style	Blend of the 2 worship styles	Blend of the 2 worship styles
	(1)	(2)	(3)	(4)	(5)	(6)
Log Infections previous week (county)	−0.001	0.001	−0.009	−0.004	−0.001	0.001
	(0.004)	(0.005)	(0.007)	(0.006)	(0.004)	(0.004)
Gatherings forbidden	0.021	0.012	0.046	0.024	0.025	0.016
	(0.020)	(0.021)	(0.031)	(0.029)	(0.021)	(0.020)
Restaurants/Entertainment closed	0.009	−0.002	0.029*	−0.003	0.011	0.0003
	(0.011)	(0.012)	(0.016)	(0.016)	(0.012)	(0.011)
During Stay Home Order	0.029***	0.013	0.021*	−0.024	0.010	−0.006
	(0.009)	(0.010)	(0.012)	(0.015)	(0.011)	(0.011)
Linear week trend		−0.004***		−0.011***		−0.004***
		(0.001)		(0.002)		(0.001)
Average in April (Sunday)	0.753	0.753	0.561	0.561	0.665	0.665
Number of churches	1222	1222	580	580	1655	1655
Number of States (clusters)	50	50	47	47	51	51
Observations	13,442	13,442	6,380	6,380	18,205	18,205
R^2	0.660	0.660	0.717	0.719	0.719	0.719
Adjusted R^2	0.626	0.626	0.688	0.691	0.691	0.691

Note: *p<0.1; **p<0.05; ***p<0.01. Dependent variable: At least one post predicted to offer an online church activity on a given Sunday. Includes church fixed effects. Standards error clustered on state level. Includes Sundays between 2020-04-15 and 2020-06-30. Worship style could be selected between traditional, contemporary, blend of contemporary and traditional, and other.

Table 11: Effect of Covid-19 and interventions on churches posting behavior on Sundays interacted with the Republic vote share in 2016 (county level): Introduction Period (before April 15)

	Dependent variable: Predicted Online Church Activity on Sunday			
	(1)	(2)	(3)	(4)
Log Infections previous week (county)	0.054***		0.027***	
	(0.002)		(0.006)	
Log deaths previous week (county)		0.063***		0.027***
		(0.003)		(0.009)
After International Travel Ban (March 11)			−0.041***	−0.044*
			(0.015)	(0.023)
After Federal guidelines issued (March 16)			−0.022*	−0.002
			(0.013)	(0.013)
After Public Schools Closed			−0.014	0.008
			(0.023)	(0.026)
Gatherings forbidden			0.141***	0.174***
			(0.024)	(0.028)
Restaurants/Entertainment closed			0.151***	0.181***
			(0.012)	(0.008)
During Stay Home Order			−0.009	−0.016
			(0.014)	(0.012)
Log Infections previous week* Percent Republic Votes 2016	0.001***		−0.0002	
	(0.0001)		(0.0002)	
Log deaths previous week* Percent Republic Votes 2016		0.0005***		0.00005
		(0.0002)		(0.0004)
After International Travel Ban* Percent Republic Votes 2016			0.001	0.002*
			(0.001)	(0.001)
After Federal guidelines issued * Percent Republic Votes 2016			0.002*	0.001
			(0.001)	(0.001)
After Public Schools Closed* Percent Republic Votes 2016			0.001	0.0003
			(0.001)	(0.002)
Gatherings forbidden* Percent Republic Votes 2016			0.002	0.002
			(0.001)	(0.002)
Restaurants/Entertainment closed* Percent Republic Votes 2016			−0.0004	−0.002***
			(0.001)	(0.001)
During Stay Home Order* Percent Republic Votes 2016			−0.0002	−0.0001
			(0.001)	(0.001)
Average in February (Sunday)	0.277	0.277	0.277	0.277
Number of churches	3888	3888	3888	3888
Number of States (clusters)	50	50	50	50
Observations	58,320	58,320	58,320	58,320
R^2	0.603	0.564	0.625	0.619
Adjusted R^2	0.575	0.533	0.598	0.592

Note: *p<0.1; **p<0.05; ***p<0.01

Note: *p<0.1; **p<0.05; ***p<0.01. Dependent variable: At least one post predicted to offer an online church activity on a given Sunday. Includes church fixed effects and an Easter Sunday dummy. Standards error clustered on state level. Percent Republican Votes 2016 measures the difference between the votes cast for the Republican party in the 2016 presidential elections on the county level and the national average. The uninteracted coefficients are thus interpreted as the relationship at the mean, the interaction as one percentage point increase in the vote share compared to the average. The Includes Sundays between 2020-01-01 and 2020-04-15.

Table 12: Effect of Covid-19 and interventions on churches posting behavior on Sundays interacted with the Republic vote share in 2016 (county level): Introduction Period (before April 15)

	Dependent variable: Predicted Online Church Activity on Sunday			
	(1)	(2)	(3)	(4)
Log Infections previous week (county)	0.028***		0.028***	
	(0.006)		(0.005)	
Log deaths previous week (county)		0.029***		0.030***
		(0.009)		(0.009)
Stay Home: with religious exemption	−0.057***	−0.057**		
	(0.016)	(0.025)		
Stay Home: no religious exemption	−0.010	−0.021		
	(0.018)	(0.022)		
Stay home: Rel. gatherings prohibited			−0.004	−0.023
			(0.023)	(0.024)
Stay home: Exempt from limits			−0.073***	−0.077***
			(0.017)	(0.027)
Stay home: Limited to 10			−0.009	−0.008
			(0.017)	(0.020)
Stay home: Limited otherwise			0.014	−0.003
			(0.046)	(0.043)
Log Infections previous week* % Republic Votes 2016	−0.0001		−0.0002	
	(0.0001)		(0.0001)	
Log deaths previous week* % Republic Votes 2016		0.0001		−0.00003
		(0.0004)		(0.0003)
Stay Home: with religious exemption* % Republic Votes 2016	0.001**	0.002*		
	(0.001)	(0.001)		
Stay Home: no religious exemption* % Republic Votes 2016	0.001	0.002		
	(0.001)	(0.002)		
Stay home: Rel. gatherings prohibited* % Republic Votes 2016			0.004**	0.006**
			(0.002)	(0.003)
Stay home: Exempt from limits* % Republic Votes 2016			0.002**	0.003**
			(0.001)	(0.001)
Stay home: Limited to 10* % Republic Votes 2016			0.001	0.001
			(0.001)	(0.001)
Stay home: Limited otherwise* % Republic Votes 2016			−0.001	−0.001
			(0.002)	(0.002)
State Intervention Indicators:	Yes	Yes	Yes	Yes
Average in February (Sunday)	0.277	0.277	0.277	0.277
Number of churches	3888	3888	3888	3888
Number of States (clusters)	50	50	50	50
Observations	58,320	58,320	58,320	58,320
Adjusted R^2	0.598	0.592	0.598	0.593

Note: *p<0.1; **p<0.05; ***p<0.01. Dependent variable: At least one post predicted to offer an online church activity on a given Sunday. Includes church fixed effects and an Easter Sunday dummy. Standards error clustered on state level. Percent Republican Votes 2016 measures the difference between the votes cast for the Republican party in the 2016 presidential elections on the county level and the national average. The uninteracted coefficients are thus interpreted as the relationship at the mean, the interaction as one percentage point increase in the vote share compared to the average. The Includes Sundays between 2020-01-01 and 2020-04-15. Columns 1 and 2: Religious exemptions according to own categorization. Columns 3 and 4: Categorization from Pew Research Center.

Table 13: Effect of Covid-19 and interventions on churches posting behavior on Sundays interacted with the Republic vote share in 2016 (county level): Relaxation Period (after April 15)

	Dependent variable: Predicted Online Church Activity on Sunday			
	(1)	(2)	(3)	(4)
Log infections previous week (county)	−0.004		−0.002	0.001
	(0.003)		(0.003)	(0.002)
Log deaths previous week (county)		0.001		
		(0.002)		
Gatherings forbidden			0.017**	−0.002
			(0.007)	(0.007)
Restaurants/Entertainment closed			0.026**	0.016
			(0.011)	(0.011)
During Stay Home Order			0.010	−0.003
			(0.007)	(0.006)
Linear week trend				−0.005***
				(0.001)
Log infections previous week* Percent Republic Votes 2016	0.00000		0.0001	0.0002
	(0.0002)		(0.0002)	(0.0002)
Log deaths previous week* Percent Republic Votes 2016		−0.0001		
		(0.0001)		
Gatherings forbidden* Percent Republic Votes 2016			0.0003	−0.00001
			(0.0004)	(0.0005)
Restaurants/Entertainment closed* Percent Republic Votes 2016			−0.0003	−0.001
			(0.001)	(0.0005)
During Stay Home Order* Percent Republic Votes 2016			0.001*	0.0004
			(0.0004)	(0.0004)
Linear week trend* Percent Republic Votes 2016				−0.0001
				(0.0001)
Average in April (Sunday)	0.688	0.688	0.688	0.688
Number of churches	3888	3888	3888	3888
Number of States (clusters)	50	50	50	50
Observations	42,768	42,768	42,768	42,768
Adjusted R^2	0.671	0.671	0.672	0.672

Note: *p<0.1; **p<0.05; ***p<0.01. Dependent variable: At least one post predicted to offer an online church activity on a given Sunday. Includes church fixed effects. Standards error clustered on state level. Percent Republican Votes 2016 measures the difference between the votes cast for the Republican party in the 2016 presidential elections on the county level and the national average. The uninteracted coefficients are thus interpreted as the relationship at the mean, the interaction as one percentage point increase in the vote share compared to the average. The Includes Sundays between 2020-04-15 and 2020-06-30.

Covid Economics Issue 61, 11 December 2020

Spatial implications of telecommuting[1]

Matthew J. Delventhal[2] and Andrii Parkhomenko[3]

Date submitted: 4 December 2020; Date accepted: 6 December 2020

If the 2020 surge in working from home became permanent, how would the distribution of jobs and residents within and across U.S. cities change? To study this question, we build a quantitative spatial equilibrium model of job and residence choice with commuting frictions between 4,502 sub-metropolitan locations in the contiguous U.S.A novel feature of our model is the heterogeneity of workers in the fraction of time they work on-site: some workers commute daily, some always work at home, while others alternate between working on-site and remotely. In a counterfactual where remote work becomes more common, residents move from central to peripheral areas within cities, and from large coastal to small interior cities, on average. The reallocation of jobs is less monotonic, with increases both in peripheral locations and in the highest-productivity metropolises. Agglomeration externalities from in-person interactions are crucial for welfare effects. If telecommuters keep contributing to productivity as if they worked on-site, better job market access drives considerable welfare gains, even for those who continue to commute. But if productivity declines in response to the reduction in face-to-face interactions, wages fall and most workers are worse off.

1 We thank seminar participants at USC Marshall brownbag and CSU Fullerton for their comments and suggestions. We are grateful to Nate Baum-Snow and Lu Han for sharing local housing supply elasticity estimates. We also thank Amanda Ang for excellent research assistance. Finally, we gratefully acknowledge financial upport provided by the USC Lusk Center for Real Estate.

2 The Robert Day School of Economics and Finance, Claremont McKenna College.

3 Department of Finance and Business Economics, Marshall School of Business, University of Southern California.

Covid Economics 61, 11 December 2020: 172-221

1 Introduction

Perhaps no event in recent history has as much potential to utterly transform the urban landscape as the surge in working from home that has occurred in 2020 following the Covid-19 pandemic. Years of steady technical progress have increased the feasibility of remote arrangements.[1] Now, in one fell swoop, one-third of the workforce has made a forced investment in the skills and equipment needed to work out of their homes.[2] Survey after survey of managers and the workers themselves indicate the likelihood that some of the increase in remote work will become permanent and will have sizable effects on location choices of workers.[3]

How would the internal structure of American cities change if the tether of commuting is cut loose for a large section of the work force? Will downtown districts be left empty, as telecommuting office workers decamp for the suburbs? And what shifts might occur across cities? Is the era of the big cities over?

In this paper we build a quantitative model of job and residence choice to address these questions. Workers compare wages, property prices, local amenities, and commuting times between 4,502 urban, suburban and rural locations in the contiguous United States. They choose one place to live and one place to work. Residential and employment density in each location endogenously determines local amenities and productivity, respectively, via agglomeration externalities. In addition to on-site workers there are telecommuters, who are also divided into groups. Some visit the office four times a week, others three times, and still others two times, or one time, or never. The less they need to visit the office, the less constrained they are in their choice of the house-job pair. Zero-time-a-weekers are able to live and work on opposite sides of the country.

Recent research by Barrero, Bloom, and Davis (2020) suggests that the fraction of workers who come to work daily will fall from 90% pre-Covid to 73% after the pandemic,

[1] Mas and Pallais (2020) provides an overview of the current state of research into remote work. Bloom, Liang, Roberts, and Ying (2015) present experimental evidence that telework increases employee work satisfaction without necessarily reducing their productivity, while another experiment by Mas and Pallais (2017) finds that, on average, workers are willing to give up 8% of wages for the option to work from home.

[2] A survey by Brynjolfsson, Horton, Ozimek, Rock, Sharma, and TuYe (2020) finds that in early May 2020, 35.2% of workers who commuted before Covid-19 were working from home.

[3] A May 2020 survey by Barrero, Bloom, and Davis (2020) finds that 16.6% of paid work days will be done from home after the pandemic ends, compared to 5.5% in 2019. Results of a survey by Bartik, Cullen, Glaeser, Luca, and Stanton (2020) also indicate that remote work will be much more common after the pandemic. These projections are supported by the findings of Dingel and Neiman (2020) who estimate that as many as 37% of U.S. jobs can feasibly be done at home. Indeed, some companies (e.g., Facebook and Twitter) announced that many of their employees could keep working from home after Covid-19. Moreover, according to a study by Upwork in October 2020, 2% of survey participants had already moved residences because of the ability to work at home and another 6% planned to do so. Of those who still planned to migrate, 40% would move more than 4 hours away from their current location (Ozimek, 2020).

while the fraction of those who commute only a few days a week or not at all will grow. Our model generates rich patterns of reallocation both within and across cities in response to this change in commuting frequencies. Residents, led by new telecommuters, move from denser and more central parts of cities to the periphery. They also move from larger to smaller, and from more coastal to more interior cities, on average. These trends have exceptions. Workers actually relocate into a handful of high-amenity locations, and some metro areas, such as Los Angeles and San Diego, grow very slightly.

The trend in job reallocation is not so monotonic. Peripheral areas with low real estate costs and central areas in the most productive cities both add jobs. While the largest percentage increases happen in smaller cities, several large metro areas, including New York and Washington, D.C., see the number of jobs increase. Even in places where jobs increase, however, more of them are held by telecommuters who visit the office less frequently or not at all and often live in different metro areas. This leads to a large decrease in the demand for commercial floorspace and drives a small average decline in real estate prices. New York and Los Angeles see real estate prices fall by about 1%, while San Francisco and San Jose see them decline by about 2%.

We find that welfare effects hinge critically on the extent to which telecommuters contribute to externalities that map local employment density into productivity. In our baseline scenario the local productivity and amenities of each location do not change in the counterfactual. Improved market access allows wages to go up, and most workers, including full time commuters, experience modest welfare gains. We also compute an alternative scenario in which productivity and amenities are determined endogenously by agglomeration externalities. Our baseline assumption is that productivity externalities arise through face-to-face interactions between workers, so teleworkers do not contribute to them when they are not in the office. In this case, the patterns of reallocation of residence and jobs are nearly the same as before, but the movements are larger due to amplifications via endogenous amenities and productivity. The welfare implications, however, are now different. The reduction in face-to-face interactions lowers overall productivity and drives wages down by over 1%. This makes workers who are still stuck commuting strictly worse off. There are still aggregate welfare gains, but only because there are now more remote workers, who can freely choose locations with better amenities and do not suffer by commuting.

We expand our analysis to explore what would happen if remote workers did make some contribution to workplace spillovers. In the extreme case where they interact in a way that is indistinguishable from on-site workers, all the negative results are reversed. By varying the contribution of telecommuters to spillovers from 0 to 100%, we are able

Covid Economics 61, 11 December 2020: 172-221

to characterize the level of contribution that would be necessary in order for all classes of workers to be no worse off after the increase in remote work, even if local productivities adjust fully.

This paper builds on previous work by Delventhal, Kwon, and Parkhomenko (2020) in which the authors model the impact of remote work on the allocation of jobs and residence within a single urban area–Los Angeles–modeled as a closed city. Including the entire system of cities changes the prediction for real estate prices–while they fell by nearly 6% in the study of L.A. as a closed city, they fall by only 1% in the current study, as workers from other parts of the country move into the L.A. area attracted by high amenities.

In modeling style our study is related to Monte, Redding, and Rossi-Hansberg (2018), who also analyze the U.S. system of cities using a model in which workers may commute between counties. Our quantitative model contains many small locations within urban counties and thus can study heterogeneous responses of many areas within metro areas. Also related are recent papers which use models of joint job and residence choice at the city level, such as Ahlfeldt, Redding, Sturm, and Wolf (2015) and Heblich, Redding, and Sturm (2020). Our study contributes to this strand of the literature by extending the toolbox to include a full-fledged model of working from home and by exploring what happens when the binding tie of the daily commute is cut for many workers. In addition, we contribute to the theoretical literature that studies telecommuting within the urban environment, e.g., Safirova (2003), Rhee (2008), and Larson and Zhao (2017). Recent work by Lennox (2020) explores the effects of working from home in an Australian context using a quantitative spatial equilibrium model.

The remainder of the paper is organized as follows. Section 2 describes the theoretical framework and the methodology of counterfactual experiments. Section 3 discusses the data, as well as estimation and calibration of model parameters. Section 4 reviews the results of counterfactual experiments in which telecommuting becomes more prevalent. Section 5 concludes and outlines possible extensions of our work.

2 Model

Consider a national economy which consists of a set $\mathcal{I} \equiv \{1, ..., I\}$ of discrete locations and is populated by workers, firms and floorspace developers. Total employment in the economy is fixed and normalized to 1.

Covid Economics 61, 11 December 2020: 172-221

2.1 Workers

2.1.1 Telecommuting

Before choosing where to work and where to live, workers draw their commuter type θ which has a distribution function $F(\theta)$ on support $[0, 1]$. The associated probability distribution function is $f(\theta)$. Parameter θ is the fraction of work time that an individual has to work on-site. In practice, $F(\theta)$ has a heavy weight on $\theta = 1$ which means that most workers cannot telecommute at all and some weight on $\theta = 0$ which means that there is a non-trivial number of workers who always work remotely. A transition toward more telecommuting corresponds to a shift to $F^*(\theta)$ which is first-order stochastically dominated by $F(\theta)$, as shown in Figure 1.

Figure 1: Distribution of commuter types.

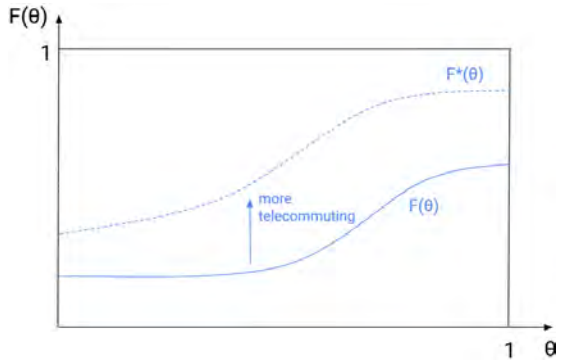

2.1.2 Preferences

A worker n who resides in location $i \in \{1, ..., I\}$, works in location j, and has to commute there a fraction θ of time, enjoys utility

$$U_{ijn}(\theta) = \frac{z_{ijn}}{d_{ij}(\theta)} \left(\frac{c}{1-\gamma} \right)^{1-\gamma} \left(\frac{h}{\gamma} \right)^{\gamma}, \tag{2.1}$$

where z_{ijn} represents an idiosyncratic preference shock for the pair of locations i and j, and $d_{ij}(\theta)$ is the disutility from commuting for type θ given by

$$d_{ij}(\theta) = e^{\theta \kappa t_{ij}}. \tag{2.2}$$

Covid Economics 61, 11 December 2020: 172-221

Individuals consume c units of the final good and h units of housing. The share of housing in expenditures is given by γ, and consumption choices are subject to the budget constraint

$$w_{ij}(\theta) = c + q_i h, \tag{2.3}$$

where $w_{ij}(\theta)$ is the wage earned by a type-θ worker who lives in i and works in j, and q_i is the price of residential floorspace in location i.

Idiosyncratic shocks z_{ijn} are drawn from a Frèchet distribution with c.d.f. $F_z(z) = e^{-z^{-\epsilon}}$. The indirect utility of worker n who lives in location i and works in location j is given by $u_{ijn}(\theta) = z_{ijn} v_{ij}(\theta)$, where

$$v_{ij}(\theta) \equiv \frac{B_{ij} w_{ij}(\theta)}{d_{ij}(\theta) q_i^{\gamma}} \tag{2.4}$$

is the utility obtained by a type-θ worker, net of the preference shock. In the above formulation, B_{ij} is a location pair-specific shifter defined as

$$B_{ij} \equiv X_i E_j b_{ij}, \tag{2.5}$$

where X_i is the average amenity derived from living in location i, E_j is the average amenity derived from working in location j, and b_{ij} is the pair-specific amenity component.

2.1.3 Location Choices

Optimal choices imply that the probability that a worker with a given θ chooses to live in location i and work in location j is

$$\pi_{ij}(\theta) = \frac{\left(v_{ij}(\theta)\right)^{\epsilon}}{\sum_{r \in \mathcal{I}} \sum_{s \in \mathcal{I}} \left(v_{rs}(\theta)\right)^{\epsilon}} = \frac{\left(B_{ij} w_{ij}(\theta)\right)^{\epsilon} \left(d_{ij}(\theta) q_i^{\gamma}\right)^{-\epsilon}}{\sum_{r \in \mathcal{I}} \sum_{s \in \mathcal{I}} \left(B_{rs} w_{rs}(\theta)\right)^{\epsilon} \left(d_{rs}(\theta) q_r^{\gamma}\right)^{-\epsilon}}. \tag{2.6}$$

As a result, the equilibrium residential population of type θ in location i is

$$N_{Ri}(\theta) = \sum_{j \in \mathcal{I}} \pi_{ij}(\theta), \tag{2.7}$$

and the equilibrium employment of type θ in location j is

$$N_{Wj}(\theta) = \sum_{i \in \mathcal{I}} \pi_{ij}(\theta). \tag{2.8}$$

Covid Economics 61, 11 December 2020: 172-221

The total amount of labor commuting from i to j is given by

$$N_{ij}^{C} \equiv \int \theta \pi_{ij}(\theta) \mathrm{d}F(\theta), \tag{2.9}$$

while the amount of labor telecommuting between i and j is

$$N_{ij}^{T} \equiv \int (1-\theta) \pi_{ij}(\theta) \mathrm{d}F(\theta). \tag{2.10}$$

Notice that the distinction between on-site and remote labor is not the same as the distinction between commuters and telecommuters, since a worker with $\theta \in (0,1)$ provides both on-site and remote labor by commuting fraction θ of time and telecommuting the remaining $1-\theta$. Thus, employment in each location consists of on-site labor

$$N_{Wj}^{C} = \sum_{i \in \mathcal{I}} N_{ij}^{C}, \tag{2.11}$$

and remote labor

$$N_{Wj}^{T} = \sum_{i \in \mathcal{I}} N_{ij}^{T}. \tag{2.12}$$

The probability of working in location j, conditional on living in i, is given by

$$\pi_{ij|i}(\theta) = \frac{\left(E_j b_{ij} w_{ij}(\theta)\right)^{\epsilon} \left(d_{ij}(\theta)\right)^{-\epsilon}}{\sum_{s \in \mathcal{I}} \left(E_s b_{is} w_{is}(\theta)\right)^{\epsilon} \left(d_{is}(\theta)\right)^{-\epsilon}}. \tag{2.13}$$

The probability of living in location i, conditional on working in i, is

$$\pi_{ij|j}(\theta) = \frac{\left(X_i b_{ij} w_{ij}(\theta)\right)^{\epsilon} \left(d_{ij}(\theta) q_i^{\gamma}\right)^{-\epsilon}}{\sum_{r \in \mathcal{I}} \left(X_r b_{rj} w_{rj}(\theta)\right)^{\epsilon} \left(d_{rj}(\theta) q_r^{\gamma}\right)^{-\epsilon}}. \tag{2.14}$$

The following commuter market clearing conditions relate the number of workers in each location to the number of residents in each location:

$$N_{Wj}(\theta) = \sum_{i \in \mathcal{I}} \pi_{ij|j}(\theta) N_{Ri}(\theta), \tag{2.15}$$

$$N_{Ri}(\theta) = \sum_{j \in \mathcal{I}} \pi_{ij|i}(\theta) N_{Wj}(\theta). \tag{2.16}$$

Covid Economics 61, 11 December 2020: 172-221

2.1.4 Welfare

The expected utility of a worker, before she knows her value of θ and before the idiosyncratic preference shocks realize, is

$$V = \varsigma \int \left[\sum_{i \in \mathcal{I}} \sum_{j \in \mathcal{I}} \left(B_{ij} w_{ij}(\theta) \right)^{\epsilon} \left(d_{ij}(\theta) q_i^{\gamma} \right)^{-\epsilon} \right]^{\frac{1}{\epsilon}} \mathrm{d}F(\theta), \tag{2.17}$$

where $\varsigma \equiv \Gamma\left(\frac{\epsilon-1}{\epsilon}\right)$ and $\Gamma(\cdot)$ is the Gamma function.

2.2 Firms

2.2.1 Production

In each location, there is a representative firm which hires both on-site and remote labor and produces a homogeneous consumption good which is traded costlessly across locations. The total output of the firm in location j is

$$Y_j = Y_j^C + Y_j^T, \tag{2.18}$$

where Y_j^C and Y_j^T are the amounts produced on-site and remotely, respectively. The on-site production function is given by

$$Y_j^C = A_j \left(N_{Wj}^C \right)^{\alpha_C} \left(H_{Wj}^C \right)^{1-\alpha_C}, \tag{2.19}$$

where N_{Wj}^C is labor, H_{Wj}^C is floorspace, and α_C is the labor share. The remote production function is also Cobb-Douglas and it combines workers from different locations as follows:

$$Y_j^T = \nu A_j \sum_{i \in \mathcal{I}} \left(N_{ij}^T \right)^{\alpha_T} \left(H_{ij}^T \right)^{1-\alpha_T}. \tag{2.20}$$

In the previous specification, N_{ij}^T is the number of telecommuters who reside in location i and work for a firm in location j, whereas H_{ij}^T is the amount of home office space the firm rents on behalf of these workers in the place of their residence.[4] Parameter ν is the productivity gap between on-site and remote work, common to all workers and firms. We

[4] We assume that the firm rents the floorspace that remote workers need in order to work from home, however this specification is isomorphic to the one in which the firm only pays for labor services of a telecommuter and the telecommuter uses his labor income to rent additional floorspace in his house.

Covid Economics 61, 11 December 2020: 172-221

let the floorspace share, $1-\alpha_m$, differ between the two modes.[5]

2.2.2 Wages

Firms take wages and floorspace prices as given, and choose the amount of on-site labor, telecommuting labor, and floorspace that maximize their profits. Equilibrium payments for on-site work are

$$w_j^C = \alpha_C A_j^{\frac{1}{\alpha_C}} \left(\frac{1-\alpha_C}{q_j}\right)^{\frac{1-\alpha_C}{\alpha_C}}, \tag{2.21}$$

where q_j is the local price of floorspace. The payments for at-home work of an individual who is employed in j and works remotely from i are given by

$$w_{ij}^T = \alpha_T \left(\nu A_j\right)^{\frac{1}{\alpha_T}} \left(\frac{1-\alpha_T}{q_i}\right)^{\frac{1-\alpha_T}{\alpha_T}}. \tag{2.22}$$

In the previous expression the relevant floorspace price is the price at the location of residence of the worker. The take-home wage of a worker with a given θ is the weighted average of payments to his commuting labor and his telecommuting labor:

$$w_{ij}(\theta) = \theta w_j^C + (1-\theta) w_{ij}^T. \tag{2.23}$$

Note that the wage of a regular commuter ($\theta = 1$) does not depend on her location of residence i. However, the wage of a worker who works some of the time remotely ($\theta < 1$) depends on his location of residence i because the home-office floorspace is used in production. The average income earned by residents of location i is

$$\tilde{w}_i = \int \sum_{j \in I} w_{ij}(\theta) \pi_{ij|i}(\theta) \mathrm{d}F(\theta). \tag{2.24}$$

[5]One may expect that $1-\alpha_C > 1-\alpha_T$ because telecommuters tend to work in industries and occupations that require little floorspace (e.g., compare software development with manufacturing). While we do not impose this inequality in our theoretical analysis, it holds in our calibration.

Covid Economics 61, 11 December 2020: 172-221

2.3 Developers

2.3.1 Supply of floorspace

There is a large number of perfectly competitive floorspace developers operating in each location. Floorspace is produced using technology

$$H_i = K_i^{1-\eta_i} \left(\phi_i L_i\right)^{\eta_i}, \tag{2.25}$$

where L_i and K_i are the amounts of land and the final good used to produce floorspace, and η_i is the location-specific share of land in the production function. Each location is endowed with Λ_i units of buildable land which is exogenous and serves as the upper bound on the developers' choice of land: $L_i \leq \Lambda_i$. Parameter ϕ_i stands for the local land-augmenting productivity of floorspace developers.[6] Let q_i be the equilibrium price of floorspace. Then the equilibrium supply of floorspace in location i is

$$H_i = \phi_i (1-\eta_i)^{\frac{1-\eta_i}{\eta_i}} q_i^{\frac{1-\eta_i}{\eta_i}} L_i. \tag{2.26}$$

The price elasticity of floorspace supply is therefore $\frac{1-\eta_i}{\eta_i}$.

2.3.2 Demand for floorspace

Floorspace is used by firms, residents, and telecommuters, and therefore is divided into commercial, residential, and home offices. The demand for commercial floorspace is

$$H_{Wi} = \left(\frac{1-\alpha_C}{q_j}\right)^{\frac{1}{\alpha_C}} N_{Wj}^C A_j^{\frac{1}{\alpha_C}}, \tag{2.27}$$

the demand for residential floorspace is

$$H_{Ri} = \frac{\gamma}{q_i} N_{Ri} \tilde{w}_i, \tag{2.28}$$

and the demand for home offices is given by

$$H_{Ti} = \left(\frac{1-\alpha_T}{q_i}\right)^{\frac{1}{\alpha_T}} N_{Ri} \sum_{j \in \mathcal{I}} \left(\nu A_j\right)^{\frac{1}{\alpha_T}} \int (1-\theta) \pi_{ij|i}(\theta) \mathrm{d}F(\theta). \tag{2.29}$$

[6] The productivity may depend on terrain, climate, land use regulations, etc.

Covid Economics 61, 11 December 2020: 172-221

In equilibrium the supply of floorspace must equal to the total demand,

$$H_i = H_{Wi} + H_{Ri} + H_{Ti}. \tag{2.30}$$

2.3.3 Land and floorspace prices

Floorspace demand also determines the demand for land. We follow Monte, Redding, and Rossi-Hansberg (2018) in assuming that land in each location is owned by local immobile landlords who only consume the final good. Thus, we can account for changes in land values when computing welfare effects, while eliminating anticipated income from land ownership as a factor in the location choice problem. In equilibrium, it is optimal for developers to use all buildable land, i.e., $L_i = \Lambda_i$. As a result, the equilibrium land price is equal to

$$l_i = \frac{\eta_i}{\Lambda_i}\left[\frac{1-\alpha_C}{\alpha_C} w_i^C \sum_{j\in\mathcal{I}} N_{ji}^C + \gamma \sum_{j\in\mathcal{I}} w_j^C N_{ij}^C + \left(\gamma + \frac{1-\alpha_T}{\alpha_T}\right)\sum_{j\in\mathcal{I}} w_{ij}^T N_{ij}^T\right]. \tag{2.31}$$

Finally, equilibrium floorspace prices are given by

$$q_i = \frac{1}{\eta_i^{\eta_i}(1-\eta_i)^{1-\eta_i}}\left(\frac{l_i}{\phi_i}\right)^{\eta_i}. \tag{2.32}$$

2.4 Externalities

Local total factor productivity and residential amenities depend on density. In particular, the productivity in location j is determined by an exogenous component, a_j, and an endogenous component that is increasing in the density of on-site labor in this location:

$$A_j = a_j\left(\frac{N_{Wj}^C + \psi N_{Wj}^T}{L_j}\right)^{\lambda}. \tag{2.33}$$

Parameter $\lambda > 0$ measures the elasticity of productivity with respect to the local density of workers. Parameter $\psi \in [0,1]$ is the degree of remote workers' participation in productive externalities. These externalities include learning, knowledge spillovers, and networking that occur as a result of face-to-face interactions between workers. When workers are not on-site, but are working remotely, they may not participate fully in the types of interactions that give rise to these externalities. As we will see, the value of ψ has important consequences for wages and welfare in our counterfactual analysis.

Covid Economics 61, 11 December 2020: 172-221

Similarly, the residential amenity in location i is determined by an exogenous component, x_j, and an endogenous component that depends on the density of residents:

$$X_i = x_i \left(\frac{N_{Ri}}{L_i} \right)^{\chi}. \tag{2.34}$$

Parameter $\chi > 0$ measures the elasticity of amenities with respect to the local density of residents.[7] The positive relationship between residential density and amenities represents in reduced form the greater propensity for both public amenities, such as parks and schools, and private amenities, such as retail shopping, to locate in proximity to greater concentrations of potential users and customers. All types of workers, commuters and telecommuters, contribute equally to amenity externalities at their location of residence.[8]

2.5 Equilibrium

Definition 2.1. A *spatial equilibrium* consists of location choice probabilities, $\pi_{ij}(\theta)$; residential and workplace employment, $N_{Ri}(\theta)$ and $N_{Wj}(\theta)$; wages, w_j^C and w_{ij}^T; land prices, l_i; floorspace prices, q_i; local productivity, A_j; and local amenities, X_j; such that equations (2.6), (2.15), (2.16), (2.21), (2.22), (2.31), (2.32), (2.33), and (2.34) are satisfied.

2.6 Counterfactual Equilibrium

In order to compute counterfactual changes in equilibrium variables, we use the "exact-hat algebra" approach pioneered by Dekle, Eaton, and Kortum (2007). For any variable with benchmark value of z and counterfactual value of z^*, define $\hat{z} \equiv z^*/z$. Then the counterfactual changes can be computed by solving the following system of equations:

$$\hat{w}_j^C = \hat{A}_j^{\frac{1}{\alpha_C}} \hat{q}_j^{-\frac{1-\alpha_C}{\alpha_C}}, \tag{2.35}$$

$$\hat{w}_{ij}^T = \left(\hat{v} \hat{A}_j \right)^{\frac{1}{\alpha_T}} \hat{q}_i^{-\frac{1-\alpha_T}{\alpha_T}}, \tag{2.36}$$

$$\hat{w}_{ij}(\theta) w_{ij}(\theta) = \theta \hat{w}_j^C w_j^C + (1-\theta) \hat{w}_{ij}^T w_{ij}^T, \tag{2.37}$$

[7] We do not include spatial spillovers of productivity and amenities between adjacent locations. These spillovers are highly localized, as found in Ahlfeldt, Redding, Sturm, and Wolf (2015) and several other studies. Given the size of locations in our quantitative economy, the effect of the spillovers is minimal. For example, the 1st percentile of one-way travel times for location pairs with positive commuting flows is 10.63 minutes (the minimum is 7.68 and the median is 26.56). With spillover decay parameters from Ahlfeldt, Redding, Sturm, and Wolf (2015), $\delta = 0.36$ and $\rho = 0.76$, only a fraction $e^{-\delta t_{ij}} = e^{-0.36 \times 10.63} = 0.0218$ of the density in one of these locations would be translated into local productivity of another location and a fraction $e^{-\rho t_{ij}} = e^{-0.76 \times 10.63} = 0.0003$ of the density would be translated into amenities.

[8] It is also possible that remote workers, by spending more time in the area of their residence, contribute more to local amenities than commuters.

Covid Economics 61, 11 December 2020: 172-221

$$\hat{q}_i = \left(\frac{\hat{l}_i}{\hat{\phi}_i}\right)^{\eta_i}, \tag{2.38}$$

$$\hat{\pi}_{ij}(\theta) = \frac{\left(\hat{X}_i \hat{E}_j \hat{b}_{ij} \hat{w}_{ij}(\theta)\right)^{\epsilon} \left(\hat{d}_{ij}(\theta)\hat{q}_i^{\gamma}\right)^{-\epsilon}}{\sum_{r \in \mathcal{I}} \sum_{s \in \mathcal{I}} \pi_{rs}(\theta) \left(\hat{X}_r \hat{E}_s \hat{b}_{rs} \hat{w}_{rs}(\theta)\right)^{\epsilon} \left(\hat{d}_{rs}(\theta)\hat{q}_r^{\gamma}\right)^{-\epsilon}}, \tag{2.39}$$

$$\hat{N}_{ij}^C N_{ij}^C = \int \theta \hat{\pi}_{ij}(\theta) \pi_{ij}(\theta) \mathrm{d}F^*(\theta), \tag{2.40}$$

$$\hat{N}_{ij}^T N_{ij}^T = \int (1-\theta) \hat{\pi}_{ij}(\theta) \pi_{ij}(\theta) \mathrm{d}F^*(\theta), \tag{2.41}$$

$$\hat{l}_i = \frac{\frac{1-\alpha_C}{\alpha_C} \hat{w}_i^C w_i^C \sum_{j \in \mathcal{I}} \hat{N}_{ji}^C N_{ji}^C + \gamma \sum_{j \in \mathcal{I}} \hat{w}_j^C w_j^C \hat{N}_{ij}^C N_{ij}^C + \left(\gamma + \frac{1-\alpha_T}{\alpha_T}\right) \sum_{j \in \mathcal{I}} \hat{w}_{ij}^T w_{ij}^T \hat{N}_{ij}^T N_{ij}^T}{\frac{1-\alpha_C}{\alpha_C} w_i^C \sum_{j \in \mathcal{I}} N_{ji}^C + \gamma \sum_{j \in \mathcal{I}} w_j^C N_{ij}^C + \left(\gamma + \frac{1-\alpha_T}{\alpha_T}\right) \sum_{j \in \mathcal{I}} w_{ij}^T N_{ij}^T}, \tag{2.42}$$

$$\hat{A}_j = \hat{a}_j \left(\frac{\hat{N}_{Wj}^C N_{Wj}^C + \psi \hat{N}_{Wj}^T N_{Wj}^T}{N_{Wj}^C + \psi N_{Wj}^T}\right)^{\lambda}, \tag{2.43}$$

$$\hat{X}_i = \hat{x}_i \left(\hat{N}_{Ri}\right)^{\chi}. \tag{2.44}$$

In equations (2.40) and (2.41), $F^*(\theta)$ denotes the counterfactual c.d.f. of θ.[9] In the last two equations, the changes in relevant workplace and residential employment are given by

$$\hat{N}_{Wj}^m N_{Wj}^m = \sum_{i \in \mathcal{I}} \hat{N}_{ij}^m N_{ij}^m, \tag{2.45}$$

for $m \in \{C, T\}$, and

$$\hat{N}_{Ri} N_{Ri} = \sum_{j \in \mathcal{I}} \left(\hat{N}_{ij}^C N_{ij}^C + \hat{N}_{ij}^T N_{ij}^T\right). \tag{2.46}$$

In order to solve the system (2.35)–(2.44), we must have data on commuting flows, $\pi_{ij}(\theta)$, wages w_i^C and w_{ij}^T, and the distribution of commuter types, $F(\theta)$. Section 3.1 describes how we obtain this data. We must also know the economy-wide elasticities, ϵ, γ, α_C, α_T, λ, and χ, as well as local floorspace supply elasticities η_i. Section 3.2 describes how we calibrate or estimate these parameters. Notably, solving the system (2.35)–(2.44) does not require any knowledge of the levels of exogenous location characteristics a_i, x_i, E_i, b_{ij}, ϕ_i, commuting costs, $d_{ij}(\theta)$, the relative productivity of telecommuters, ν, floorspace prices q_i, and buildable land areas Λ_i. This system can be solved recursively and we follow a procedure similar to the one in Monte, Redding, and Rossi-Hansberg (2018).

[9] We do not use the hat-algebra notation for F in order to allow that $F(\theta) = 0$ and $F^*(\theta) > 0$ for some θ.

Covid Economics 61, 11 December 2020: 172-221

Counterfactual Welfare Changes. The counterfactual change in the consumption-equivalent welfare is given by

$$\widehat{V} = \frac{\int \hat{w}_{ij}(\theta) w_{ij}(\theta) \left(\hat{\pi}_{ij}(\theta)\pi_{ij}(\theta)\right)^{-\frac{1}{\epsilon}} \left(\hat{d}_{ij}(\theta) d_{ij}(\theta)\right)^{-1} \mathrm{d}F^*(\theta)}{\int w_{ij}(\theta)\pi_{ij}(\theta)^{-\frac{1}{\epsilon}} d_{ij}(\theta)^{-1} \mathrm{d}F(\theta)}. \tag{2.47}$$

Note that the previous expression yields the same value of $\widehat{V}$ for any pair (i, j). While we can compute counterfactual changes in all equilibrium variables without knowing commuting costs, $d_{ij}(\theta)$, we need to know them to compute counterfactual changes in welfare.[10] Appendix A.1 discusses how counterfactual welfare changes can be calculated for each type θ separately and decomposed into various channels (consumption, amenities, commuting, etc.).

3 Data, Calibration, and Estimation

3.1 Data

3.1.1 Locations

The set of model locations is the intersection of the Census Public Use Microdata Areas (PUMA) and counties. The benefit of using PUMAs is that they are defined based on population and therefore allow for rich variation within large urban areas. However, in rural areas PUMAs may be very large and comprise several counties.[11] Using PUMAs, when they are contained within a county, and counties, when they are contained within PUMAs, results in 4,504 locations. Two of these locations do not have wage data.[12] Hence, we exclude them from the analysis and end up with 4,502 model locations.

3.1.2 Employment, commuters and telecommuters

We use the LEHD Origin-Destination Employment Statistics (LODES) data provided by the Census Bureau to construct employment by residence and workplace for each of our model locations. We also use LODES to build the commuting matrix between each pair of locations, as discussed in Section 3.2.3. LODES provides employment and commuting

[10] In many gravity models, exact-hat algebra enables expressions for welfare changes which only depend on changes. Here, however, counterfactual changes are driven by a shift in $F(\theta)$. Hence, welfare gains depend on the change in the number of workers who face commuting costs for a particular θ.

[11] By construction, PUMAs are between 100,000 and 200,000 residents.

[12] These two locations have a total population of only 8,000.

Covid Economics 61, 11 December 2020: 172-221

flows at the level of Census blocks, and we aggregate the data to the level of our model locations, i.e., PUMAs and counties. This data, however, does not distinguish workers who commute to work from those who work from home. We use survey evidence from Barrero, Bloom, and Davis (2020) to build the distribution of commuter types $F(\theta)$ before Covid-19 and the predicted distribution after Covid-19, as described in Section 4.1.

3.1.3 Commuting times and distances

The Census Transportation Planning Products (CTPP) reports commuting time data for origin-destination pairs of Census tracts across the contiguous United States for 2012–2016. Travel times are reported for over four million trajectories, which is a small fraction of all possible bilateral trajectories, because most pairs of tracts are far enough apart and do not have any commuters traveling between them. We transform this data into bilateral matrix of travel times in two steps. First, we calculate the average location to location travel times as the average of all tract-level travel times reported in the data where the origin is in one model location and the destination is in the other. This provides us with links for the subset of location pairs that are closest to each other.[13] Then we use these links as the first-order connections in a transport network, and use the Dijkstra's algorithm to calculate the quickest path through this network between each pair of model locations. Further details of our methodology are contained in Appendix A.3.

3.1.4 Wages

Our tract-level wage estimates are also taken from the database of Census Transportation Planning Products (CTPP), in combination with the microdata from the American Community Survey (ACS). We use these two datasets from 2012–2016 to calculate the quality-adjusted wage index for each model location. For additional details, see Appendix A.2.

Existing empirical evidence finds a wage premium of around 10% for telecommuters over regular commuters (Gariety and Scaffer, 2007). Yet, it is not clear if this premium will persist if many more workers telecommute. In addition, our data does not allow us to observe the location of employer of a telecommuter. To be conservative, in the benchmark economy we set $w_{ij}^T = w_j^C$ for all i, where w_j^C equals the wage index described above.

[13] We perform the same calculation for the average distance of each location *from itself*, thereby obtaining data-based estimates of the average internal travel time for each location as well.

Covid Economics 61, 11 December 2020: 172-221

Covid Economics 61, 11 December 2020: 172-221

3.1.5 Floorspace supply elasticities and prices

Location-specific housing supply elasticities, $(1 - \eta_i)/\eta_i$, are taken from Baum-Snow and Han (2020). They estimate elasticities of floorspace supply with respect to prices at the Census tract level for over 300 metropolitan areas. We aggregate their estimates to the level of our model locations using population weights. They do not have estimates for locations outside MSAs and these are predominantly rural locations with population densities lower than in metro areas. Because there is a strong negative relationship between population density and the supply elasticity, we assume that locations with missing estimates have the same elasticity as the location with the highest elasticity. At the level of model locations, elasticities vary from 2.07 to 4.82, and the population-weighted mean is 3.38. This implies that η_i ranges from 0.21 to 0.33, and the mean is 0.24.[14]

Note that our method of computing counterfactual changes in equilibrium variables and welfare does not require any information on floorspace prices. Yet, in order to calculate changes in prices at higher levels of geography than our model locations (e.g., metropolitan area or the entire country), we need to know price levels in the benchmark economy. To obtain the prices, we estimate hedonic rent indices for each PUMA using self-reported housing rents from the ACS. We follow the procedure in Eeckhout, Pinheiro, and Schmidheiny (2014) and, as regression controls, we include the age of the building, the number of rooms, and the type of the structure (single-family, multi-family, etc.).

3.2 Estimation and Calibration

3.2.1 Externally calibrated parameters

Using similar gravity models of commuting, Ahlfeldt, Redding, Sturm, and Wolf (2015) estimate that the sensitivity of the disutility of commuting to commuting time, κ, is equal to 0.01, while Tsivanidis (2019) estimates a value of 0.012. We set $\kappa = 0.011$, the average of these two estimates. We borrow the estimates of the elasticities of local productivity and amenities with respect to density from Heblich, Redding, and Sturm (2020), and set $\lambda = 0.086$ and $\chi = 0.172$.[15]

The share of housing in expenditures, γ, is equal to 0.24, following Davis and Ortalo-Magné (2011). The labor share of commuters in the production function, α, is set to 0.8, following Valentinyi and Herrendorf (2008). We borrow the value for the labor share of

[14]Recall that in our model η_i also corresponds to the land share in the production function for floorspace. Hence, the mean η_i in our model aligns well with existing estimates of the land share. For instance, Albouy and Ehrlich (2018) find that the land share is about 1/3 for the U.S., while Combes, Duranton, and Gobillon (2019) estimate a value of about 0.2 for France.

[15]In a future version of this paper we will estimate these two elasticities from our data.

telecommuters, $\alpha_T = 0.934$, from Delventhal, Kwon, and Parkhomenko (2020).[16] Due to the lack of empirical evidence and appropriate calibration targets, we do not take a stance on the relative contribution of remote workers to productive externalities, ψ. Instead, we will consider counterfactual scenarios with $\psi = 0$ and $\psi = 1$.

3.2.2 Estimated parameters

Estimate ϵ. First, we estimate the product $\epsilon\kappa$ following the approach in Heblich, Redding, and Sturm (2020). To do this, we take the log of the gravity equation (2.6) evaluated at $\theta = 1$,

$$\ln \pi_{ij} = -\epsilon\kappa t_{ij} + \varphi_i^R + \varphi_j^W + \ln b_{ij}, \tag{3.1}$$

where the location-specific fixed effects φ_i^R and φ_j^W subsume local amenities, wages, and floorspace prices. Before estimating this equation, we set $\pi_{ij} = 0$ for all pairs with commuting times of more than 3 hours one way.[17]

We first estimate the previous equation by OLS and obtain $\epsilon\kappa = 0.03199$ (Table 1 reports regression results). However, t_{ij} may be endogenous to π_{ij} due to traffic congestion or because the supply of infrastructure responds to commuting demand.[18] Hence, we instrument for t_{ij} with straight-line distance between i and j, δ_{ij}, and obtain $\epsilon\kappa = 0.03409$. To recover the Frèchet shape parameter ϵ we use the calibrated value $\kappa = 0.011$, as discussed above. Our estimate of ϵ is therefore equal to $3.099 = 0.03409/0.011$.[19]

[16]Since α_T determines the teleworkers' demand for floorspace, it was calibrated to the observed difference between house sizes of commuters and telecommuters. See Delventhal, Kwon, and Parkhomenko (2020) for details.

[17]Out of around 139 mln commuters that we observe in LODES, 9.8 mln travel between locations that are more than 3 hours apart. We believe that most of these observations are due to errors in assigning locations of work or residence, and therefore drop them from our sample.

[18]See Heblich, Redding, and Sturm (2020) for a more detailed discussion.

[19]Our value of ϵ is on the lower end of the range of estimates in the literature. Monte, Redding, and Rossi-Hansberg (2018) estimate 3.3, Heblich, Redding, and Sturm (2020) find a value of 5.25, and Ahlfeldt, Redding, Sturm, and Wolf (2015) estimate 6.65.

Covid Economics 61, 11 December 2020: 172-221

Table 1: Estimation of the gravity equation

	(1) OLS	(2) IV
Second stage		
t_{ij}	-0.03199	-0.03409
	(0.000046)	(0.000050)
Residence f.e.	yes	yes
Workplace f.e.	yes	yes
Observations	318,870	318,870
R^2	0.792	–
First stage		
δ_{ij}		0.8970
		(0.000018)
Residence f.e.		yes
Workplace f.e.		yes
Observations		318,870
R^2		0.996

Note: This table reports estimates of equation (3.1). Standard errors are in parentheses. See the text for details.

Estimate b_{ij}. Notice that the location pair-specific shifter, b_{ij}, can be identified from the residual in equation (3.1). However, since the estimation procedure only uses location pairs with positive commuting flows, we cannot infer the value of b_{ij} for pairs with zero flows. In this class of models, it is common to set $b_{ij} = 0$ for zero-flow pairs.[20] However, our counterfactual experiments study environments in which many more individuals gain the ability to work remotely and may choose residence-workplace location pairs that have not been chosen in the benchmark economy.

In order to resolve this problem, we specify b_{ij} as a function of straight-line distance between i and j,

$$\ln b_{ij} = \beta_0 + \beta_1 \ln \delta_{ij}, \tag{3.2}$$

and estimate this relationship on the sample of pairs with positive flows. Our hypothesis is that, even though many location pairs have zero commuters due to the high commuting costs, they would have positive number of commuters if the costs were lower and that the flows between such locations depend on the distance between them. Table 2 reports the regression results. We find that the there is a statistically significant negative relationship between b_{ij} and δ_{ij}, albeit the distances do not explain much of the variation in the pair-

[20] As, for example, in Monte, Redding, and Rossi-Hansberg (2018) or Heblich, Redding, and Sturm (2020). Dingel and Tintelnot (2020) show that dropping pairs with zero flows may bias the estimates of the Frèchet shape parameter.

specific shifter. Table 3 provides summary statistics of the estimated values of b_{ij} for pairs with zero flows in the data and shows that b_{ij} varies from around 0.5 to 1.2.

Table 2: Relationship between the pair-specific shifter, b_{ij}, and distance

Dependent variable:	$\ln b_{ij}$
$\ln \delta_{ij}$	-0.1671
	(0.0027)
Observations	318,629
R^2	0.012

Note: This table reports estimates of equation (3.2). Standard errors are in parentheses.

Table 3: Summary statistics of the pair-specific commuting flow shifter, b_{ij}

	Mean	S.d.	Min	Max	Observations
b_{ij}	0.6339	0.0732	0.5109	1.2260	19,949,134

Note: This table reports summary statistics of b_{ij} as predicted by the estimated relationship (3.2).

3.2.3 Commuting flow matrix

The benchmark economy consists of both commuters and telecommuters, however we cannot tell them apart in the LODES data. Hence, we resort to our model and use the estimated equation (3.1) in order to construct commuting flow matrices for each θ.[21] Because the gravity equation was estimated at $\theta = 1$ and because b_{ij} are derived from regression residuals, our model will match the observed bilateral flows of commuters nearly exactly. However, since $b_{ij} > 0$ for all pairs with zero observed flows, our model will have positive, even if negligible, flows between each pair of locations. Figure A.8 shows the relationship between commuting flows in the model and the data for $\theta = 1$. Panel (a) demonstrates that the data and the model match up nearly exactly for pairs with positive flows in the data. Yet, as panel (b) shows, zooming into the lower left corner of the scatter plot, one can see that there are small positive flows in the model between locations with zero flows in the data. These flows are negligible–their total volume corresponds to 0.6% of total employment in the economy, even though they account for 98.4% of all location pairs.

[21] Dingel and Tintelnot (2020) also suggest using a model-based commuting matrix to run counterfactuals in settings when there are many zero-flow location pairs in the data.

Covid Economics 61, 11 December 2020: 172-221

4 Implications of an Increase in Telecommuting

In this section, we study a simulated increase in the number of telecommuters and its effect on the location of residents and jobs, floorspace prices, wages, commuting costs, and welfare.

4.1 The Counterfactual Experiment

The counterfactual experiment consists of changing the distribution of commuter types from $F(\theta)$ to $F^*(\theta)$, as shown in Figure 1, while keeping all other parameters at the benchmark level.[22] First, we study a counterfactual economy in which local productivity A_i and amenities X_i are fixed at the benchmark level, by setting $\lambda = \chi = 0$. This allows us to isolate the first-order effects of changing commuting requirements from the amplifications via endogenous productivity and amenities. Then, we turn "on" productive and amenity externalities, one by one, by restoring λ and χ to their calibrated levels and let these externalities affect the counterfactual changes. In all previous experiments, we set $\psi = 0$ in equation (2.34), i.e., we disallow remote workers to contribute to productive externalities. In the last two experiments, we let remote workers to fully contribute to productive externalities as if they were physically present in the office, by setting $\psi = 1$; we calculate results when amenities are exogenous, and again when they are endogenous.

Distribution of commuter types. We discretize the distribution of commuter types, $F(\theta)$, to six support points, $\theta \in \{0, 0.2, 0.4, 0.6, 0.8, 1\}$. We chose this support so that each value of θ can be interpreted as the number of days per week that an individual commutes to work. For example, a worker with $\theta = 0$ always works at home, a worker with $\theta = 0.2$ commutes one day a week, and a worker with $\theta = 1$ commutes five days a week.

In order to build empirical benchmark and counterfactual distributions of θ we turn to Barrero, Bloom, and Davis (2020). Using evidence from a survey of employers conducted in May 2020, they find that in 2019, 3.4% of employees worked at home 5 or more days a week, 2.9% did so 2–4 days, another 3.4% worked from home one day, and the remaining 90.3% rarely or never worked at home. Thus, in the benchmark economy, the probability distribution of commuter types is $f = (0.034, 0.01, 0.01, 0.01, 0.034, 0.903)$, where we split the 2.9% who worked at home 2–4 days a week equally between 2, 3, and 4 days. The survey also asks about plans of employers after Covid-19 as to how often their employees would work at home and on-site. They find that 10.3% will work at home 5 or more days

[22] When we solve the system of counterfactual changes (2.35)–(2.44), $\hat{a}_i$, $\hat{x}_i$, $\hat{E}_i$, $\hat{b}_{ij}$, $\hat{\phi}_i$, $\hat{v}$, and $\hat{d}_{ij}(\theta)$ are all equal to 1 for all locations i and j and types θ.

Covid Economics 61, 11 December 2020: 172-221

a week, 9.9% will do so 2–4 days a week, 6.9% will work from home one day a week, and only 73% will rarely or never work at home. Therefore, the counterfactual distribution is $f^* = (0.103, 0.033, 0.033, 0.033, 0.069, 0.73)$. This shift in the distribution implies that in the counterfactual economy 17.6% of work days will be done from home, a more than a threefold increase compared to 5.8% in the benchmark.[23] Figure 2 demonstrates the benchmark and the counterfactual distributions of commuter types.

Figure 2: Change in the distribution of commuting frequency

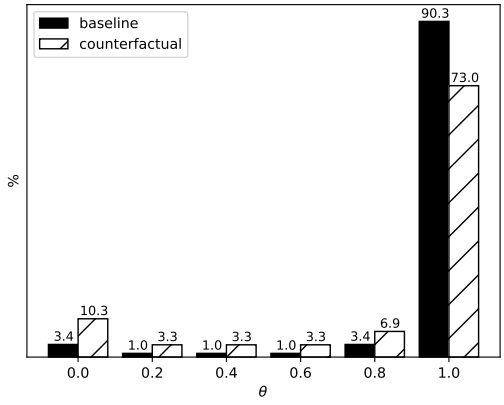

4.2 Results

When more workers gain the ability to commute less frequently or not at all and when there are no agglomeration effects in productivity or amenities, two immediate effects occur. First, the importance of distance between employers and employees weakens, and workers who experience a fall in θ relocate further from their jobs.[24] Second, as the supply of on-site labor falls and the supply of remote labor increases, the demand for commercial real estate plummets and the demand for residential real estate goes up. The rest of the section describes how these two basic mechanisms change residential and employment density, floorspace prices, wages, and discusses welfare implications of more widespread

[23] $\sum_{\theta\in\{0,\ldots,1\}}(1-\theta)f(\theta) = 0.058$ and $\sum_{\theta\in\{0,\ldots,1\}}(1-\theta)f^*(\theta) = 0.176$. The latter number is less than half of 0.37 which, according Dingel and Neiman (2020), is the fraction of jobs in the United States that can be done at home. It reasonable to expect, however, that employers and employees may prefer to conduct a significant amount of work on-site even when it can feasibly be done from home.

[24] For example, the benchmark economy has few commuters from San Diego to Los Angeles, CA. These cities are 120 miles apart and a one-way commute takes about 3 hours, either by car or train. In the counterfactual economy, there is a 149% jump in the number of weekly commuter trips from locations in San Diego county to Downtown L.A., largely driven by those who commute once or twice a week.

Covid Economics 61, 11 December 2020: 172-221

telecommuting. We conclude the section by discussing the importance of agglomeration externalities and the contribution of teleworkers to productive externalities for our results.

4.2.1 Residential density

More telework leads to the increased sprawl of residents who leave dense and expensive urban cores for less dense suburbs and rural areas, as panel (a) in Figure 3 shows. The map in panel (a) of Figure 9 confirms that most locations that gain density are located in suburban and rural areas, while locations that lose density are primarily in urban areas.[25]

Does this mean that telecommuting will create a massive exodus from cities to rural areas? Panel (b) of Figure 9 demonstrates that even though many rural and suburban locations experience a large *percentage* increase in residents, in the vast majority of them the *absolute* changes in density are small. We find that most people will keep living in cities–the fraction of workers that reside in the 397 largest MSAs only declines from 85.9% in the benchmark to 84.6% in the counterfactual.[26] Moreover, as panel (b) of Figure 3 shows, not all large metro areas shrink: Los Angeles, as well as the neighboring Riverside-San Bernardino and San Diego grow larger.

A closer look at the two largest metro areas, New York and Los Angeles, unveils a rich pattern of reallocations. In Los Angeles (panels (c) and (e) of Figure 9), the crescent between Santa Monica and Downtown loses residents. This area is characterized by proximity to jobs and sky-high real estate prices. As it becomes less important to be close to jobs, people move to more affordable suburbs in San Fernando Valley, San Bernardino County, and Orange County. In contrast, most areas in the New York metro area (panels (d) and (f) of Figure 9) lose residents. The biggest reductions occur in Manhattan and adjacent parts of Brooklyn and Queens, while parts of the Bronx and the Staten Island, as well as some far-flung suburbs attract new residents.

[25] In accordance with these results, Althoff, Eckert, Ganapati, and Walsh (2020) find that in the few months after the beginning of the COVID-19 pandemic there was a sizable reallocation of residents from the densest to the least dense commuting zones in the U.S.

[26] We use Core-Based Statistical Areas (CBSAs) for our MSA-level results.

Covid Economics 61, 11 December 2020: 172-221

Figure 3: Change in Residents

Panel (a): model locations

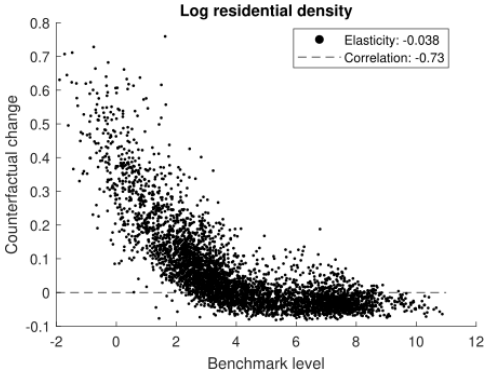

Panel (b): metropolitan areas

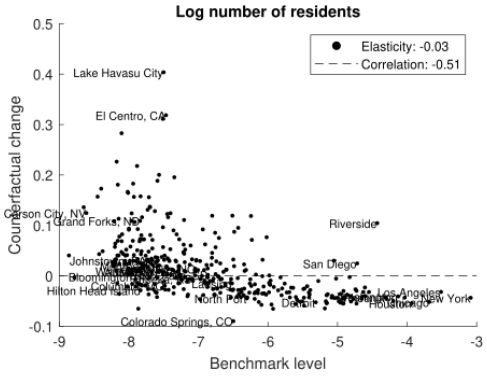

Note: These scatterplots show the relationship between the benchmark residential density and the counterfactual change in log density. Panel (a) shows this relationship for model locations, panel (b) shows this relationship for metropolitan areas. "Elasticity" is the coefficient of the OLS regression of the counterfactual change on the benchmark level.

4.2.2 Employment density

We find that telecommuting also results in the outflow of employment from high-density to low-density locations, albeit the effect is much weaker than for residents (panel (a) of Figure 4). In fact, as panel (b) in Figure 4 demonstrates, many of these reallocations occur within metropolitan areas, and there is virtually no relationship between the initial size of an MSA and the change in its employment. Indeed, some metro areas, such as New York and Washington, D.C., experience moderate increases in employment. The maps in Figure 10 confirm that in many urban locations employment grows.

How is it possible that some places lose residents and gain workers at the same time? This happens because a large portion of the increase in employment comes from telecommuters. With less frequent commutes, more workers combine the benefits of working in high-wage cities, such as Washington, D.C., and living in more affordable places nearby, such as Richmond, VA. Similarly, firms located in highly productive metro areas can increase their size by hiring more workers from distant places. Figure 5 focuses on five metropolitan areas and shows that areas which experience employment growth in the counterfactual do so thanks to a jump in the number of telecommuters, while on-site employment falls in all places shown in the figure. In addition, Table A.1 in

Covid Economics 61, 11 December 2020: 172-221

Covid Economics 61, 11 December 2020: 172-221

Appendix displays changes in jobs, residents, and floorspace prices for each of the 100 largest metropolitan areas.

Figure 4: Change in Employment

Panel (a): model locations

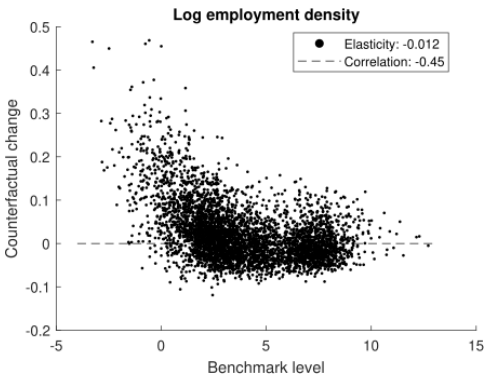

Panel (b): metropolitan areas

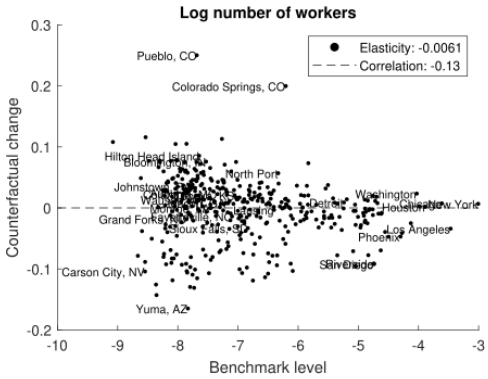

Note: These scatterplots show the relationship between the benchmark employment density and the counterfactual change in log density. Panel (a) shows this relationship for model locations, panel (b) shows this relationship for metropolitan areas. "Elasticity" is the coefficient of the OLS regression of the counterfactual change on the benchmark level.

Figure 5: Changes in total, on-site, and remote employment in selected metro areas

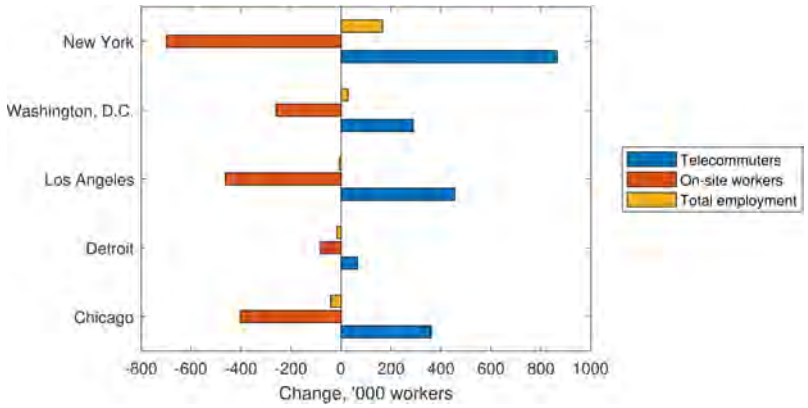

Note: This figure shows the counterfactual change in total, on-site, and remote employment in several metropolitan areas. Since a given worker can provide on-site and remote labor at the same time, these changes are converted from changes in total, on-site, and remote work days in each workplace location.

4.2.3 Floorspace prices

The rise of telecommuting reallocates the demand for floorspace across uses–commercial and residential–and across locations. In particular, as fewer workers spend time in offices, the stock of commercial real estate declines. At the same time, these workers require more residential floorspace to be able to work at home productively, and therefore the supply of residential real estate goes up. The rise in residential demand is further exacerbated by the migration of residents to suburban and rural areas where housing is cheaper and therefore large houses are more affordable.

We find that, on average, floorspace prices only fall by 2%. However, there are sizable differences in price changes across locations. As panel (a) in Figure 11 and panel (a) in Figure 6 show, many suburban and rural areas experience large increases in prices. This happens because some residents and employers relocate to these areas. However, as panels (b) and (c) in Figure 11 demonstrate, even within the largest cities, some locations see an increase in prices. While the densest places, such as Manhattan in New York and Downtown Los Angeles, become cheaper, several peripheral areas become more expensive.

The aggregate average fall in floorspace prices is due to the combination of two effects: First, residents move on average to less dense places, where in the benchmark economy prices were lower. Second, residents move on average to places with a higher elasticity of floorspace supply to price. To assess the importance of the second channel we run an alternative counterfactual exercise in which the elasticity of housing supply is uniform across space and equal to the population-weighted national average. Housing costs only fall by 1.82% in this alternative exercise, indicating that about 7% of the total fall in prices is due to reallocation to more flexible housing markets.

Even when many more workers can telecommute, large metropolitan areas remain attractive places to live and run businesses, and real estate there does not become dramatically cheaper (see panel (b) in Figure 6 and Table A.1 in Appendix).[27] Having said that, while telecommuting is unlikely to improve housing affordability in the "superstar" cities, it offers the opportunity for many workers to move to more affordable places while retaining their jobs in major economic hubs.

[27]These results contrast with Delventhal, Kwon, and Parkhomenko (2020) who find that floorspace prices in Los Angeles would fall by nearly 6% with more telecommuting. However, that paper models Los Angeles as a closed city and does not consider the possibility that residents and firms may move in and out of the city. In this paper, we allow such migration and find that, as more widespread telecommuting increases the population and employment in Los Angeles, floorspace prices only fall by 1%.

Covid Economics 61, 11 December 2020: 172-221

Figure 6: Floorspace prices

Panel (a): model locations

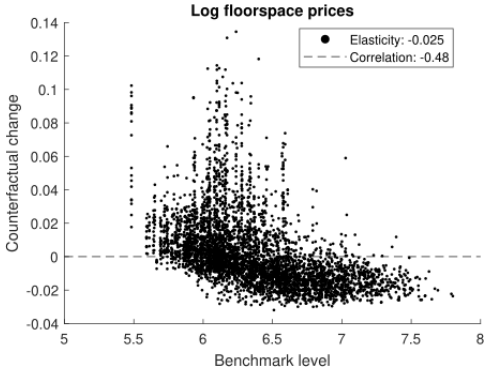

Panel (b): metropolitan areas

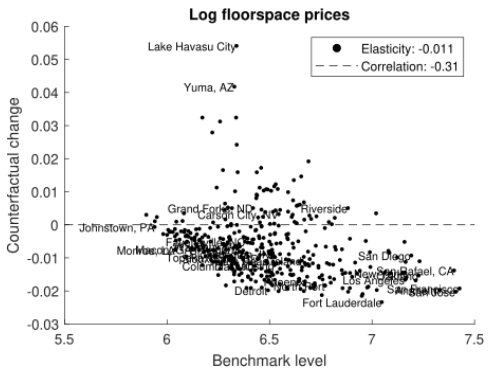

Note: These scatterplots show the relationship between the benchmark log floorspace prices and the counterfactual change in log floorspace prices. "Elasticity" is the coefficient of the OLS regression of the variable on the vertical axis on the variable on the horizontal axis.

4.2.4 Wages

One important effect of the rise in telecommuting is that it increases resident market access for many workers by lowering their commuting frequency. This implies that more individuals have access to the most productive locations and many of them switch from less productive jobs they held before. As a result, as panel (a) in Figure 7 demonstrates, telecommuting increases the dispersion of wages across model locations and also across metropolitan areas. These findings suggest that, even though remote work may bring greater employment opportunities to workers who do not currently live in the most successful local labor markets, it is unlikely to make the distribution of income more equal. However, since the importance of living close to jobs fades, the competition for expensive real estate in the most successful places becomes less intense and results in greater spatial mixing of people with different income levels. As panel (b) in Figure 7 shows, the dispersion of income at the place of residence declines.

Figure 7: Wages

Panel (a): model locations

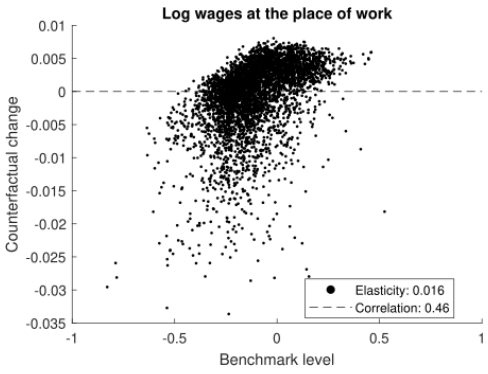

Panel (b): metropolitan areas

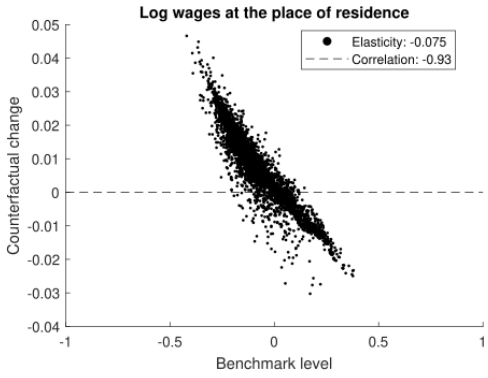

Note: Panel (a) show the relationship between the benchmark log wages of commuters at the place of work, w_j^C, and the counterfactual change in log wages. Panel (b) shows this relationship for wages at the place of residence, $\tilde{w}_i$. "Elasticity" is the coefficient of the OLS regression of the variable on the vertical axis on the variable on the horizontal axis.

4.2.5 Aggregate Results and Welfare Effects

We find that, by weakening the link between the place of work and the place of residence, a shift toward more telework results in modest wage gains, especially for telecommuters, and a slight reduction in real estate prices (column (1) in Table 4). Both of these effects result in a 0.8% larger aggregate consumption (column (1) in Table 5). Individuals further gain by spending less time on commuting (column (1) in Table 4 and column (1) in Table 5). In addition, as many workers commute to work less frequently or not at all, they can pick location pairs with better residential and workplace amenities, X_i and E_j (column (1) in Table 5).

Yet, most of the welfare gains can be attributed to better matches between firms and workers, as measured by the value of the Frèchet preference shock. Because a commuter must reside close to her job and because the distribution of preference shocks is i.i.d. across pairs of locations, it is unlikely that she would be able to choose a pair of locations i and j with a high value of z_{ijn}. A telecommuter places a lesser importance on the disutility of commuting and can therefore choose a pair with a higher value of z_{ijn}. We find that gains from greater consumption, less commuting, and better access to amenities increase aggregate welfare by almost 5%, however, better access to location pairs with higher values

CEPR PRESS

of preference shocks further increases aggregate welfare gains to nearly 35%.

These welfare gains took into account those workers who experienced a decrease in θ, i.e., switched from more to less commuting. What are the welfare effects on workers who did not change their commuting frequency in the counterfactual? Column (1) in Table 5 lists welfare gains for workers with each θ and demonstrates that welfare gains are larger for those who commute more frequently. Commuters experience an increase in wages and a fall in housing costs. In addition, as the demand for living close to places with good employment opportunities recedes, commuters gain from being able to pick residence locations with shorter commutes and better amenities. At the same time, full-time remote workers experience a slight reduction in expected utility. The main reason for that is that in the benchmark economy telecommuters tended to live in less dense areas with cheap housing. As the number of telecommuters grows, these areas experience a surge in housing demand and increasing floorspace prices, thereby harming those telecommuters who lived there before.

Table 4: Aggregate results

Productive externalities ($\lambda > 0$):	no	no	yes	yes	yes	yes
Amenity externalities ($\chi > 0$):	no	yes	no	yes	no	yes
Remote labor adds to productive externalities ($\psi = 1$):	no	no	no	no	yes	yes
	(1)	(2)	(3)	(4)	(5)	(6)
Wages, all workers, % chg	0.28	0.17	-0.98	-1.14	0.29	0.11
Wages, on-site labor, % chg	0.47	0.36	-0.82	-0.99	0.45	0.26
Wages, remote labor, % chg	0.09	-0.01	-1.08	-1.21	0.24	0.10
Floorspace prices, % chg	-1.95	-2.69	-2.15	-3.02	-1.96	-2.90
Time spent commuting, all workers, % chg	-7.04	-6.44	-7.00	-6.34	-6.90	-6.20
Time spent commuting, commuters ($\theta = 1$), % chg	-0.13	0.44	-0.09	0.53	0.01	0.67
Distance traveled, all workers, % chg	-6.42	-5.06	-6.49	-4.88	-6.27	-4.57
Distance traveled, commuters ($\theta = 1$), % chg	-0.46	0.92	-0.54	1.12	-0.31	1.43

Note: Columns (1)–(6) present results from models with different combinations of productive and amenity externalities, and whether remote labor contributes to productive externalities, as specified in the header of the table.

Covid Economics 61, 11 December 2020: 172-221

Table 5: Welfare Decomposition

Productive externalities ($\lambda > 0$):	no	no	yes	yes	yes	yes
Amenity externalities ($\chi > 0$):	no	yes	no	yes	no	yes
Remote labor adds to productive externalities ($\psi = 1$):	no	no	no	no	yes	yes
	(1)	(2)	(3)	(4)	(5)	(6)
Welfare by source, % chg						
consumption only	0.81	0.86	-0.42	-0.38	0.82	0.87
+ commuting	4.01	3.90	2.73	2.59	3.98	3.83
+ amenities	4.90	5.26	3.66	4.09	5.00	5.50
+ Frèchet shocks	34.92	35.84	33.28	34.31	35.05	36.13
Welfare by commuter type, % chg						
$\theta = 0$	-0.05	1.69	-1.19	0.72	0.20	2.20
$\theta = 0.2$	0.21	0.76	-0.95	-0.31	0.32	1.00
$\theta = 0.4$	0.33	0.56	-0.86	-0.57	0.39	0.69
$\theta = 0.6$	0.43	0.48	-0.80	-0.71	0.44	0.53
$\theta = 0.8$	0.51	0.45	-0.75	-0.79	0.50	0.45
$\theta = 1$	0.57	0.46	-0.72	-0.82	0.55	0.44

Note: Columns (1)–(6) present results from models with different combinations of productive and amenity externalities, and whether remote labor contributes to productive externalities, as specified in the header of the table. Appendix A.1 provides more details on welfare results by type and source.

4.2.6 Role of Agglomeration Externalities

Next, we consider what would happen if local productivity, A_j, and amenities, X_i, adjusted endogenously to changes in employment and residential density (see equations 2.33 and 2.34). In the context of these counterfactual exercises, it is important that workers only contribute to agglomeration externalities when they are on-site ($\psi = 0$): a one-day-per-week commuter only contributes to these externalities one fifth as much, and a full-time telecommuter does not contribute at all. As a result, even if no workers changed their residences or jobs, more telework would result in lower aggregate productivity. Yet, when the productivity in a given location falls, wages fall as well making some workers seek employment elsewhere and therefore amplifying the initial reduction in productivity. Similarly, when some individuals move to suburban or rural areas from dense urban locations, amenities in these places decline and, as a result, even more residents leave. Figures (A.1)–(A.7) in the Appendix repeat Figures (3)–(11) and show that all of the effects described in Sections 4.2.1–4.2.4 are stronger when the agglomeration externalities are present. There is more reallocation of residents and jobs toward less dense places, greater convergence in floorspace prices, and larger divergence in wages.

Covid Economics 61, 11 December 2020: 172-221

The changes in density and prices with agglomeration externalities do not bring any real quantitative surprises–almost all the same locations and variables see changes in the same direction as before, the changes are just bigger. In terms of welfare, however, we find that the picture is now completely changed. Tables 4 and 5 show this change in steps. Column (1) of each table corresponds to the baseline counterfactual, when endogeniety for both amenities and productivity is turned "off." Column (2) shows the effect of turning "on" endogeneity only for amenities. Column (3) shows the effect of turning endogeneity "on" only for productivity. Finally, column (4) shows the effect of turning endogeneity "on" for both at once.

Endogenous amenities. When only amenities are endogenous, the reduction in distance traveled and time spent commuting for commuters, is reversed. This is because telecommuters bring amenities out to the periphery with them when they move, and commuters are thus induced to follow them, and accept longer commutes in exchange for better residential amenities. The small increases in wages for all categories of workers are attenuated because the migration of commuters to higher-productivity tracts is thus less pronounced and because increased demand for floorspace in the periphery induces telecommuters to slightly reduce the sizes of their home offices and, thus, their productivity. In terms of welfare, commuters still experience some gains but the gradient in welfare gains is now reversed–now telecommuters benefit most, because they take the amenities with them. Overall welfare gains are still positive due to the increase in at-home work days for most workers.

Endogenous amenities also considerably increase the role of the relocation of residents to places with more elastic housing supply in accounting for the reduction in floorspace prices. In an alternative exercise in which only amenities are endogenous but the floorspace supply elasticity takes the average value everywhere, floorspace prices fall by only 2.43%. This indicates that nearly 10% of the total reduction is due to the improvement in the average housing supply elasticity, as compared to 7% in the "basic" counterfactual in column (1).

Endogenous productivity. When only productivity is endogenous, small gains in wages turn into a nearly 1% drop. This is because telecommuters no longer contribute to externalities when working remotely, reducing the productivity especially of those work locations which are most accessible to commuters. The effect on commuting times and distances barely changes compared to the baseline counterfactual. In terms of welfare, each category individually now suffers losses between 0.7% and 1.2%, with reductions

Covid Economics 61, 11 December 2020: 172-221

larger for telecommuters than commuters. Overall welfare gains are negative when only accounting for consumption, because wages and overall productivity are now lower. Once commuting and amenities are taken into account, the overall welfare effect is positive, due to the reallocation of workers from commuting to telecommuting, which offers reduced time on the road and a freer choice of residence.

Endogenous amenities and productivity. When both amenities and productivity are endogenous, wages fall further and commute times and distances traveled by commuters go up. Average floorspace prices fall by over 3%, more than in the baseline scenario or either of the "piecemeal" scenarios, which helps to offset the consumption cost of lower wages. Everyone now earns less, but they have access to more affordable housing on average. When accounting for consumption, commuting disutility, and amenities together, the overall increase in welfare is now only 4.1%. This increase is due entirely to an improved situation for the lucky commuters who can now work from home. Commuters who are "stuck" working on-site full-time see their welfare fall by 0.8%.

One way to think about the counterfactual results with agglomeration effects, is that they give us a peek at what could happen in the long run. In the short and medium run, the levels of productivity and amenities may not change much even if many more people telecommute. Co-workers can still connect via Zoom, while restaurants or schools may remain open at the same capacity levels. In the long run, however, a permanent reduction in face-to-face interactions and a fall in the demand for living and working in dense urban places, may result in a permanent blow to productivity and a reallocation of neighborhood amenities.

4.2.7 Telecommuters' contribution to workplace externalities

But what if future advances allow telecommuters to participate in all work-related activities just as efficiently as they would in person? In the preceding discussion, we have only considered scenarios in which remote workers do not contribute at all to productive externalities which, in terms of our model, means setting $\psi = 0$.

One alternative is to make the opposite extreme assumption, and set $\psi = 1$. Column (5) in Tables 4 and 5 shows the results when $\psi = 1$ and only productivity externalities are turned "on." Column (6) in each table shows the results when amenity externalities are "on" also. The contrast between columns (4) and (6) is striking. Allowing telecommuters to contribute to local productivity externalities reverses most of the negative effects of the increase in telecommuting which showed up in columns (3) and (4) when we turned endogenous productivity "on." Instead of falling, wages now rise modestly. Instead

Covid Economics 61, 11 December 2020: 172-221

of disadvantaging left-behind commuters, this group now benefits considerably, their expected utility increasing by 0.44%. The reduction in real estate prices, combined with the rise in wages allows a larger gain in average consumption welfare than in any of the other scenarios.

In other ways, the results for columns (4) and (6) are similar. Just as was the case when telecommuters did not contribute to externalities, full commuters end up travelling farther and spending more time on the road. The motivations are the same: an increase in the relative wage advantage of jobs in the city centers, and an increase in the amenities of farther-flung suburbs. When telecommuters improve productivity, too, the city center wage advantage is made bigger, hence larger changes in average commute time and distance.[28]

As ψ changes from 0 to 1, all of the aggregate results shown in Tables 4 and 5 transition smoothly from column (4) to column (6).[29] Figure 8 shows this transition for average wages, for consumption utility, and for the utility of left-behind commuters. These are three aggregate outcomes for which, if telecommuters make no contribution to production externalities, the effect of increased telecommuting is negative. Varying ψ between 0 and 1 suggests another way to think about its importance: What would the contribution of telecommuters to externalities have to be in order to turn these negative results positive?

Average consumption utility is the first to turn positive as ψ increases: if remote workers contribute 30% as much to workplace spillovers as on-site workers, that is enough for the utility derived from consumption of goods and housing, averaged across all types of workers in the economy, to increase. The next to turn is overall utility for left-behind full-time commuters. If telecommuters contribute to workplace spillovers 60% as much as their on-site colleagues, this is enough to erase the losses suffered by every-day commuters. The hardest nut to crack, so to speak, is the average wage. For the counterfactual increase in telecommuting we consider, the average wage will go down unless remote labor contributes fully 90% as much as local labor to productive externalities.

Is it likely that the "true" value of ψ could be as high as 0.3, or 0.6, or 0.9? There is

[28]The direction and size of the change in aggregate commuting is almost exactly the same if we compare columns (3) and (5), when endogenous amenities are absent. Therefore, the difference between (3) and (5), or (4) and (6), give an estimate of the importance of telecommuters' productivity contribution in drawing workers into city centers. In contrast, the change in commuting variables between columns (5) and (6) highlights the considerably larger role of endogenous amenities in the suburbs of promoting long commutes. The fact that the change from (3) to (4) is also nearly the same as the change from (5) to (6) indicates that the two influences on commuting–that of endogenous amenities and that of improved center-city productivity–operate independently of one another, without amplifying or canceling each other out in a major way.

[29]The transition from column (3) to column (5) is also smooth.

Covid Economics 61, 11 December 2020: 172-221

little information available to form the basis of an objective answer to this question. Any assessment, therefore, will depend heavily on the priors held by the individual observer.

Figure 8: Remote workers' workplace externalities: wages and welfare

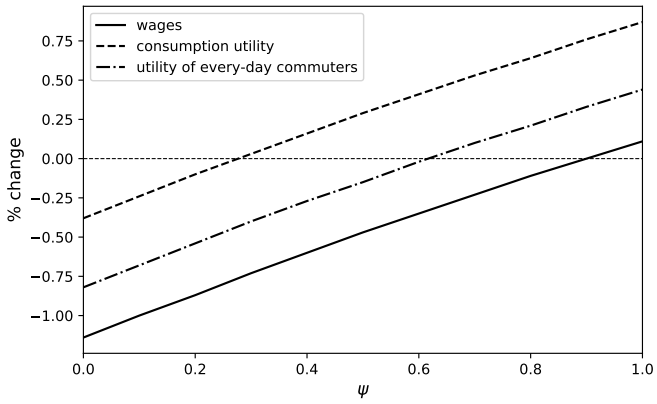

5 Conclusions and Further Work

In this paper we have built a quantitative general equilibrium model of employment and residence choice in which a portion of workers work from home either some or all of the time. In a counterfactual experiment, we increased the share of telecommuters, and saw that the model predicted rich patterns of reallocation both within and across metropolitan areas. In particular, there is a mostly monotonic shift of residents from central locations to the periphery, while jobs go up both in very small and very big cities. The question of how a decrease in face-to-face interaction will affect productivity in the long run is the key to predicting the overall welfare impact of such a change.

Our analysis has a number of limitations which open opportunities for extensions. First, our model does not consider trade between locations and its impact on wages and prices. Costly trade would probably act as a centripetal force, increase the cost of living in remote areas that otherwise might receive more migration from new telecommuters. Second, it might be useful to introduce multiple occupations to our analysis. Considering local differences in industrial and occupational structure could be central to understand quantitative implications of telecommuting, since the ability to work remotely varies across industries and occupations. Considering trade costs could tone down our findings, since some of the firms, especially those that produce non-traded goods, and therefore some of their workers, would have to remain in dense urban areas because this is where most

Covid Economics 61, 11 December 2020: 172-221

of their customers are. Third, our model does not distinguish between transportation modes and our counterfactual scenarios assume that commuting costs do not change. With fewer commuters traffic congestion may become less severe, though after Covid-19 many workers may switch from public transit to private cars.

Covid Economics 61, 11 December 2020: 172-221

Covid Economics 61, 11 December 2020: 172-221

Maps

Figure 9: Density of residents

Panel (a): United States, relative changes

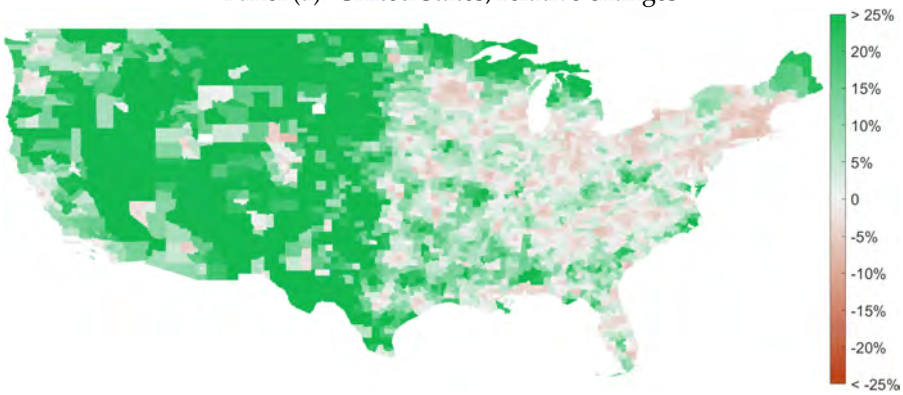

Panel (b): United States, absolute changes

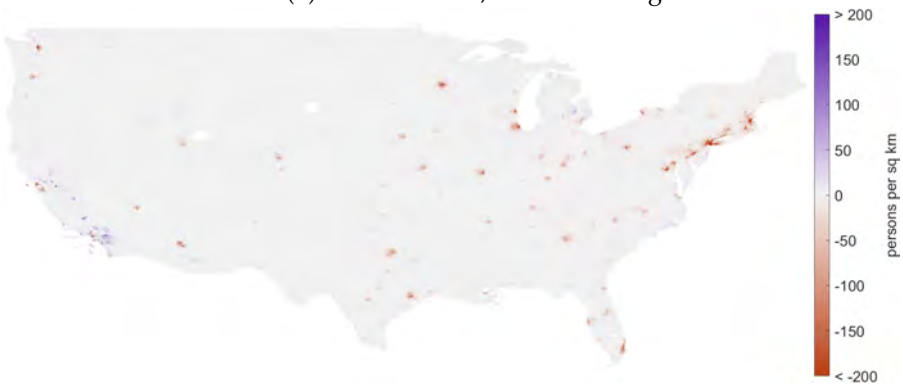

Panel (c): Los Angeles, relative changes

Panel (d): New York, relative changes

Panel (e): Los Angeles, absolute changes

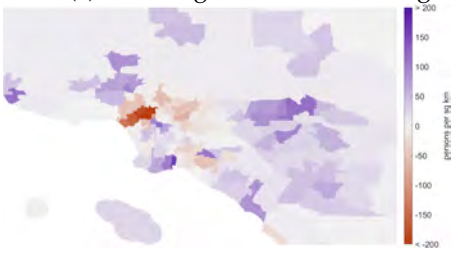

Panel (f): New York, absolute changes

Covid Economics 61, 11 December 2020: 172-221

Figure 10: Density of workers

Panel (a): United States, relative changes

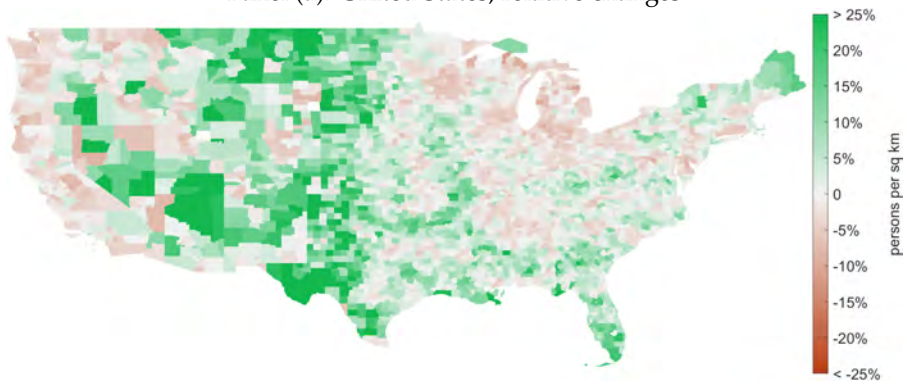

Panel (b): United States, absolute changes

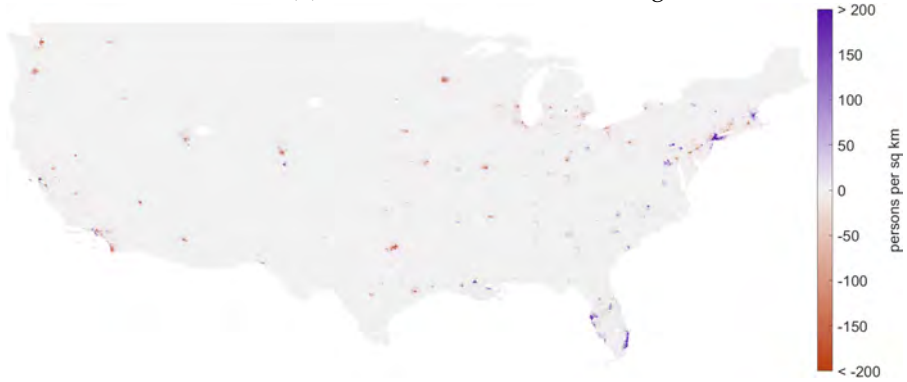

Panel (c): Los Angeles, relative changes

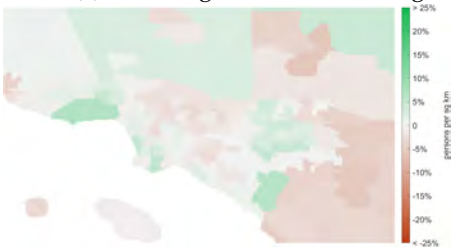

Panel (d): New York, relative changes

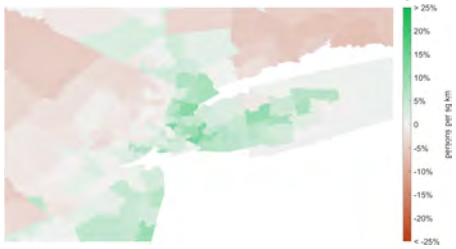

Panel (e): Los Angeles, absolute changes

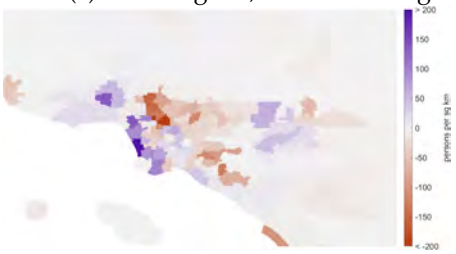

Panel (f): New York, absolute changes

Covid Economics 61, 11 December 2020: 172-221

Figure 11: Floorspace Prices

Panel (a): United States, percentage changes

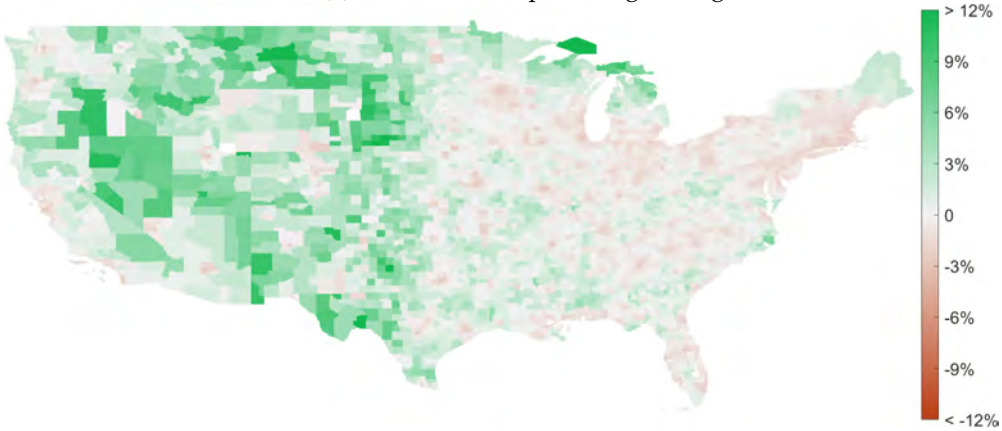

Panel (b): Los Angeles, percentage changes

Panel (c): New York, percentage changes

Bibliography

Ahlfeldt, G. M., S. J. Redding, D. M. Sturm, and N. Wolf (2015): "The Economics of Density: Evidence From the Berlin Wall," *Econometrica*, 83(6), 2127–2189.

Albouy, D., and G. Ehrlich (2018): "Housing productivity and the social cost of land-use restrictions," *Journal of Urban Economics*, 107, 101 – 120.

Althoff, L., F. Eckert, S. Ganapati, and C. Walsh (2020): "The City Paradox: Skilled Services and Remote Work," Working paper.

Barrero, J. M., N. Bloom, and S. J. Davis (2020): "COVID-19 Is Also a Reallocation Shock," Working Paper.

Bartik, A. W., Z. B. Cullen, E. L. Glaeser, M. Luca, and C. T. Stanton (2020): "What Jobs are Being Done at Home During the Covid-19 Crisis? Evidence from Firm-Level Surveys," NBER Working Paper 27422.

Baum-Snow, N., and L. Han (2020): "The Microgeography of Housing Supply," Working Paper.

Bloom, N., J. Liang, J. Roberts, and Z. J. Ying (2015): "Does working from home work? Evidence from a Chinese experiment," *The Quarterly Journal of Economics*, 130(1), 165–218.

Brynjolfsson, E., J. J. Horton, A. Ozimek, D. Rock, G. Sharma, and H.-Y. TuYe (2020): "COVID-19 and Remote Work: An Early Look at US Data," NBER Working Paper 27344.

Combes, P.-P., G. Duranton, and L. Gobillon (2019): "The Production Function for Housing: Evidence from France," Working Paper.

Davis, M. A., and F. Ortalo-Magné (2011): "Household Expenditures, Wages, Rents," *Review of Economic Dynamics*, 14(2), 248 – 261.

Dekle, R., J. Eaton, and S. Kortum (2007): "Unbalanced Trade," *American Economic Review*, 97(2), 351–355.

Delventhal, M. J., E. Kwon, and A. Parkhomenko (2020): "How Do Cities Change When We Work from Home?," Working Paper.

Dingel, J. I., and B. Neiman (2020): "How Many Jobs Can Be Done at Home?," *Journal of Public Economics*, 189, 104235.

Dingel, J. I., and F. Tintelnot (2020): "Spatial Economics for Granular Settings," Working Paper.

Eeckhout, J., R. Pinheiro, and K. Schmidheiny (2014): "Spatial Sorting," *Journal of Political Economy*, 122(3), 554 – 620.

Gariety, B. S., and S. Scaffer (2007): "Wage Differentials Associated with Working at Home," Monthly labor review, Bureau of Labor Statistics.

Heblich, S., S. J. Redding, and D. M. Sturm (2020): "The Making of the Modern Metropolis: Evidence from London," *Quarterly Journal of Economics*, 135(4), 2059–2133.

Covid Economics 61, 11 December 2020: 172-221

Larson, W., and W. Zhao (2017): "Telework: Urban form, energy consumption, and greenhouse gas implications," *Economic Inquiry*, 55(2), 714–735.

Lennox, J. (2020): "More working from home will change the shape and size of cities," Centre of Policy Studies/IMPACT Centre Working Papers g-306, Victoria University, Centre of Policy Studies/IMPACT Centre.

Mas, A., and A. Pallais (2017): "Valuing alternative work arrangements," *American Economic Review*, 107(12), 3722–59.

——— (2020): "Alternative Work Arrangements," *Annual Review of Economics*.

Monte, F., S. J. Redding, and E. Rossi-Hansberg (2018): "Commuting, Migration, and Local Employment Elasticities," *American Economic Review*, 108(12), 3855–90.

Ozimek, A. (2020): "Remote Workers on the Move," Upwork Economist Report.

Rhee, H.-J. (2008): "Home-based telecommuting and commuting behavior," *Journal of Urban Economics*, 63(1), 198–216.

Safirova, E. (2003): "Telecommuting, traffic congestion, and agglomeration: a general equilibrium model," *Journal of Urban Economics*, 52(1), 26–52.

Spear, B. D. (2011): *NCHRP 08-36, Task 098 Improving Employment Data for Transportation Planning*. American Association of State Highway and Transportation Officials.

Tsivanidis, N. (2019): "The Aggregate and Distributional Effects of Urban Transit Infrastructure: Evidence from Bogotá's TransMilenio," Working Paper.

Valentinyi, A., and B. Herrendorf (2008): "Measuring factor income shares at the sectoral level," *Review of Economic Dynamics*, 11(4), 820–835.

Covid Economics 61, 11 December 2020: 172-221

A Appendix

A.1 Welfare Decomposition

Welfare by type. The expected utility of a worker after he learns his type θ but before location preference shocks are realized, is given by

$$V(\theta) = \varsigma \pi_{ij}(\theta)^{-\frac{1}{\epsilon}} \frac{X_i E_j b_{ij} w_{ij}(\theta)}{d_{ij}(\theta) q_i^{\gamma}}. \tag{A.1}$$

Hence, we compute counterfactual changes in welfare for each worker who did not switch his commuter type θ as

$$\widehat{V}(\theta) = \hat{\pi}_{ij}(\theta)^{-\frac{1}{\epsilon}} \frac{\hat{X}_i \hat{E}_j \hat{b}_{ij} \hat{w}_{ij}(\theta)}{\hat{d}_{ij}(\theta) \hat{q}_i^{\gamma}}. \tag{A.2}$$

Note that the previous expression yields the same value of $\widehat{V}(\theta)$ for any pair (i, j).

Welfare by source. Aggregate composite consumption (i.e., $c^{1-\gamma} h^{\gamma}$) is given by

$$\int \sum_{i \in \mathcal{I}} \sum_{j \in \mathcal{I}} w_{ij}(\theta) q_i^{-\gamma} \pi_{ij}(\theta) \mathrm{d}F(\theta). \tag{A.3}$$

Therefore welfare gains resulting from changes in *consumption* are calculated as the ratio of aggregate counterfactual and benchmark consumption levels:

$$\widehat{V}_{\mathrm{C}} = \frac{\int \sum_{i \in \mathcal{I}} \sum_{j \in \mathcal{I}} \hat{w}_{ij}(\theta) w_{ij}(\theta) \left(\hat{q}_i q_i\right)^{-\gamma} \hat{\pi}_{ij}(\theta) \pi_{ij}(\theta) \mathrm{d}F^*(\theta)}{\int \sum_{i \in \mathcal{I}} \sum_{j \in \mathcal{I}} w_{ij}(\theta) q_i^{-\gamma} \pi_{ij}(\theta) \mathrm{d}F(\theta)}. \tag{A.4}$$

Similarly, we calculate welfare gains resulting from changes in *consumption and commuting* by adjusting the previous expression by the commuting cost of traveling from i to j:

$$\widehat{V}_{\mathrm{C,C}} = \frac{\int \sum_{i \in \mathcal{I}} \sum_{j \in \mathcal{I}} \hat{w}_{ij}(\theta) w_{ij}(\theta) \left(\hat{q}_i q_i\right)^{-\gamma} \hat{\pi}_{ij}(\theta) \pi_{ij}(\theta) \hat{d}_{ij}(\theta) d_{ij}(\theta) \mathrm{d}F^*(\theta)}{\int \sum_{i \in \mathcal{I}} \sum_{j \in \mathcal{I}} w_{ij}(\theta) q_i^{-\gamma} \pi_{ij}(\theta) d_{ij}(\theta) \mathrm{d}F(\theta)}. \tag{A.5}$$

Then, we calculate welfare gains resulting from changes in *consumption, commuting, and amenities* by adding relevant residential, workplace, and bilateral amenity levels to the previous expression:

$$\widehat{V}_{\mathrm{C,C,A}} = \frac{\int \sum_{i \in \mathcal{I}} \sum_{j \in \mathcal{I}} \hat{X}_i X_i \hat{E}_j E_j \hat{b}_{ij} b_{ij} \hat{w}_{ij}(\theta) w_{ij}(\theta) \left(\hat{q}_i q_i\right)^{-\gamma} \hat{\pi}_{ij}(\theta) \pi_{ij}(\theta) \hat{d}_{ij}(\theta) d_{ij}(\theta) \mathrm{d}F^*(\theta)}{\int \sum_{i \in \mathcal{I}} \sum_{j \in \mathcal{I}} X_i E_j b_{ij} w_{ij}(\theta) q_i^{-\gamma} \pi_{ij}(\theta) d_{ij}(\theta) \mathrm{d}F(\theta)}. \tag{A.6}$$

Finally, welfare gains resulting from changes in *consumption, commuting, amenities, and Frèchet shocks* correspond to total welfare gains and are given by equation (2.47).

Covid Economics 61, 11 December 2020: 172-221

A.2 Local Wage Indices

Our source of wage data is the Census Transportation Planning Products (CTPP). CTPP data sets produce tabulations of the American Community Survey (ACS) data, aggregated at the Census tract level. We use the data reported for the five-year period from 2012 to 2016. We use the variable "earnings in the past 12 months (2016 $), for the workers 16-year-old and over," which is based on the respondents' workplace locations. The variable provides the estimates of the number of people in each of the several earning bins in each workplace tract.[30]

We calculate mean tract-level labor earnings as

$$\hat{w}_j = \frac{\Sigma_b nworkers_{b,j} \times \hat{meanw}_b}{\Sigma_b nworkers_{b,j}}, \tag{A.7}$$

where $nworkers_{b,j}$ is the number of workers in bin b in tract j, and $\hat{meanw}_b$ is mean earnings in bin b for each PUMA, calculated from the ACS microdata.

Next, to control for possible effects of workers' heterogeneity on tract-level averages, we run the following Mincer regression,

$$\hat{w}_j = \alpha + \beta_1 age_j + \beta_2 sexratio_j + \Sigma_r \beta_{2,r} race_{r,j} + \Sigma_i \beta_{3,i} ind_{i,j} + \Sigma_o \beta_{4,o} occ_{o,j} + \epsilon_j, \tag{A.8}$$

where age_j is the average age of workers; $sexratio_j$ is the proportion of males to females in the labor force; $race_{r,j}$ is the share of race $r \in \{Asian, Black, Hispanic, White\}$; $ind_{i,j}$ is the share of jobs in industry i; $occ_{o,j}$ is share of jobs in occupation o in tract j.[31] The estimated tract-level wage index corresponds to the sum of the constant and the tract fixed effect, $\hat{\alpha} + \hat{\epsilon}_j$. Finally, we aggregate the tract-level wage indices to the level of our model locations using employment weights.

A.3 Estimation of Travel Times

In constructing a matrix of location to location travel times, we follow the practice recommended by Spear (2011) and use LODES data as a measure of commuting flows and Census Transportation Planning Products (CTPP) data to provide information on commute times. The CTPP database reports commuting time data for origin-destination pairs of Census tracts across the contiguous United States for 2012–2016, and is tabulated using

[30] The bins are ≤ $9,999; $10,000–$14,999; $15,000–$24,999; $25,000–$34,999; $35,000–$49,999; $50,000–$64,999; $65,000–$74,999; $75,000–$99,999; and ≥ $100,000.

[31] We use the following *industry* categories: Agricultural; Armed force; Art, entertainment, recreation, accommodation; Construction; Education, health, and social services; Finance, insurance, real estate; Information; Manufacturing; Other services; Professional scientific management; Public administration, Retail. We use the following *occupation* categories: Architecture and engineering; Armed Forces; Arts, design, entertainment, sports, and media; Building and grounds cleaning and maintenance; Business and financial operations specialists; Community and social service; Computer and mathematical; Construction and extraction; Education, training, and library; Farmers and farm managers; Farming, fishing, and forestry; Food preparation and serving related; Healthcare practitioners and technicians; Healthcare support; Installation, maintenance, and repair; Legal; Life, physical, and social science; Management; Office and administrative support; Personal care and service; Production;Protective service; Sales and related.

Covid Economics 61, 11 December 2020: 172-221

American Community Survey (ACS) data.[32] Travel times are reported for a little over four million trajectories, which is a small fraction of all possible bilateral trajectories, because most pairs of tracts are far enough apart that the ACS survey does not observe anyone commuting between those two points. We process this data in the following three steps:

1. We calculate the average travel time between each pair of locations as the average of all reported tract-to-tract travel times with an origin inside one location and a destination in the other. To minimize the influence of outliers on these estimates, we throw out the calculation for any pair of locations for which less than 10% of all possible tract-to-tract travel times is reported by CTPP. We also exclude average travel times that imply a travel speed of more than 100 kilometers per hour or less than 5 kilometers per hour. We perform this same calculation for the average distance of each location *from itself*, thereby obtaining data-based estimates of the average internal travel time for each location as well.

2. To prevent "breaks" in the network, we check to see if any location does not have an estimated travel time to its 5 nearest neighbors. If travel times are missing for any of these location-to-location trajectories, we project a travel time using the estimated coefficients of a regression of average location-to-location travel times on average great circle distance and an indicator variable that takes the value one if the origin is the same as the destination. This procedure adds about 10,000 additional links, out of 20,268,004 possible location-to-location trajectories.

3. We take the approximately 34,000 primitive connections, the travel times for which we have calculated as detailed above, as the first-order connections in a transport network. We use Dijkstra's algorithm to find the least possible travel times through this network between each pair of model locations.

[32]The CTPP data divides commuting times into 10 bins: less than 5 minutes, 5 to 14 minutes, 15 to 19 minutes, 20 to 29 minutes, 30 to 44 minutes, 45 to 59 minutes, 60 to 74 minutes, 75 to 89 minutes, 90 or more minutes, and work from home.

Covid Economics 61, 11 December 2020: 172-221

CEPR PRESS

A.4 MSA-level results

Table A.1: Changes in residents, jobs, and floorspaces prices for 100 largest CBSAs

CBSA	Change in residents				Change in jobs				Change in
	all workers		on-site	remote	all workers		on-site	remote	floorspace
	%	'000	'000	'000	%	'000	'000	'000	prices, %
New York-Jersey City-Wh..., NY-NJ	-3.0	-186	-683	497	2.5	166	-699	865	-1.2
Los Angeles-Long Beach-..., CA	0.7	29	-458	486	-0.2	-8	-463	455	-1.0
Chicago-Naperville-Arli..., IL	-2.7	-94	-397	303	-1.2	-43	-404	361	-1.5
Houston-The Woodlands-S..., TX	-2.4	-67	-317	250	-1.0	-28	-316	289	-1.5
Atlanta-Sandy Springs-R..., GA	-3.0	-73	-285	212	0.9	23	-284	307	-1.3
Washington-Arlington-Al..., DC-VA-MD-WV	-2.6	-59	-252	193	1.1	27	-262	289	-1.4
Dallas-Plano-Irving, TX	-2.5	-53	-247	194	-3.7	-82	-258	176	-1.4
Minneapolis-St. Paul-Bl..., MN-WI	-5.2	-100	-229	130	-4.7	-92	-231	139	-1.9
Phoenix-Mesa-Scottsdale..., AZ	-3.0	-57	-224	167	-1.2	-23	-222	200	-1.5
Riverside-San Bernardin..., CA	8.4	133	-167	300	-0.5	-7	-152	145	0.4
Nassau County-Suffolk C..., NY	-3.1	-45	-158	113	4.7	63	-142	205	-1.6
Seattle-Bellevue-Everet..., WA	-3.3	-46	-168	122	-3.3	-51	-181	130	-1.7
Denver-Aurora-Lakewood, CO	-2.2	-31	-167	136	-4.4	-61	-169	109	-1.5
Anaheim-Santa Ana-Irvin..., CA	1.0	13	-152	165	-0.7	-10	-161	151	-1.1
Baltimore-Columbia-Tows..., MD	-3.2	-43	-154	111	-1.6	-22	-155	133	-1.5
St. Louis, MO-IL	-4.6	-61	-161	100	-3.5	-48	-162	114	-1.7
San Diego-Carlsbad, CA	0.1	1	-152	154	-4.6	-58	-156	99	-1.1
Cambridge-Newton-Framin..., MA	-5.7	-70	-141	71	3.4	44	-139	183	-2.0
Newark, NJ-PA	-4.3	-52	-134	82	-1.1	-13	-131	118	-1.7
Warren-Troy-Farmington ..., MI	0.2	3	-142	145	-2.5	-29	-142	113	-1.0
Oakland-Hayward-Berkele..., CA	-0.4	-5	-136	131	-0.0	-0	-118	118	-1.1
Tampa-St. Petersburg-Cl..., FL	-2.3	-27	-132	105	6.3	76	-132	209	-1.4
Pittsburgh, PA	-5.2	-60	-137	78	-2.9	-35	-139	105	-1.8
Portland-Vancouver-Hill..., OR-WA	-2.6	-29	-136	107	-4.8	-54	-138	84	-1.6
Charlotte-Concord-Gasto..., NC-SC	-3.4	-37	-128	91	1.7	20	-128	148	-1.3
Fort Worth-Arlington, TX	-1.6	-17	-123	106	-3.3	-32	-117	85	-1.3
Cincinnati, OH-KY-IN	-4.2	-43	-122	78	-3.2	-33	-122	89	-1.5
Kansas City, MO-KS	-4.6	-47	-125	77	-3.3	-35	-126	92	-1.8
Miami-Miami Beach-Kenda..., FL	-3.1	-32	-114	82	6.0	66	-120	186	-1.7
Boston, MA	-5.9	-60	-117	57	5.4	68	-133	201	-2.0
Montgomery County-Bucks..., PA	-4.0	-41	-116	75	-1.9	-20	-119	100	-1.6
Cleveland-Elyria, OH	-1.4	-14	-119	106	-3.0	-31	-128	96	-1.3
Orlando-Kissimmee-Sanfo..., FL	-3.3	-33	-115	82	3.0	34	-125	159	-1.5
Indianapolis-Carmel-And..., IN	-3.4	-33	-117	83	-0.5	-6	-118	113	-1.5
Columbus, OH	-0.9	-9	-114	105	1.8	19	-116	135	-1.1
Las Vegas-Henderson-Par..., NV	-3.2	-30	-116	86	-3.7	-35	-116	81	-1.5
San Antonio-New Braunfe..., TX	-1.2	-11	-109	98	-2.0	-18	-109	90	-1.3
Sacramento–Roseville–..., CA	2.9	26	-103	129	-2.2	-20	-106	86	-0.6
San Jose-Sunnyvale-Sant..., CA	-2.3	-20	-101	81	-1.7	-16	-108	92	-1.7
Philadelphia, PA	-4.1	-35	-100	64	-1.4	-13	-104	91	-1.7
Austin-Round Rock, TX	-1.0	-8	-99	91	0.5	5	-101	106	-1.1
Nashville-Davidson–Mur..., TN	-4.1	-34	-101	67	-1.2	-11	-104	93	-1.4
Milwaukee-Waukesha-West..., WI	-5.0	-41	-97	56	-3.3	-30	-103	74	-2.0
San Francisco-Redwood C..., CA	-1.5	-12	-92	80	0.4	4	-108	112	-1.5
Providence-Warwick, RI-MA	-6.4	-51	-94	43	-3.1	-23	-87	64	-2.1
Fort Lauderdale-Pompano..., FL	-4.8	-38	-90	52	6.2	49	-83	132	-2.0
Virginia Beach-Norfolk-..., VA-NC	-2.8	-20	-85	64	-0.6	-4	-85	81	-1.5
Detroit-Dearborn-Livoni..., MI	-1.6	-11	-81	70	-2.3	-17	-83	66	-1.3
Camden, NJ	-0.1	-1	-70	69	-0.1	-0	-62	62	-0.9
Louisville/Jefferson Co..., KY-IN	-4.2	-27	-75	49	-0.4	-3	-76	73	-1.6
Hartford-West Hartford-..., CT	-7.1	-44	-74	30	-4.2	-28	-79	51	-2.2
Richmond, VA	-0.0	-0	-72	72	2.6	17	-74	91	-0.9
Silver Spring-Frederick..., MD	-1.4	-9	-67	59	2.1	13	-65	77	-1.2
Oklahoma City, OK	-0.5	-3	-74	70	2.3	15	-75	90	-1.1
Memphis, TN-MS-AR	-4.0	-23	-72	49	-4.4	-26	-73	47	-1.7
Jacksonville, FL	-3.9	-23	-71	49	-0.5	-3	-73	69	-1.5
Salt Lake City, UT	-2.8	-16	-73	56	-5.6	-38	-84	47	-1.7
Raleigh, NC	-3.9	-22	-69	47	3.8	23	-67	91	-1.3

Covid Economics 61, 11 December 2020: 172-221

CEPR PRESS

Table A.2: Changes in residents, jobs, and floorspaces prices for 100 largest CBSAs (cont'd)

CBSA	Change in residents				Change in jobs				Change in floorspace prices, %
	all workers		on-site	remote	all workers		on-site	remote	
	%	'000	'000	'000	%	'000	'000	'000	
Buffalo-Cheektowaga-Nia..., NY	-6.0	-34	-68	35	-3.1	-18	-70	52	-2.0
New Orleans-Metairie, LA	-2.7	-14	-62	48	5.0	29	-64	93	-1.6
Rochester, NY	-4.0	-21	-64	43	1.2	7	-64	71	-1.5
West Palm Beach-Boca Ra..., FL	-2.5	-13	-59	46	12.1	69	-59	129	-1.5
Birmingham-Hoover, AL	0.9	5	-61	65	1.4	8	-63	71	-0.7
Omaha-Council Bluffs, NE-IA	-4.8	-23	-59	36	-5.6	-28	-60	33	-1.9
Grand Rapids-Wyoming, MI	-1.4	-7	-60	53	-4.0	-21	-65	44	-1.2
Worcester, MA-CT	-4.9	-23	-54	31	0.2	1	-46	47	-1.6
Tulsa, OK	0.9	4	-56	60	-1.3	-6	-57	51	-0.8
Bridgeport-Stamford-Nor..., CT	-5.6	-24	-48	24	-3.3	-15	-51	36	-2.1
Lake County-Kenosha Cou..., IL-WI	-1.8	-8	-48	40	-1.1	-4	-45	41	-1.3
New Haven-Milford, CT	-6.7	-28	-49	21	-5.3	-21	-47	26	-2.2
Allentown-Bethlehem-Eas..., PA-NJ	-2.7	-11	-45	34	-2.6	-9	-43	34	-1.2
Albany-Schenectady-Troy..., NY	-5.1	-21	-49	28	1.8	8	-51	59	-1.5
Albuquerque, NM	-0.9	-4	-50	46	0.0	0	-49	49	-1.1
Greenville-Anderson-Mau..., SC	-5.1	-19	-44	25	-2.8	-11	-46	35	-1.5
Baton Rouge, LA	-1.6	-6	-44	38	9.6	39	-42	82	-1.1
Knoxville, TN	-1.0	-3	-44	41	-0.5	-2	-47	45	-0.9
Oxnard-Thousand Oaks-Ve..., CA	4.8	17	-41	58	-0.8	-2	-35	32	-0.3
Madison, WI	-2.9	-10	-42	32	-4.5	-18	-47	29	-1.4
Tacoma-Lakewood, WA	0.9	3	-43	46	-3.4	-10	-35	26	-0.7
Wilmington, DE-MD-NJ	-5.2	-18	-41	23	-6.1	-22	-43	21	-1.8
Dayton, OH	-4.7	-16	-42	25	-3.5	-13	-43	31	-1.7
Columbia, SC	0.2	1	-41	41	5.4	21	-42	62	-0.8
Fresno, CA	7.0	24	-43	67	-3.8	-12	-44	32	-0.3
Little Rock-North Littl..., AR	0.9	3	-42	45	4.2	15	-44	59	-0.7
Akron, OH	-2.8	-9	-40	30	-4.3	-14	-41	27	-1.5
Tucson, AZ	6.0	20	-42	62	0.5	2	-43	45	0.1
Des Moines-West Des Moi..., IA	-3.2	-10	-40	30	1.4	5	-42	47	-1.5
Greensboro-High Point, NC	-1.0	-3	-37	34	0.7	2	-42	44	-1.1
El Paso, TX	-1.7	-5	-41	36	-5.6	-18	-42	24	-1.3
Gary, IN	-1.3	-4	-37	33	-4.7	-13	-35	22	-1.2
Charleston-North Charle..., SC	2.6	8	-39	47	7.0	23	-39	62	-0.3
Boise City, ID	2.3	7	-41	48	-5.5	-16	-42	25	-0.4
Wichita, KS	-3.5	-10	-37	27	-0.9	-3	-38	35	-1.5
Elgin, IL	-2.7	-8	-34	26	-2.6	-7	-30	23	-1.4
Springfield, MA	-1.0	-3	-32	29	3.2	9	-33	42	-1.1
Ogden-Clearfield, UT	-2.2	-6	-37	30	-5.7	-13	-30	17	-1.2
Winston-Salem, NC	-2.7	-8	-34	26	1.7	4	-30	35	-1.0
Bakersfield, CA	12.8	35	-33	68	-2.0	-5	-35	30	0.6
Toledo, OH	-2.8	-8	-32	24	-4.8	-14	-35	21	-1.6
Syracuse, NY	-1.3	-3	-33	29	1.1	3	-34	38	-1.1

Covid Economics 61, 11 December 2020: 172-221

Covid Economics 61, 11 December 2020: 172-221

A.5 Counterfactual Results with Agglomeration Effects

Figure A.1: Change in Residents

Panel (a): model locations

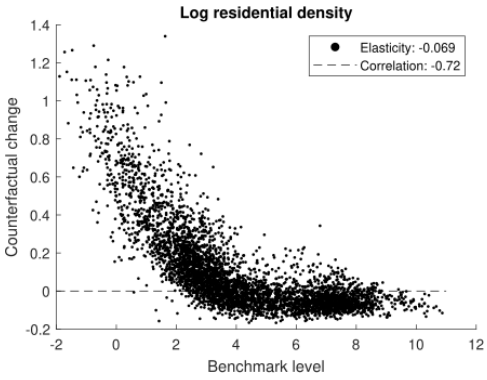

Panel (b): metropolitan areas

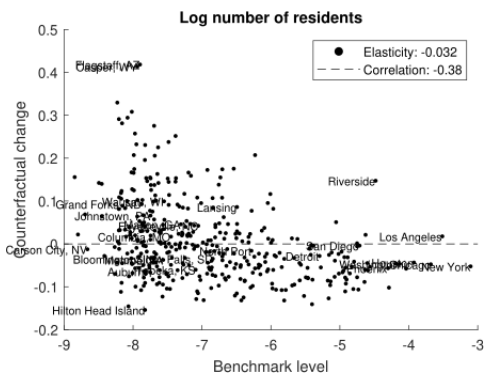

Note: These scatterplots show the relationship between the benchmark residential density and the counterfactual change in log density. Panel (a) shows this relationship for model locations, panel (b) shows this relationship for metropolitan areas. "Elasticity" is the coefficient of the OLS regression of the counterfactual change on the benchmark level.

Figure A.2: Change in Employment

Panel (a): model locations

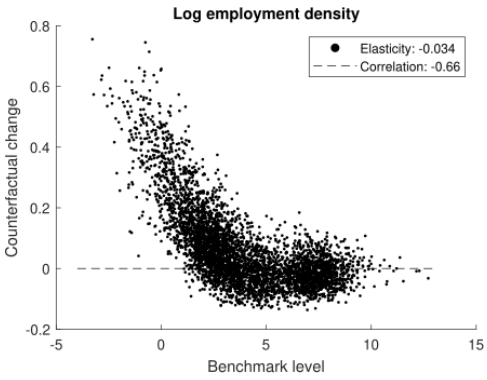

Panel (b): metropolitan areas

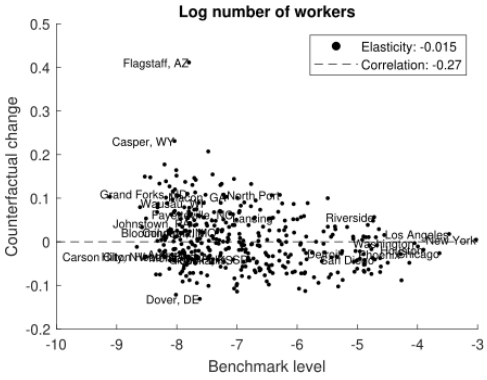

Note: These scatterplots show the relationship between the benchmark employment density and the counterfactual change in log density. Panel (a) shows this relationship for model locations, panel (b) shows this relationship for metropolitan areas. "Elasticity" is the coefficient of the OLS regression of the counterfactual change on the benchmark level.

Covid Economics 61, 11 December 2020: 172-221

Figure A.3: Density of residents

Panel (a): United States, relative changes

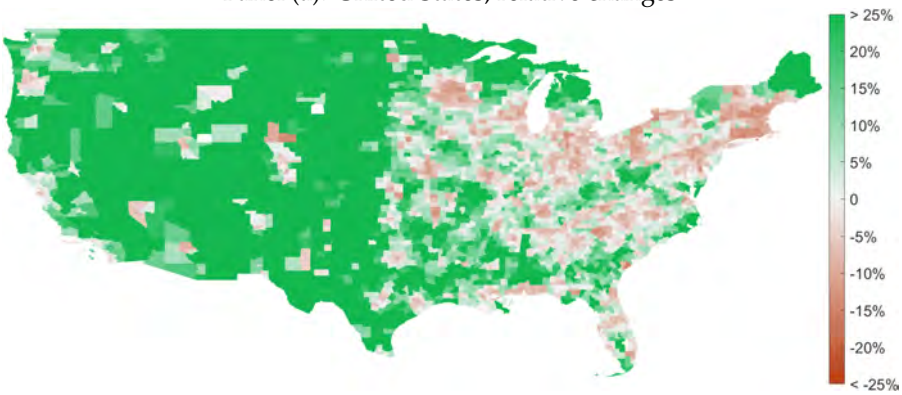

Panel (b): United States, absolute changes

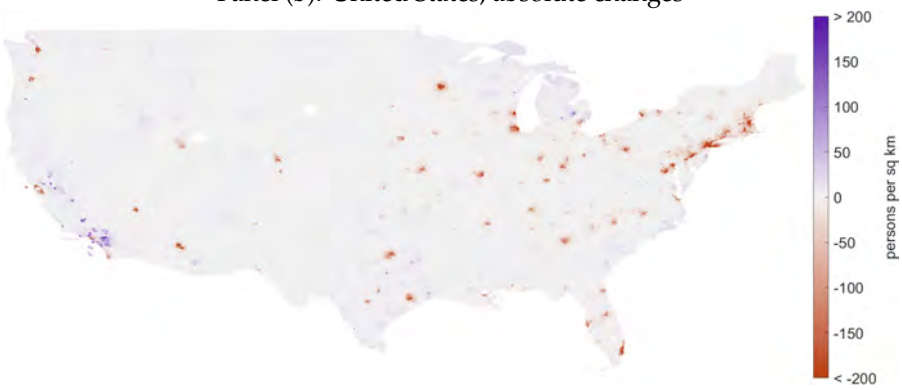

Panel (c): Los Angeles, relative changes

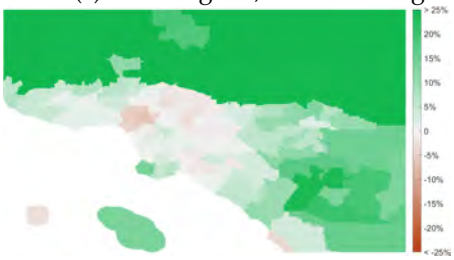

Panel (d): New York, relative changes

Panel (e): Los Angeles, absolute changes

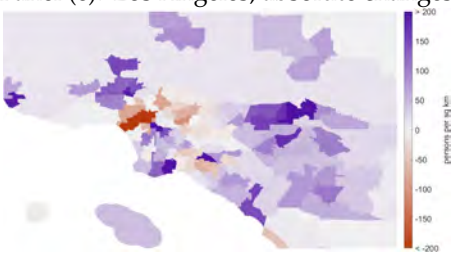

Panel (f): New York, absolute changes

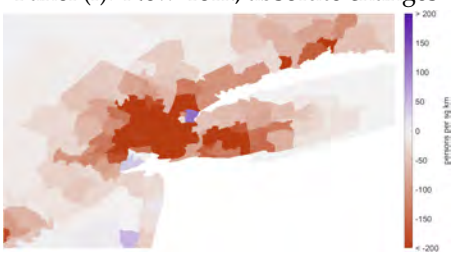

Covid Economics 61, 11 December 2020: 172-221

Figure A.4: Density of workers

Panel (a): United States, relative changes

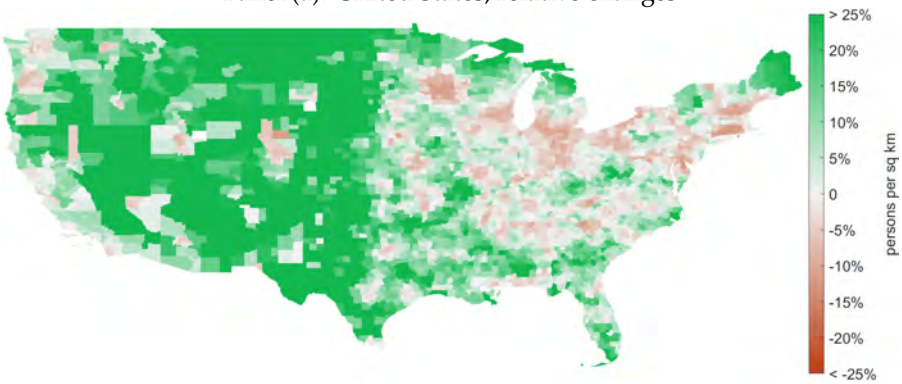

Panel (b): United States, absolute changes

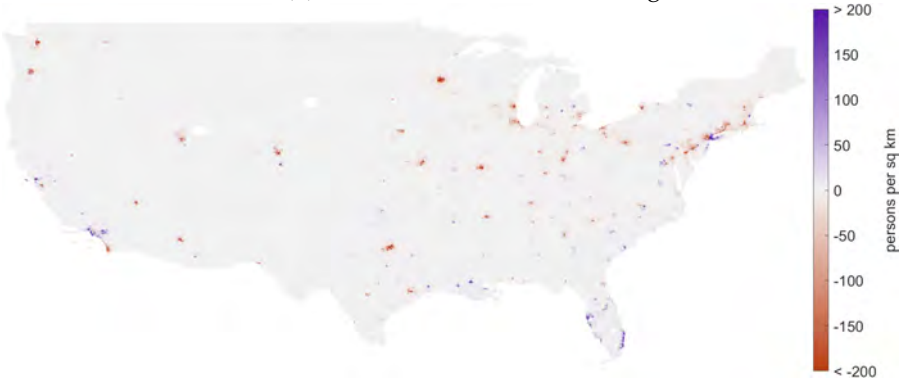

Panel (c): Los Angeles, relative changes

Panel (d): New York, relative changes

Panel (e): Los Angeles, absolute changes

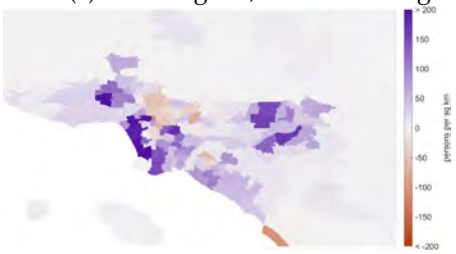

Panel (f): New York, absolute changes

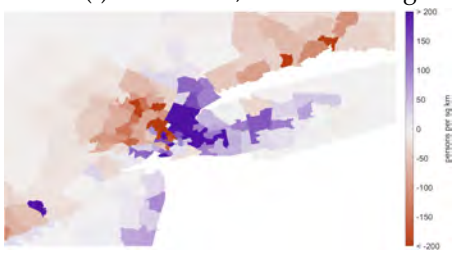

Figure A.5: Real Estate Prices

Panel (a): United States, percentage changes

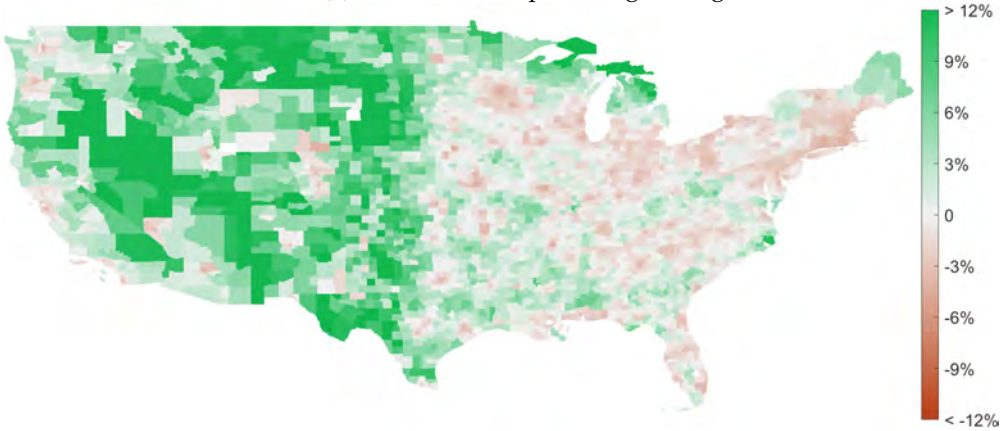

Panel (b): Los Angeles, percentage changes

Panel (c): New York, percentage changes

Covid Economics 61, 11 December 2020: 172-221

Covid Economics 61, 11 December 2020: 172-221

Figure A.6: Floorspace prices

Panel (a): model locations

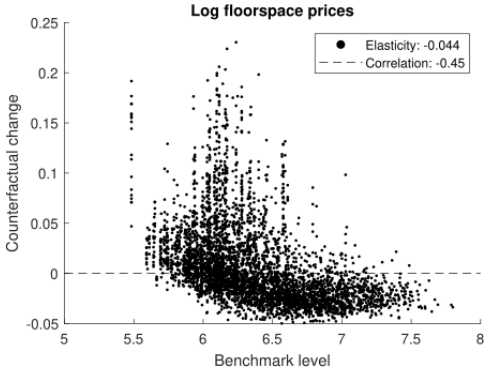

Panel (b): metropolitan areas

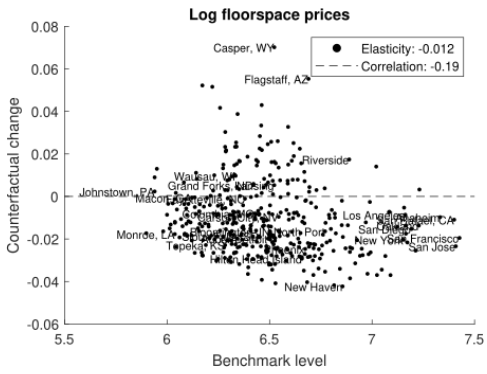

Note: These scatterplots show the relationship between the benchmark log floorspace prices and the counterfactual change in log floorspace prices. "Elasticity" is the coefficient of the OLS regression of the variable on the vertical axis on the variable on the horizontal axis.

Figure A.7: Wages

Panel (a): model locations

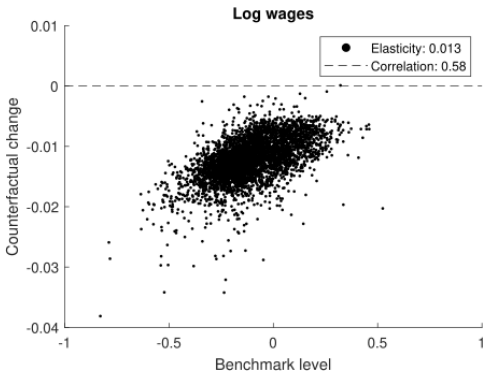

Panel (b): metropolitan areas

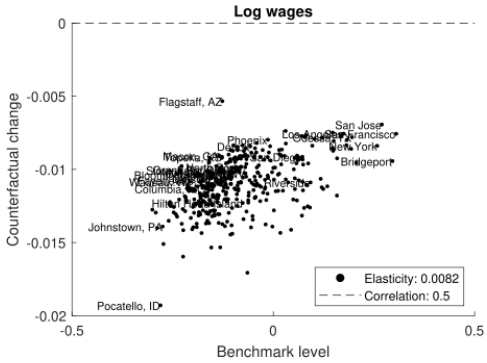

Note: These scatterplots show the relationship between the benchmark log wages of commuters at the place of work, w_j^C, and the counterfactual change in log wages. "Elasticity" is the coefficient of the OLS regression of the variable on the vertical axis on the variable on the horizontal axis.

A.6 Additional Figures and Tables

Figure A.8: Commuting flows

Panel (a): all pairs

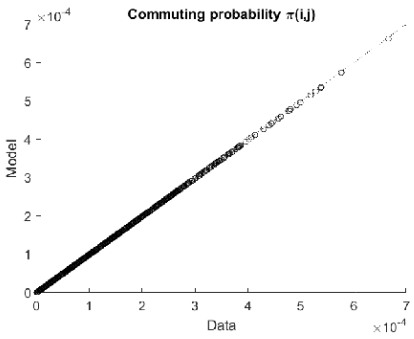

Panel (b): pairs with small flows

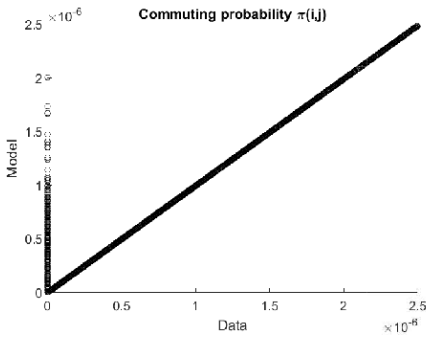

Note: These scatterplots show the relationship between commuting probabilities in the LODES data and their counterparts in the model. Panel (a) shows all pairs, panel (b) shows pairs with $\pi_{ij} < 2.5 \times 10^{-6}$. The dotted line is the 45-degree line.

Covid Economics 61, 11 December 2020: 172-221

Covid Economics Issue 61, 11 December 2020

Covid-19, trade collapse and GVC linkages: European experience[1]

Katja Zajc Kejzar[2] and Alan Velic[3]

Date submitted: 6 December 2020; Date accepted: 8 December 2020

This paper aims to highlight the role of supply chain linkages for the transmission of Covid-19 induced shocks based on the monthly trade of the European Union member states. The paper distinguishes demand and supply shocks as of either domestic or partner country origin and further characterizes the role of the latter based on the bilateral GVC positions, thereby taking into account the possibility of transmission through forward and backward linkages. Using the framework of the gravity model, we find a general decline in trade following the Covid-19 outbreak and significantly negative trade effects associated with Covid-19 cases per capita in both origin and destination country. The combined trade effect of Covid-19 is almost minus 20% for both exports and imports, taking into account the average Covid-19 infection rates in the EU and partner countries from April 2020. While export decreases twice as much in response to an increase in the current number of Covid-19 cases in the destination country than in the origin country, it becomes more sensitive to the Covid-19 situation in the origin country over time, suggesting that import demand shocks have a more immediate effect than export supply ones. Moreover, the results confirm that forward GVC linkages act as a channel for the transmission of (demand) shocks in the supply chain trade. An increase in the incidence of destination's Covid-19 cases, namely, induces a steeper decline in domestic exports of intermediate products in those destinations with which a country has stronger forward linkages, i.e. in partners positioned further downstream. On the other hand, we fail to find robust evidence for the transmission of Covid-19-induced shocks via backward linkages.

1 This research was sponsored by the Slovenian Research Agency (Research Programme P5-0117).
2 Full Professor of International Economics, University of Ljubljana, School of Economics and Business.
3 Graduate from University of Ljubljana, School of Economics and Business.

Covid Economics 61, 11 December 2020: 222-244

1. Introduction

As a result of the Covid-19 pandemic, predictions show the global economy contracting sharply by -4.9 percent in 2020 (IMF, 2020)[1], whilst all regions will suffer double-digit declines in exports and imports (WTO, 2020)[2], much worse than during the 2008-09 global financial crisis (hereinafter GFC). It is projected for the European Union to be among the most affected economies, with a drop in GDP by 8.3 percent in 2020 (European Commission, 2020)[3]. Estimates of the expected recovery of Europe in 2021 are uncertain, with outcomes depending significantly on the duration of the outbreak and the effectiveness of the policy responses. An economic downturn, increased uncertainty and simultaneous supply chain disruptions have been putting tremendous pressure on the reorganisation and reconfiguration of the global value chains (GVC hereafter). Covid-19 has hit at the core of GVC hub regions, including Europe, China, and the US.

The lessons from recent global crises and shocks, such as GFC in 2008 and the Japanese earthquake/tsunami in 2011, showed that companies react by reorienting their sourcing strategies towards more diversification of risk and breaking the value chains into shorter and less complex ones (OECD, 2013). However, the Covid-19 crisis differs from the GFC mainly in that it involves lockdown and social distancing which has led to major GVC disruptions. Trade is likely to fall more steeply in sectors characterized by complex value chain linkages, particularly in electronics and automotive products. This is closely tied to the nature of certain jobs that cannot be sufficiently performed remotely and thus result in lesser output by the industry, consequentially amplifying trade effects due to the supply chain linkages. Dingel and Neiman (2020) estimated, using survey data for the US, an upper bound of 22% that represents a share of jobs in manufacturing that can be performed remotely, which helps explain negative trade effects from exporting countries due to lesser export supply as a consequence of imposed measures.

On top of this, as pointed out by Evenett (2020), a troubling trade policy dimension is now coming to light. Over 80 countries have introduced export prohibitions or restrictions as a result of the Covid-19 pandemic, predominantly on medical supplies, pharmaceuticals, and medical equipment, but also additional products, such as foodstuffs and toilet paper (WTO, 2020)[4]. At the same time, politicians' calls for "sovereign" or "national" supply chains and re-thinking of domestic companies' approaches to international outsourcing of production are becoming louder (Serič, Görg, Mösle, and Windisch, 2020). These processes and developments might lead as well to the break of the existing GVCs and their readjustment.

[1] Available at https://www.imf.org/en/Publications/WEO/Issues/2020/06/24/WEOUpdateJune2020
[2] Available at https://www.wto.org/english/news_e/pres20_e/pr855_e.htm
[3] Available at https://ec.europa.eu/info/sites/info/files/economy-finance/ip132_en.pdf
[4] More on this https://www.wto.org/english/tratop_e/covid19_e/export_prohibitions_report_e.pdf

Covid Economics 61, 11 December 2020: 222-244

Friedt and Zhang (2020) estimated that GVC contagion effect explains around two-thirds of the total reduction in Chinese exports thus providing support for the decisive role of GVC participation for the trade response to Covid-19 pandemic situation. In line with this observation, Figure 1 placed later in Section 3.5 illustrates that during the first wave of the pandemic EU member states overall recorded the largest decline in trade with intermediated goods. Though, differences in the trade contraction that unfolded at the beginning of the second quarter of 2020 among the EU member states do not reflect, at least, at first sight, differences in the incidence of Covid-19 cases. As exemplified in Figures 2 and 3 in Section 3.5, despite having relatively fewer Covid-19 cases per capita, the new EU member states experienced above-average import and export contraction. Can this discrepancy be explained by differences in GVC participation and position among the member states? According to World Development Report 2020, the type of GVC participation significantly differs among the EU member state; while most of the old EU member states are specialized in innovative GVCs activities, CEE-11 are mostly specialized in advanced manufacturing and services GVCs with a high share of manufacturing and business services exports and high backward GVC integration. Overall, the old member states occupy a more upstream position in GVCs compared to the new EU member states.

Understanding the severity and nature of trade collapse in EU member states in the wake of the Covid-19 pandemic requires knowledge about the structure of value chains and subsequent level of integration by countries. In this paper, we intend to add to the growing literature on the disruptions of the real economic activity caused by the pandemic by empirically evaluating how involvement and position in the GVCs determine the trade adjustment to Covid-19 induced shocks. We augment the gravity model with the backward and forward GVC linkages to account for various trade-related transmission mechanisms of the Covid-19 shocks in partner countries. We find that among the identified transmission channels, forward linkages played the most prominent role in transmitting the pandemic induced shocks through the supply chains. A significant contraction in both exports and imports is directly attributed to a country's forward participation.

Our work is closely related to Baldwin and Freeman (2020), Baldwin and Tomiura (2020) and Friedt and Zhang (2020) who investigate the so-called 'triple pandemic effect' on trade through the pandemic-induced domestic supply, international demand, and GVC contagion shocks. The transmission role of the GVCs has been addressed also from the perspective of its impact on real economic activity and prices (Meier and Pinto, 2020), output adjustments to cross-sectoral effects of labour supply shocks (Bonadio et al., 2020; McCann and Myers, 2020), and aggregate welfare, through both deaths and reduced gains from trade (Antras et al., 2020). While the literature on demand and supply shocks includes Farhi and Baqaee (2020) who study how Covid-19 induced supply and demand shocks affect real economic variables and Hassan et al. (2020) who identify negative demand shock and supply chain disruptions as one of the prevailing concerns when conducting a firm-level analysis of earnings' calls.

The rest of the paper is organised as follows. Section 2 discusses transmission mechanisms of Covid-19 shocks through supply chain linkages. Section 3 sets gravity-model-based empirical specifications, discusses methodological issues and presents stylised facts on trade performance and Covid-19 pandemic situation across EU member states. Section 4 shows the estimates and discusses the results of the Covid-19 impact on bilateral trade flows and provides some robustness checks. Section 5 concludes the paper.

2. Background on GVC linkages and transmission of Covid-19 induced shocks

In many countries, several drastic measures have been taken in response to the Covid-19 pandemic, such as lockdowns and social distancing, with direct impact on both the demand and the supply side of the domestic economy and thus on its trade performance. Moreover, due to strong supply chain linkages, the Covid-19 induced shocks spread quickly across countries. Baldwin and Freeman (2020), Baldwin and Tomiura (2020) and Friedt and Zhang (2020) conceptualize this diverse set of effects as the 'triple pandemic effect' on trade through direct supply disruption due to various containment efforts, the supply-chain contagion due to the disruptions of the international flow of intermediate inputs, and the decline in global demand due to reduction in consumer spending and investment delays.

We build upon this classification by further acknowledging that supply and demand shocks transmit through the GVC linkages in both directions via forward and backward linkages, i.e. upstream and downstream, giving rise to complex interplay of the trade effects of Covid-19 pandemic which we summarize in Table 1. Based on their position in GVCs, countries can be classified as more upstream or downstream, each category of countries being subject to different dynamics of shock transmission.

On the supply side, lockdown measures, subsequent closing of local businesses as well as fear of infection result in a labour supply shock. On a domestic level, lockdown-induced labour supply shock is manifested in lesser export supply due to lower output. Moreover, labour supply shocks in partner countries affect domestic trade through (see Table 1): (i) lower domestic imports of final consumption goods due to ravaged supply in a partner country, and (ii) reduced imports of intermediates via backward linkages, i.e. supply-chain disruption from foreign upstream suppliers conveyed to domestic downstream customers. Bonadio et al. (2020), for instance, showed that a quarter of the average real GDP downturn due to lockdown-induced labour supply shocks could be contributed to the transmission through global supply chains.

Covid Economics 61, 11 December 2020: 222-244

On the demand side, increased uncertainty and fall in the household disposable income propagate decreased demand for products, mostly consumer goods, which means lower import quantities. Hassan et al. (2020) confirmed by employing text-based measures of the costs, benefits and risks firms associate with the spread of Covid-19 disease in the first quarter of 2020 that collapse of demand and increased uncertainty were among firms' primary concerns. Transmission of demand-side shocks from partner countries come through multiple channels, trade in final goods and supply chain trade (intermediates and capital goods). While the impact on trade in final goods is relatively straightforward, corresponding directly to the decreased exports to partner country which experiences a demand shock (i.e. partner country's demand shock resulting in lesser imports will translate directly to lesser domestic export), supply chain trade transmission depends upon the GVC interrelations. In particular, the demand-side shock in a partner country results in lower demand for intermediated goods sourced from more upstream domestic suppliers via forward GVC linkages, hence lower exports of intermediate goods from domestic to partner country. We summarize these potential channels and expected effects of Covid-19 on trade in Table 1.

Table 1: Domestic and transmitted effects of Covid-19 pandemic on the domestic country's trade

	Domestic Covid-19 shock in *i*	**Transmission of Covid-19 shock from partner country *j***		
		Final good trade	*Supply chain trade (intermediates and capital goods)*	
			From downstream customers in j to domestic upstream suppliers (via FP_{ij})	From upstream suppliers in j to domestic downstream customers (via BP_{ij})
Demand side	IM_i ⇩	EX_i ⇩	EX_i ⇩	
Supply side	EX_i ⇩	IM_i ⇩		IM_i ⇩

Friedt and Zhang (2020) estimated that the impact of GVC contagion explains around 75% of the total reduction in Chinese exports, while the domestic supply shock in China accounts for around 10% to 15% and the international demand shock only explains around 5% to 10%. McCann and Myers (2020) studied the nature of transmission of Covid-19 shock through inter-sectoral supply-chain linkages and found that in particular upstream sectors without direct Covid-19 exposure containment policies can still be affected if their downstream (customer) firms suffer acute revenue losses, while the transmission from upstream suppliers to downstream firms is likely to be smaller. In line with this evidence, we expect that transmission of supply-chain shocks operates primarily from downstream customers to their upstream suppliers. It does so by initially affecting the exports of the intermediate goods via forward linkages. On the other hand, Meier and Pinto (2020) provide indirect evidence of the transmission of shocks through backward linkages. They found that US

Covid Economics 61, 11 December 2020: 222-244

sectors with greater exposure to intermediate goods imports from China contracted significantly more than other sectors coupled with their relative input and output price increase. As per direct impact of Covid-19 crisis, Hayakawa and Mukunoki (2020) found that in the early stage of the pandemics Covid-19 burden in exporting countries, but not in importing countries, has a significantly negative effect on trade.

3. Conceptual framework, methodology and data

3.1. Gravity model framework

The identified channels of Covid-19 trade effects are tested within a gravity model framework. The gravity model is a workhorse for testing various determinants of international trade and the effect of trade policy measures. It adopts the logic of Newton's law of universal gravitation for explaining the bilateral trade flows stating that trade between two economic areas will be directly proportional to the product of their market sizes (e.g. GDPs) and inversely proportional to the square of the distance between their centres.

We will follow the approach of Anderson and van Wincoop (2003) who had shown that proper specification of the gravity model grounded in the trade theory requires the inclusion of the inward and outward multilateral resistance terms (MRT) which take into consideration how "remote" both regions are from the rest of the world. The main idea is that bilateral trade flows between trading partners "i" and "j" depend on bilateral trade barriers relative to average trade barriers that both trading partners face with all their trading partners. Their formulation of the structural gravity equation, which is the basis for almost all subsequent papers using gravity models to explain bilateral trade flows, is as follows:

$$trade_{ijt} = \frac{Y_{it}Y_{jt}}{Y_t}\left(\frac{t_{ijt}}{\pi_{it}P_{jt}}\right)^{1-\sigma}, \qquad [1]$$

where Y_{it} and Y_{jt} stand for particular countries' GDP and Y_t for the world aggregate GDP, while t_{ijt} stands for the tariff equivalent of overall trade costs. The elasticity of substitution between goods is represented with σ, while π_{it} and P_{jt} represent multilateral resistance terms (in other words – exporter and importer ease of market access).

By log-linearizing structural gravity eq. [1], we obtain the most common theory-consistent gravity model specification:

Covid Economics 61, 11 December 2020: 222-244

$$\ln trade_{ijt} = \ln Y_{it} + \ln Y_{jt} - \ln Y_t + (1-\sigma)\left[\ln t_{ijt} - \ln \Pi_{it} - \ln P_{jt}\right] + \varepsilon_{ij} \,. \qquad [2]$$

3.2. Accounting for transmission of Covid-19 induced shocks via GVC linkages

To account for the role of both the extent of participation in and the position along GVCs in cross-country transmission of Covid-19 shocks we augment eq. [2] with GVC participation indices which measure to what extent are countries involved in a vertically fragmented production and resulting supply chain trade flows. The GVC participation is decomposed in the two indices: forward participation (FP) and backward participation (BP). Forward GVC participation refers to the type of participation where an economy joins the global production by exporting domestically produced inputs to partners who are in charge of downstream production stages, while backward GVC participation is the type of integration where the country participates by importing foreign inputs to produce the goods and services for its export. Backward linkages are measured as foreign value-added (FVA) in domestic exports, while forward ones by the domestic value-added embodied in foreign exports (DVAFX). Hence, the FVA in the exports indicates the country's "downstreamness" in global production chains and the DVAFX indicates "upstreamness".

The GVC indices are calculated using the following equations:

$$FP_{ijt} = \frac{DVAFX_{ijt}}{grossEX_{it}} \cdot 100 \qquad [3]$$

$$BP_{ijt} = \frac{FVA_{ijt}}{grossEX_{it}} \cdot 100 \qquad [4]$$

Where $DVAFX_{ijt}$ n eq. [3] denotes domestic value-added of country *i* embodied in exports of country *j* in a year *t*, and FVA_{ijt} in eq. [4] represents foreign value-added of a country *j* embedded in exports of a country *i*. *G*rossEX_{it} represents gross exports of a country *i* in that same year.

To portray the bilateral GVC position of EU countries we use the log ratio of a country's forward and backward participation as proposed by Koopman, Powers, Wang, & Wei, (2010). The higher the value of the ratio the more upstream position in the GVC a country holds. This measure characterises the relative upstreamness of a country by comparing the importance of forward and backward participation, as opposed to "distance to final demand" based measures, proposed by e.g. Fally (2012) and Antràs et al. (2012), which measure how many stages of production are left before the goods or services produced by an industry reach their final consumers. We adjust the GVC position measure to be country-pair specific by using bilateral participation indices that we specified in eq. [3] and eq. [4] to obtain a bilateral GVC participation index (eq. [5]).

Covid Economics 61, 11 December 2020: 222-244

$$GVC_{ijt} = \text{Ln}(1 + FP_{ijt}/100) - \ln(1 + BP_{ijt}/100) \quad [5]$$

To account for the impact of the Covid-19 pandemic situation in domestic and partner countries on bilateral trade both directly and via supply-chain linkages summarized in Table 1 we augment gravity model specification [2] in the following way:

$$\begin{aligned}\ln trade_{ijt} = {} & \beta_0 + \beta_1 covid\_period_t + \beta_2 covid\_cases\_o_{it} + \beta_3 covid\_cases\_d_{jt} + \beta_4 FP_{ijt} + \\ & + \beta_5 BP_{ijt} + \beta_6 FP_{ijt} * covid\_cases\_d_{jt} + \beta_7 BP_{ijt} * covid\_cases\_d_{jt} + \beta_8 \ln y_{it} + \beta_9 \ln y_{jt} + \\ & + X'_{ij}\beta_{10} + \sum \beta_{11.t}\, month_t + \sum \beta_{12.t}\, year_t + \sum \beta_{12.it} year_t * reporter_i + \\ & + \sum \beta_{13.jt} year_t * partner_j + \sum \beta_{14.ij} country\_pair_{ij} + \varepsilon_{ijt}\end{aligned} \quad [6]$$

Where, $trade_{ijt}$ denotes export and import flows between countries *i* and *j* in time *t*, while *covid_period* is a dummy variable which takes value one during the Covid-19 pandemic situation, i.e. from February 2020 on, and zero otherwise. The latter variable tests the general drop in trade during the first wave of the Covid-19 pandemic situation. Regressors *Covid_cases_o* and *covid_cases_d* count the number of affected people per 1000 population in the reporter (origin) and partner (destination) country in *t* to account for domestic and international supply and demand Covid-19 induced shocks. As explained above, FP_{ijt} and BP_{ijt} indicate bilateral forward and backward participation based on equations [3] and [4], respectively, while their interaction with the number of affected people per 1000 population in partner country tests the presence of supply-chain transmission of shocks from partner country to domestic exports/imports via both forward and backward linkages. Vector X' includes country-pair, time-invariant specific variables such as *lnDist* measuring log value of the weighted distance between country *i* and country *j*, and dummy variables indicating whether countries *i* and *j* share a common border (*contig)*, language is spoken by at least 9% of the population in both countries (*comlang_ethno*), have had a common colonizer after 1945 (*comcol*), have had a colonial relationship after 1945 (*col45*), were/are the same country (*smctry*). Specification includes various sets of fixed effects including time-varying reporter and partner fixed effects, country-pair fixed effects and annual and monthly fixed effects.

3.3.Methodological issues

There are certain potential econometric concerns of estimating gravity model in a panel data setting that deserve discussion. The first issue that arises in our estimation is zero trade values that are relatively common in the trade matrix and are dropped from the OLS model due to undefined logarithm value of number zero. Ignoring this issue might result in inefficient and biased estimates. To deal with this issue of zero values we use the Poisson Maximum Likelihood Estimator (PPML) which effectively solves this potential selection bias (Burger et al. 2009). The next issue is a problem of endogeneity (see Baier & Bergstrand, 2007 for discussion). Contrary to exogenous

Covid Economics 61, 11 December 2020: 222-244

variables, endogenous variables are systematically affected by the changes in other variables within the model. Among the gravity equation variables in our specification, the GVC indices are most likely candidates for endogenous variables. To reduce the risk of endogeneity in our specifications, the FP and BP GVC participation indices are entered in the model in their lagged forms. We also lagged the GDP and Covid-19 variables due to potential simultaneity. Third, following the abovementioned findings from Anderson & van Wincoop (2003) multilateral trade-resistance terms (MRT) are also important when estimating the gravity model. Under MRT we understand a number of different trade barriers that a country faces in trade with all its trading partners, and not just with one particular partner. Without respecting the MRT the only factors that influence the trade between countries i and j are included in the analysis, which is creating a so-called omitted variable bias in the intuitive equation. To control for MRT we use a wide set of fixed effects including time-varying reporter and partner fixed effects, country-pair fixed effects and annual and monthly fixed effects. We implement Poisson pseudolikelihood regression with multiple levels of fixed effects as described by Correia, Guimarães, and Zylkin (2020) which is robust to statistical separation and convergence issues and allows any number and combination of fixed effects and individual slopes based on procedures developed in Correia, Guimarães, and Zylkin (2019). Moreover, the estimations under [6] are obtained through the clustering on the country-pair indicator variable and are therefore robust to cross-sectional heteroscedasticity and serial correlation.

3.4.Data and descriptive statistics

The empirical specification [6] will be applied to monthly bilateral trade data of EU member states covering the five-year period, i.e. from June 2015 till May 2020. Gross trade data used in the analysis is obtained from the Comext trade database. It includes monthly intra- and extra-EU export and import flows that are grouped into three product categories according to their broad economic purpose (BEC classification): intermediates, consumption and capital goods. The data on the nominal GDP of destination/origin countries were taken from World Development Indicators database (The World Bank, 2020), while bilateral distances and a number of country-pair dummy variables from CEPII database (Head, Mayer & Ries, 2010; Head & Mayer, 2014).

Data for the number of affected people and deaths caused by Covid-19 is taken from the European Centre for Disease Prevention and Control. Their data is sourced from health authorities worldwide, comprising from but not limited to official reports from countries' ministries of health, public health institutes, World Health Organisation, and other national authorities.

To calculate the GVC indices, we use data from the Eora Multi-Region Input-Output (MRIO) database (henceforth referred to as Eora (see Lenzen et al. (2012) and Lenzen et al. (2013)), which has a considerably broader geographic coverage than the TiVA database. It includes virtually all

Covid Economics 61, 11 December 2020: 222-244

countries in the world and starts in 1990. Thus, it also provides information on countries without I-O tables based on optimisation algorithms for estimating intra- and interregional transaction matrices for all countries worldwide. Additionally, the robustness check estimations are performed on the TiVA database that excludes non-OECD partner countries from our sample.

3.5.Some stylized facts on EU trade during Covid-19 pandemics

As per the data published by the Comext database, trade among the EU member states and with third countries decreased notably following the outbreak of Covid-19. A decrease in the total intra- and extra-EU imports was led mostly by the decrease in the imports of the intermediate goods as presented in Figure 1 which plots year on year relative changes in monthly imports of the EU member states. We can observe that the negative trend in imports of intermediate goods started already in the second half of the year 2019. With the outbreak of Covid-19 pandemics, imports of intermediate goods further dropped sharply by over 30% in April 2020 compared to its level in April 2019.

Figure 1: Monthly imports (intra- and extra-EU) of EU-27 according to BEC (indices defined as $Import_t/Import_{t-12}$·100)

Source: Authors' calculations based on the Comext database (Eurostat, 2020).

Covid Economics 61, 11 December 2020: 222-244

Figure 2 presents cumulative Covid-19 cases per capita for 27 EU member states in the time span from January through April 2020. Notably, Central and Eastern European Countries (CEECs) had seen a lesser number of cases, while Luxembourg, Spain, and Belgium respectively had the most officially confirmed cases per capita. Figure 3 shows relative changes in trade for each European country, comparing the April 2020 values to those in April 2019 to present the trade situation that unfolded at the beginning of the second quarter of 2020 in the EU. Further division to relative changes to exports (Figure 3a) and relative changes to imports (Figure 3b) aims to portray different initial dynamics that may be dominantly affected by either supply or demand shock. These figures signify notable differences in the trade contraction among member states, which cannot be directly related to the severity of the pandemic situation in terms of the number of Covid-19 patients.

Figure 2: Cumulative cases of Covid-19 per 100,000 inhabitants on a country level (period January-April 2020)

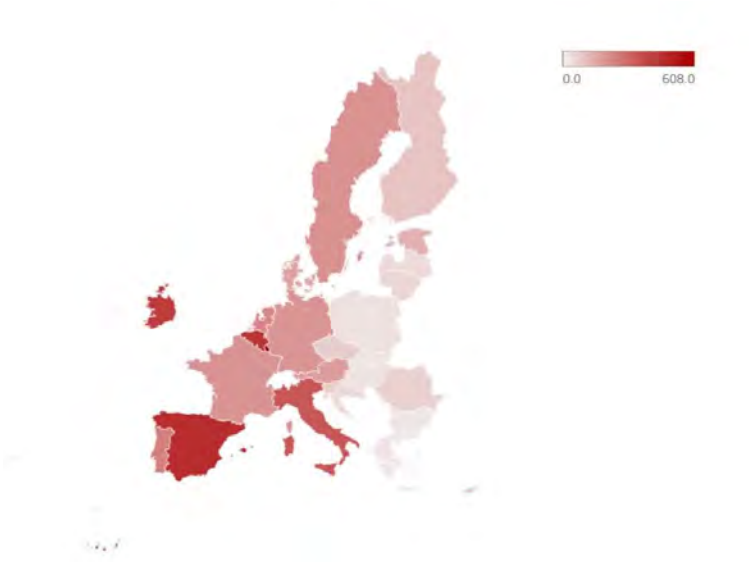

Source: Authors' calculations based on the European CDC data (ECDC, 2020).

Notably, we can see that despite having relatively fewer Covid-19 cases per capita, peripheral countries nonetheless experienced a significant import and export contraction. In the observed time period, for instance, a CEE country, Slovakia, had an average of 25.50 cases per 100000 inhabitants, one of the lowest among the member states, yet its trade contracted more than in the average EU country. The imports decreased by 46.58% on a year-on-year basis while the exports sector experienced a 40.85% reduction. For reference, Spain ranked 2nd among cases per capita and had a sharper decline in intermediate goods trade (37.44 % for imports and approximately 40 % decline in exports). Germany, the largest EU economy, had the 10th highest cases per capita

Covid Economics 61, 11 December 2020: 222-244

among the EU countries and saw a 25.96 % decline in imports and exports of intermediate goods. An interesting case was Bulgaria, a country with then the lowest number of officially recorded cumulative cases per capita. In Bulgaria, imports fell by almost 32 % while the exports decreased by a much lesser amount (16.18 %). While some countries, like Spain and Italy, saw an above-average rise in the number of cases early on, other countries did not experience a surge until later on. An overall decline in both imports and exports was expected, thus our paper focuses more on the aspect of shock transmission and supply chain amplification during the period of lockdowns and government-imposed restrictions.

Figure 3: Percentage change in trade in intermediate goods (YoY comparison April 2019-April 2020)

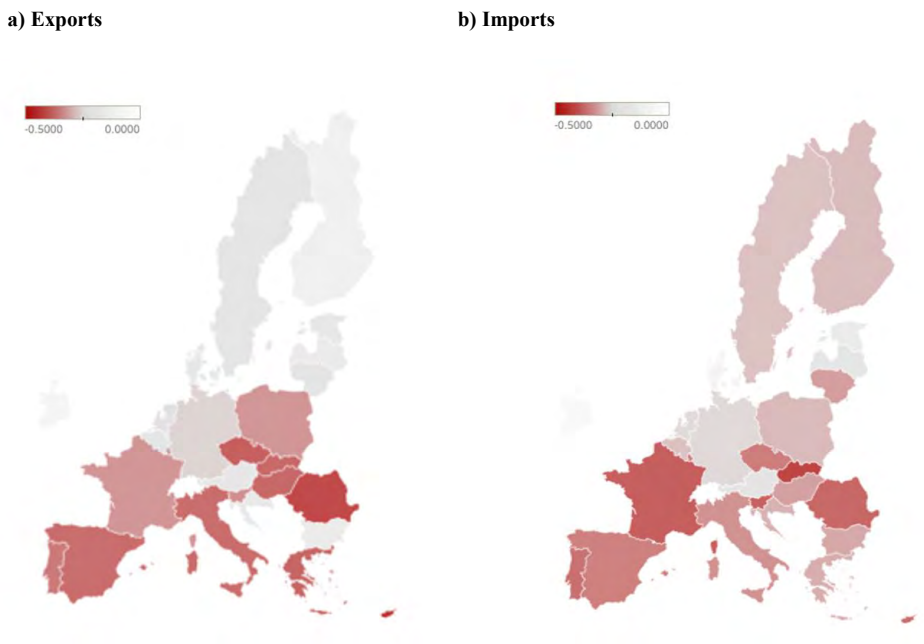

Source: Authors' calculations based on the Comext database (Eurostat, 2020).

4. Empirical results

4.1 Baseline results for total export s and imports

In this section, we present the results for the transmission channels discussed in section 2 and summarized in Table 1. First, we focus on total imports and exports (Table 2). As expected, the

results confirm the general drop in trade in the range of 9.5 % - 11 % during the pandemic time, i.e. since February 2020, as indicated with the significantly negative coefficient for the *covid_period* dummy variable. Furthermore, there is a highly significant, negative impact of per capita number of Covid-19 cases both in origin and destination country on imports and exports indicating the presence of both supply and demand shocks. Taking into account the average Covid-19 infection rates in the EU and partner countries from April 2020, i.e. 1.066 and 0.489 affected people per 1000 population, respectively, the combined trade effect of Covid-19 is around minus 19% for both exports and import (based on specifications in columns 1 and 5 in Table 2).

However, results show that exports decrease more with a higher Covid-19 count in the destination country as opposed to the origin country. This means that for each additional Covid-19 case in the originating country exports will decrease relatively less compared to a decrease due to an additional case in the destination country. These results imply that demand induced shocks through contraction of imports by partner country play an important and immediate role in the transmission of them. Interestingly, we get the opposite result for the total exports when we introduce Covid-19 as a lagged variable (column 4 in Table 2). Introducing Covid-19 as a lagged variable is important as many of the effects of an increased number of cases have a time component (ie. a government imposes stricter measures and lockdowns after the spike). Here the number of cases in exporting country plays a relatively more important role in the decrease in exports. This turnaround might be attributed to the fact that at the start of the pandemic, less strict measures were imposed, that induced uncertainty and the consumption of people decreased. When the more prominent measures were taken by the governments, not only did demand decrease further, there was a labour supply shortage and production halted, resulting in lesser exports supply. When looking at imports (columns 5 through 8 in Table 2), the difference between the impact of Covid-19 cases in origin and destination country becomes evident only for lagged Covid-19 variable (column 8) suggesting the transmission of shocks through demand side is gradually reinforced, as this time the imports contract more depending on the number of cases in the origin country.

Comparing regression coefficients of interaction terms between GVC indices accounting for forward and backward linkages and Covid-19 cases in a partner country we observe that forward participation interaction plays a statistically significant role and is more prominent and instant when it comes to exports. Strong bilateral forward linkages reinforce the negative impact of the covid-19 cases in the destination country on home exports signifying the transmission of the Covid-19 induced shocks from foreign downstream customers to more upstream domestic suppliers. We expect this channel to be particularly relevant for the supply-chain exports which we test on the disaggregated trade flows according to broad economic purpose in the next step. Impact of forward participation for transmission of Covid-19 related shocks can be explained through the GVC composition. With higher bilateral forward participation, the country has a larger share of its domestic value added relative to its gross exports embodied in exports of a particular

Covid Economics 61, 11 December 2020: 222-244

partner country. Since the home country's exports are reliant on the exports of a partner country, the decrease in exports of a partner country, and hence its demand for intermediate goods from domestic country, will have an amplified effect on the home country's exports. Consequentially with the elapsed time, this channel leads to a higher contraction of imports as well confirmed by significantly negative interaction term in case of considering lagged Covid-19 cases in import specification (column 8 in Table 2). On the other hand, we haven't found any empirical support for immediate transmission of Covid-19 induced supply shocks trough the backward linkages from foreign upstream suppliers to domestic downstream customers. As per the traditional regressors in gravity model specifications, e.g. distance and various country-pair dummy variables, all have expected signs and are mostly highly significant in all specifications.

Table 2: Poisson pseudolikelihood estimates of gravity model for total trade of EU-27 member states

	(1) EXPORTS total	(2) EXPORTS total	(3) EXPORTS total	(4) EXPORTS total	(5) IMPORTS total	(6) IMPORTS total	(7) IMPORTS total	(8) IMPORTS total
				Lagged Covid-19 variables				Lagged Covid-19 variables
covid_period	-0.102***	-0.099***	-0.102***	-0.115***	-0.112***	-0.110***	-0.110***	-0.107***
	[0.008]	[0.008]	[0.008]	[0.007]	[0.008]	[0.008]	[0.008]	[0.008]
Covid_cases_o	-0.051***	-0.045***	-0.049***	-0.095***	-0.063***	-0.056***	-0.059***	-0.091***
	[0.008]	[0.009]	[0.009]	[0.013]	[0.009]	[0.010]	[0.009]	[0.017]
Covid_cases_d	-0.113***	-0.096***	-0.103***	-0.084***	-0.068***	-0.054***	-0.062***	-0.059***
	[0.011]	[0.014]	[0.012]	[0.013]	[0.010]	[0.013]	[0.011]	[0.015]
FP(-1)		0.082***	0.008	0.008		0.051**	-0.002	-0.002
		[0.014]	[0.010]	[0.010]		[0.022]	[0.010]	[0.010]
Covid_cases_d		-0.013**	-0.009**	-0.011**		-0.005	-0.007	-0.011**
# FP(-1)		[0.006]	[0.005]	[0.005]		[0.007]	[0.005]	[0.006]
BP(-1)		0.018	0.005	0.005		0.094***	0.002	0.002
		[0.022]	[0.006]	[0.006]		[0.020]	[0.004]	[0.004]
Covid_cases_d		-0.000	0.002	0.007		-0.005	0.002	0.001
# BP(-1)		[0.007]	[0.005]	[0.006]		[0.010]	[0.006]	[0.007]
lndistw	-1.092***	-1.052***			-0.817***	-0.721***		
	[0.072]	[0.072]			[0.103]	[0.095]		

contig	0.180**	0.105			0.366***	0.252***		
	[0.074]	[0.069]			[0.081]	[0.078]		
comlang_ethno	0.107	0.062			0.133	0.008		
	[0.123]	[0.117]			[0.143]	[0.115]		
comcol	1.860***	1.860***			1.755***	1.848***		
	[0.147]	[0.149]			[0.221]	[0.227]		
col45	1.003***	0.996***			0.597***	0.504***		
	[0.129]	[0.123]			[0.133]	[0.134]		
smctry	0.015	-0.079			-0.140	-0.215		
	[0.144]	[0.155]			[0.186]	[0.191]		
Constant	28.610***	28.154***	20.851***	20.851***	26.560***	25.571***	20.888***	20.888***
	[0.540]	[0.544]	[0.025]	[0.025]	[0.774]	[0.732]	[0.026]	[0.026]
Monthly FE	yes	yes	yes	yes	yes	yes	yes	yes
Annual FE	yes	yes	yes	yes	yes	yes	yes	yes
Reporter-year FE	yes	yes	yes	yes	yes	yes	yes	yes
Partner-year FE	yes	yes	yes	yes	yes	yes	yes	yes
Country-pair FE	no	no	yes	yes	no	no	yes	yes
Observations	272,798	242,758	242,318	242,682	272,798	242,758	239,371	239,720
Pseudo R^2	0.963	0.964	0.994	0.994	0.948	0.950	0.992	0.992

Note: Robust standard errors in brackets. *** p<0.01, ** p<0.05, * p<0.1

4.2 Accounting for the supply-chain trade

We further analyse the trade effects by breaking down the exports and imports using the broad economic purpose classification in Tables 3 and 4, respectively to address the supply-chain trade effects. Here, we observe the difference among the intermediate, consumer and capital goods. Overall, exports of consumer goods seem to be least affected over the course of the first wave of Covid-19 pandemic, contracting in the range of 7.2 % to 8.3 % opposed to 10.2 %-10.7% and 7.2 %-10.9 % reduction in intermediate and capital goods, respectively. As expected, the interaction term between Covid-19 cases in a destination country and forward GVC participation exhibits significant impact only for the exports of intermediate goods providing further support for the supply chain transmission of Covid-19 induced shocks through forward GVC linkages (see columns 1 and 2 in Table 3). This implies that an increase in the incidence of Covid-19 cases induces a steeper decline of supply chain exports of intermediates to those destinations with which a country has stronger forward linkages, i.e. to partner positioned further downstream. In other

Covid Economics 61, 11 December 2020: 222-244

words, an increase in bilateral forward participation amplifies the effect of Covid-19 cases in the destination country on decrease of exports of intermediate goods to this destination.

Table 3: Poisson pseudolikelihood estimates of gravity model for EU-27 exports according to BEC categories

VARIABLES	(1) EXPORTS Intermediate goods	(2) EXPORTS Intermediate goods Lagged Covid-19 variables	(3) EXPORTS Consumer goods	(4) EXPORTS Consumer goods Lagged Covid-19 variables	(5) EXPORTS Capital goods	(6) EXPORTS Capital goods Lagged Covid-19 variables
covid_period	-0.113***	-0.108***	-0.075***	-0.087***	-0.075***	-0.115***
	[0.009]	[0.009]	[0.012]	[0.010]	[0.017]	[0.016]
Covid_cases_o	-0.028***	-0.077***	-0.029***	-0.067***	-0.102***	-0.138***
	[0.010]	[0.015]	[0.008]	[0.011]	[0.018]	[0.020]
Covid_cases_d	-0.084***	-0.087***	-0.081***	-0.056***	-0.132***	-0.086***
	[0.012]	[0.015]	[0.011]	[0.014]	[0.018]	[0.018]
FP(-1)	0.004	0.004	0.009	0.009	0.004	0.004
	[0.011]	[0.011]	[0.018]	[0.018]	[0.030]	[0.030]
Covid_cases_d	-0.017***	-0.023***	-0.001	0.000	0.002	0.005
# FP(-1)	[0.005]	[0.007]	[0.004]	[0.005]	[0.006]	[0.006]
BP(-1)	-0.004	-0.004	0.006	0.006	0.035***	0.035***
	[0.010]	[0.010]	[0.014]	[0.014]	[0.011]	[0.011]
Covid_cases_d	0.006	0.013*	0.000	0.002	0.000	-0.001
# BP(-1)	[0.006]	[0.007]	[0.005]	[0.005]	[0.008]	[0.006]
Constant	20.208***	20.208***	19.459***	19.459***	19.100***	19.100***
	[0.035]	[0.035]	[0.055]	[0.055]	[0.053]	[0.053]
Monthly FE	yes	yes	yes	yes	yes	yes
Annual FE	yes	yes	yes	yes	yes	yes
Reporter-year FE	yes	yes	yes	yes	yes	yes
Partner-year FE	yes	yes	yes	yes	yes	yes
Country-pair FE	yes	yes	yes	yes	yes	yes
Observations	240,643	241,088	239,474	239,803	238,285	238,614
Pseudo R^2	0.993	0.993	0.993	0.993	0.978	0.978

Note: Robust standard errors in brackets. *** p<0.01, ** p<0.05, * p<0.1

Covid Economics 61, 11 December 2020: 222-244

Table 4: Poisson pseudolikelihood estimates of gravity model for EU-27 imports according to BEC categories

	IMPORTS Intermediate goods	IMPORTS Intermediate goods Lagged Covid-19 variables	IMPORTS Consumer goods	IMPORTS Consumer goods Lagged Covid-19 variables	IMPORTS Capital goods	IMPORTS Capital goods Lagged Covid-19 variables
covid_period	-0.132***	-0.115***	-0.064***	-0.071***	-0.087***	-0.107***
	[0.009]	[0.010]	[0.014]	[0.012]	[0.016]	[0.014]
Covid_cases_o	-0.057***	-0.120***	-0.040***	-0.013	-0.051*	-0.033
	[0.010]	[0.014]	[0.009]	[0.026]	[0.028]	[0.026]
Covid_cases_d	-0.049***	-0.032**	-0.026**	-0.061***	-0.116***	-0.120***
	[0.014]	[0.015]	[0.010]	[0.021]	[0.024]	[0.024]
FP(-1)	-0.006	-0.005	0.014	0.014	-0.018	-0.018
	[0.013]	[0.013]	[0.017]	[0.017]	[0.025]	[0.025]
Covid_cases_d	-0.004	-0.013**	-0.005	-0.002	-0.019**	-0.016*
# FP(-1)	[0.006]	[0.006]	[0.004]	[0.004]	[0.008]	[0.009]
BP(-1)	-0.002	-0.002	-0.003	-0.002	0.009	0.009
	[0.006]	[0.006]	[0.007]	[0.007]	[0.009]	[0.009]
Covid_cases_d	-0.002	-0.001	-0.001	-0.004	0.024**	0.017
# BP(-1)	[0.006]	[0.008]	[0.003]	[0.004]	[0.010]	[0.012]
Constant	20.254***	20.253***	19.533***	19.533***	19.500***	19.500***
	[0.034]	[0.034]	[0.038]	[0.038]	[0.062]	[0.062]
Monthly FE	yes	yes	yes	yes	yes	yes
Annual FE	yes	yes	yes	yes	yes	yes
Reporter-year FE	yes	yes	yes	yes	yes	yes
Partner-year FE	yes	yes	yes	yes	yes	yes
Country-pair FE	yes	yes	yes	yes	yes	yes
Observations	231,648	232,099	228,903	229,464	219,154	219,504
Pseudo R^2	0.988	0.988	0.994	0.994	0.984	0.984

Note: Robust standard errors in brackets. *** p<0.01, ** p<0.05, * p<0.1

In Table 4 we present the import breakdown by the product category. Observing the import trade flows, the role of forward linkages as a channel for Covid-19 induced shocks is further confirmed (columns 2 and 5) for intermediate and capital goods, with changes to intermediate goods being on a lower scale than for the exports. This follows our notion that the decrease in imports through forward linkages comes after the decrease in exports, due to producers not needing the inputs as they have to lower the production. Again, no evidence provided for the magnification effect of the backward linkages for the destination country's Covid-19 impact on the imports, but surprisingly the interaction becomes even positive for the category of capital goods. On top of that, we see that a decrease of 10.9 %-12.4 % in imports of intermediate goods was more substantial than in the exports, showcasing the role of demand shock in supply chain trade.

4.3 Robustness checks

Table 5 reports regression results using a different approach to the country's GVC involvement. Here we use the upstreamness index that measures a country's bilateral GVC position based on the forward and backward participation values. Results are in support of conclusions following from baseline results presented in Tables 3 and 4 on importance of forward linkages for the transmission of the Covid-19 shocks from partner countries to domestic country's exports of intermediate goods. Namely, a significantly negative interaction term between upstreamness and Covid-19 cases in partner country for this type of exports (column 1) indicates that the adverse impact of the seriousness of destination country's pandemic situation is larger the more upstream is the position of the country in trade relations with the particular partner country, i.e. higher the forward relative to backward participation.

We perform second robustness check using the data from the OECD TiVA database to calculate the corresponding GVC indices based on the 2015 data (see Table 6) which limits our sample to OECD partner countries. Results are in line with our previous findings on GVC contagion effect through forward linkages resulting in lower exports of intermediate goods. However, the interaction term with backward participation is of the opposite sign suggesting that certain reorientation of exports of intermediate goods towards traditionally more upstream positioned partners took place during the pandemic period. Furthermore, using the TiVA trade data, we get a statistically significant effect of backward linkages in transmitting the supply chain shocks from partner countries resulting in a sharper drop in imports of intermediate goods. Through these linkages, we provide indication that the supply side shocks/disruptions are transmitted from foreign upstream suppliers to downstream domestic importers. A country's reliance on foreign value added in exports will cause its imports to decrease following the supply side shock caused by lesser output due to lockdown measures in partner countries.

Covid Economics 61, 11 December 2020: 222-244

Table 5: Poisson pseudolikelihood estimates of gravity model for EU-27 trade according to BEC categories

VARIABLES	(1) EXPORTS Intermediate goods	(2) EXPORTS Consumer goods	(3) EXPORTS Capital goods	(4) IMPORTS Intermediate goods	(5) IMPORTS Consumer goods	(5) IMPORTS Capital goods
covid_period	-0.110***	-0.087***	-0.115***	-0.118***	-0.072***	-0.106***
	[0.010]	[0.011]	[0.016]	[0.010]	[0.012]	[0.014]
Covid_cases_o(-1)	-0.079***	-0.067***	-0.137***	-0.124***	-0.015	-0.033
	[0.014]	[0.011]	[0.019]	[0.014]	[0.026]	[0.025]
Covid_cases_d(-1)	-0.108***	-0.052***	-0.076***	-0.060***	-0.074***	-0.119***
	[0.013]	[0.012]	[0.017]	[0.014]	[0.021]	[0.020]
Upstream(-1)	0.420	-0.418	-3.298***	0.094	0.396	-0.969
	[0.954]	[1.233]	[1.169]	[0.560]	[0.716]	[0.982]
Covid_cases_d(-1)	-1.855**	-0.069	0.457	-0.530	0.231	-1.795
# Upstream(-1)	[0.757]	[0.504]	[0.626]	[0.769]	[0.395]	[1.114]
Constant	20.208***	19.490***	19.172***	20.237***	19.558***	19.479***
	[0.005]	[0.006]	[0.007]	[0.003]	[0.004]	[0.012]
Monthly FE	yes	yes	yes	yes	yes	yes
Annual FE	yes	yes	yes	yes	yes	yes
Reporter-year FE	yes	yes	yes	yes	yes	yes
Partner-year FE	yes	yes	yes	yes	yes	yes
Country-pair FE	yes	yes	yes	yes	yes	yes
Observations	241,088	239,803	238,614	232,099	229,464	219,504
Pseudo R^2	0.993	0.993	0.977	0.988	0.994	0.984

Note: Robust standard errors in brackets. *** p<0.01, ** p<0.05, * p<0.1

Covid Economics 61, 11 December 2020: 222-244

Table 6: Poisson pseudolikelihood estimates of gravity model for EU-27 trade according to BEC categories based on TiVA data

VARIABLES	(1) EXPORTS Intermediate goods	(2) EXPORTS Consumer goods	(3) EXPORTS Capital goods	(4) IMPORTS Intermediate goods	(5) IMPORTS Consumer goods	(6) IMPORTS Capital goods
covid_period	-0.116***	-0.067***	-0.069***	-0.123***	-0.064***	-0.088***
	[0.008]	[0.012]	[0.018]	[0.009]	[0.015]	[0.014]
Covid_cases_o(-1)	-0.025**	-0.024***	-0.092***	-0.041***	-0.040***	-0.044
	[0.010]	[0.008]	[0.019]	[0.011]	[0.010]	[0.027]
Covid_cases_d(-1)	-0.080***	-0.081***	-0.142***	-0.056***	-0.016	-0.090***
	[0.014]	[0.015]	[0.020]	[0.017]	[0.011]	[0.025]
Covid_cases_d(-1)	-0.040***	-0.015	0.013	0.005	-0.010	0.002
# FP_TiVA2015	[0.010]	[0.011]	[0.016]	[0.013]	[0.011]	[0.010]
Covid_cases_d(-1)	0.011***	0.007	-0.006	-0.014**	-0.005	-0.003
# BP_TiVA2015	[0.004]	[0.005]	[0.005]	[0.007]	[0.005]	[0.005]
Constant	20.356***	19.658***	19.396***	20.347***	19.610***	19.471***
	[0.001]	[0.001]	[0.001]	[0.001]	[0.001]	[0.001]
Monthly FE	yes	yes	yes	yes	yes	yes
Annual FE	yes	yes	yes	yes	yes	yes
Reporter-year FE	yes	yes	yes	yes	yes	yes
Partner-year FE	yes	yes	yes	yes	yes	yes
Country-pair FE	yes	yes	yes	yes	yes	yes
Observations	84,058	84,005	83,899	83,846	83,846	83,740
chi2	641.9	211.2	233.7	436.0	113.1	129.1
r2_p	0.994	0.994	0.976	0.991	0.993	0.980

Note: Robust standard errors in brackets. *** p<0.01, ** p<0.05, * p<0.1

5. Concluding remarks

Although several months have already passed since the beginning of the Covid-19 outbreak in Europe, uncertainty regarding the future of international trade and supply chain reorganisation remains. In this paper, we have performed gravity model analysis of final good and supply chain trade of EU member states to identify the transmission channels of the shocks caused by the

Covid Economics 61, 11 December 2020: 222-244

pandemic. To account for various mechanisms we distinguish demand and supply shocks as of either domestic or partner country origin. We further characterize the latter on the basis of the country's GVC position, thus accommodating for a possibility of transmission through forward and backward linkages. We argue that the identified transmission channels of demand shocks and forward linkages play an important role in the supply chain trade. Results show that an increase in the incidence of Covid-19 cases induces a steeper decline of supply chain exports of intermediates in those destinations with which a country has stronger forward linkages, i.e. in partners positioned further downstream. Furthermore, a decrease in exports of inputs is followed by a contraction in imports. Although our study demonstrates some of the important GVC trade dynamics during the Covid-19 pandemic, we are aware that certain outcomes remain unexplained. This may be attributed to the limitations of the existing model as well as to the current unavailability of important data. We, therefore, leave possible extensions of the model for future work as some of our findings may have long-lasting effects such as reshaping of the supply chains, whilst others will only be temporary. As some of the findings suggest, identifying the proper cause is important in explaining the trade dynamics, especially in a complex environment of GVCs. Thus, they should be recognised by policymakers, as the policies ought to address right causes for optimal outcomes, whether those concern demand or supply side.

Covid Economics 61, 11 December 2020: 222-244

References

Anderson, J.E., van Wincoop, E. (2003). "Gravity with Gravitas: A Solution to the Border Puzzle," *The American Economic Review*, 93(1), pp.170-192.

Antras, P., Chor, D., Fally, T. & Hillberry, R. (2012). Measuring the Upstreamness of Production and Trade Flows. American Economic Review, American Economic Association, vol. 102(3), pages 412-16, May.

Antras, P., Redding, S.J., and Rossi-Hansberg, E. (2020). "Globalization and pandemics," *Covid Economics* 49, 1-84. https://cepr.org/sites/default/files/CovidEconomics49.pdf#Paper1

Baier, S. L., and Bergstrand, J. H. (2007). "Do free trade agreements actually increase members' international trade?," *Journal of international Economics*, 71(1), 72-95.

Baldwin, R., and Freeman, R. (2020). "Supply chain contagion waves: Thinking ahead on manufacturing 'contagion and reinfection' from the covid concussion". Retrieved from: https://voxeu.org/article/covidconcussion-and-supply-chain-contagion-waves, 2020.

Baldwin, R., and Tomiura, E. (2020). "Thinking ahead about the trade impact of covid-19." Economics in the Time of COVID-19, 59, 2020.

Bonadio, B., Huo, Z., Levchenko, A. A., & Pandalai-Nayar, N. (2020). *Global supply chains in the pandemic* (No. w27224). National Bureau of Economic Research.

Burger, M., van Oort, F., and Linders., G-J. (2009). "On The Specification of The Gravity Model of Trade: Zeros, Excess Zeros and Zero-inflated Estimation," *Spatial Economic Analysis, (4)*2, 167-190.

Correia, S., Guimarães, P., & Zylkin, T. (2019). "Verifying the existence of maximum likelihood estimates for generalized linear models". arXiv preprint arXiv:1903.01633.

Correia, S., Guimarães, P., & Zylkin, T. (2020). "Fast Poisson estimation with high-dimensional fixed effects," *The Stata Journal*, 20(1), 95-115.

Dingel, J., and Neiman, B. (2020). "How many jobs can be done at home?," *Journal of Public Economics,* vol 189.

European Centre for Disease Prevention and Control (ECDC) (2020). Retrieved from: https://www.ecdc.europa.eu/en/publications-data/download-todays-data-geographic-distribution-covid-19-cases-worldwide

Eurostat (2020). Comext trade database. Retrieved from: http://epp.eurostat.ec.europa.eu/newxtweb/

Evenett, S. (2020). "Sickening thy neighbour: Export restraints on medical supplies during a pandemic". Retrieved from: https://voxeu.org/article/export-restraints-medical-supplies-during-pandemic

Fally, T. (2012). Has production become more fragmented? International vs domestic perspective, VoxEU Policy Brief, retrieved from: https://voxeu.org/article/has-production-become-more-fragmented-international-vs-domestic-perspectives

Farhi, E., & Baqaee, D. R. (2020). "Supply and Demand in Disaggregated Keynesian Economies with an Application to the Covid-19 Crisis" CEPR Discussion Paper DP14743.

Friedt, F. L., and Zhang, K. (2020). "The triple effect of Covid-19 on Chinese exports: First evidence of the export supply, import demand and GVC contagion effects," *Covid Economics* 53, 72-109. https://cepr.org/sites/default/files/CovidEconomics53.pdf#Paper1

Hassan, T. A., Hollander, S., van Lent, L., Tahoun, A. (2020). "Firm-level Exposure to Epidemic Diseases: Covid-19, SARS, and H1N1", NBER Working Paper No. 26971.

Hayakawa, K., and Mukunoki, H. (2020). "Impacts of covid-19 on international trade: evidence from the first quarter of 2020", IDE Discussion Paper Vol. 791.

Head, K., Mayer, T. & Ries, J. (2010). "The erosion of colonial trade linkages after independence", *Journal of International Economics*, 81(1):1-14.

Head, K. and T. Mayer, (2014). "Gravity Equations: Toolkit, Cookbook, Workhorse." *Handbook of International Economics*, Vol. 4,eds. Gopinath, Helpman, and Rogoff, Elsevier.

Koopman, R., Powers, W., Wang, Z., & Wei, S.-J. (2010). Give Credit Where Credit Is Due: Tracing Value Added in Global Production Chains: National Bureau of Economic Research, Inc.

Covid Economics 61, 11 December 2020: 222-244

Lenzen M., Kanemoto K., Moran D. & Geschke A. (2012). Mapping the structure of the world economy. Environmental Science & Technology, 46(15) pp 8374–8381. doi: 10.1021/es300171x

Lenzen, M., Moran, D., Kanemoto, K. & Geschke, A. (2013). Building Eora: A Global Multi-regional Input-Output Database at High Country and Sector Resolution. Economic Systems Research, 25:1, 20-49, doi:10.1080/09535314.2013.769938

McCann, F., and Myers, S. (2020). "COVID-19 and the transmission of shocks through domestic supply chains," Financial Stability Notes Vol. 2020 No. 3, Central Bank of Ireland.

Meier, M., and Pinto, E. (2020). "Covid-19 supply chain disruptions", *Covid Economics* 48, 139-170. https://cepr.org/sites/default/files/CovidEconomics48.pdf#Paper4

OECD (2013). Interconnected economies: Benefiting from Global Value Chains. Synthesis Report, OECD. https://www.oecd.org/mcm/C-MIN(2013)15-ENG.pdf

OECD (2020). "Trade in value added", *OECD Statistics on Trade in Value Added* (database), retrieved from: https://doi.org/10.1787/data-00648-en

Serič, A., Görg, H., Mösle, S., and Windisch, M. (2020). "Managing COVID-19: How the pandemic disrupts global value chains," *UNIDO's Department of Policy Research and Statistics*. Retrieved from: https://iap.unido.org/articles/managing-covid-19-how-pandemic-disrupts-global-value-chains
the Pandemic," NBER Working Paper No. 27224.

World Bank (2020). "World Development Report 2020," World Bank Publications, The World Bank, number 32437, June.

Covid Economics 61, 11 December 2020: 222-244